Structure Property Relationships of Proton Exchange Membranes

Abhishek Roy

Dissertation submitted to the faculty of the Virginia Polytechnic Institute and State University in partial fulfillment of the requirements for the degree of

Doctor of Philosophy
In
Macromolecular Science and Engineering

Dr. James E. McGrath

Dr. Judy S. Riffle
Dr. Donald G. Baird
Dr. John J. Lesko
Dr. Richey M. Davis

(02.19.08)
(Blacksburg, VA)

Keywords: (Proton Exchange Membranes, Block Copolymer, Transport, Morphology, States of Water)

Copyright 2008, Abhishek Roy

Structure Property Relationships of Proton Exchange Membranes

Abhishek Roy

ABSTRACT

The major challenge of the research was to characterize and develop concepts for establishing structure/property relationships between the functionality of the polymer backbone, the states of water and the membrane transport properties. Most of the hydrocarbon based random copolymers reported in the literature show reduced proton conductivity at low water content. This was attributed to the formation of an isolated morphology. Over the last few years our group has synthesized thermally stable multiblock copolymers with varying chemical structures and compositions. Block copolymers consist of two or more incompatible polymers (i.e. blocks) that are chemically conjoined in the same chain. The transport properties of the multiblock copolymers showed a strong dependence on the morphology in contrast to the random copolymers. Irrespective of the nature of the backbone, the transport properties scaled with the block lengths of the copolymers. An increase in block length for a given series of block copolymer was associated with improved proton conduction, particularly under partially hydrated conditions compared to the random copolymers. The structure-property relationship of the proton conductivity and self-diffusion coefficient of water was obtained as a function of the volume fraction of water for all the random and block copolymers. At a given volume fraction, the block copolymers displayed both higher self-diffusion coefficients of water and proton conductivities relative to the random

copolymers. This improvement in transport properties indicates the presence of desired and favorable morphology for the blocks. For DMFC applications, the block copolymers also showed low methanol permeability and high selectivity. The states of water in the copolymers were characterized using DSC and NMR relaxation techniques. At similar ionic contents, the free water concentration increased with increasing block lengths. The distribution of the states of water in the copolymers correlates to transport properties. This knowledge, coupled with the state of water experiments, transport measurements, and chemical structure of the copolymers provided a fundamental picture of how the chemical nature of a phase separated copolymer influences its transport properties. The experimental procedure involved impedance spectroscopy, DSC, TGA, FTIR, DMA, pulse gradient stimulated echo (PGSE) NMR, NMR relaxation experiments and various electrochemical fuel cell performance experiments.

Dedicated to my loving parents Mrs. Manju Roy & Mr. Arunabha Roy

for

their love, support, sacrifice and encouragement

Acknowledgements

I would like to begin by thanking my advisor Prof. James E. McGrath for his immense support and guidance throughout my entire Ph.D. work. Without his enormous contribution, my research would not have been complete and successful. I am deeply enthralled by his profound knowledge in polymer science which helped me in several ways to shape my educational and professional life. His mentorship and his dedication to his students will always be an inspiration in my life. I would also like to express my gratitude to my advisory committee members, Prof. Judy S. Riffle, Prof. Donald G. Baird, Prof. John J. Lesko, and Prof. Richey M. Davis for their valuable suggestions and thoughtful discussions for completing this dissertation.

Special thanks go to my mentor and friend Prof. Michael A. Hickner. He was instrumental in helping me to develop an analytical mind critically needed for Ph.D. research. I would also like to thank the synthesis connoisseurs in our group; Mr. Hae-Sung Lee, Dr. Xiang Yu and Dr. Yanxiang Li for providing me their wonderful samples. I would like to thank Dr. Brain R. Einsla, Dr. William L. Harrison, Dr. Yu Seung Kim, Dr. Chris J. Cornelius, Dr. Subiman Ghosh, Dr. Anand S. Badami, Dr. Hang Wang, Mrs. Rachael A. VanHouten, Miss Natalie Arnett and Miss Ozzie Lane for valuable discussions and friendship.

Many thanks go to Mrs. Laurie Good and Mrs. Millie Ryan for their constant assistance and cooperativeness over these past years. Their contribution is truly helpful for running this big group smoothly.

I would like to express my deepest gratitude to my parents Mr. Arunabha Roy and Mrs. Manju Roy for their selfless contribution, constant support and endless love without which I could not have reached to this point of my life. Thank you ma and baba, for your life long sacrifice and the encouragement you have always provided in every situation of my life. Thanks to my sweet little younger sister Miss. Abhinanda Roy for her constant

loving support throughout my life. I will always remember the cherished moments of our growing up together and the innumerable ways by which she has made my life happier. I want to specially thank my father in-law Mr. Amal Paul and my mother in-law Mrs. Sabita Paul for all their good wishes and love.

Finally, I like to thank my loving wife, best friend and soul mate, Mou, for her love, support and patience. I felt her presence and contributions in every aspect of my life. Her interest and suggestions for my research have been a boon to my Ph.D. work. Most of all, I thank Dear God for being with me.

Attribution

Several colleagues and coworkers aided in the research behind several of the chapters of this dissertation. A brief description of their background and their contributions are included here.

Prof. James E. McGrath (Department of Chemistry, Virginia Tech) is the primary advisor and the committee chair. Prof. McGrath helped the author and guided him for this work.

Prof. Michael A. Hickner (Sandia National Laboratory), currently faculty at The Pennsylvania State University, contributed to the discussion in Chapter 2, 3, 4, 5, 6 and 11.

Dr. Brian R. Einsla (Macromolecular Science and Engineering Program, Virginia Tech), currently employee at Rohm and Haas and **Dr. William L. Harrison** (Department of Chemistry, Virginia Tech), currently employee at Nano Sonic, Inc., helped the author in the synthesis of HQSH-xx copolymers in chapter 2.

Mr. Hae-Seung Lee (Macromolecular Science and Engineering Program, Virginia Tech), contributed towards the synthesis of BPSH-PI(x:y) multiblocks in chapter 4,5 & 6; in the synthesis of BPSH-BPS(A:B) multiblocks in chapter 8 and also in the synthesis of BPS-PBI(x:y) in chapter 9.

Mr. Xiang Yu (Macromolecular Science and Engineering Program, Virginia Tech), currently employee at Henkel, contributed towards the synthesis of BPSH-BisAF(x:y) multiblocks in chapter 3 and also in the synthesis of BPSH-BisSF(x:y) multiblocks in chapter 8.

Dr. Yanxiang Li (Macromolecular Science and Engineering Program, Virginia Tech), currently employee at The Dow Chemical Company, contributed towards the synthesis of B-ketone-xx and PB-diketone-xx copolymers in chapter 3; and B-ketone-xx copolymers in chapter 5 & 6.

Mr. Tom Glass (Department of Chemistry, Virginia Tech) helped the author in the NMR experiments for chapter 5 and 6.

Dr. Linda Harris (Department of Chemistry, Virginia Tech) aided in the discussion in chapter 12.

Mr. Stuart Dunn (Department of Chemistry, Virginia Tech), currently a graduate student at University of North Carolina at Chapel Hill, contributed towards the research in chapter 8.

Table of Contents

1.0 LITERATURE REVIEW 1

1.1 INTRODUCTION TO FUEL CELLS 1
1.2 MEMBRANE ELECTRODE ASSEMBLY 6
1.3 PROTON EXCHANGE MEMBRANES 8
1.3.1 Fluorinated membranes 8
1.3.2 Non-fluorinated membranes 9
1.3.3 Poly(arylene ether)s 9
1.3.3.1 Post sulfonation method 10
1.3.3.2 Direct sulfonation methods 11
1.3.3.3 Synthesis of the monomer 12
1.4 MORPHOLOGY OF PEMS 16
1.5 PROTON CONDUCTIVITY 20
1.6 SELF-DIFFUSION COEFFICIENT OF WATER 22
1.7 ELECTRO-OSMOTIC DRAG 29
1.8 METHANOL PERMEABILITY 30
1.9 STATES OF WATER 31
1.10 DESIGN FOR NEXT GENERATION PROTON EXCHANGE MEMBRANES. 35
1.11 REFERENCES 37

2.0 SYNTHESIS AND CHARACTERIZATION OF PARTIALLY DISULFONATED HYDROQUINONE BASED POLY(ARYLENE ETHER SULFONE)S RANDOM COPOLYMERS FOR APPLICATION AS PROTON EXCHANGE MEMBRANES 51

2.1 INTRODUCTION 52
2.2 EXPERIMENTAL 53
2.2.1 Materials 53
2.2.2 Synthesis of hydroquinone based partially disulfonated poly(arylene ether sulfone) random copolymers (HQSH-xx) 54
2.2.3 Membrane preparation 54
2.2.4 NMR, ATR-FTIR spectroscopy, DSC and intrinsic viscosity 55
2.2.5 Measurement of proton conductivity 55
2.2.6 Determination of water uptake, hydration number, density and effective proton concentration (C_{H^+}) 55
2.2.7 Methanol permeability and DMFC performance 56
2.3 RESULTS AND DISCUSSION 57
2.3.1 Copolymer synthesis 57
2.3.2 Water uptake 59
2.3.3 Proton conductivity 60
2.3.4 DMFC performance and methanol permeability 61
2.4 CONCLUSIONS 65
2.5 REFERENCES 66

3.0 INFLUENCE OF CHEMICAL COMPOSITION AND SEQUENCE LENGTH ON THE TRANSPORT PROPERTIES OF PROTON EXCHANGE MEMBRANES 69

3.1 INTRODUCTION 70
3.1.1 Proton conductivity 71
3.1.2 Methanol permeability 74
3.1.3 Self-diffusion coefficient of water 74
3.2 EXPERIMENTAL 75
3.2.1 Materials 75
3.2.2 Synthesis of disulfonated poly(arylene ether) random copolymers (BPSH-xx, HQSH-xx, B-ketone-xx and PB-diketone-xx) 75
3.2.3 Synthesis of the hydrophilic/hydrophobic multiblock copolymers: 76
3.2.4 Membrane preparation: 77
3.2.5 Proton conductivity 77
3.2.6 Water uptake 77
3.2.7 Methanol permeability 78
3.2.8 Pulsed-field gradient spin echo nuclear magnetic resonance (PGSE NMR). 78
3.2.9 NMR spectroscopy, gel permeation chromatography (GPC), intrinsic viscosity and atomic force microscopy characterization (AFM). 80
3.3 RESULTS AND DISCUSSIONS 80
3.3.1 NMR spectroscopy, GPC, intrinsic viscosity and AFM characterization of the multiblock copolymer 80
3.3.2 Proton conductivity and water uptake 83
3.3.3 Self-diffusion coefficient of water 90
3.3.4 Methanol permeability 93
3.4 CONCLUSIONS 95
3.5 REFERENCES 96

4.0 STRUCTURE-PROPERTY RELATIONSHIPS OF SEGMENTED SULFONATED POLY(ARYLENE ETHER SULFONE)-B-POLYIMIDE MULTIBLOCK COPOLYMERS FOR APPLICATION IN PROTON EXCHANGE MEMBRANE FUEL CELLS 101

4.1 INTRODUCTION 102
4.2 EXPERIMENTAL 104
4.2.1 Materials 104
4.2.2 Multiblock copolymer synthesis 105
4.2.3 Membrane preparation 105
4.2.4 Measurement of proton conductivity 105
4.2.5 Determination of water uptake 106
4.2.6 Determination of swelling ratio and density 107
4.2.7 Methanol permeability and DMFC performance 107
4.2.8 Pulsed-field gradient spin echo nuclear magnetic resonance (PGSE NMR) 107
4.3 RESULTS AND DISCUSSION 108
4.3.1 Multiblock copolymer synthesis 108

4.3.2 Water uptake, volume fraction, swelling and IEC *109*
4.3.3 Self-diffusion coefficient of water *112*
4.3.4 Proton Conductivity *116*
4.3.5 Partially hydrated conditions: water absorption and proton conduction .. *118*
4.4 CONCLUSIONS 126
4.5 REFERENCES 127

5.0 STATES OF WATER OF PROTON EXCHANGE MEMBRANES PART-A-INFLUENCE OF CHEMICAL STRUCTURES AND COMPOSITIONS 131

5.1 INTRODUCTION 132
5.2 EXPERIMENTAL 134
5.2.1 Materials *134*
5.2.2 Synthesis of partially disulfonated poly(arylene ether) random copolymers (HQSH-xx and B-ketone-xx) *135*
5.2.3 Synthesis of disulfonated poly(arylene ether sulfone)-b-polyimide (BPSH-x-PI-y) multiblock copolymers *136*
5.2.4 Membrane preparation *136*
5.2.5 Differential scanning calorimetry (DSC) and nuclear magnetic resonance (NMR) and thermo gravimetric Analyzer (TGA) *137*
5.3 RESULTS 138
5.3.1 Model copolymers *138*
5.3.2 Water uptake *139*
5.3.3 DSC results *142*
5.3.4 NMR relaxation measurements (T_2 and T_1) *146*
5.4 DISCUSSION AND CONCLUSIONS 150
5.5 REFERENCES 153

6.0 STATES OF WATER IN PROTON EXCHANGE MEMBRANES-PART-B-INFLUENCE ON TRANSPORT PROPERTIES 157

6.1 INTRODUCTION 158
6.2 EXPERIMENTAL 159
6.2.1 Materials *159*
6.2.2 Pulsed-field gradient spin echo nuclear magnetic resonance (PGSE NMR). 160
6.2.3 Thermogravimetric analysis (TGA) *161*
6.3 RESULTS AND DISCUSSION 161
6.3.1 Proton conductivity *161*
6.3.2 Self-diffusion coefficient of water *164*
6.3.3 Methanol permeability *167*
6.3.4 Importance of bound water on freezing and high temperature transport processes *168*
6.4 CONCLUSIONS 171
6.5 REFERENCES 172

7.0 HYDROPHILIC-HYDROPHOBIC MULTIBLOCK COPOLYMERS BASED ON POLY(ARYLENE ETHER SULFONE)S AS NOVEL PROTON EXCHANGE MEMBRANES-PART-B 175

7.1 INTRODUCTION 176
7.2 EXPERIMENTAL 178
7.2.1 Materials 178
7.2.2 Multiblock and random copolymer synthesis 178
7.2.3. Membrane preparation 179
7.2.4. Measurement of proton conductivity 179
7.2.5. Determination of water uptake 180
7.2.6. Determination of swelling ratio and density 181
7.2.7. Determination of self-diffusion coefficient of water 181
7.2.8. Differential scanning calorimetry (DSC) and nuclear magnetic resonance (NMR) 181
7.3. RESULTS AND DISCUSSION 182
7.3.1 Summary of the copolymers synthesized 182
7.3.2 Physical properties: IEC, density, water uptake and water volume fraction 183
7.3.3 States of water 190
7.3.3.1 Water absorption 191
7.3.3.2 DSC studies 192
7.3.3.3 NMR relaxation measurements 194
7.4 CONCLUSIONS 197
7.5 REFERENCES 198

8.0 INFLUENCE OF MICROSTRUCTURE AND CHEMICAL COMPOSITION ON PROTON EXCHANGE MEMBRANE PROPERTIES OF SULFONATED-FLUORINATED, HYDROPHILIC-HYDROPHOBIC MULTIBLOCK COPOLYMERS 202

8.1 INTRODUCTION 203
8.2 EXPERIMENTAL 206
8.2.1 Materials 206
8.2.2 Synthesis 206
8.2.3 NMR spectroscopy 207
8.2.4 Proton conductivity 207
8.2.5 Water uptake 207
8.2.6 Determination of swelling ratio and density 208
8.2.7 Pulsed-field gradient spin echo nuclear magnetic resonance (PGSE NMR) 208
8.3 RESULTS AND DISCUSSION 209
8.3.1 Multiblock synthesis and structural variables 209
8.3.2 Water uptake and Hydration number 210
8.3.3 Self-diffusion coefficient of water and proton conductivity 212
8.3.4 Selectivity 221
8.4 CONCLUSIONS 222
8.5 REFERENCES 223

9.0 INVESTIGATION OF PROTON TRANSPORT PHENOMENON IN PHOSPHORIC ACID DOPED POLY(ARYLENE ETHER SULFONE)-*B*-POLYBENZIMIDAZOLE COPOLYMERS 227

9.1 INTRODUCTION 228
9.2 EXPERIMENTAL 230
9.2.1 Materials 230
9.2.2 Multiblock Copolymer Synthesis 231
9.2.3 Film casting and H_3PO_4 doping 232
9.2.4 Determination of proton conductivity 232
9.3 RESULTS AND DISCUSSION 233
9.3.1 Proton conductivity 233
9.4 CONCLUSIONS 239
9.5 REFERENCES 240

10.0 OPTIMIZATION OF MEA PROCESSING PARAMETERS 244

10.1 INTRODUCTION 245
10.1.1 Importance of molecular weight of the copolymer on processing temperature 247
10.1.2 The impact of water content in a copolymer on the processing temperature during MEA fabrication 247
10.2 EXPERIMENTAL 249
10.2.1 Copolymers studied 249
10.2.2 Differential scanning calorimetry (DSC) and thermogravimetric analysis (TGA) 249
10.2.3 Proton conductivity 250
10.2.4 MEA preparation and fuel cell characterization 250
10.2.5 Experimental design 250
10.3 RESULTS AND DISCUSSION 251
10.3.1 Water uptake 251
10.3.2 Effect of hot pressing conditions on proton conductivity of the blanks and MEAs 252
10.4 CONCLUSIONS 256
10.5 REFERENCES 256

11.0 STRUCTURE PROPERTY RELATIONSHIPS OF PROTON EXCHANGE MEMBRANES 258

11.1 INTRODUCTION 259
11.2 EXPERIMENTAL 263
11.2.1 Copolymers studied 263
11.2.2 Characterization properties 263
11.3 RESULTS AND DISCUSSION 266
11.3.1 Water absorption 266
11.3.2 Water transport 268
11.3.3 Proton transport 270
11.3.4 States of water 276
11.4 CONCLUSIONS 278
11.5 REFERENCES 279

12.0 SUGGESTED FUTURE RESEARCH 284

12.1 SCOPE 284

12.2 SYNTHETIC STRATEGIES 285
12.3 CHARACTERIZATION 288
12.4 REFERENCES 289

LIST OF SYMBOLS 290

VITA 291

List of Figures

FIGURE 1-1 REPRESENTATIVE V-I CURVE FOR AN H_2/AIR TYPE PEMFC FUEL CELL. REPRINTED WITH PERMISSION.[5] COPYRIGHT 2004 AMERICAN CHEMICAL SOCIETY.... 5

FIGURE 1-2 MEMBRANE ELECTRODE ASSEMBLY. REPRINTED WITH PERMISSION.[15] COPYRIGHT 2004 AMERICAN CHEMICAL SOCIETY 6

FIGURE 1-3 SCHEMATIC DIAGRAM OF H_2 / AIR MEA FABRICATION TECHNIQUE 7

FIGURE 1-4 MODULUS VS. TEMPERATURE 7

FIGURE 1-5 CHEMICAL STRUCTURE OF NAFION®[23] 9

FIGURE 1-6 GENERAL STRUCTURE OF POLY(ARYLENE ETHER)S. REPRINTED WITH PERMISSION.[15] COPYRIGHT 2004 AMERICAN CHEMICAL SOCIETY 10

FIGURE 1-7 CHEMICAL STRUCTURES OF COMMERCIALLY AVAILABLE PEEKS. REPRINTED WITH PERMISSION.[17] COPYRIGHT 2003 ANNUAL REVIEW OF MATERIALS RESEARCH 11

FIGURE 1-8 PLACEMENT OF THE SULFONIC ACID GROUP IN POST SULFONATION (ACTIVATED RING) VS. DIRECT COPOLYMERIZATION OF A DISULFONATED MONOMER (DEACTIVATED RING). REPRINTED WITH PERMISSION.[15] COPYRIGHT 2004 AMERICAN CHEMICAL SOCIETY 12

FIGURE 1-9 SYNTHETIC ROUTE FOR SDCDPS REPRINTED WITH PERMISSION.[15] COPYRIGHT 2004 AMERICAN CHEMICAL SOCIETY 13

FIGURE 1-10 SYNTHETIC ROUTE FOR BPSH-XX COPOLYMER REPRINTED WITH PERMISSION.[15] COPYRIGHT 2004 AMERICAN CHEMICAL SOCIETY 13

FIGURE 1-11 3000 H STABILITY FOR 6F 35 UNDER DMFC CONDITIONS AT 80 ^{O}C 15

FIGURE 1-12 DMFC FUEL CELL PERFORMANCE CURVE FOR 6FCN 35, BPSH 40 AND NAFION® 117. REPRINTED WITH PERMISSION.[49] COPYRIGHT [2004], THE ELECTROCHEMICAL SOCIETY 15

FIGURE 1-13 CONCEPTUAL MODEL FOR MORPHOLOGY OF DRY AND SWOLLEN NAFION®. REPRINTED FROM [71] WITH PERMISSION FROM ELSEVIER 17

FIGURE 1-14 AFM IMAGES OF NAFION® 117 (K^+) FORM A) HEIGHT IMAGE B) PHASE IMAGE; 300 NM X 300 NM. REPRINTED WITH PERMISSION.[63] COPYRIGHT 2000 AMERICAN CHEMICAL SOCIETY 19

FIGURE 1-15 WATER UPTAKE SCALES WITH MORPHOLOGY AND DEGREE OF DISULFONATION FOR BPSH-XX COPOLYMERS REPRINTED FROM[73] WITH PERMISSION FROM ELSEVIER 19

FIGURE 1-16 PULSE SEQUENCE OF PGSE NMR 22

FIGURE 1-17 INTENSITY OF THE WATER SIGNAL AS A FUNCTION OF GRADIENT STRENGTH IN AN IDEAL PGSE EXPERIMENT 23

FIGURE 1-18 LINEAR CURVE FITTING OF THE PGSE EXPERIMENTAL RESULTS 24

FIGURE 1-19 PROTON CONDUCTIVITY SCALES WITH WATER CONTENT IN NAFION® 117. REPRINTED WITH PERMISSION.[82] COPYRIGHT 1991 AMERICAN CHEMICAL SOCIETY 25

FIGURE 1-20 PROTON CONDUCTIVITY AND WATER UPTAKE FOR BPSH-XX COPOLYMERS AS A FUNCTION OF RELATIVE HUMIDITY. REPRINTED WITH PERMISSION FROM JOHN WILEY & SONS, INC[36] 26

FIGURE 1-21 SELF-DIFFUSION COEFFICIENT OF WATER AS A FUNCTION OF WATER CONTENT FOR (A) NAFION® AND (B) SULFONATED PEEK. REPRINTED WITH PERMISSION.[17] COPYRIGHT 2003 ANNUAL REVIEW OF MATERIALS RESEARCH 27

FIGURE 1-22 PROTON CONDUCTIVITY AS A FUNCTION OF TEMPERATURE AND RELATIVE HUMIDITY FOR NAFION.® REPRINTED FROM [102] WITH PERMISSION FROM ELSEVIER .. 28

FIGURE 1-23 DSC COMPARISON OF NAFION® 117 AND BPSH 40 AT VARIOUS WATER CONTENTS SHOWING THE DIFFERENCE IN THE STATE OF WATER FOR EACH MEMBRANE. REPRINTED WITH PERMISSION.[103] COPYRIGHT 2003 AMERICAN CHEMICAL SOCIETY 34

FIGURE 2-1 SYNTHETIC SCHEME FOR HQS-XX RANDOM COPOLYMERS..... 57

FIGURE 2-2 ^{1}H NMR SPECTRUM OF HQS-25 RANDOM COPOLYMER; ONLY THE AROMATIC REGION IS DISPLAYED..... 58

FIGURE 2-3 ATR-FTIR SPECTRA OF HQS-XX COPOLYMERS CONFIRMING THE PRESENCE OF SULFONATE GROUPS..... 59

FIGURE 2-4 WATER UPTAKE AS A FUNCTION OF IEC FOR HQSH-XX AND BPSH-XX RANDOM COPOLYMERS 60

FIGURE 2-5 DMFC PERFORMANCE OF HQSH-XX RANDOM COPOLYMERS AS A FUNCTION OF DEGREE OF DISULFONATION; THE THICKNESS OF THE MEMBRANES IN MILS IS PROVIDED IN THE LEGEND 62

FIGURE 2-6 METHANOL PERMEABILITY AS A FUNCTION OF TEMPERATURE FOR THE HQSH-XX COPOLYMERS 63

FIGURE 2-7 AROMATIC COPOLYMERS DISPLAY HIGHER SELECTIVITY WITH LOWER METHANOL PERMEABILITY COMPARED TO NAFION® 117 64

FIGURE 3-1 COPOLYMER CHEMICAL STRUCTURES SYNTHESIZED IN THIS WORK (A) BPSH-XX; (B) HQSH-XX, (C) B-KETONE-XX & PB-DIKETONE-XX, (D) BLOCK BISAF-BPSH(X:Y)K 71

FIGURE 3-2 PULSE SEQUENCE SCHEMATIC FOR PGSE NMR EXPERIMENTS 79

FIGURE 3-3 A.. ^{1}H NMR SPECTRA OF HYDROPHILIC TELECHELIC OLIGOMER(TOP) AND MULTIBLOCK (BOTTOM) BISAF-BPSH(8:8)K COPOLYMER 81

FIGURE 1-3 B ^{19}F NMR SPECTRA OF HYDROPHOBIC TELECHELIC OLIGOMER(TOP) AND MULTIBLOCK BISAF-BPSH(8:8)K (BOTTOM) COPOLYMER.....81

FIGURE 3-4 TAPPING MODE AFM HEIGHT IMAGE(LEFT) ,PHASE IMAGE(RIGHT)OF BLOCK BISAF-BPSH(5:5)K INDICATING NANO-PHASE SEPARATION BETWEEN HYDROPHILIC AND HYDROPHOBIC DOMAINS 82

FIGURE 3-5 PROTON CONDUCTIVITY FOR HQSH-XX, B-KETONE-XX AND PB-DIKETONE-XX INCREASES WITH INCREASE IN IEC..... 85

FIGURE 3-6 PROTON CONDUCTIVITY FOR HQSH –XX RANDOM COPOLYMERS FOLLOWS ARRHENIUS RELATIONSHIP WITH TEMPERATURE 85

FIGURE 3-7 PROTON CONDUCTIVITY FOR PB–DIKETONE-XX RANDOM COPOLYMERS AS A FUNCTION OF TEMPERATURE..... 86

FIGURE 3-8 PROTON CONDUCTIVITY FOR COPOLYMERS SCALES LINEARLY WITH HYDRATION NUMBER AT IEC OF 1.4 MEQ/G 86

FIGURE 3-9 PROTON CONDUCTIVITY AS A FUNCTION OF RELATIVE HUMIDITY FOR NAFION® 117, HQSH-30 AND PB-DIKETONE-50 AT 80°C 88

FIGURE 3-10 ACTIVATION ENERGY FOR PROTON CONDUCTION FOR HQSH-30 RANDOM COPOLYMER DECREASES WITH INCREASE IN RELATIVE HUMIDITY OVER A TEMPERATURE RANGE OF 30-80°C..... 88

FIGURE 3-11 PROTON CONDUCTIVITY FOR BLOCK BISAF-BPSH(X:Y)K UNDER PARTIALLY HYDRATED CONDITION INCREASES WITH INCREASE IN BLOCK LENGTH AT 80°C 90

FIGURE 3-12 SELF-DIFFUSION COEFFICIENT FOR WATER AS A FUNCTION OF IEC FOR THE RANDOM AND BLOCK COPOLYMERS AND NAFION® 112 91

FIGURE 3-13 SELF-DIFFUSION COEFFICIENT OF WATER IN THE POLYMER SAMPLES AS A FUNCTION OF EFFECTIVE DIFFUSION TIME INDICATING PRESENCE OF A LOWER MORPHOLOGICAL BARRIER TO TRANSPORT FOR NAFION®112 AND BLOCK BISAF-BPSH(8:8)K. 92

FIGURE 3-14 METHANOL PERMEABILITY FOR HQSH-XX, B-KETONE-XX, BLOCK BISAF-BPSH(X:Y)K SERIES AND NAFION®117 AS A FUNCTION OF IEC AT 80 °C 94

FIGURE 4-1 CHEMICAL STRUCTURES OF A) BPSH-XX RANDOM COPOLYMER, B) BPSH-X-PI-Y MULTIBLOCK COPOLYMER WHERE X AND Y REPRESENT THE MOLECULAR WEIGHT OF THE HYDROPHILIC AND HYDROPHOBIC BLOCKS RESPECTIVELY IN KG/MOLE 104

FIGURE 4-2 STIMULATED ECHO PULSE SEQUENCE SCHEMATIC FOR PGSE NMR EXPERIMENTS 108

FIGURE 4-3 INFLUENCE OF BLOCK LENGTH AND IEC ON WATER UPTAKE 111

FIGURE 4-4 A) TAPPING MODE AFM IMAGES OF THE MULTIBLOCKS. REPRINTED WITH PERMISSION FROM JOHN WILEY & SONS, INC.[17] B) WATER SWELLING IN BOTH IN-PLANE AND THROUGH-PLANE AS A FUNCTION OF THE BLOCK LENGTHS 112

FIGURE 4-5 SELF-DIFFUSION COEFFICIENTS OF WATER SCALE WITH THE WATER VOLUME FRACTIONS FOR THE MULTIBLOCKS, NAFION® AND BPSH 35 AT 25 ^{O}C 114

FIGURE 4-6 SELF-DIFFUSION COEFFICIENTS OF WATER AS A FUNCTION OF THE EFFECTIVE DIFFUSION TIME SCALE WITH THE MORPHOLOGY OF THE BLOCK COPOLYMER 114

FIGURE 4-7 WATER DIFFUSION CHANGES FROM RESTRICTED TO TORTUOUS IN NATURE WITH INCREASING BLOCK LENGTH 116

FIGURE 4-8 PROTON CONDUCTION UNDER FULLY HYDRATED CONDITIONS AT 30 ^{O}C IS A FUNCTION OF THE WATER OR HYDROPHILIC VOLUME FRACTIONS 118

FIGURE 4-9 WATER ABSORPTION UNDER PARTIALLY HYDRATED CONDITIONS AS A FUNCTION OF THE BLOCK LENGTH. 119

FIGURE 4-10 PROTON CONDUCTION VS. VOLUME FRACTION OF WATER AS A FUNCTION OF BLOCK LENGTH 120

FIGURE 4-11 PROTON CONDUCTION UNDER PARTIALLY HYDRATED CONDITIONS AT 80 ^{O}C INCREASES WITH INCREASING BLOCK LENGTH OR WITH THE EXTENT OF PHASE SEPARATION IN MULTIBLOCKS 121

FIGURE 4-12 METHANOL PERMEABILITY AS A FUNCTION OF ION EXCHANGE CAPACITY FOR SEVERAL SYSTEMS AT 80 °C REPRODUCED WITH PERMISSIONS FROM ECS TRANSACTIONS.[25] COPYRIGHT [2007], THE ELECTROCHEMICAL SOCIETY 123

FIGURE 4-13 PHASE SEPARATED MORPHOLOGY OF MULTIBLOCKS ALLOWS TO ACHIEVE HIGH SELECTIVITY AT LOW METHANOL PERMEABILITY. REPRODUCED WITH PERMISSIONS FROM ECS TRANSACTIONS.[25] COPYRIGHT [2007], THE ELECTROCHEMICAL SOCIETY 124

FIGURE 4-14 DMFC PERFORMANCES OF NAFION®117 AND BPSH-PI MULTIBLOCK COPOLYMERS, THE MEMBRANE THICKNESSES (DRIED) ARE GIVEN ALONG WITH THE COPOLYMER NAMES IN THE LEGEND. REPRODUCED WITH PERMISSIONS FROM ECS TRANSACTIONS.[31] COPYRIGHT [2007], THE ELECTROCHEMICAL SOCIETY. 125

FIGURE 5-1 COPOLYMER CHEMICAL STRUCTURES: (A) HQSH-XX; (B) BPSH-XX, (C) B-KETONE-XX, (D) BPSH-X-PI-Y MULTIBLOCKS 138

FIGURE 5-2 INFLUENCE OF IEC AND BLOCK LENGTHS ON WATER UPTAKE AT FULLY HYDRATED CONDITIONS 139

FIGURE 5-3A) WATER ABSORPTION UNDER PARTIALLY HYDRATED CONDITIONS FOR THE RANDOM HQSH-XX COPOLYMERS AS A FUNCTION OF IEC. 141

FIGURE 5-3 B) WATER ABSORPTION UNDER PARTIALLY HYDRATED CONDITIONS FOR THE BLOCK COPOLYMERS BPSH-X-PI-Y AS A FUNCTION OF THE BLOCK LENGTH 141

FIGURE 5-4 A) MELTING ENDOTHERMS OF THE FREEZING WATER IN HQSH-XX COPOLYMERS AS A FUNCTION OF DEGREE OF DISULFONATION UNDER FULLY HYDRATED CONDITION 142

FIGURE 5-4 B) MELTING ENDOTHERMS OF THE FREEZING WATER IN BPSH-X-PI-Y MULTIBLOCK COPOLYMERS AS A FUNCTION OF BLOCK LENGTH UNDER FULLY HYDRATED CONDITION 143

FIGURE 5-5 A) INFLUENCE OF WATER CONTENT ON ENDOTHERMIC PEAKS AND T_GS OF HQSH 35 144

FIGURE 5-5 B) INFLUENCE OF WATER CONTENT ON ENDOTHERMIC PEAKS AND TGS OF BPSH-15-PI-15THE NUMBERS IN THE LEFT SIDE REPRESENT WATER UPTAKE AND ON RIGHT TGS RESPECTIVELY 144

FIGURE 5-6 NORMALIZED ENTHALPY CHANGES OF WATER AS A FUNCTION OF THE HYDRATION NUMBER FOR HQSH-XX RANDOM COPOLYMERS; THE INTERCEPTS ARE THE TIGHTLY BOUND WATER CONTENTS 145

FIGURE 5-7 INFLUENCE OF DISULFONIC ACID CONCENTRATIONS ON ^1H T_2 DECAYS FOR THE B-KETONE-XX COPOLYMERS. THE MARKERS REPRESENT ACTUAL EXPERIMENTAL DATA AND THE LINES REPRESENT THE FITTED FUNCTIONS 147

FIGURE 5-8 RETENTION OF WATER AS A FUNCTION OF TEMPERATURE FOR THE HQSH-XX AND NAFION® COPOLYMERS 150

FIGURE 6-1 COPOLYMER CHEMICAL STRUCTURES: (A) HQSH-XX; (B) BPSH-XX, (C) B-KETONE-XX, (D) BPSH-X-PI-Y MULTIBLOCKS 161

FIGURE 6-2 INFLUENCE OF FREE WATER CONTENT ON PROTON CONDUCTIVITY IN LIQUID WATER AT 30 ^{O}C 162

FIGURE 6-3 ACTIVATION ENERGY FOR PROTON TRANSPORT DECREASES WITH INCREASING FREE WATER CONTENT 163

FIGURE 6-4 PROTON CONDUCTIVITY AS A FUNCTION OF THE RELATIVE HUMIDITY FOR MULTIBLOCK AND RANDOM COPOLYMERS AT 80 ^{O}C 164

FIGURE 6-5 INTENSITY OF THE WATER SIGNAL AS A FUNCTION OF GRADIENT STRENGTH IN AN IDEAL PGSE EXPERIMENT; A MONO EXPONENTIAL RELATIONSHIP WAS OBSERVED 165

FIGURE 6-6 LINEAR CURVE FITTING OF THE PGSE EXPERIMENTAL RESULTS 166

FIGURE 6-7 SELF-DIFFUSION COEFFICIENTS OF WATER AS A FUNCTION OF FREE WATER CONTENT; MULTIBLOCK COPOLYMERS AT 25 ^{O}C SHOW BETTER WATER TRANSPORT THAN RANDOM COPOLYMERS AT A GIVEN FREE WATER CONTENT 166

FIGURE 6-8 METHANOL PERMEABILITY AT 30 ^{O}C INCREASES WITH INCREASING FREE WATER CONTENT 168

FIGURE 6-9 WATER RETENTION AS A FUNCTION OF TEMPERATURE DEPENDS ON THE MORPHOLOGY OF THE PEMS 170

FIGURE 6-10 WATER TRANSPORT UNDER FREEZING CONDITIONS IS A FUNCTION OF THE NON-FREEZING WATER CONTENT 170

FIGURE 7-1 CHEMICAL STRUCTURE OF A) BPSH-BPS(A:B) MULTIBLOCK AND B) BPSH-XX RANDOM COPOLYMER 182

FIGURE 7-2 IN-PLANE AND THROUGH PLANE SWELLING RATIOS FOR THE COPOLYMERS; MULTIBLOCK COPOLYMERS SHOW ANISOTROPIC SWELLING AFTER A CERTAIN BLOCK LENGTH 184

FIGURE 7-3 PROTON CONDUCTIVITY SCALES WITH THE VOLUME FRACTION OF WATER 186

FIGURE 7-4 INFLUENCE OF TEMPERATURE ON PROTON CONDUCTIVITY AS A FUNCTION OF BLOCK LENGTHS; ACTIVATION ENERGY IN KJ/MOLE REPRESENTED WITHIN BOXES DECREASES WITH INCREASING BLOCK LENGTH 187

FIGURE 7-5 PROTON CONDUCTIVITY UNDER PARTIALLY HYDRATED CONDITIONS INCREASES WITH INCREASING BLOCK LENGTHS AT 80 ^{O}C 188

FIGURE 7-6 PROTON CONDUCTIVITY AS A FUNCTION OF RELATIVE HUMIDITY FOR THE MULTIBLOCKS WITH HIGHER IECS AT 80 ^{O}C 189

FIGURE 7-7 PROTON CONDUCTIVITY AS A FUNCTION OF VOLUME FRACTION OF WATER IN THE COPOLYMERS AT 30 ^{O}C; MORPHOLOGY DOMINATES TRANSPORT AT LOW WATER CONTENT 190

FIGURE 7-8 WATER ABSORPTION OF COPOLYMERS UNDER PARTIALLY HYDRATED CONDITIONS 191

FIGURE 7-9 DSC THERMOGRAMS OF THE MELTING ENDOTHERM OF WATER AS A FUNCTION OF BLOCK LENGTHS 193

FIGURE 7-10 DSC THERMOGRAMS OF BPSH-BPS (10:10) MULTIBLOCK AT VARIOUS WATER CONTENT, THE NUMBERS REPRESENT THE WATER UPTAKE ON MASS BASIS .. 194

FIGURE 7-11 ^{1}H NMR T_2 RELAXATION (TRI-EXPONENTIAL FIT) BEHAVIOR OF BPSH-BPS (10:10) MULTIBLOCK COPOLYMER 195

FIGURE 8-1 STRUCTURES OF SULFONATED-FLUORINATED MULTIBLOCK COPOLYMERS... 204

FIGURE 8-2 PULSE SEQUENCE SCHEMATIC FOR PGSE NMR EXPERIMENTS 209

FIGURE 8-3 SELF-DIFFUSION COEFFICIENT OF WATER VS. THE EFFECTIVE DIFFUSION TIME 213

FIGURE 8-4 INFLUENCE OF TEMPERATURE ON SELF-DIFFUSION COEFFICIENTS OF WATER 213

FIGURE 8-5 INFLUENCE OF TEMPERATURE ON PROTON CONDUCTIVITY AS A FUNCTION OF BLOCK LENGTH; ACTIVATION ENERGY IN KJ/MOLE REPRESENTED WITHIN BOXES DECREASES WITH INCREASING BLOCK LENGTH 215

IGURE 8-6 INFLUENCE OF BLOCK LENGTH ON PROTON CONDUCTION UNDER PARTIALLY HYDRATED CONDITIONS AT 80 ^{O}C FOR THE BISSF-BPSH MULTIBLOCKS AT SIMILAR IECS 216

FIGURE 8-7 MULTIBLOCK COPOLYMERS DISPLAY REDUCED IN-PLANE SWELLING; THE NUMBERS IN THE PARENTHESIS REPRESENTS IEC IN MEQ/G 218

FIGURE 8-8 PROTON CONDUCTIVITY AS A FUNCTION OF RELATIVE HUMIDITY FOR THE BISSF-BPSH (17:12) WITH VARYING IECS; THE NUMBER AFTER THE PARENTHESIS REPRESENT IEC IN MEQ/G 220

FIGURE 8-9 PROTON CONDUCTIVITY AS A FUNCTION OF RELATIVE HUMIDITY FOR THE BISSF-BPSH (25:16) WITH VARYING IECS; THE NUMBER AFTER THE PARENTHESIS REPRESENTS IEC IN MEQ/G 220

FIGURE 8-10 SELECTIVITY OF PEMS AS A FUNCTION OF HYDRATION NUMBER 222

FIGURE 9-1 SYNTHESIS SCHEME OF POLY(ARYLENE ETHER SULFONE)-*B*-POLYBENZIMIDAZOLE COPOLYMERS 231

FIGURE 9-2 INFLUENCE OF TEMPERATURE ON PROTON CONDUCTIVITY FOR BPS-PBI(15-15) SAMPLES AT VARYING PHOSPHORIC ACID DOPING LEVELS. 235

FIGURE 9-3 INFLUENCE OF TEMPERATURE ON PROTON CONDUCTIVITY FOR BPS-PBI(10-10) SAMPLES AT VARYING PHOSPHORIC ACID DOPING LEVELS 235

FIGURE 9-4 INFLUENCE OF TEMPERATURE ON PROTON CONDUCTIVITY FOR BPS-PBI(5-5) SAMPLES AT VARYING PHOSPHORIC ACID DOPING LEVELS 236

FIGURE 9-5 INFLUENCE OF PHOSPHORIC ACID CONTENT ON ACTIVATION ENERGY FOR PROTON CONDUCTION 236

FIGURE 9-6 INFLUENCE OF BLOCK LENGTH ON PROTON CONDUCTION AT VARYING PHOSPHORIC ACID DOPING LEVELS AT 140 ^{O}C 238

FIGURE 9-7 INFLUENCE OF RELATIVE HUMIDITY ON PROTON TRANSPORT FOR THE PHOSPHORIC ACID DOPED BPS-PBI (10-10) MULTIBLOCK AT 80 ^{O}C; THE NUMBER AFTER THE PARENTHESIS IN THE LEGEND REPRESENTS THE DOPING LEVEL 239

FIGURE 10-1 MEMBRANE ELECTRODE ASSEMBLY. REPRINTED WITH PERMISSIONS.[1] COPYRIGHT 2004 AMERICAN CHEMICAL SOCIETY. 245

FIGURE 10-2 MEA FABRICATION TECHNIQUE 246

FIGURE 10-3 MODULUS VS. TEMPERATURE 247

FIGURE 10-4 CHEMICAL STRUCTURE OF BPSH-XX RANDOM COPOLYMER 249

FIGURE 10-5 RETENTION OF WATER AS A FUNCTION OF TEMPERATURE OF THE BPSH-35 RANDOM COPOLYMER EQUILIBRATED AT DIFFERENT RELATIVE HUMIDITIES 251

FIGURE 10-6 CONDUCTIVITY VS. CURRENT DENSITY FOR THE MEAS 253

FIGURE 10-7 AFM IMAGES OF THE EXPOSED BPSH 35 AT DIFFERENT CONDITIONS. REPRINTED FROM [9] WITH PERMISSION FROM ELSEVIER 254

FIGURE 11-1 CHEMICAL STRUCTURES OF A) HQSH-XX, B) BPSH-XX, C) 6FSH-XX, D) BPSH-PI (X:Y), E) BPSH-BPS (X:Y), F) BPSH-BISSF (X:Y) 262

FIGURE 11-2 INFLUENCE OF PEM MICROSTRUCTURE ON WATER ABSORPTION BEHAVIOR 267

FIGURE 11-3 SELF-DIFFUSION COEFFICIENTS OF WATER SCALE WITH THE VOLUME FRACTION OF WATER 269

FIGURE 11-4 PROTON CONDUCTIVITY MEASURED IN LIQUID WATER AT 30 ^{O}C AS A FUNCTION OF THE VOLUME FRACTION OF WATER 271

FIGURE 11-5 THE EFFECTIVE PROTON CONCENTRATION IN PEMS DECREASES AT HIGHER WATER CONTENT 272

FIGURE 11-6 MULTIBLOCKS DISPLAY HIGHER PROTON DIFFUSIVITY THAN THE RANDOM COPOLYMERS AT A GIVEN VOLUME FRACTION OF WATER 273

FIGURE 11-7 INFLUENCE OF MULTIBLOCK CHEMICAL STRUCTURE ON PROTON CONDUCTION UNDER PARTIALLY HYDRATED CONDITIONS AT 80 ^{O}C 275

FIGURE 11-8 DISTRIBUTION OF DIFFERENT STATES OF WATER IN THE PEMS AS A FUNCTION OF THE COPOLYMER MORPHOLOGY AND CHEMICAL COMPOSITIONS 277

FIGURE 12-1 VARIATION IN CHEMICAL STRUCTURES FOR THE PROPOSED MULTIBLOCK COPOLYMERS 286

List of Tables

TABLE 1-1 COMPARATIVE STUDY OF DIFFERENT TYPES OF FUEL CELL. REPRINTED WITH PERMISSION. [5] COPYRIGHT 2004 AMERICAN CHEMICAL SOCIETY 2

TABLE 2-1 SUMMARY OF THE PROPERTIES OF HQSH-XX COPOLYMERS 58

TABLE 2-2 PROTON EXCHANGE MEMBRANE PROPERTIES OF HQSH-XX AND BPSH-XX[19] COPOLYMERS 61

TABLE 3-1 BLOCK LENGTHS, IV, M_N, IEC, WATER UPTAKE, AND PROTON CONDUCTIVITY OF THE MULTIBLOCK BISAF-BPSH(X:Y)K COPOLYMERS 82

TABLE 3-2 WATER UPTAKE, PROTON CONDUCTIVITY AT 30 AND 80 °C AND ACTIVATION ENERGIES FOR PROTON TRANSPORT FOR HQSH-XX, PB-DIKETONE-XX, AND B-KETONE-XX RANDOM COPOLYMERS 84

TABLE 4-1 SUMMARY OF THE PROPERTIES OF THE BPSH-X-PI-Y MULTIBLOCKS 110

TABLE 4-2 SUMMARY OF DMFC PERFORMANCE RESULTS FOR THE COPOLYMERS STUDIED. REPRODUCED WITH PERMISSIONS FROM ECS TRANSACTIONS.[31] COPYRIGHT [2007], THE ELECTROCHEMICAL SOCIETY. 126

TABLE 5-1 SUMMARY OF COPOLYMER PROPERTIES 146

TABLE 5-2 QUANTIFICATION OF THE DIFFERENT STATES OF WATER AND THE $1/T_1$ RELAXATION TIME 149

TABLE 7-1 SUMMARY OF THE PROPERTIES OF COPOLYMERS 183

TABLE 7-2 STATES OF WATER QUANTIFICATION FOR THE BPSH-BPS(A:B) MULTIBLOCKS AND BPSH- XX RANDOM[13] COPOLYMERS 196

TABLE 8-1 SUMMARY OF PROPERTIES FOR BISSF-BPSH(X:Y) COPOLYMERS WITH IEC 1.3 MEQ/G 211

TABLE 8-2 SUMMARY OF THE PROPERTIES FOR BISSF-BPSH (X:Y) MULTIBLOCKS WITH VARYING IECS 217

TABLE 10-1 DEPRESSION OF GLASS TRANSITION TEMPERATURE UNDER HYDRATED CONDITIONS[4] 248

TABLE 10-2 EXPERIMENTAL DESIGN 251

TABLE 10-3 DEPRESSION OF GLASS TRANSITION TEMPERATURE OF BPSH35 WITH WATER UPTAKE 252

TABLE 10-4 PROTONIC CONDUCTIVITY OF THE HOT PRESSED SAMPLES IN LIQUID WATER253

TABLE 10-5 PROTON CONDUCTIVITY VALUES AFTER HYDROTHERMAL TREATMENT FOR THE HOT PRESSED SAMPLES..... 255

TABLE 11-1 SUMMARY OF THE PHYSICAL PROPERTIES OF RANDOM COPOLYMERS 264

TABLE 11-2 PHYSICAL PROPERTIES OF MULTIBLOCK COPOLYMERS 265

1.0 Literature Review

1.1 Introduction to fuel cells

Fuel cells are defined as energy producing devices that convert chemical energy directly to electrical energy.[1-3] The concept is not new to the world. In 1839, William Grove first demonstrated the possibility of producing electric power from H_2 and O_2. However, it took over a century before NASA utilized the concept in providing power to their space shuttle.[4] The long delay was mainly due to the availability of ample amounts of conventional fuel. Thus, there was no urgency for developing fuel cell technologies. In the late 20th century, however, people became aware of the importance of electrical energy, our over-dependence on conventional fuels, and more recently, the deleterious environmental aspects of continuing to use fossil fuels to power the world. These factors have all combined to support the development and commercialization of fuel cell technologies.

Fuel cells are classified according to the nature of the electrolyte.[5-8] The most promising ones are alkaline fuel cells (AFCs), proton exchange membrane fuel cells (PEMFCs), phosphoric acid based fuel cells (PAFCs), molten carbonate fuel cells (MCFCs) and solid oxide fuel cells (SOFCs). PEMFCs can be further subdivided based on the nature of the fuel. The fuel may be nonvolatile in nature, for example H_2 (H_2/Air fuel cells), or volatile as in the case of methanol (direct methanol fuel cells). Fuel cells can also be classified according to their operating temperatures. AFCs and PEMFCs, for example, belong to the low temperature category (< 200 ^{o}C), while PAFCs, MCFCs, and SOFCs all fall into the high temperature category (> 200 ^{o}C). Winter et al.[5] have reported a comparative study on the various types of fuel cell as given in Table (1-1).

Table 1-1 Comparative study of different types of fuel cell. Reprinted with permission. [5]

Copyright 2004 American Chemical Society

Advantages	Disadvantages	Comments
	Alkaline (AFC)	
Mechanically rechargeable low cost KOH electrolyte	Limited activated life Intolerant of impurities in gas streams Pure H_2 only suitable fuel	Original development > 30 years ago Apollo fuel cell Operates at room temp to 80 ^oC
	Polymer electrolyte membrane Fuel Cell (PEMFC)	
Nonvolatile electrolyte Few materials problems CO_2 rejecting electrolyte Polymer electrolyte Only byproduct is water, green technology	Expensive catalyst required CO poisoning High cost electrolyte Water management issues Limited life	Operates best at 60-90 ^oC Originally developed for space by GE Main development efforts for automotive and stationary applications
	Direct Methanol Fuel Cell (DMFC)	
Direct fuel conversion Slow electrode kinetics Improved wt and vol Polymer electrolyte	High catalyst loading Low overall efficiency Methanol hazardous	Operates best at 60-90 ^oc Methanol fuel eliminates reformer Lower current capability Methanol crossover reduces efficiency
	Phosphoric Acid Fuel Cell (PAFC)	
CO_2 rejecting electrolyte High fuel efficiency Ability to operate in absence of water	H_2 only suitable fuel Anode Co catalyst poison Leaching out of phosphoric acid Limited life	Operates best at 200 ^oC Stationary energy storage Available commercially
	Molten carbonate Fuel Cell (MCFC)	
Fast electrode kinetics High efficiency Co/CH_4 usable fuel Direct reforming feasible	Materials problems and life Low sulfur tolerance High ohmic electrolyte	Operates best at 550 ^oC Nickel catalyst, ceramic separator membrane Hydrocarbon fuels reformed in situ
	Solid Oxide Fuel Cell (SOFC)	
High grade heat available Fast electrode kinetics High system efficiency	High fabrication cost Operates only at higher temperature ~ 900 ^oC Mechanically not stable	Conducting ceramic oxide electrodes Hydrocarbon fuels reformed in situ

Although all five fuel cell types have shown promise, our research is concerned mainly with PEMFCs and phosphoric acid based fuel cells.

A typical operating principle for a PEMFC involves oxidation of the fuel at the anode to produce hydrogen ions and electrons.[1] The hydrogen ions or the protons are then transported across the proton exchange membrane (PEM) to the cathode and react with oxygen to form water. The "half cell reaction" at the anode with H_2 as the fuel, is provided in Equation (1-1).

$$\mathbf{2H_2 \longrightarrow 4\,H^+ + 4e^-} \qquad \textbf{Equation 1-1}$$

The half cell oxidation reaction depends upon the catalytic activity of the catalyst and the diffusive nature of the fuel. Physically, the oxidation involves three simultaneous processes: diffusion of H_2 across the electrodes, adsorption onto the catalyst, and dissociation. Thus, both the catalytic activity and the permeability of the fuel determine the overall rate of oxidation.

An anodic cell reaction can be summarized by Equation (1-1a)

$$2Pt_s + H_2 \longrightarrow Pt\text{-}H_{ads} + Pt\text{-}H_{ads}$$
$$Pt\text{-}H_{ads} \longrightarrow H^+ + e^- + Pt_s \qquad \textbf{Equation 1-1a}$$

One of the major problems associated with this reaction is the reduction in the catalytic activity due to the CO poisoning of the platinum catalyst.[3, 7] This can be eliminated by using pure H_2 or by raising the temperature of the reaction. An increase in temperature would also enhance the rate of the reaction. However, there are proven disadvantages associated with higher temperature operations. For example, recent studies have indicated the possibility of Pt dissolution around 120 °C, causing a decrease in catalytic activity.[9] The half cell reaction at the cathode is given in Equation (1-2).

$$\mathbf{\tfrac{1}{2}\,O_2 + 2H^+ + 2e^- \longrightarrow H_2O} \qquad \textbf{Equation 1-2}$$

The electrochemical reaction at the cathode involves reduction of gaseous oxygen by electrons in the presence of a Pt catalyst and combination with protons to form H_2O. Excess water accumulation at the cathode restricts the diffusion of oxygen to the catalyst. This is often referred to as cathode flooding, which reduces overall fuel cell performance. Hence, water management in fuel cells is an important issue which will be addressed later. From Equations (1-1 and 1-2), the overall cell reaction can be written as:

$$\mathbf{H_2 + \tfrac{1}{2}\, O_2 \longrightarrow H_2O} \qquad \textbf{Equation 1-3}$$

The overall theoretical cell potential for this reaction is reported to be 1.229V.[1] This is in consideration of the fact that the anode half cell has a standard half cell potential of 0.00V and the cathode has 1.229V.

In the case of direct methanol fuel cells (DMFCs), the fuel introduced at the anode is methanol.[10] The catalyst typically used for the oxidation of methanol is a Pt-Ru alloy.[1, 11-14] However, the amount of Pt tends to be much higher than that for the H_2/Air system because of the difficulty in oxidizing methanol. The anodic reaction is summarized in Equation (1-4).

$$\mathbf{CH_3OH + H_2O - 6e \longrightarrow 6H^+ + CO_2} \qquad \textbf{Equation 1-4}$$

The half cell reaction at the cathode is the same as that for the H_2/Air systems.

$$\mathbf{\tfrac{1}{2}\, O_2 + 2\, H^+ + 2e \longrightarrow 2\, H_2O} \qquad \textbf{Equation 1-5}$$

The overall cell reaction is given as,

$$\mathbf{CH_3OH + 3/2\, O_2 \longrightarrow CO_2 + 2\, H_2O} \qquad \textbf{Equation 1-6}$$

Fuel cell performance is generally represented by the V-i curve as shown in Figure (1-1). The curve represents a graph of voltage vs. current density. The current is normalized by the area of the fuel cell. Ideally, the voltage should be independent of the current drawn from the cell and should be close to the thermodynamic voltage. However, in the case of an actual fuel

cell, voltage decreases with increasing drawn current, as depicted in Figure (1-1). The loss from theoretical voltage values can be divided into three major types. The activation loss is represented by Region 1 in the performance curve, while the ohmic loss is shown as Region 2, and the concentration loss as Region 3.

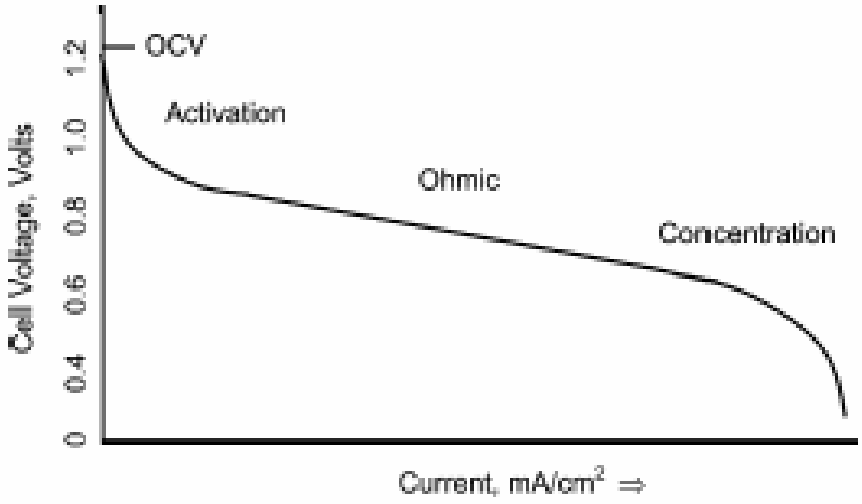

Figure 1-1 Representative V-i curve for an H_2/Air type PEMFC fuel cell. Reprinted with permission.[5] Copyright 2004 American Chemical Society

Activation loss is mainly due to the loss associated with an electrochemical reaction. The health of the electrodes (and primarily the health of the cathode) governs this region. The ohmic loss is solely due to the resistance offered by the membrane itself and depends largely on the membrane morphology and hydration level. The lower the resistance, the lower is the slope of the curve. Concentration loss is mainly due to mass transport loss. High current density results in high water production leading to cathode flooding. This hampers the oxygen diffusion process and reduces the concentration of the fuel.

Another way of judging fuel cell performance is by the power density curve. Power density can be obtained by multiplying the voltage by current density at each point and plotting this as a function of current density. Typically, power density increases with increasing current density up to a maximum and then decreases. Ideally, one should operate the fuel cell at a voltage close to the maximum power density.

1.2 Membrane electrode assembly

The heart of the fuel cell is generally considered to be the membrane electrode assembly (MEA). The MEA consists of a proton exchange membrane (PEM) bonded to two electrodes (Fig. 1-2).[1, 15]

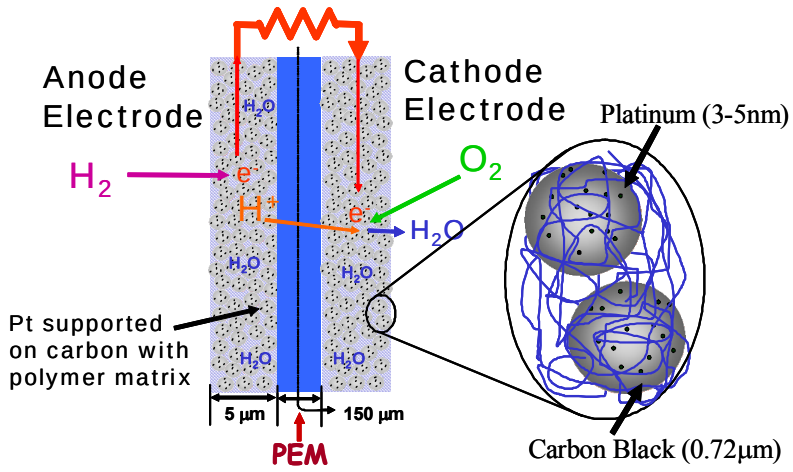

Figure 1-2 Membrane electrode assembly. Reprinted with permission.[15] Copyright 2004 American Chemical Society

The electrodes are carbon supported platinum particles dispersed in a polymer matrix. The first step in making an MEA is preparing a Nafion® Pt dispersion or an "ink," which is painted onto decals to obtain ~0.2–0.4 mg/cm^2 of Pt loadings. The decals are then hot pressed onto the PEM to form the MEA.[16] This process is schematically represented in Figure (1-3).

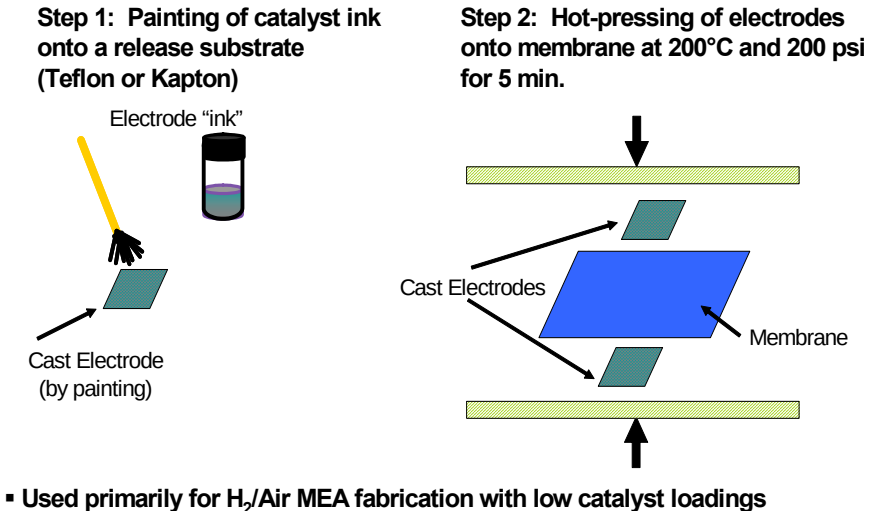

Figure 1-3 Schematic diagram of H_2 / Air MEA fabrication technique

One of the most important objectives in MEA fabrication is to achieve a good bond between the electrodes and the membrane. The MEA bonding region represents the area wherein the flow of the polymer can facilitate good adhesion with the electrodes. Therefore, it is apparent that the parameters controlling polymer flow are critical in optimizing the processing temperature. The MEA bonding temperature has been determined to be close to the hydrated glass transition temperature of the polymer, as illustrated by Figure (1-4).

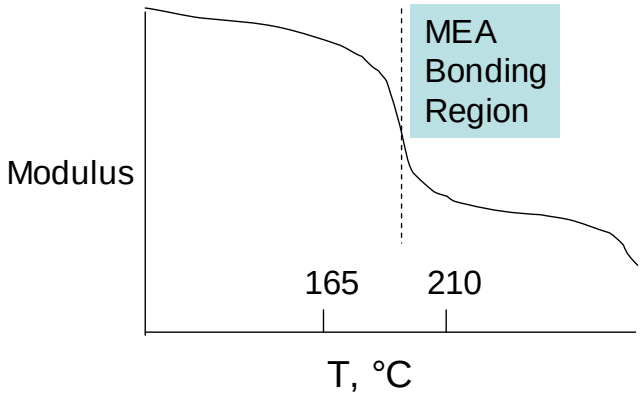

Figure 1-4 Modulus vs. temperature

1.3 Proton exchange membranes

Over the last century, substantial research has been conducted in developing new proton exchange membranes.[15, 17-21 22] These membranes can be broadly classified into fluorinated and non-fluorinated, and hydrocarbon membranes. A significant difference in the morphology and transport processes between these two types has been observed. This review will address this issue, which will include a discussion of the chemical structure and synthesis of these materials.

1.3.1 Fluorinated membranes

Nafion®, which has long been considered the state-of-the-art material for proton exchange membranes, is commercially produced by DuPont and has a polyperfluoroacid structure as shown in Figure (1-5).[23] Nafion® is synthesized by free radical polymerization and is extruded in the sulfonyl fluoride form. It is then hydrolyzed and acidified to convert it to the membrane form. Typically, about 13 mole% of the vinyl ether monomer containing the pendent sulfonyl group is employed to achieve an optimized equivalent weight of 1100 (meq of sulfonic acid/ g of the dry polymer). Commercially, Nafion® is available by their trade names Nafion®117, 115 and 112. In the case of Nafion®117, the first two numbers represent 1100 equivalent weight, while the 7 represents the thickness in mils.

Similar to Nafion®, other perfluorosulfonate membranes have been developed by the Asahi Chemical Company and the Asahi Glass Company.[3] Dow Chemical developed a similar perfluorosulfonate material, but with shorter side chains as compared to Nafion®.[24]

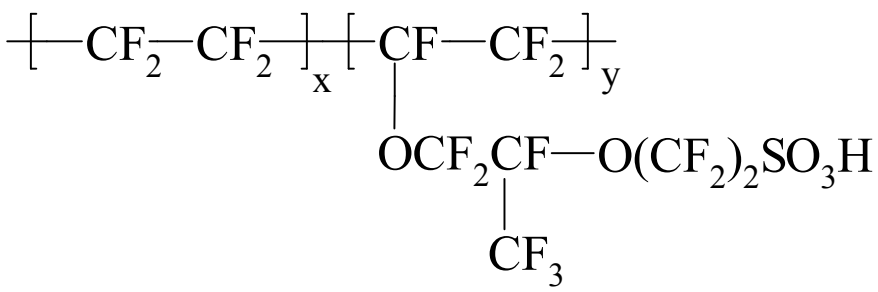

Figure 1-5 Chemical structure of Nafion®[23]

1.3.2 Non-fluorinated membranes

Although the Nafion® and Dow membranes have shown excellent fuel cell properties, a major drawback of fluorinated materials is cost. Moreover, recent research has indicated the need for electrochemically and mechanically stable membranes capable of operating under low humidity and high temperature conditions. These factors have all prompted the need for developing alternative proton exchange membranes.

1.3.3 Poly(arylene ether)s

Poly(arylene ether)s are considered promising candidates for proton exchange membranes due to their excellent chemical and thermal stability under fuel cell operating conditions. The general chemical structure is given in Figure (1-6), where X and Y represent various functional groups. By varying the chemical functional group one can control the structure-property relationships of these polymers.[25] The most common poly(arylene ether)s are poly(arylene ether sulfone)s and ketones. The aromatic ether unit provides flexibility, whereas the sulfone or ketone functional groups provide oxidative stability.

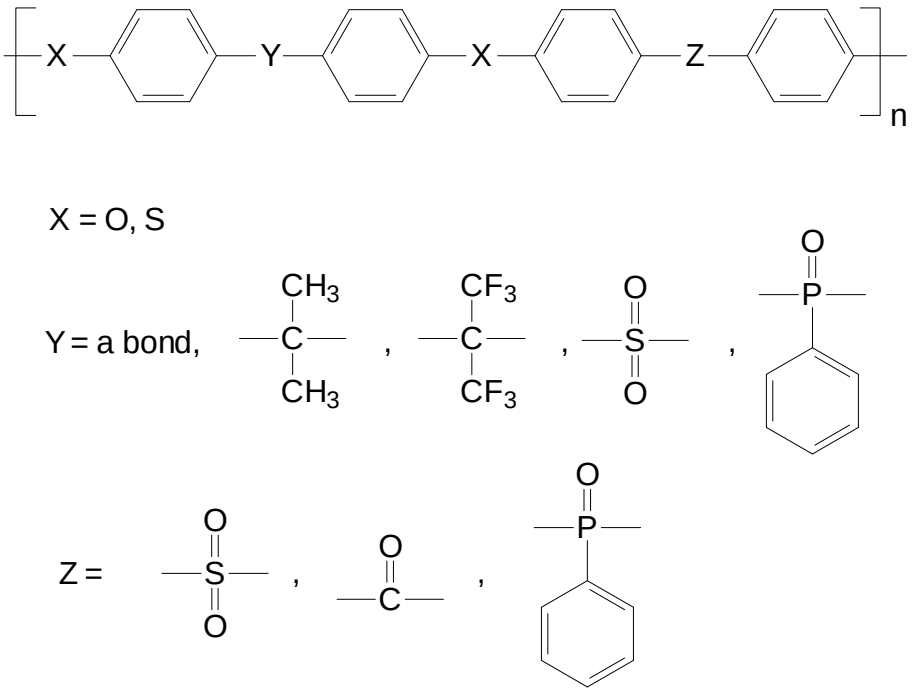

Figure 1-6 General structure of poly(arylene ether)s. Reprinted with permission.[15] Copyright 2004 American Chemical Society

The copolymers were converted into ion containing proton exchange membranes by introducing sulfonic acid groups into the backbone.[26] Sulfonation can be done either by post sulfonation or by direct sulfonation, and each method has both advantages and disadvantages.[26]

1.3.3.1 Post sulfonation method

The most common technique for the post sulfonation of these materials utilizes sulfuric or chlorosulfuric acid. Because the mechanism for post sulfonation follows electrophilic aromatic substitution on the activated ortho position of the aromatic ring,[27] the resulting materials are not considered to be very stable.[28] Post sulfonation by various sulfonating agents also results in chemical degradation of the backbone and lack of precise control of the degree of disulfonation. These drawbacks can be overcome by using mild sulfonating agents, such as

trimethylsilyl-chlorosulfonate, as reported by Genova-Demitrova.[29] However, the disadvantages of using mild sulfonating reagents are lower reaction rates and lower efficiencies of sulfonation.

Among the poly(arylene ether)s, the poly(arylene ether ketone)s (PEEK) have been the most widely studied. Poly(arylene ether ketone)s are semicrystalline thermoplastic polymers with enhanced oxidative and hydrolytic stability.[15, 17, 19] They are commercially available in different chemical structures, as shown in Figure (1-7), with the most common one being Victrex PEEK. Sulfonation can be carried out using concentrated sulfuric acid with up to one sulfonic acid group per repeat unit. The sulfonation rate can be controlled by reaction time, temperature, and acid concentration.[30, 31]

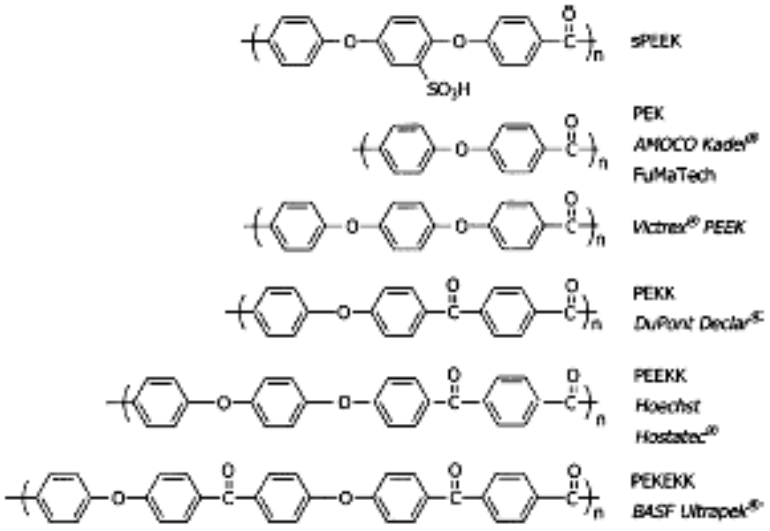

Figure 1-7 Chemical structures of commercially available PEEKs. Reprinted with permission.[17] Copyright 2003 Annual Review of Materials Research

1.3.3.2 Direct sulfonation methods

A major drawback of the post sulfonated system is the lack of control over the reproducibility of the degree and location of sulfonation and on the thermal stability of the polymers. This is a critical disadvantage given the fact that good control over the position, number and distribution of sulfonic acid groups will lead to better tailoring of the microstructures

and, hence, performance properties. To obtain comparable higher proton conductivity, one has to move towards higher degrees of sulfonation, which is also unfortunately associated with higher degrees of water swelling and poor mechanical properties. In contrast, the monomer sulfonation method results in the placement of two sulfonic groups per repeat unit at a deactivated position on the aromatic ring. The difference between the sulfonic acid placements in the two methods is shown in Figure (1-8). Hence, one might expect higher acidity, better thermal stability and better control over the microstructure of the ionomer. And, indeed, reasonable proton conductivities can be achieved with modest levels of disulfonation.

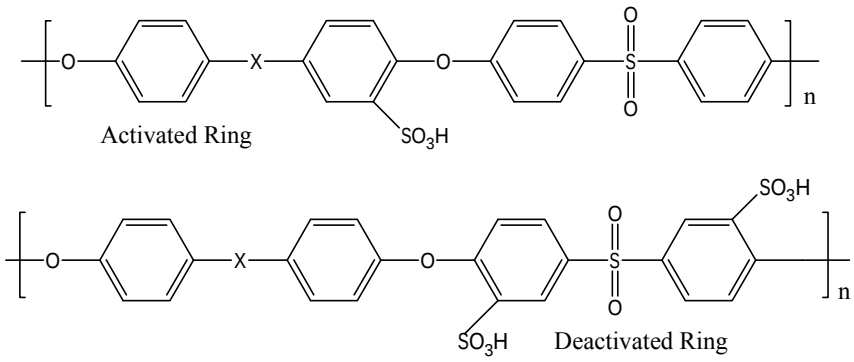

Figure 1-8 Placement of the sulfonic acid group in post sulfonation (activated ring) vs. direct copolymerization of a disulfonated monomer (deactivated ring). Reprinted with permission.[15] Copyright 2004 American Chemical Society

1.3.3.3 Synthesis of the monomer

Robeson and Matzner first reported the sulfonated monomer, for use in a flame retardant material.[32] Recently, McGrath et al. refined the sulfonation technique, as shown in Figure (1-9).[33] The direct copolymerization of disulfonated poly(arylene ether sulfone)s was carried out by an aromatic nucleophilic substitution reaction.[34, 35]

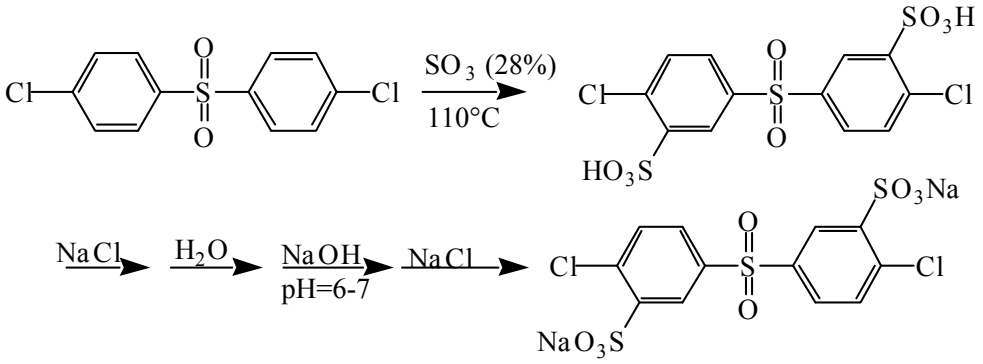

Figure 1-9 Synthetic route for SDCDPS Reprinted with permission.[15] Copyright 2004 American Chemical Society

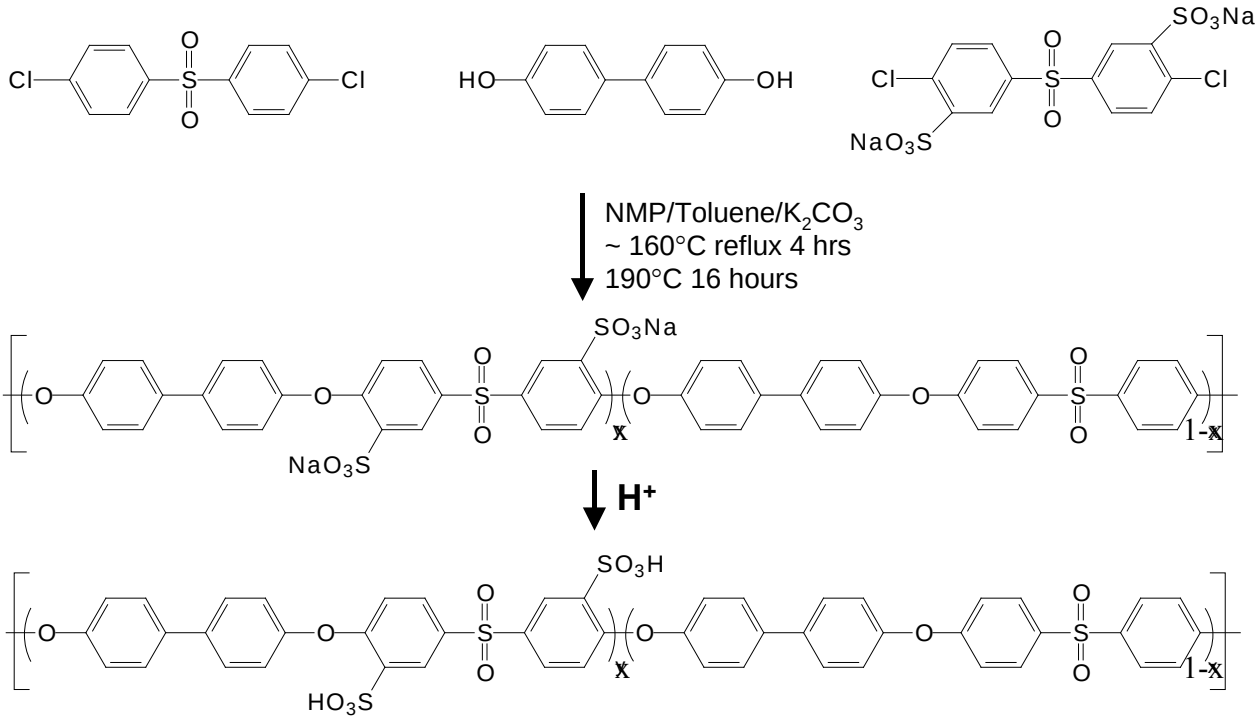

Figure 1-10 Synthetic route for BPSH-xx copolymer Reprinted with permission.[15] Copyright 2004 American Chemical Society

The acronym for the material is BPSH–xx, where BP stands for biphenol, S for sulfonation, H for the acidified form of the membrane, and xx for the degree of disulfonation.[15, 36] The influence of the bisphenol structure on resulting properties was studied by varying the bisphenol structure from hydroquinone, hexafluoroisopropylidene bisphenol (6F), 4,4`-biphenol to bisphenol A.[37-42] The functional groups were also varied to synthesize poly(arylene ether ketone)s[43] and poly(arylene thioether sulfone)s.[44] All of the copolymers showed similar properties and the electrochemical properties corresponded well with the ion exchange capacities.

The 6F materials showed distinct advantages over the Nafion® benchmark materials in a number of fuel cell tests. For example, Kim et al. reported 3000 h stability in DMFC fuel cell conditions (Fig. 1-11).[45] Similar water swelling values between the electrode and the PEMs and chemical similarity with Nafion® electrodes were observed, which are considered to be key factors. Moreover, the BPSH 35 copolymer has demonstrated excellent oxidative stability as shown in the Open Circuit Voltage (OCV) test,[46] which was conducted at 100 ^{o}C under an H_2 / O_2 environment at 25 % RH. In fact, BPSH outperformed the Nafion® benchmark material in this test and was stable up to 300 h. This inherent stability was attributed to the extremely low oxygen permeability (10x lower than Nafion®). Thermal properties were also characterized by dynamic mechanical analysis (DMA) and differential scanning calorimetry (DSC).[47]

Similar to the BPSH systems, novel poly(arylene ether benzonitrile) copolymers were synthesized.[48] For DMFC applications, this particular copolymer with a 35% degree of disulfonation showed very good performance—namely, a 50% increase in selectivity and at 0.5 V, a current density of 200 mA/cm^2.[49] The DMFC performance curve compared favorably with Nafion® and BPSH-40 as shown in Figure (1-12).

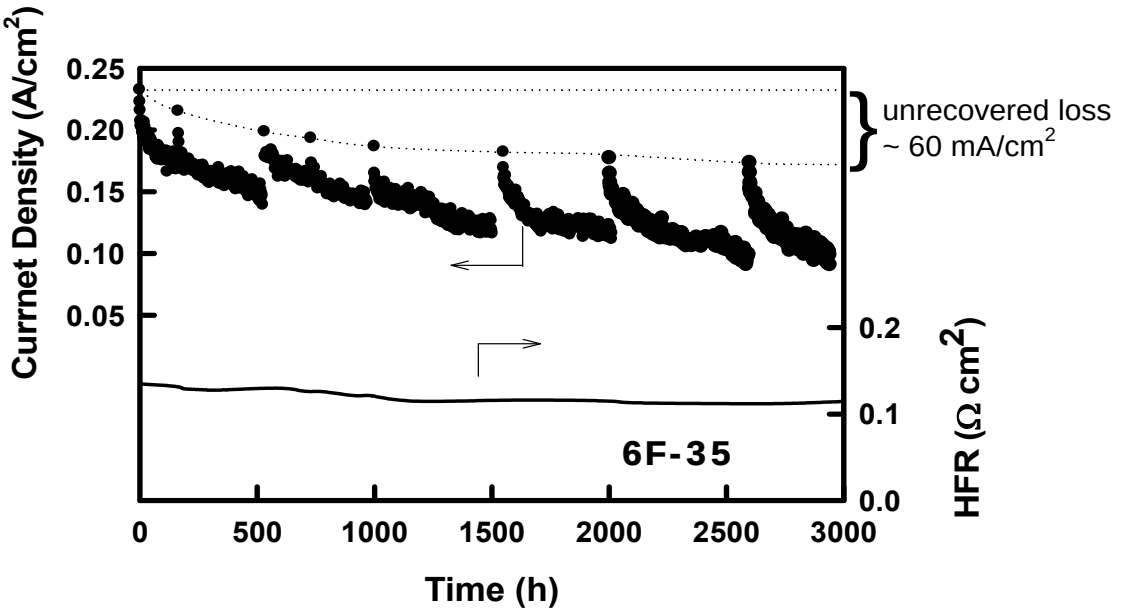

Figure 1-11 3000 h stability for 6F 35 under DMFC conditions at 80 °C

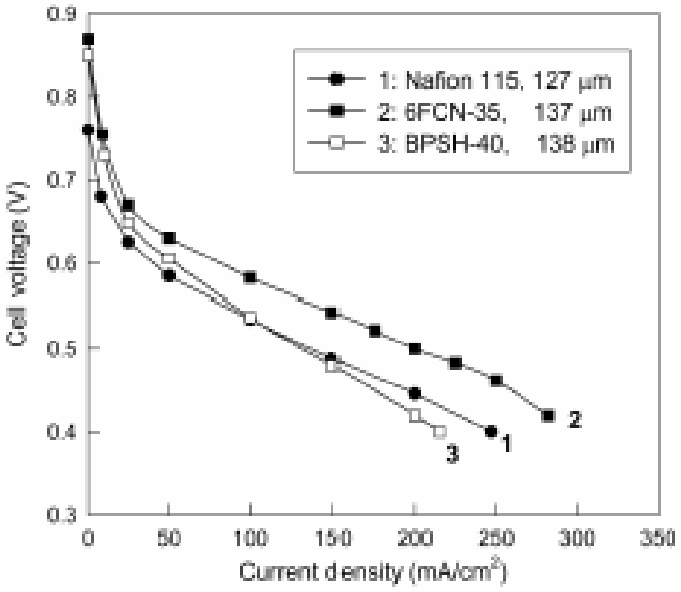

Figure 1-12 DMFC fuel cell performance curve for 6FCN 35, BPSH 40 and Nafion® 117. Reprinted with permission.[49] Copyright [2004], The Electrochemical Society

1.4 Morphology of PEMs

Ion containing polymeric materials are known to have very complex morphologies.[50-52] All the electrochemical properties of proton exchange membranes are strongly dependent on the morphology of the copolymer.[53-55] For example, the sulfonic acid containing copolymers phase separate to form hydrophilic and hydrophobic domains. Under hydrated conditions, these hydrophilic domains play an important role in the transport process. The morphology of sulfonated copolymers is influenced by many factors such as chemical composition, distribution of the sulfonic acid groups, selection of casting solvent, and the hydrothermal history.[56-58] The morphology can be studied by various experimental techniques, including small angle X-ray scattering,[59, 60] neutron scattering,[60, 61] transmission electron microscopy (TEM),[62] atomic force microscopy (AFM)[63] and NMR relaxation and diffusion experiments.[64 65]

As noted earlier, the most studied material in the literature is the perfluorinated sulfonic acid containing membrane, Nafion®. "Nafion® is considered to have a random chemical structure that is capable of organizing the complex formation of ionic and crystalline domains with a significant distribution in dimensions over a wide range of length scales."[54] Gierke and co workers were the first to propose the cluster-network model using SAXS and wide angle X-ray diffraction.[59, 66-69] They studied both the hydrolyzed and unhydrolyzed forms of Nafion®. They observed a low angle SAXS minimum around 0.5^{o} 2θ and diffraction peak at 18^{o} 2θ for the unhydrolyzed sample. The peak increased with increasing equivalent weights of the PTFE segments and was assigned to the crystalline organization within the fluorocarbon matrix. An additional peak at 1.6^{o} 2θ was observed for the hydrolyzed sample and was assigned to the ionic clusters. This peak increased with decreasing equivalent weights and increasing water content. Under hydrated conditions, the ionic clusters were proposed to be spherical in shape with an inverted micelle structure, as reported.[69] The transport processes were assumed to be controlled by the cluster network or the "channels," while the PTFE units provided mechanical support. In contrast to the cluster-network model, Fujimura et al.[70] proposed an interparticle core-shell model. In this model, an ion rich core is believed to be surrounded by an ion poor shell composed of PTFE units.

The structural evolution of Nafion® from the dry state to the hydrated state was extensively studied by Gebel using small angle scattering techniques.[71] A conceptual model depicting the swelling and dissolution processes was developed, which is shown in Figure (1-13).[71]

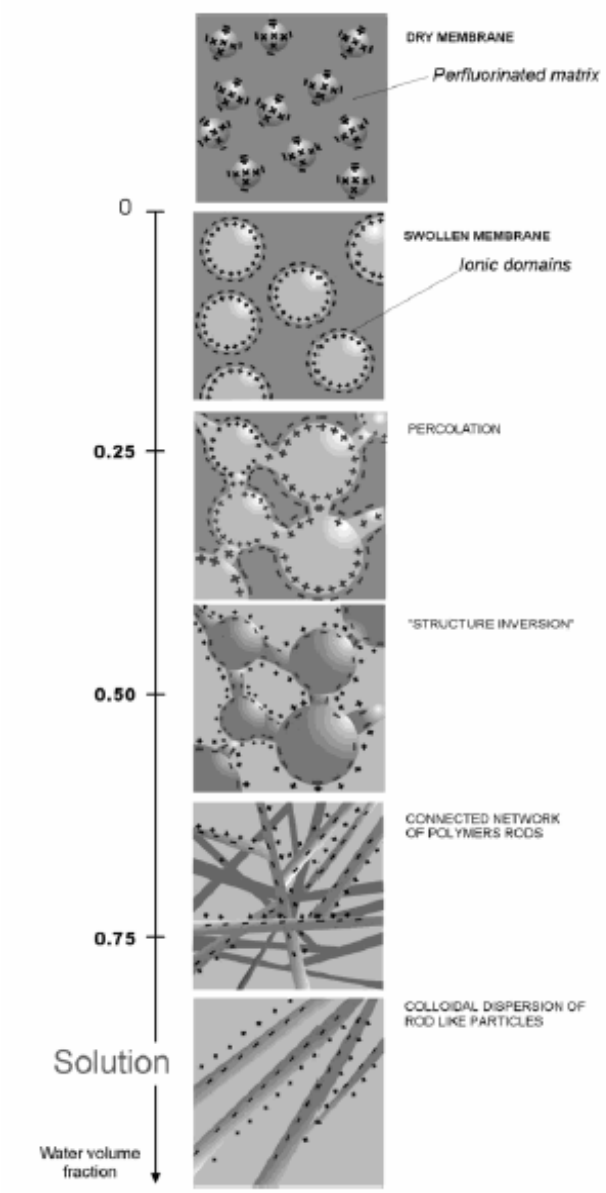

Figure 1-13 Conceptual model for morphology of dry and swollen Nafion®. Reprinted from [71] with permission from Elsevier

As shown, the dry membrane is thought to contain isolated, spherical ionic clusters with diameters of ~ 1.5 nm. With increasing water content, these clusters swell and at water activities of 0.3 to 0.5, structural reorganization takes place to form a percolated well connected network. However, with increasing water uptake an inversion of structure is thought to take place with the evolution of rod-like morphology. At a higher water uptake, the membrane dissolves and the morphology resembles an isolated colloidal of rods.

In recent years, substantial research has been conducted on characterizing Nafion® morphology by microscopic techniques. Xue et al.[62] reported the presence of a three phase morphology in solution cast Nafion® 117 using TEM studies. Spherical clusters in the diameter range of 25-50^{o} A were found to be surrounded by an interphase and dispersed in a hydrophobic fluorocarbon matrix.

McLean et al.[63] studied the near surface morphology of the ionic domains in Nafion® membranes using various AFM techniques (Fig.1-14). For example, sequential AFM imaging proved that the softer fluorocarbon regions contained spherical ionic domains in the same topographical areas, while tapping mode AFM was useful in probing the stiffer fluorocarbon aggregates. The results supported the Gierkie model in that spherical ionic domains were related to the inverted micelle structure. AFM was also used to study the hydrated morphology of the Nafion® membranes. Expansions in the ionic clusters were observed with increasing hydration levels, followed by aggregation, to form long structures.

This concept was further expanded by Kreuer in his nanoscopic hydrated model.[72] He compared the morphology of Nafion® and poly(arylene ether ketone)s to understand the influence of microstructures. Specifically, he considered an arrangement of ionic clusters and the water-filled spaces in between. The water acts as a second phase, which help in forming the percolated structure and ensures connectivity between the ionic clusters. Kreuer concluded that Nafion® displayed better connectivity and wider channels when compared to PEEK. These differences were attributed to the presence of more hydrophobic, higher acidic groups, as well as the flexible backbone of Nafion®.

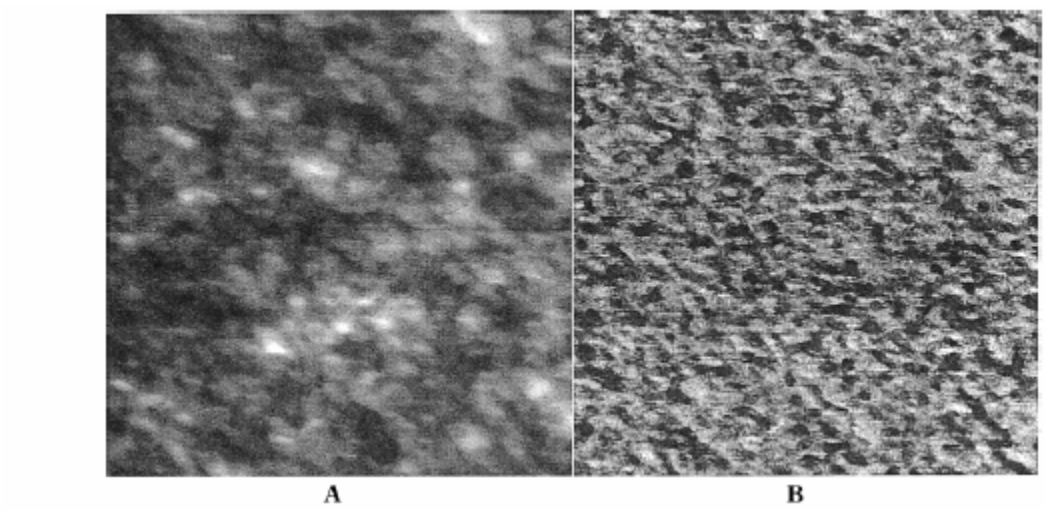

Figure 1-14 AFM images of Nafion® 117 (K^+) form A) height image B) phase image; 300 nm x 300 nm. Reprinted with permission.[63] Copyright 2000 American Chemical Society

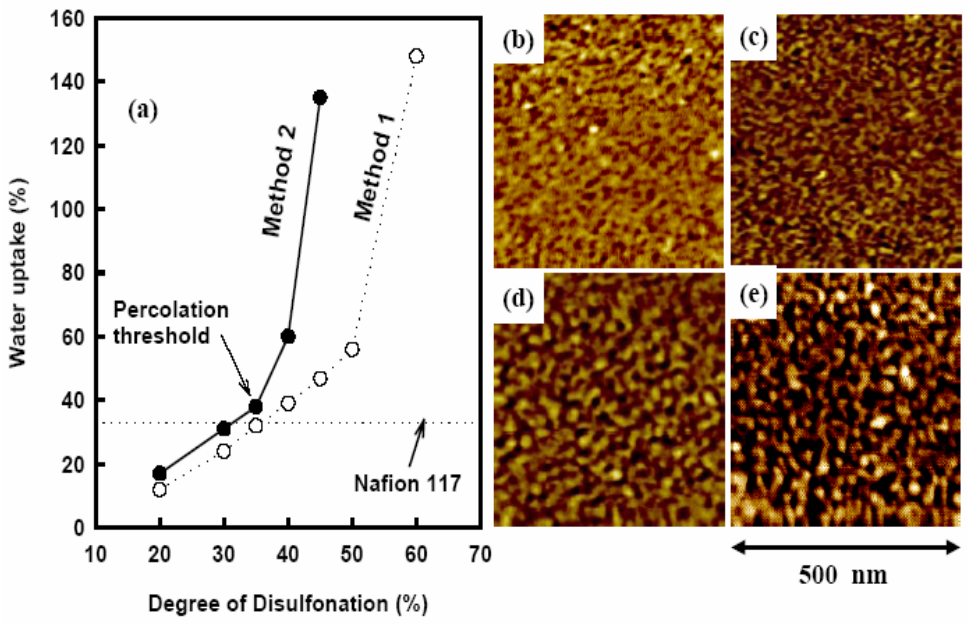

Figure 1-15 Water uptake scales with morphology and degree of disulfonation for BPSH-xx copolymers. Reprinted from[73] with permission from Elsevier

McGrath et al.[73 36] reported the morphological structure of ion containing random non-fluorinated membranes using AFM and DMA techniques. The random copolymers showed a hydrophilic/hydrophobic morphology that depended strongly on the degree of disulfonation. At

low degree of disulfonation, the hydrophilic phase was found to be discontinuous, and the hydrophobic phase was determined to be continuous. Moreover, phase separation increased with increasing degrees of disulfonation. After a particular degree of disulfonation, however, the hydrophilic phase was found to be the continuous or percolated phase. A sudden increase in water uptake was associated with this percolation threshold, as displayed in Figure (1-15).

The importance of the acidification method was also studied. While room temperature acidification yielded a mainly closed morphological structure acidifying under boiling conditions followed by a hydrothermal treatment resulted in a much open network,[36] resulting in higher water and proton transport at a given IEC.

1.5 Proton conductivity

Proton flux for ion containing copolymers can be described by the Nernst Plank equation, as follows[74]

$$-j_p = D_p C_p \left(\frac{\nabla C_p}{C_p} + z_p \frac{F \nabla \psi}{RT} \right) \qquad \textbf{Equation 1-7}$$

where j_p is the proton flux, C_p is the concentration of protons, D_p is the diffusion coefficient of the protons, z_p is the proton charge, Ψ is the electrostatic potential, R is the gas constant, and F is the faraday constant. For a membrane with a constant thickness and a proton charge of +1, the proton flux can be related to proton conductivity (σ).

$$\sigma \propto j_p \propto D_p C_p \qquad \textbf{Equation 1-8}$$

Thus, proton conductivity is a function of both the concentration of the protons and the diffusion coefficients of the protons.

$$\sigma = f(C, D) \qquad \textbf{Equation 1-9}$$

Proton transport in aqueous environments has been studied extensively and can be described by two principal mechanisms.[75-77] The first is the Grotthuss[78] mechanism, wherein protons are transferred down a chain of correlated hydrogen bonds, forming and reforming hydronium cations (H_3O^+). The second mechanism, described by Kreuer[75, 76, 79-81] is known as the vehicle mechanism. It is believed to occur via the bulk diffusion of a proton and its associated water molecules or "vehicle" in an H_3O^+, H_5O^{2+}, or other $H_{2n+1}O^{n+}$ cation species. Hence, the self-diffusion coefficient of water is critical in understanding the transport behavior of protons as shown by both Kreuer et al.[76] and Zawodzinski et al.[82] In fact, both these reports have proved that the vehicle mechanism is dominant at low water contents (or hydration number, λ) where the diffusion coefficients of protons and water are similar; thus, water and protons move in concert.[77] At higher water contents, however, the Grotthuss mechanism dominates proton conduction where the computed diffusion coefficients of protons is higher than that of the measured water self-diffusion coefficients. In other words, protons are moving faster across the membrane than is the water.

The most common method for measuring proton conductivity is by impedance spectroscopy as reported [82] using an Impedance/Gain-Phase Analyzer over the frequency range of 10 Hz - 1 MHz. The cell geometry was chosen to ensure that the membrane resistance dominated the response of the system. The resistance of the film was measured at the frequency which produced the minimum imaginary response.[83] Therefore, the conductivity of a membrane can be calculated from the measured resistance and the geometry of the cell according to Equation (1-10),

$$\sigma = \frac{l}{Z' A} \qquad \textbf{Equation 1-10}$$

where σ is the proton conductivity, l is the length between the electrodes, A is the cross sectional area available for proton transport, and Z' is the real impedance response.

1.6 Self-diffusion coefficient of water

The self-diffusion coefficient of water is a weighted average of the diffusion coefficients of water and protons for separate environments. In a hydrated PEM, ^{1}H nuclei exchange rapidly between the H_2O and H^+ environments. Thus, the diffusion of water within the membrane is not considered to be a one dimensional mass transfer problem. The self-diffusion coefficient of water tends to depend upon the tortuosity and the local morphology of the membranes and is defined by the following Equation (1-11), [84]

$$J_1 = \left[\frac{D_{eff}\, H}{l}\right](C_1 - C_2) \qquad \textbf{Equation 1-11}$$

where J is the flux, H is the partition coefficient (i.e., the concentration of the membrane divided by that in adjacent solution), D_{eff} is the effective diffusion coefficient, and C_1 and C_2 are the concentrations of the components across the length l. One of the most important techniques for measuring the self-diffusion coefficient of water is via pulsed-field gradient spin echo nuclear magnetic resonance (PGSE NMR).[85-92] The standard pulse sequence is given in Figure (1-16).

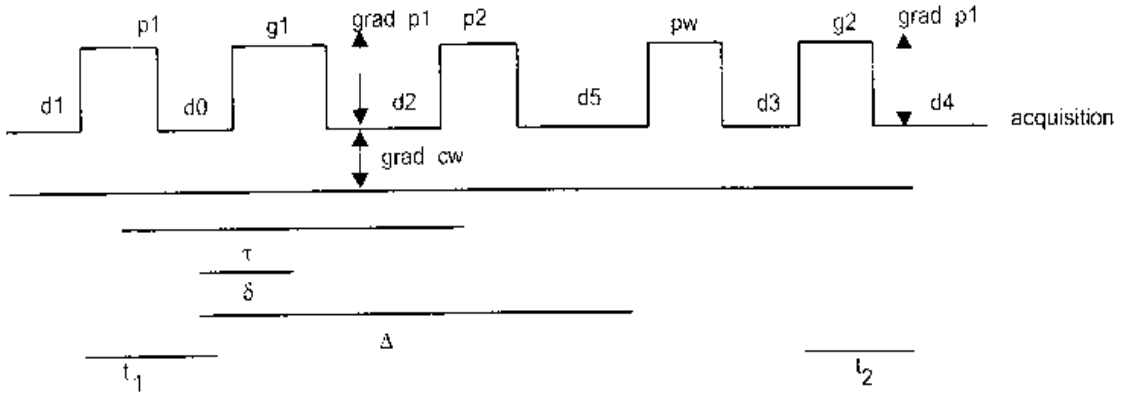

Figure 1-16 Pulse sequence of PGSE NMR

The measurement is obtained by observing the echo signal intensity (A) as a function of the gradient strength (g) (Fig. 1-17). The diffusion coefficient (D) is determined by fitting the data (Fig 18) to the Equation (1-12),[88]

$$A(g) = A(o)\exp[-\gamma^2 D g^2 \delta^2 (\Delta - \delta/3)] \qquad \textbf{Equation 1-12}$$

where, A is the NMR signal intensity as a function of gradient strength, γ is the gyromagnetic ratio (26752 $radG^{-1}s^{-1}$ for protons), δ is length of the gradient pulse, and Δ is the time between gradient pulses.

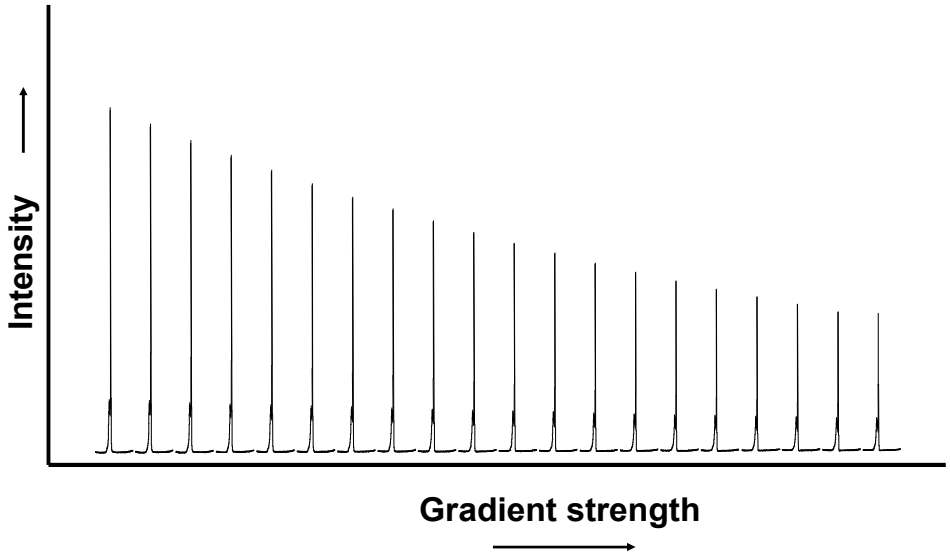

Figure 1-17 Intensity of the water signal as a function of gradient strength in an ideal PGSE experiment

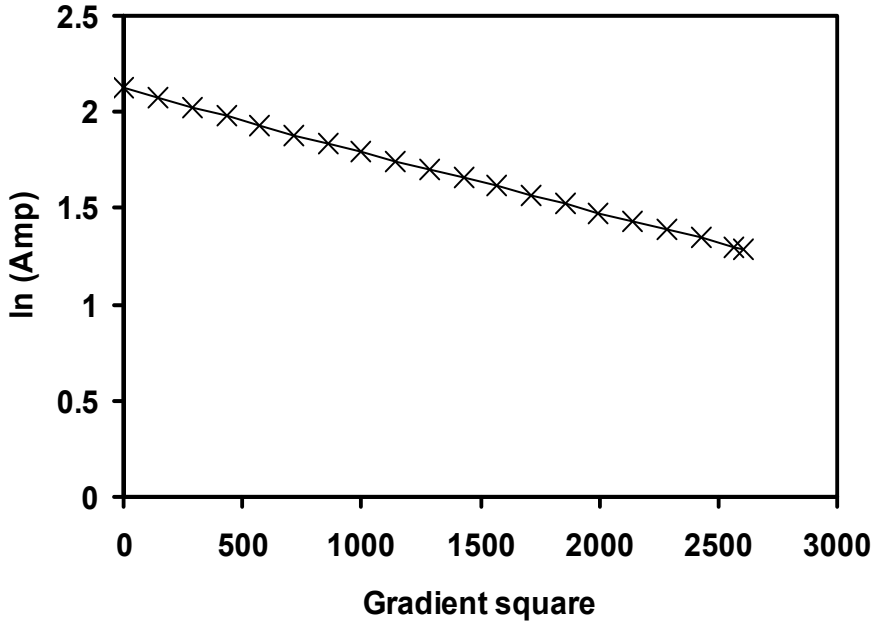

Figure 1-18 Linear curve fitting of the PGSE experimental results

One of the advantages of this method is that the measured diffusion coefficients can be related to the mean square displacement of the water molecule or the effective diffusion length scale[86, 88, 89, 93, 94] because the time (Δ) during which the diffusion measurement is assessed is known. The displacement (Δr) is given by:

$$\langle \Delta r \rangle = \sqrt{2 D_{eff} \Delta} \qquad \textbf{Equation 1-13}$$

for a gradient in one direction. This will provide insight for probing the influence of a restricted morphology on transport properties. The effective diffusion time (and hence the length over which the diffusion coefficient is measured) can be modified by varying the (Δ-δ/3) term in the NMR pulse sequence. Thus, probing the morphology of the interconnected channels between the hydrophilic domains will provide a better understanding of important transport mechanisms. The mathematical interpretation of this phenomenon was reported by Callaghan and coauthors.[95]

Comparative study of proton and water transport for Nafion® and non-fluorinated hydrocarbon PEMs

The proton conductivity of Nafion® has been extensively studied over a long period of time,[21, 76, 80, 81, 96-100] with most researchers in agreement that it tends to depend strongly on the water content of the membrane.[97, 98] Zawodzinski et al.[82] showed (Fig. 1-19) a linear relationship between the water content expressed as moles of water per equivalent of sulfonic acid and proton conductivity. A similar correlation between proton conduction and water content has also been observed for non-fluorinated hydrocarbon based random copolymers. However, the extent of decrease is more pronounced for the random copolymers in comparison to Nafion® as reported for BPSH-xx copolymers. Kim et al. noted that the water uptake and proton conductivity of BPSH-xx was a function of relative humidity (Fig. 1-20).[36] Although BPSH-xx tends to hold more water than Nafion®, particularly under partially hydrated conditions, the proton conductivity shows a reverse trend. It is thought that morphology and/or chemical structure may be critical for proton transport under partially hydrated conditions.

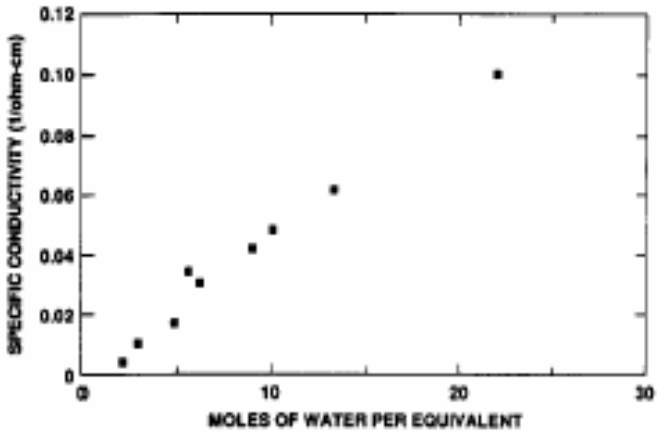

Figure 1-19 Proton conductivity scales with water content in Nafion® 117. Reprinted with permission.[82] Copyright 1991 American Chemical Society

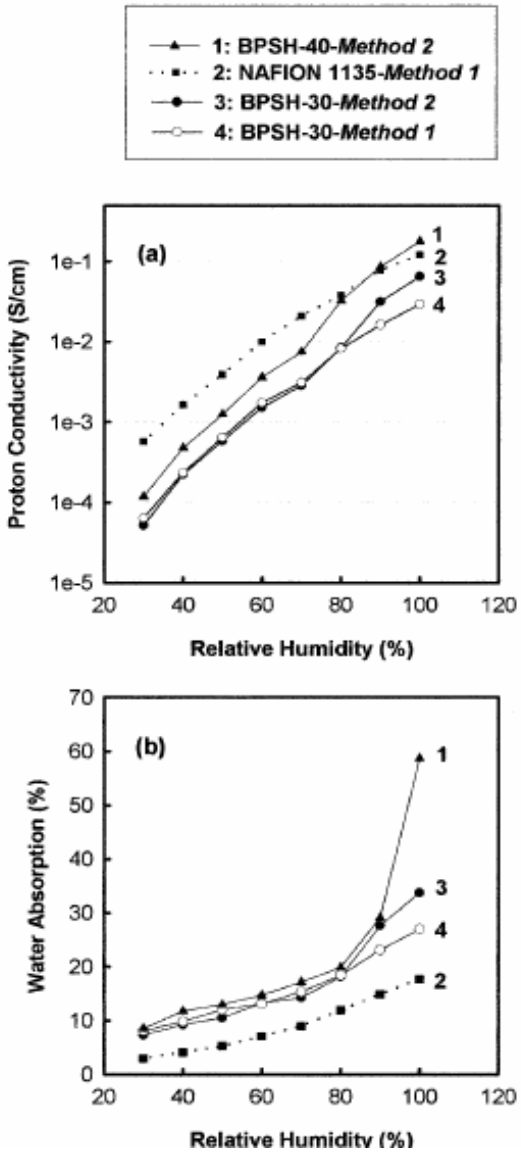

Figure 1-20 Proton conductivity and water uptake for BPSH-xx copolymers as a function of relative humidity. Reprinted with permission from John Wiley & Sons, Inc[36]

The self-diffusion coefficients of water for these random copolymers has been shown to be much lower than Nafion.® For example, Shuster et al. reported the self-diffusion coefficients of water as a function of water content for both poly(ether ketone)s and Nafion®, as shown in Figure (1-21).[101] As this figure depicts, the values tend to decrease significantly for the random

copolymer at lower water content. In fact, at low hydration levels most of the water is tightly associated with the sulfonic groups for the random copolymers, as evidenced by the low diffusion coefficient. This encourages the formation of isolated domain morphology over the percolated morphology. Thus, although there may be significant concentrations of protons, transport is limited by the discontinuous morphological structure. Under fully hydrated condition, water assisted percolated transport pathway develops.

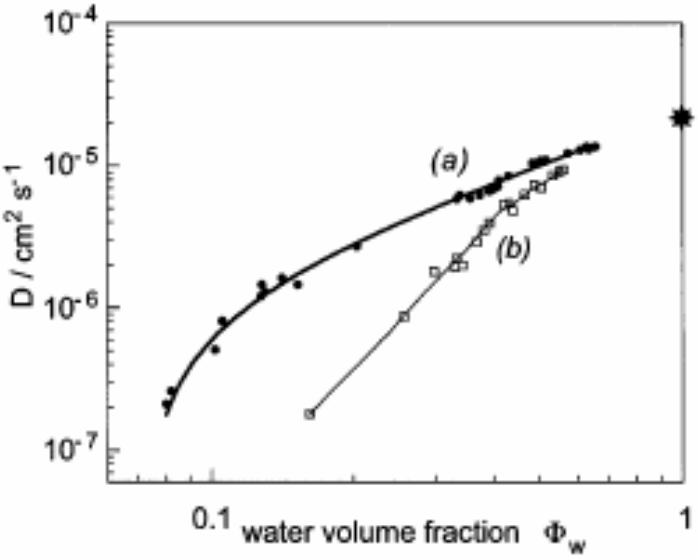

Figure 1-21 Self-diffusion coefficient of water as a function of water content for (a) Nafion® and (b) sulfonated PEEK. Reprinted with permission.[17] Copyright 2003 Annual Review of Materials Research

It is also understood that proton conductivity is strongly associated with both water content and ion exchange capacity (IEC). As has been documented, for BPSH-xx and all other random copolymers, proton conductivities and the self-diffusion coefficients of water increase linearly with ion exchange capacity and water uptake.[34, 36, 87]

Both proton conductivity and the self-diffusion coefficient of water depend strongly on temperature over a wide range of water contents. However, the activation energy for transport is a function of the molecular mobility and chemical structure of the copolymers. Alberty et al. studied the proton conductivity of Nafion® over a wide range of temperatures and relative

humidities.[18] As they documented, an irreversible decay in proton conductivity occurred after a specific temperature was reached.[102]

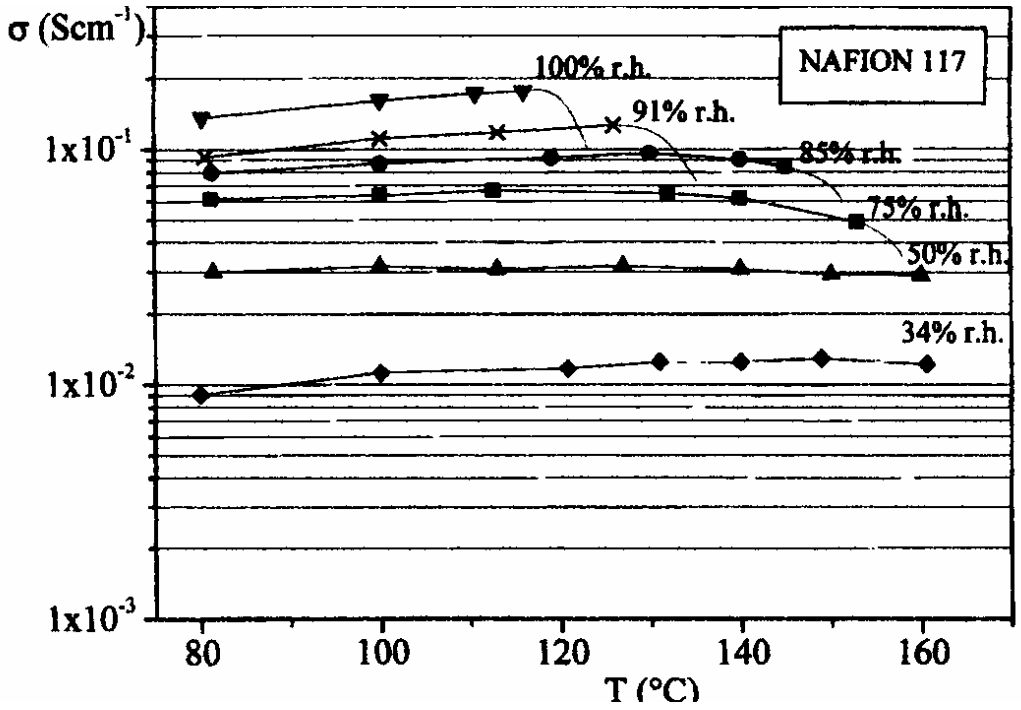

Figure 1-22 Proton conductivity as a function of temperature and relative humidity for Nafion®. Reprinted from [102] with permission from Elsevier

As shown in Figure 1-22, the upper limit temperature was found to strongly depend on relative humidity. It was also observed to increase with decreasing relative humidity. A similar observation was also reported by McGrath et al. for the BPSH copolymers.[103] However, the threshold temperature was found to be higher than for Nafion®.

Several explanations have been suggested for this phenomenon. Initially, it was thought to result from the loss of water or because of the chemical degradation of Nafion®. However, the increase in the upper threshold temperature at lower relative humidity overruled those arguments. McGrath et al. related threshold temperature to hydrated glass transition temperature.[103] Water is known to act as a plasticizer, which lowers the glass transition

temperature of an ion containing copolymer. Hence, when a membrane passes through its hydrated glass transition temperature it undergoes morphological relaxations that disrupt proton transport. Moore et al. refined this concept with elegant NMR relaxations and DMA measurements.[56] They reported the presence of α and β relaxations in Nafion®. The β relaxation was related to molecular chain mobility. Hydrated Nafion® was actually found to have a β relaxation temperature lower than room temperature. This also explains the higher proton conductivity of Nafion®. The α relaxation is related to the complete disruption of the ionic domains. The temperature at which Nafion® undergoes an irreversible change in proton conductivity can be related to the hydrated α relaxation temperature. Under partially hydrated conditions, the hydrated α relaxation temperature increases, which corresponds to the increasing upper threshold temperature.

1.7 Electro-osmotic drag

Under the influence of an electric field, ions are transported across a membrane along with a solvent, which is a phenomenon known as electro-osmosis. The electro-osmotic drag coefficient is defined as the number of water molecules transported per proton. This transport parameter is important in understanding the water management issues of a fuel cell. Protons, along with water, are transported across a membrane from anode to cathode. A high electro-osmotic coefficient results in the depletion of water at the anode side, while flooding occurs at the cathode side—particularly at high current densities. Depletion of water at the anode affects the hydration state of a membrane and increases ohmic loss. High water content at the cathode leads to mass transport problems and reduces the overall fuel cell performance. In their review, Pivovar et al. described the various experimental techniques for determining the electro-osmotic drag coefficient.[104] The electro-osmotic drag cell, membrane electrode assembly cells,[105] activity gradient method[106] and recently electrophoretic NMR [107] are the notable ones. Chemical structure and morphology both play important roles in governing the electro-osmotic drag coefficient, which increases with increasing water content in a polymer.[108-110] For Nafion® the value ranges from 3.3-3.9 at room temperature.[105] Electro-osmotic drag typically occurs in temperatures ranging from 2.0 (15 ^{o}C) to 5.1 (130 ^{o}C).[105] Compared to Nafion®, hydrocarbon membranes have much lower electro-osmotic drag coefficients. For the 6FCN 35 material, for

example, the value is around 1.3, which may explain its higher MEA selectivity in DMFC fuel cells.[49] It has also been shown that values increase with the temperature and ion exchange capacities of the copolymers.[111]

1.8 Methanol permeability

Methanol permeability is a critical transport property of a proton exchange membrane, especially for use in liquid-fed direct methanol fuel cells.[12, 112, 113] Methanol that is unoxidized at the anode can "cross over" through the membrane and be oxidized at the cathode.[114-116] This methanol "short circuit" decreases the fuel efficiency of the system, lowers the cell voltage by causing a mixed potential at the cathode, and increases cell heating. In general, the methanol crossover through the membrane in an MEA scales with the feed concentration of methanol. This is why most active DMFC systems are supplied with very low (e.g. 0.5 M) methanol feed concentrations.[14] Creating low crossover membranes that are relatively impermeable to methanol may be a strategy for increasing the feed concentration in DMFC systems without sacrificing cell performance. Increasing the fuel feed concentration would be desirable with respect to both system energy density and system complexity. Many novel PEMs have low methanol permeability, but their proton conductivity tends to decrease as well. An ideal membrane would be one with low crossover and high conductivity, which could still maintain the ability to form robust junctions at the membrane-electrode interface.

There are two common methods for measuring the methanol permeability of PEMs. The first involves a membrane separated cell,[117] and the second determines open circuit electrochemical crossover measurements in a DMFC.[118] It should also be noted that the methanol permeability of a membrane tends to track with electro-osmotic drag, which provides insight into the domain structure of the membrane.

One of the major disadvantages of Nafion® is its higher methanol permeability, which is related to its open morphological structure.[119, 120] In contrast, the aromatic hydrocarbon based materials display much lower methanol permeability. For random copolymers, methanol permeability has been found to decrease with decreasing ion exchange capacities. However,

proton conductivity is a linear function of ion exchange capacity under fully hydrated conditions. Polyimide based PEMs synthesized by the McGrath group are reported to have very low methanol permeabilities and high proton conductivities.[121, 122] However the hydrolytic stability of these copolymers was not as good compared to the poly(arylene ether)s. Post or directly sulfonated poly(arylene ether)s are reported to have much lower methanol permeabilities. However, the selectivity of the post sulfonated materials is much lower. Directly polymerized BPSH and 6FCN based poly(arylene ether sulfone)s are reported to have 3~4 times higher selectivity than Nafion®.[37, 49, 73]

1.9 States of water

For a PEMFC, membrane hydration is critical to fuel cell performance because it influences proton conductivity, methanol permeability, and electro-osmotic drag. However, the degree of water absorption on a weight basis does not correlate well with these variables, especially when comparing the different copolymer systems. Our group recently proposed that the state of water, as assessed when confined within the membrane, plays a more significant role in determining the membrane transport properties than previously suggested.[103] There are at least three states of water associated with the hydrophilic phases of a polymer,[65, 103, 123-128] and the presence of these thee states can be defined by thermal properties. *Non-freezing bound water* is strongly associated with the polymer and depresses its T_g, but the water shows no melting endotherm as determined by DSC. *Freezable bound water* is weakly bound to the polymer (or weakly bound to the non-freezing water), and displays a broad melting behavior at around 0 °C. *Free water* exhibits a sharp melting point at 0 °C.

A model for three states of water in hydrogels was first proposed by Jhon and Andrade more than 30 years ago.[129] They classified the states of water based on the type of interactions between the water and the polymer. If water interacts strongly with functional groups present in the polymer it is termed “bound.” “Loosely bound” refers to water molecules that display weaker interactions with polymer chains, while “free” water is thought to have insignificant or no interactions with a polymer.

The variations in water-polymer interactions play a major role in the distribution of the different types of water. The effect of binding sites on water-polymer interactions in polymers was studied by Rowland and Kuntz.[130, 131] They reported that interactions were found to decrease in the following order, ion-ion > water-ion>water-polar= polar-polar=water-water> water-hydrophobic. Similar water-polymer interactions are known to occur in other hydrated polymers as well. For example, water-polymer interactions were studied for hydrazine and hydrazine hydrate in ethyl cellulose membranes.[132] The binding capacity, i.e., the interactions of the hydrazine with the functional groups in the polymer, was found to be much higher than water. The nature of water-polymer interactions in synthetic polymers is mainly a hydrogen bonding type. Polymers with amide, carboxyl, ester and ionic clusters are found to hydrogen bond with water, resulting in the distribution of different types of water in the membrane.

The states of water for hydrophilic polymers have been characterized by various methods, such as DSC and NMR relaxation measurements.[94, 103, 128, 133-136] In the case of frozen hydrogels, Hodge et al.[127] observed the presence of two endothermic peaks using slow heating DSC experimentation. The sharp peak corresponds to the melting point of ice (273) K and a broader one below at 10-40 K. In the case of pHEMA hydrogels, Roodra et al. reported an alternative explanation for the two peaks. They believed that the two endothermic peaks are actually one peak separated by an exothermic peak, which is attributed to the crystallization of the amorphous ice.[137]

Previous work has shown that DSC thermograms are a function of the water content in a polymer, showing the melting endotherms of both loosely bound and free water. It is also believed that at low hydration levels, only tightly bound water is associated with a polymer. With an increase in the hydration level, loosely bound water is manifested first, followed by free water. Tightly bound water can be correlated to the maximum amount of water for which there is no melting endotherm.[65, 127] However, it is very difficult to separate the two melting endotherms of free and loosely bound water; thus, quantifying the states of water would be ineffective. Quinn et al.[128, 134, 138] have proposed a better mathematical technique to estimate the distribution of each type of water. They showed that when the integrated change in enthalpy (per gram of dry polymer) from a DSC thermogram is plotted against water content, the intercept

identifies the tightly bound water. By subtracting the tightly bound water from the total water, the combined content of the loosely bound water and free water can be obtained.

Yoshida et al. studied the different states of water from Nafion® samples in a Li^+, Na^+, K^+, NH_4^+ and alkylammonium counterion form using DSC.[139] The presence of an exothermic peak was observed during the cooling cycle. The peak width decreased with in the order of the counterion, while the magnitude of the peaks increased with increasing water content. These peaks were assigned as a result of the crystallization of water inside the membrane. In addition, the presence of a single endothermic peak was observed for the heating curves, which broadened and shifted to a lower temperature with decreasing water content. A similar study was also conducted using ethanol instead of water.[140]

NMR relaxation (T_2) experiments[94, 135, 141, 142] have provided improved quantification of the three states of water as reported by Whittaker et al.[94] They showed that for a hydrophilic polymer with three states of water, the decay in transverse relaxation magnetization of water can be modeled to a tri- exponential function. The shortest component of the decay with the fastest relaxation time corresponds to the tightly bound water having the shortest diffusive path length. The intermediate component represents the loosely bound water, while the long component of T_2 corresponds to the bulk or free water. The relative fractions of the coefficients of the exponential terms are proportional to the respective types of water, allowing quantification of each.

The presence of different states of water and an investigation of molecular mobility was undertaken by Boyle et al. using NMR techniques.[143-146] ^1H, ^2H, and ^{19}F NMR analysis was reported by McMillan et al.[147, 148] with respect to low temperature molecular dynamics. A change in the slope of the relaxation times was observed as a function of temperature.

The three states of water have been explored in proton exchange membranes using DSC by Kim et al.[103] A comparison of a series of DSC scans for two different membrane samples at various levels of water content is shown in Figure (1-23).[103] At low water contents, up to 3.9 weight % for Nafion® 117 and up to 20.1 weight % for BPSH 40 were observed. These scans show no indication of thermal transitions occurring around 0 °C. At low water contents, the only observable feature associated with the strongly bound water in the polymer was a depression in

the glass transition temperature (T_g), as indicated by a short vertical dash. Thermal transitions of freezable bound water (broad peaks) were observed at 11.7 weight % and 24.0 weight % for Nafion® 117 and BPSH 40, respectively.

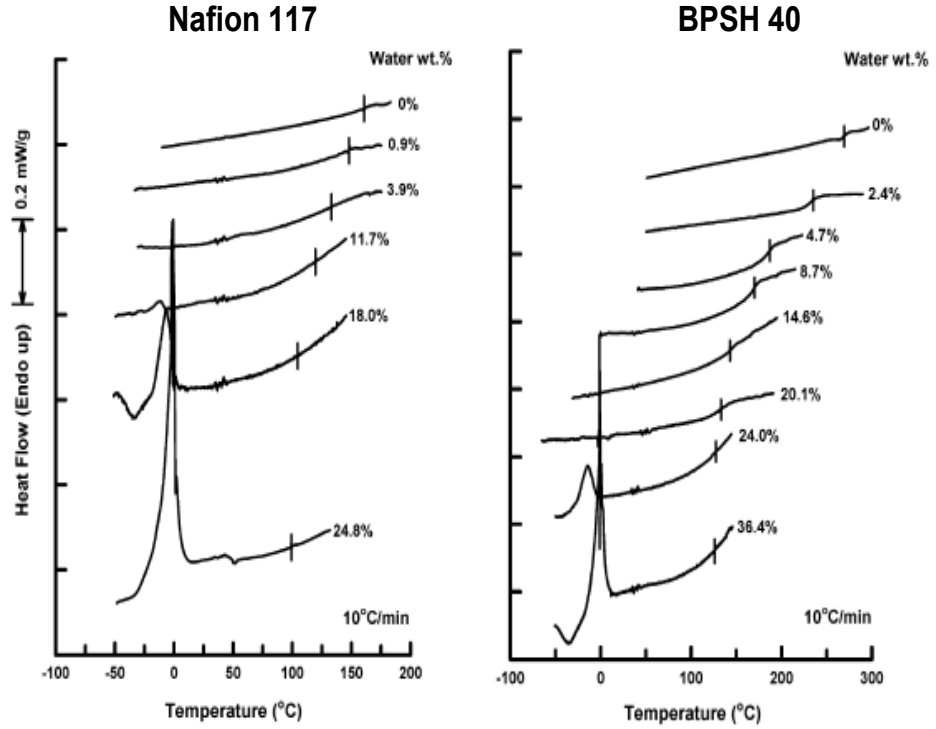

Figure 1-23 DSC comparison of Nafion® 117 and BPSH 40 at various water contents showing the difference in the state of water for each membrane. Reprinted with permission.[103] Copyright 2003 American Chemical Society

In addition, evidence of bulk-like, free water (sharp peak) was observed in the DSC scans for Nafion® at 24.8 weight % and for BPSH 40 at 36.4 weight %. In comparing the two membrane samples and their thermal transition behaviors when hydrated, it is evident that the water contained within each sample behaves differently. Specifically, the water contained in the nano-phase structure of Nafion® is not as tightly bound as the water in the BPSH 40 structure.

The state of water in sulfonated copolymers clearly has a critical influence on the electro-chemical properties of the membranes, which is very important for PEM fuel cells. For example,

tightly bound water results in a T_g depression. Under hydrated conditions this indirectly affects the proton conductivity of the sulfonated copolymers by influencing the temperature at which a viscoelastic induced morphological relaxation occurs. The temperature at which this relaxation occurs has important implications when the operating temperature of fuel cells is increased. The free water content was found to influence the transport properties.

1.10 Design for next generation proton exchange membranes.

The challenge in designing next generation PEMs lies in how to modify the chemistry of the polymers to obtain significant proton conductivity at low hydration levels, especially when the self-diffusion coefficient of water may still be quite low due to its association with the acid groups. One proposal for increasing proton conductivity in the absence of a large amount of water is to develop the associated structure of the ionic groups at low hydration levels. This can be achieved by increasing the ionic concentration, which in turn increases the degree of sulfonation. This increase in the concentration of sulfonic groups may help to form associated domain structures—even at low hydration levels—and may contribute to enhanced proton conductivity. The major drawback of a higher degree of sulfonation is that the polymer will experience excessive water uptake at higher water activities. This results in poor dimensional stability and significant depression of the glass transition temperature.[47] It has been reported that for BPSH-xx copolymers, water uptake increases to a very high value after approximately 55%. degree of disulfonation.[36, 103, 149] This relatively high degree of disulfonation has been correlated to the continuity of the hydrophilic phase, which varies depending on the polymer's chemical features. High conductivity at both low degrees of disulfonation and low hydration levels may be possible if one can alter the sequential chemical structure of the polymer backbone to produce block copolymers.

Block copolymers consist of two or more chemically dissimilar backbone segments (i.e. blocks) that are chemically conjoined through covalent bonds in the same chain.[150] In many cases where the blocks are immiscible, improved morphological control can be achieved by tailoring the chemical composition, molecular weight, and volume fraction of the blocks. Thus, new materials with attractive properties can be created, which would not have been possible in a single phase.[151] Block copolymer ionomers can be obtained when one of the blocks is fully or

partially modified with ion containing groups. In block ionomer proton exchange membranes, the ionic groups act as proton conducting sites, while the non-ionic component provides dimensional strength and, in the case of DMFCs, may serve as a barrier for methanol transport. Among the most extensively studied block ionomers as potential PEMs are the sulfonated polystyrene-based triblock copolymers. Another example is sulfonated poly(styrene-isobutylene-styrene) (SPSIS),[74, 152] with varying block lengths and degrees of sulfonation of the PS block, synthesized by living cationic polymerization. Although these block copolymer ionomers have been shown to have acceptable proton conductivity and fuel cell performance characteristics,[74, 152] their major disadvantage is the poor chemical stability of their aliphatic backbones. This limits their applicability to low temperature and low power density devices.

Relatively few attempts have been made to develop block copolymer ionomers having thermally and chemically stable aromatic backbones.[153-155] Synthesizing this type of system is possible via step growth polymerization whereby hydrophobic and hydrophilic telechelic oligomers with appropriate end groups are copolymerized to obtain multiblock, or segmented, copolymer ionomers. McGrath et al. have recently synthesized a series of multiblock ionomers having highly fluorinated hydrophobic blocks and poly(arylene ether sulfone)s hydrophilic blocks with a 100% degree of sulfonation.[156] Unlike the BPSH-xx copolymers, where the sulfonic acid groups are randomly distributed in pairs along the chain, the multiblock copolymers feature an ordered sequence of hydrophilic and hydrophobic segments. If connectivity is established between the hydrophilic domains in these multiblock copolymers, they will not need as much water to form a percolated structure. Hence, they will exhibit much better proton conductivity than the random copolymers (with similar degrees of sulfonation, or IEC) under partially hydrated conditions.

1.11 References

1. Zalbowitz, M.; S, T., Green Power. *Fuel Cells* **1999**.

2. Cleghorn, S. J. C.; Ren, X.; Springer, T. E.; Wilson, M. S.; Zawodzinski, C.; Zawodzinski, T. A.; Gottesfeld, S., PEM fuel cells for transportation and stationary power generation applications. *International Journal of Hydrogen Energy* **1997,** 22, (12), 1137-1144.

3. Carrette, L.; Friedrich, K. A.; Stimming, U., Fuel cells: Principles, types, fuels, and applications. *Chemphyschem* **2000,** 1, (4), 162-193.

4. Appelby, A., 1999. *Scientific American* 74-79.

5. Winter, M.; Brodd, R. J., What are batteries, fuel cells, and supercapacitors? *Chemical Reviews* **2004,** 104, (10), 4245-4269.

6. Winter, M.; Brodd, R. J., What are batteries, fuel cells, and supercapacitors? (vol 104, pg 4245, 2003). *Chemical Reviews* **2005,** 105, (3), 1021-1021.

7. Acres, G. J. K., Recent advances in fuel cell technology and its applications. *Journal of Power Sources* **2001,** 100, (1-2), 60-66.

8. Brandon, N. P.; Skinner, S.; Steele, B. C. H., Recent advances in materials for fuel cells. *Annual Review of Materials Research* **2003,** 33, 183-213.

9. Mathias, M.; Gasteiger, H.; Makharia, R.; Kocha, S.; Fuller, T.; Xie, T.; Pisco, J., Can available membranes and catalysts meet automotive polymer electrolyte fuel cell requirements? *Preprints of Symposia - American Chemical Society, Division of Fuel Chemistry* **2004,** 49, (2), 471-474.

10. Ren, X.; Zelenay, P.; Thomas, S.; Davey, J.; Gottesfeld, S., Recent advances in direct methanol fuel cells at Los Alamos National Laboratory. *Journal of Power Sources* **2000,** 86, (1-2), 111-116.

11. Dinh, H. N.; Ren, X. M.; Garzon, F. H.; Zelenay, P.; Gottesfeld, S., Electrocatalysis in direct methanol fuel cells: in-situ probing of PtRu anode catalyst surfaces. *Journal of Electroanalytical Chemistry* **2000,** 491, (1-2), 222-233.

12. Ren, X. M.; Zelenay, P.; Thomas, S.; Davey, J.; Gottesfeld, S., Recent advances in direct methanol fuel cells at Los Alamos National Laboratory. *Journal of Power Sources* **2000,** 86, (1-2), 111-116.

13. Thomas, S. C.; Ren, X. M.; Gottesfeld, S.; Zelenay, P., Direct methanol fuel cells: progress in cell performance and cathode research. *Electrochimica Acta* **2002,** 47, (22-23), 3741-3748.

14. Gottesfeld, S., Direct methanol fuel cells for portable power applications. *Abstracts of Papers of the American Chemical Society* **2004,** 228, U653-U653.

15. Hickner, M. A.; Ghassemi, H.; Kim, Y. S.; Einsla, B. R.; McGrath, J. E., Alternative polymer systems for proton exchange membranes (PEMs). *Chemical Reviews* **2004,** 104, (10), 4587-4611.

16. Wilson, M., The Regents of the University of California. *U.S. 5,211,984* **1993**.

17. Roziere, J.; Jones, D. J., Non-fluorinated polymer materials for proton exchange membrane fuel cells. *Annual Review of Materials Research* **2003,** 33, 503-555.

18. Alberti, G.; Casciola, M., Composite membranes for medium-temperature PEM fuel cells. *Annual Review of Materials Research* **2003,** 33, 129-154.

19. Kerres, J. A., Development of ionomer membranes for fuel cells. *Journal of Membrane Science* **2001,** 185, (1), 3-27.

20. Kerres, J.; Ullrich, A.; Hein, M., Preparation and characterization of novel basic polysulfone polymers. *Journal of Polymer Science Part a-Polymer Chemistry* **2001,** 39, (17), 2874-2888.

21. Zawodzinski, T. A.; Springer, T. E.; Uribe, F.; Gottesfeld, S., Characterization of Polymer Electrolytes for Fuel-Cell Applications. *Solid State Ionics* **1993,** 60, (1-3), 199-211.

22. Hickner, M. A.; Pivovar, B. S., The chemical and structural nature of proton exchange membrane fuel cell properties. *Fuel Cells* **2005,** 5, (2), 213-229.

23. Grot, W., du Pont de Nemours and Company. *U.S. 3,718,627* **1968**.

24. Tant, M. R.; Darst, K. P.; Lee, K. D.; Martin, C. W., Structure and Properties of Short-Side-Chain Perfluorosulfonate Ionomers. *Acs Symposium Series* **1989,** 395, 370-400.

25. Wang, S.; McGrath, J. E., Synthesis of Poly(arylene ether)s. *Synthetic methods in Step-Growth Polymers* **2003,** Wiley:New York, p 327.

26. Noshay, A.; Robeson, L. M., Sulfonated Polysulfone. *Journal of Applied Polymer Science* **1976,** 20, (7), 1885-1903.

27. Johnson, B. C.; Yilgor, I.; Tran, C.; Iqbal, M.; Wightman, J. P.; Lloyd, D. R.; Mcgrath, J. E., Synthesis and Characterization of Sulfonated Poly(Arylene Ether Sulfones). *Journal of Polymer Science Part a-Polymer Chemistry* **1984,** 22, (3), 721-737.

28. Nolte, R.; Ledjeff, K.; Bauer, M.; Mulhaupt, R., Partially Sulfonated Poly(Arylene Ether Sulfone) - a Versatile Proton Conducting Membrane Material for Modern Energy-Conversion Technologies. *Journal of Membrane Science* **1993,** 83, (2), 211-220.

29. Genova-Dimitrova, P.; Baradie, B.; Foscallo, D.; Poinsignon, C.; Sanchez, J. Y., Ionomeric membranes for proton exchange membrane fuel cell (PEMFC): sulfonated polysulfone associated with phosphatoantimonic acid. *Journal of Membrane Science* **2001,** 185, (1), 59-71.

30. Bauer, B.; Jones, D. J.; Roziere, J.; Tchicaya, L.; Alberti, G.; Casciola, M.; Massinelli, L.; Peraio, A.; Besse, S.; Ramunni, E., Electrochemical characterisation of sulfonated polyetherketone membranes. *Journal of New Materials for Electrochemical Systems* **2000,** 3, (2), 93-98.

31. Bailly, C.; Williams, D. J.; Karasz, F. E.; Macknight, W. J., The Sodium-Salts of Sulfonated Poly(Aryl-Ether-Ether-Ketone) (Peek) - Preparation and Characterization. *Polymer* **1987,** 28, (6), 1009-1016.

32. Robeson, L. M.; Matzner, M., US Patent. *to Union carbide,Inc* **1983,** 4,380,598.

33. Sankir, M.; Bhanu, V. A.; Harrison, W. L.; Ghassemi, H.; Wiles, K. B.; Glass, T. E.; Brink, A. E.; Brink, M. H.; McGrath, J. E., Synthesis and characterization of 3,3 '-disulfonated-4,4 '-dichlorodiphenyl sulfone (SDCDPS) monomer for proton exchange membranes (PEM) in fuel cell applications. *Journal of Applied Polymer Science* **2006,** 100, (6), 4595-4602.

34. Wang, F.; Hickner, M.; Kim, Y. S.; Zawodzinski, T. A.; McGrath, J. E., Direct polymerization of sulfonated poly(arylene ether sulfone) random (statistical) copolymers: candidates for new proton exchange membranes. *Journal of Membrane Science* **2002,** 197, (1-2), 231-242.

35. Wang, F.; Hickner, M.; Ji, Q.; Harrison, W.; Mecham, J.; Zawodzinski, T. A.; McGrath, J. E., Synthesis of highly sulfonated poly(arylene ether sulfone) random (statistical) copolymers via direct polymerization. *Macromolecular Symposia* **2001,** 175, 387-395.

36. Kim, Y. S.; Wang, F.; Hickner, M.; McCartney, S.; Hong, Y. T.; Harrison, W.; Zawodzinski, T. A.; McGrath, J. E., Effect of acidification treatment and morphological stability

of sulfonated poly(arylene ether sulfone) copolymer proton-exchange membranes for fuel-cell use above 100 degrees C. *Journal of Polymer Science Part B-Polymer Physics* **2003,** 41, (22), 2816-2828.

37. Kim, Y. S.; Einsla, B.; Sankir, M.; Harrison, W.; Pivovar, B. S., Structure-property-performance relationships of sulfonated poly(arylene ether sulfone)s as a polymer electrolyte for fuel cell applications. *Polymer* **2006,** 47, (11), 4026-4035.

38. Harrison, W. L.; Wang, F.; Kim, Y.; Hickner, M.; McGrath, J. E., Synthesis, characterization and morphologial influence of bisphenol structure on the direct synthesis of sulfonated poly(arylene ether sulfone) copolymers. *Abstracts of Papers of the American Chemical Society* **2002,** 223, D16-D16.

39. Hickner, M. A.; Wang, F.; Kim, Y. S.; Privovar, B.; Zawodzinski, T. A.; McGrath, J. E., Chemistry-morphology-property relationships of novel proton exchange membranes for direct methanol fuel cells. *Abstracts of Papers of the American Chemical Society* **2001,** 222, U467-U467.

40. Harrison, W. L.; Wang, F.; Mecham, J. B.; Glass, T. E.; Hickner, M. A.; McGrath, J. E., Influence of bisphenol structure on the direct synthesis of sulfonated poly(arylene ether)s. *Abstracts of Papers of the American Chemical Society* **2001,** 221, U415-U415.

41. Harrison, W. L.; Wang, F.; Mecham, J. B.; Bhanu, V. A.; Hill, M.; Kim, Y. S.; McGrath, J. E., Influence of the bisphenol structure on the direct synthesis of sulfonated poly(arylene ether) copolymers. I. *Journal of Polymer Science Part a-Polymer Chemistry* **2003,** 41, (14), 2264-2276.

42. Roy, A.; Einsla, B.; Harrison, W.; McGrath, J. E., Synthesis and characterization of hydroquinone based disulfonated poly(arylene ether sulfone)s via direct copolymerization. *Abstracts of Papers of the American Chemical Society* **2004,** 228, U663-U663.

43. Li, Y. X.; Mukundan, T.; Harrison, W. L.; Hill, M.; Sankir, M.; Yang, J.; McGrath, J. E., Direct synthesis of disulfonated poly(arylene ether ketone)s and investigation of their behavior as proton exchange membrane (PEM). *Abstracts of Papers of the American Chemical Society* **2004,** 228, U657-U657.

44. Wiles, K. B.; Bhanu, V. A.; Wang, F.; Hickner, M. A.; McGrath, J. E., Poly(arylene thioether sulfone) copolymers for PEM-based fuel cell systems. *Abstracts of Papers of the American Chemical Society* **2003,** 225, U640-U640.

45. Kim, Y. S., *Los Alamos National Laboratory* Unpublished results.

46. *DOE Program Review* **2005,** May 23-26, (Arlington,VA).

47. Kim, Y. S.; Dong, L. M.; Hickner, M. A.; Pivovar, B. S.; McGrath, J. E., Processing induced morphological development in hydrated sulfonated poly(arylene ether sulfone) copolymer membranes. *Polymer* **2003,** 44, (19), 5729-5736.

48. Summer, M. J.; Harrison, W. L.; Weyers, R. M.; Kim, Y. S.; McGrath, J. E.; Riffle, J. S.; Brink, A.; Brink, M. H., Novel proton conducting sulfonated poly(arylene ether) copolymers containing aromatic nitriles. *Journal of Membrane Science* **2004,** 239, (2), 199-211.

49. Kim, Y. S.; Sumner, M. J.; Harrison, W. L.; Riffle, J. S.; McGrath, J. E.; Pivovar, B. S., Direct methanol fuel cell performance of disulfonated poly-arylene ether benzonitrile) copolymers. *Journal of the Electrochemical Society* **2004,** 151, (12), A2150-a2156.

50. Eisenberg, A., Structure and Viscoelastic Properties of Ion-Containing Polymers in Solid-State. *Pure and Applied Chemistry* **1976,** 46, (2-4), 171-175.

51. Yeager, H. L.; Eisenberg, A., Perfluorinated Ionomer Membranes - Introduction. *Acs Symposium Series* **1982,** 180, 1-6.

52. Eisenberg, A., Bulk Properties of Ionomers. *Abstracts of Papers of the American Chemical Society* **1988,** 196, 212-POLY.

53. Hsu, W. Y.; Gierke, T. D., Ion-Transport and Clustering in Nafion Perfluorinated Membranes. *Journal of Membrane Science* **1983,** 13, (3), 307-326.

54. Mauritz, K. A.; Moore, R. B., State of Understanding of Nafion. *Chem. Rev.* **2004,** 104, (10), 4535-4586.

55. Paddison, S. J.; Elliott, J. A., Molecular Modeling of the short-side-chain perfluorosulfonic acid membrane. *Journal of Physical Chemistry A* **2005,** 109, (33), 7583-7593.

56. Page, K. A.; Cable, K. M.; Moore, R. B., Molecular Origins of the Thermal Transitions and Dynamic Mechanical Relaxations in Perfluorosulfonate Ionomers. *Macromolecules* **2005,** 38, (15), 6472-6484.

57. Phillips, A. K.; Moore, R. B., Mechanical and transport property modifications of perfluorosulfonate ionomer membranes prepared with mixed organic and inorganic counterions. *Journal of Polymer Science, Part B: Polymer Physics* **2006,** 44, (16), 2267-2277.

58. Taylor, E. P.; Landis, F. A.; Page, K. A.; Moore, R. B., Counterion dependent crystallization kinetics in blends of a perfluorosulfonate ionomer with poly(vinylidene fluoride). *Polymer* **2006,** 47, (21), 7425-7435.

59. Gierke, T. D.; Munn, G. E.; Wilson, F. C., The Morphology in Nafion Perfluorinated Membrane Products, as Determined by Wide-Angle and Small-Angle X-Ray Studies. *Journal of Polymer Science Part B-Polymer Physics* **1981,** 19, (11), 1687-1704.

60. Gebel, G.; Moore, R. B., Small-angle scattering study of short pendant chain perfuorosulfonated ionomer membranes. *Macromolecules* **2000,** 33, (13), 4850-4855.

61. Gebel, G.; Loppinet, B.; Hara, H.; Hirasawa, E., Small-angle neutron scattering study of polyethylene-co-methacrylate ionomer aqueous solutions. *Journal of Physical Chemistry B* **1997,** 101, (20), 3980-3987.

62. Xue, T.; Trent, J. S.; Osseoasare, K., Characterization of Nafion Membranes by Transmission Electron-Microscopy. *Journal of Membrane Science* **1989,** 45, (3), 261-271.

63. McLean, R. S.; Doyle, M.; Sauer, B. B., High-resolution imaging of ionic domains and crystal morphology in ionomers using AFM techniques. *Macromolecules* **2000,** 33, (17), 6541-6550.

64. Meresi, G.; Wang, Y.; Bandis, A.; Inglefield, P. T.; Jones, A. A.; Wen, W. Y., Morphology of dry and swollen perfluorosulfonate ionomer by fluorine-19 MAS, NMR and xenon-129 NMR. *Polymer* **2001,** 42, (14), 6153-6160.

65. Sivashinsky, N.; Tanny, G. B., The State of Water in Swollen Ionomers Containing Sulfonic-Acid Salts. *Journal of Applied Polymer Science* **1981,** 26, (8), 2625-2637.

66. Gierke, T. D., Morphology and Its Relationship to Efficiency of Nafion Perfluorosulfonic Acid Membranes. *Journal of the Electrochemical Society* **1978,** 125, (3), C163-C163.

67. Gierke, T. D., The Morphology in Nafion Perfluorinated Membranes and Its Effect on Ion-Transport. *Bulletin of the American Physical Society* **1981,** 26, (3), 462-462.

68. Gierke, T. D.; Hsu, W. Y., The Cluster-Network Model of Ion Clustering in Perfluorosulfonated Membranes. *Acs Symposium Series* **1982,** 180, 283-307.

69. Gierke, T. D.; Munn, G. E.; Wilson, F. C., Morphology of Perfluorosulfonated Membrane Products - Wide-Angle and Small-Angle X-Ray Studies. *Acs Symposium Series* **1982,** 180, 195-216.

70. Fujimura, M.; Hashimoto, T.; Kawai, H., Small-Angle X-Ray-Scattering Study of Perfluorinated Ionomer Membranes .1. Origin of 2 Scattering Maxima. *Macromolecules* **1981,** 14, (5), 1309-1315.

71. Gebel, G., Structural evolution of water swollen perfluorosulfonated ionomers from dry membrane to solution. *Polymer* **2000,** 41, (15), 5829-5838.

72. Kreuer, K. D., Handbook of Fuel Cells-Fundamentals, Technology and Applications; Vielstich, W., Lamm, A., gasteiger, h.A., Eds.;. *John Wiley & Sons Ltd: Chichester, U.K.,* **2003,** Vol. 3, (Part 3).

73. Kim, Y. S.; Hickner, M. A.; Dong, L. M.; Pivovar, B. S.; McGrath, J. E., Sulfonated poly(arylene ether sulfone) copolymer proton exchange membranes: composition and morphology effects on the methanol permeability. *Journal of Membrane Science* **2004,** 243, (1-2), 317-326.

74. Elabd, Y. A.; Napadensky, E.; Sloan, J. M.; Crawford, D. M.; Walker, C. W., Triblock copolymer ionomer membranes Part I. Methanol and proton transport. *Journal of Membrane Science* **2003,** 217, (1-2), 227-242.

75. Kreuer, K. D., Proton conductivity: Materials and applications. *Chemistry of Materials* **1996,** 8, (3), 610-641.

76. Kreuer, K. D., On the complexity of proton conduction phenomena. *Solid State Ionics* **2000,** 136, 149-160.

77. Paddison, S. J., Proton conduction mechanisms at low degrees of hydration in sulfonic acid-based polymer electrolyte membranes. *Annual Review of Materials Research* **2003,** 33, 289-319.

78. Van Grotthuss, C. J. D., *Ann. Chim* **1806,** 58, (54).

79. Kreuer, K. D.; Rabenau, A.; Weppner, W., Vehicle Mechanism, a New Model for the Interpretation of the Conductivity of Fast Proton Conductors. *Angewandte Chemie-International Edition in English* **1982,** 21, (3), 208-209.

80. Kreuer, K. D.; Ise, M.; Fuchs, A.; Maier, J., Proton and water transport in nano-separated polymer membranes. *Journal De Physique Iv* **2000,** 10, (P7), 279-281.

81. Kreuer, K. D.; Paddison, S. J.; Spohr, E.; Schuster, M., Transport in proton conductors for fuel-cell applications: Simulations, elementary reactions, and phenomenology. *Chemical Reviews* **2004,** 104, (10), 4637-4678.

82. Zawodzinski, T. A.; Neeman, M.; Sillerud, L. O.; Gottesfeld, S., Determination of Water Diffusion-Coefficients in Perfluorosulfonate Ionomeric Membranes. *Journal of Physical Chemistry* **1991,** 95, (15), 6040-6044.

83. Springer, T. E.; Zawodzinski, T. A.; Wilson, M. S.; Gottesfeld, S., Characterization of polymer electrolyte fuel cells using AC impedance spectroscopy. *Journal of the Electrochemical Society* **1996,** 143, (2), 587-599.

84. Cussler, E. L., Diffusion Mass Transfer in Fluid Systems. *2nd Ed. Cambridge University Press, New York,* **1997**.

85. Hill, D. J. T.; Lim, M. C. H.; Whittaker, A. K., Water diffusion in hydroxyethyl methacrylate (HEMA)-based hydrogels formed by gamma-radiolysis. *Polymer International* **1999,** 48, (10), 1046-1052.

86. Ghi, P. Y.; Hill, D. J. T.; Whittaker, A. K., PFG-NMR measurements of the self-diffusion coefficients of water in equilibrium poly(HEMA-co-THFMA) hydrogels. *Biomacromolecules* **2002,** 3, (3), 554-559.

87. Dong, L. M.; Kim, Y. S.; Wang, F.; Hickner, M.; Glass, T. E.; McGrath, J. E., Self-diffusion of water in sulfonated poly(arylene ether sulfone) copolymers by pulse field gradient NMR. *Abstracts of Papers of the American Chemical Society* **2003,** 225, U631-U631.

88. Stejskal, E. O.; Tanner, J. E., *J.chem.Phys* **1965**, (42), 288.

89. Zawodzinski, T. A.; Springer, T. E.; Neeman, M.; Sillerud, L. O., Diffusion-Barriers in Pulsed-Gradient Spin-Echo Nmr Microscopy. *Israel Journal of Chemistry* **1992,** 32, (2-3), 281-289.

90. Matsukawa, S.; Yasunaga, H.; Zhao, C.; Kuroki, S.; Kurosu, H.; Ando, I., Diffusion processes in polymer gels as studied by pulsed field-gradient spin-echo NMR spectroscopy. *Progress in Polymer Science* **1999,** 24, (7), 995-1044.

91. Matsukawa, S.; Ando, I., Study of self-diffusion of molecules in polymer gel by pulsed-gradient spin-echo H-1 NMR. 3. Stearyl itaconamide N,N-dimethylacrylamide copolymer gels. *Macromolecules* **1999,** 32, (6), 1865-1871.

92. Zhao, C. H.; Matsukawa, S.; Kurosu, H.; Ando, I., Self-diffusion behavior of solvents in polypeptide gel as studied by pulsed-gradient spin-echo H-1 NMR spectroscopy. *Macromolecules* **1998,** 31, (9), 3139-3141.

93. Ghi, P. Y.; Hill, D. J. T.; Maillet, D.; Whittaker, A. K., Nmr imaging of the diffusion of water into poly(tetrahydrofurfuryl methacrylate-co-hydroxyethyl methacrylate). *Polymer* **1997,** 38, (15), 3985-3989.

94. Ghi, P. Y.; Hill, D. J. T.; Whittaker, A. K., H-1 NMR study of the states of water in equilibrium Poly(HEMA-co-THFMA) hydrogels. *Biomacromolecules* **2002,** 3, (5), 991-997.

95. Callaghan, P. T.; Coy, A.; Halpin, T. P. J.; Macgowan, D.; Packer, K. J.; Zelaya, F. O., Diffusion in Porous Systems and the Influence of Pore Morphology in Pulsed Gradient Spin-Echo Nuclear-Magnetic-Resonance Studies. *Journal of Chemical Physics* **1992,** 97, (1), 651-662.

96. Paddison, S. J.; Paul, R., The nature of proton transport in fully hydrated Nafion (R). *Physical Chemistry Chemical Physics* **2002,** 4, (7), 1158-1163.

97. Zawodzinski, T. A.; Derouin, C.; Radzinski, S.; Sherman, R. J.; Smith, V. T.; Springer, T. E.; Gottesfeld, S., Water-Uptake by and Transport through Nafion(R) 117 Membranes. *Journal of the Electrochemical Society* **1993,** 140, (4), 1041-1047.

98. Zawodzinski, T. A.; Springer, T. E.; Davey, J.; Jestel, R.; Lopez, C.; Valerio, J.; Gottesfeld, S., A Comparative-Study of Water-Uptake by and Transport through Ionomeric Fuel-Cell Membranes. *Journal of the Electrochemical Society* **1993,** 140, (7), 1981-1985.

99. Kreuer, K. D.; Munch, W.; Maier, J., About the complexity of proton conduction mechanisms in electrolytes for high drain applications. *Abstracts of Papers of the American Chemical Society* **2000,** 220, U180-U180.

100. Kreuer, K. D., On the development of proton conducting polymer membranes for hydrogen and methanol fuel cells. *Journal of Membrane Science* **2001,** 185, (1), 29-39.

101. Kreuer, K. D., In Solid State Ionics: Science and Technology, ed.DVR Chowdhari *London: World Scientific* **1998**, pp. 263-74.

102. Alberti, G.; Casciola, M.; Massinelli, L.; Bauer, B., Polymeric proton conducting membranes for medium temperature fuel cells (110-160 degrees C). *Journal of Membrane Science* **2001,** 185, (1), 73-81.

103. Kim, Y. S.; Dong, L. M.; Hickner, M. A.; Glass, T. E.; Webb, V.; McGrath, J. E., State of water in disulfonated poly(arylene ether sulfone) copolymers and a perfluorosulfonic acid copolymer (nafion) and its effect on physical and electrochemical properties. *Macromolecules* **2003,** 36, (17), 6281-6285.

104. Pivovar, B. S., An overview of electro-osmosis in fuel cell polymer electrolytes. *Polymer* **2006,** 47, (11), 4194-4202.

105. Ren, X. M.; Henderson, W.; Gottesfeld, S., Electro-osmotic drag of water in ionomeric membranes - New measurements employing a direct methanol fuel cell. *Journal of the Electrochemical Society* **1997,** 144, (9), L267-L270.

106. Fuller, T. F.; Newman, J., Experimental-Determination of the Transport Number of Water in Nafion-117 Membrane. *Journal of the Electrochemical Society* **1992,** 139, (5), 1332-1337.

107. Ise, M.; Kreuer, K. D.; Maier, J., Electroosmotic drag in polymer electrolyte membranes: an electrophoretic NMR study. *Solid State Ionics* **1999,** 125, (1-4), 213-223.

108. Zawodzinski, T. A.; Davey, J.; Valerio, J.; Gottesfeld, S., The Water-Content Dependence of Electroosmotic Drag in Proton-Conducting Polymer Electrolytes. *Electrochimica Acta* **1995,** 40, (3), 297-302.

109. Pivovar, B. S.; Smyrl, W. H.; Cussler, E. L., Electro-osmosis in Nafion 117, polystyrene sulfonic acid, and polybenzimidazole. *Journal of the Electrochemical Society* **2005,** 152, (1), A53-A60.

110. Pivovar, A. A.; Pivovar, B. S., Dynamic behavior of water within a polymer electrolyte fuel cell membrane at low hydration levels. *Journal of Physical Chemistry B* **2005,** 109, (2), 785-793.

111. Wiles, K. B.; Akle, B. J.; Hickner, M. A.; Bennett, M.; Leo, D. J.; McGrath, J. E., Directly copolymerized poly(arylene sulfide sulfone) and poly(arylene ether sulfone) disulfonated copolymers for use in ionic polymer transducers. *Journal of the Electrochemical Society* **2007,** 154, (6), P77-P85.

112. Gottesfeld, S., Polymer electrolyte and direct methanol fuel fells: A tutorial. *Abstracts of Papers of the American Chemical Society* **2001,** 222, U460-U460.

113. Gottesfeld, S., Polymer electrolyte and Direct Methanol Fuel Cells: Technical challenges and commercial opportunities. *Abstracts of Papers of the American Chemical Society* **2001,** 222, U466-U466.

114. Ren, X.; Springer, T. E.; Gottesfeld, S., Direct methanol fuel cell: transport properties of polymer electrolyte membrane and cell performance. *Proceedings - Electrochemical Society* **1999,** 98-27, (Proton Conducting Membrane Fuel Cells II), 341-357.

115. Ren, X.; Springer, T. E.; Gottesfeld, S., Water and methanol uptakes in Nafion membranes and membrane effects on direct methanol cell performance. *Journal of the Electrochemical Society* **2000,** 147, (1), 92-98.

116. Ren, X.; Zawodzinski, T.; Gottesfeld, S., Water and methanol transport in membranes for direct methanol fuel cells. *Polymeric Materials Science and Engineering* **1999,** 80, 601-602.

117. Pivovar, B. S.; Wang, Y. X.; Cussler, E. L., Pervaporation membranes in direct methanol fuel cells. *Journal of Membrane Science* **1999,** 154, (2), 155-162.

118. Ren, X. M.; Springer, T. E.; Zawodzinski, T. A.; Gottesfeld, S., Methanol transport through nafion membranes - Electro-osmotic drag effects on potential step measurements. *Journal of the Electrochemical Society* **2000,** 147, (2), 466-474.

119. Mauritz, K. A.; Moore, R. B., State of understanding of Nafion. *Chemical Reviews* **2004,** 104, (10), 4535-4585.

120. Nicholas W. DeLuca, Y. A. E., Polymer electrolyte membranes for the direct methanol fuel cell: A review. In 2006; Vol. 44, pp 2201-2225.

121. Li, Y.; Yang, J.; Roy, A.; Einsla, B.; Wang, F.; McGrath, J. E., Partially fluorinated disulfonated poly (arylene ether sulfone) copolymers with controlled molecular weights and their applications to proton exchange membrane fuel cells. *Preprints of Symposia - American Chemical Society, Division of Fuel Chemistry* **2005,** 50, (2), 573-574.

122. Einsla, B. R.; Hong, Y. T.; Kim, Y. S.; Wang, F.; Gunduz, N.; Mcgrath, J. E., Sulfonated naphthalene dianhydride based polyimide copolymers for proton-exchange-membrane fuel cells. I. Monomer and copolymer synthesis. *Journal of Polymer Science Part a-Polymer Chemistry* **2004,** 42, (4), 862-874.

123. Mcbrierty, V. J.; Quinn, F. X.; Keely, C.; Wilson, A. C.; Friends, G. D., Water in Hydrogels .4. Poly(N-Vinyl-2-Pyrrolidinone Methyl-Methacrylate) Saline Systems. *Macromolecules* **1992,** 25, (17), 4281-4284.

124. Hodge, R. M.; Edward, G. H.; Simon, G. P., The States of Water within Poly(Vinyl Alcohol) Thin-Films .2. Investigation by Differential Scanning Calorimetry and Thermogravimetric Analysis. *Abstracts of Papers of the American Chemical Society* **1993,** 205, 448-POLY.

125. Hodge, R. M.; Edward, G. H.; Simon, G. P.; Hill, A. J., The States of Water within Poly(Vinyl Alcohol) Thin-Films .1. Investigation by Positron-Annihilation Lifetime Spectroscopy. *Abstracts of Papers of the American Chemical Society* **1993,** 205, 447-POLY.

126. Hodge, R. M.; Bastow, T. J.; Edward, G. H.; Simon, G. P.; Hill, A. J., Free volume and the mechanism of plasticization in water-swollen poly(vinyl alcohol). *Macromolecules* **1996,** 29, (25), 8137-8143.

127. Hodge, R. M.; Edward, G. H.; Simon, G. P., Water absorption and states of water in semicrystalline poly(vinyl alcohol) films. *Polymer* **1996,** 37, (8), 1371-1376.

128. Quinn, F. X.; Kampff, E.; Smyth, G.; Mcbrierty, V. J., Water in Hydrogels .1. A Study of Water in Poly(N-Vinyl-2-Pyrrolidone Methyl-Methacrylate) Copolymer. *Macromolecules* **1988,** 21, (11), 3191-3198.

129. Mu Shik Jhon, J. D. A., Water and hydrogels. *Journal of Biomedical Materials Research* **1973,** 7, (6), 509-522.

130. Kuntz, I., D., *ADV PROTEIN CHEM* **1974,** 28, 239.

131. Rowland, S., P., *ACS Symp. Series* **1980,** 127.

132. Ravindra, R.; Sridhar, S.; Khan, A. A., Separation studies of hydrazine from aqueous solutions by pervaporation. *Journal of Polymer Science Part B-Polymer Physics* **1999,** 37, (16), 1969-1980.

133. Barbieri, R.; Quaglia, M.; Delfini, M.; Brosio, E., Investigation of water dynamic behaviour in poly(HEMA) and poly(HEMA-co-DHPMA) hydrogels by proton T-2 relaxation time and self-diffusion coefficient nmr measurements. *Polymer* **1998,** 39, (5), 1059-1066.

134. Quinn, F. X.; Mcbrierty, V. J.; Wilson, A. C.; Friends, G. D., Water in Hydrogels .3. Poly(Hydroxyethyl Methacrylate) Saline Solution Systems. *Macromolecules* **1990,** 23, (21), 4576-4581.

135. McConville, P.; Pope, J. M., H-1 NMR T-2 relaxation in contact lens hydrogels as a probe of water mobility. *Polymer* **2001,** 42, (8), 3559-3568.

136. Lee, H. B.; Jhon, M. S.; Andrade, J. D., Nature of Water in Synthetic Hydrogels .1. Dilatometry, Specific Conductivity, and Differential Scanning Calorimetry of Polyhydroxyethyl Methacrylate. *Journal of Colloid and Interface Science* **1975,** 51, (2), 225-231.

137. Roorda, W., Do Hydrogels Contain Different Classes of Water. *Journal of Biomaterials Science-Polymer Edition* **1994,** 5, (5), 383-395.

138. Smyth, G.; Quinn, F. X.; Mcbrierty, V. J., Water in Hydrogels .2. A Study of Water in Poly(Hydroxyethyl Methacrylate). *Macromolecules* **1988,** 21, (11), 3198-3204.

139. Yoshida, H.; Miura, Y., Behavior of Water in Perfluorinated Ionomer Membranes Containing Various Monovalent Cations. *Journal of Membrane Science* **1992,** 68, (1-2), 1-10.

140. Miura, Y.; Yoshida, H., Effects of Water and Alcohols on Molecular-Motion of Perfluorinated Ionomer Membranes. *Thermochimica Acta* **1990,** 163, 161-168.

141. McConville, P.; Whittaker, M. K.; Pope, J. M., Water and polymer mobility in hydrogel biomaterials quantified by H-1 NMR: A simple model describing both T-1 and T-2 relaxation. *Macromolecules* **2002,** 35, (18), 6961-6969.

142. Starkweather, H. W.; Chang, J. J., Water Relaxation in Perfluorosulfonate Ionomers. *Macromolecules* **1982,** 15, (3), 752-756.

143. Boyle, N. G.; Coey, J. M. D.; Mcbrierty, V. J., Low-Temperature Behavior of Water in Nafion Membranes. *Chemical Physics Letters* **1982,** 86, (1), 16-19.

144. Boyle, N. G.; Mcbrierty, V. J.; Douglass, D. C., A Study of the Behavior of Water in Nafion Membranes. *Macromolecules* **1983,** 16, (1), 75-80.

145. Boyle, N. G.; Mcbrierty, V. J.; Eisenberg, A., Nmr Investigation of Molecular-Motion in Nafion Membranes. *Macromolecules* **1983,** 16, (1), 80-84.

146. Boyle, N. G.; Coey, J. M. D.; Meagher, A.; Mcbrierty, V. J.; Nakano, Y.; Macknight, W. J., Aqueous Phase in a Perfluorocarboxylate Membrane. *Macromolecules* **1984,** 17, (7), 1331-1334.

147. MacMillan, B.; Sharp, A. R.; Armstrong, R. L., An nmr investigation of the dynamical characteristics of water absorbed in Nafion. *Polymer* **1999,** 40, (10), 2471-2480.

148. MacMillan, B.; Sharp, A. R.; Armstrong, R. L., Nmr relaxation in Nafion - the low temperature regime. *Polymer* **1999,** 40, (10), 2481-2485.

149. Kim, Y. S.; Wang, F.; Hickner, M.; Zawodzinski, T. A.; McGrath, J. E., Fabrication and characterization of heteropolyacid (H3PW12O40)/directly polymerized sulfonated poly(arylene ether sulfone) copolymer composite membranes for higher temperature fuel cell applications. *Journal of Membrane Science* **2003,** 212, (1-2), 263-282.

150. Noshay, A.; McGrath, J. E., *Block Copolymers: Overview and Critical Survey,Academic Press, New York* **1977**, 91.

151. Leibler, L., Theory of Microphase Separation in Block Copolymers. *Macromolecules* **1980,** 13, (6), 1602-1617.

152. Storey, R. F.; Baugh, D. W.; Choate, K. R., Poly(styrene-b-isobutylene-b-styrene) block copolymers produced by living cationic polymerization - I. Compositional analysis. *Polymer* **1999,** 40, (11), 3083-3090.

153. Shin, C. K.; Maier, G.; Andreaus, B.; Scherer, G. G., Block copolymer ionomers for ion conductive membranes. *Journal of Membrane Science* **2004,** 245, (1-2), 147-161.

154. Ghassemi, H.; McGrath, J. E., Synthesis and properties of new sulfonated poly(p-phenylene) derivatives for proton exchange membranes. I. *Polymer* **2004,** 45, (17), 5847-5854.

155. Ghassemi, H.; Ndip, G.; McGrath, J. E., New multiblock copolymers of sulfonated poly(4 '-phenyl-2,5-benzophenone) and poly(arylene ether sulfone) for proton exchange membranes. II. *Polymer* **2004,** 45, (17), 5855-5862.

156. Yu, X.; Roy, A.; Dunn, S.; Yang, J.; McGrath, J. E., Synthesis and characterization of sulfonated-fluorinated, hydrophilic-hydrophobic multiblock copolymers for proton exchange membranes. *Macromolecular Symposia* **2006,** 245/246, (World Polymer Congress--MACRO 2006), 439-449.

2.0 Synthesis and Characterization of Partially Disulfonated Hydroquinone Based Poly(arylene ether sulfone)s Random Copolymers for Application as Proton Exchange Membranes

Abhishek Roy,[1] Michael A. Hickner,[2] Brian R. Einsla,[1] William L. Harrison,[1] and James E. McGrath[1]

[1]Macromolecules and Interfaces Institute
Virginia Polytechnic Institute and State University, Blacksburg, VA 24061
[2] Present Address: Department of Materials Science and Engineering
The Pennsylvania State University, University Park, PA 16802

Abstract

Partially disulfonated hydroquinone based poly(arylene ether sulfone) random copolymers were synthesized and characterized for application as proton exchange membranes. The copolymer composition was varied in degree of disulfonation. The copolymers were characterized by ^{1}H NMR, FTIR, DSC and other analytical techniques. The copolymer with a 25 % degree of disulfonation showed the best optimized balance between water uptake and proton conductivity. The copolymers showed substantially reduced methanol permeability compared to Nafion® and satisfactory DMFC performance. The methanol selectivity improved significantly in comparison to Nafion® 117. At a given ionic composition, the hydroquinone based system showed higher water uptake and proton conductivity than the biphenol based (BPSH-xx) poly(arylene ether sulfone)s copolymers.

2.1 Introduction

Fuel cells are defined as electrochemical devices that convert chemical energy into electrical energy. Fuel cells are classified according to the nature of their electrolyte.[1-4] Among the different types of fuel cells, alkaline fuel cells (AFCs), proton exchange membrane fuel cells (PEMFCs), phosphoric acid based fuel cells (PAFCs), molten carbonate fuel cells (MCFCs) and solid oxide fuel cells (SOFCs) have all shown promise. PEMFCs can be further subdivided based on the nature of the fuel. Specifically, the fuel may be non-volatile in nature—for example, H_2 (H_2/Air)—or volatile as in the case of methanol, which is used in direct methanol fuel cells (DMFCs). The typical operating temperature of a fuel cell is from 80-120 ^oC, and it requires the presence of water for satisfactory performance.[5, 6] The electrolyte employed is typically a sulfonic acid containing polymeric membrane. The ionic groups in presence of water provide the pathway for proton conduction and the chemical polymeric backbone provides the mechanical support. The typical criteria for effective proton exchange membranes are high proton conductivity, excellent oxidative and mechanical durability, reduced fuel permeability, low water uptake, reduced swelling-deswelling characteristics, ability to be fabricated to MEA, and overall cost effectiveness.[5]

Over the last several years, our group has been involved in the synthesis of 4,4'-biphenol based disulfonated poly(arylene ether sulfone)s copolymers.[5] These copolymers (of varying degrees of molar disulfonation) are synthesized by the direct copolymerization of disulfonated monomers.[7] The corresponding acronym is known as BPSH-xx, where BP stands for the biphenol, S for sulfone, H for the acid form, and xx for the degree of disulfonation. The materials show very good proton conductivity at higher degrees of disulfonation. Comparable H_2/Air fuel cell performance to the commercially available Nafion® has been achieved. The materials also display significantly lower methanol permeability with improved DMFC performance than Nafion®.[8, 9]

In this paper, the current research has been extended towards the synthesis and characterization of partially disulfonated hydroquinone based poly(arylene ether sulfone)s. The corresponding acronym is defined as HQSH-xx, where HQ stands for hydroquinone, S for sulfone, H for the acid form, and xx for the degree of disulfonation. Hydroquinone with only one benzene ring is expected to impart less rigidity in the copolymer compared to biphenol in BPSH-xx. From an economic standpoint, hydroquinone is also less expensive than biphenol, making it much more commercially viable. In this paper, HQSH-xx copolymers with varying degrees of disulfonation were synthesized and characterized using ^{1}H NMR and FTIR spectroscopic techniques.[10, 11] A number of fundamental transport properties were evaluated to optimize the ionic content for achieving the desired properties. Membrane electrode assemblies were constructed for DMFC applications and fuel cell performance was evaluated.

2.2 Experimental

2.2.1 Materials

Highly purified 4,4'-dichlorodiphenylsulfone (DCDPS) was provided by Solvay Advanced Polymers. Hydroquinone (HQ) was obtained from Eastman Chemical Company. All the monomers were dried under vacuum prior to use. The disulfonated comonomer (SDCDPS) was synthesized according to the modified literature methods[12] and dried under vacuum before copolymerization. The solvents N,N-dimethylacetamide (DMAc, Fisher) and N-methyl-2-pyrrolidinone (NMP, Fisher) were vacuum-distilled from calcium hydride onto molecular sieves. Potassium carbonate (Aldrich) was dried in vacuum before copolymerization. Toluene, sodium chloride, 30% fuming sulfuric acid and methanol were obtained from Aldrich and used as received. The fuming sulfuric acid was further analyzed for active SO_3 concentration.[13] Nafion® 117 was obtained from ElectroChem, Inc and used as received. BPSH-xx copolymers were used as controls. The data presented for the BPSH-xx random copolymers in this paper were obtained from previously reported studies.[5, 7-9]

2.2.2 Synthesis of hydroquinone based partially disulfonated poly(arylene ether sulfone) random copolymers (HQSH-xx)

The synthesis of disulfonated poly(arylene ether sulfone) copolymers was successfully achieved via aromatic nucleophilic substitution as described previously.[10-12] One typical copolymerization for a HQSH-40 copolymer was as follows: Hydroquinone (10 mmole), 4,4'-dichlorodiphenylsulfone (6 mmole), and 3,3'-disulfonated-4,4'-dichlorodiphenylsulfone (4 mmole) were charged to the flame dried 3-neck flask, which was equipped with a mechanical stirrer, nitrogen inlet and a Dean-Stark trap. Potassium carbonate (11.5 mmole) was added to the system. Dry NMP was introduced to afford about a 20% solids concentration and toluene (NMP/toluene = 2/1 v/v) was used as an azeotropic agent. The reaction mixture was heated under reflux at 150 ºC for 4 h to remove the water. Then, the bath temperature was raised slowly to 180 ºC and reacted for an additional 24 h. The viscous solution was cooled to room temperature, and then diluted with NMP. The copolymer solution was filtered to remove the salt byproduct and then isolated by precipitation in deionized water. The copolymer was separated by filtration and dried in a vacuum oven at 120 °C for 24 h.

2.2.3 Membrane preparation

The salt form copolymers were redissolved in DMAc to afford transparent 5 wt % solutions, which were then cast onto clean glass substrates. The films were slowly dried for 2 days with infrared heat at gradually increasing temperatures, and then dried under vacuum at 110 ^{o}C for 2 days. The membranes were converted to their acid form by boiling in 0.5 M H_2SO_4 for 2 h, and were then boiled in deionized water for 2 h to remove any residual acid. Membranes were stored in deionized water until used for measurement.

2.2.4 NMR, ATR-FTIR spectroscopy, DSC and intrinsic viscosity

^{1}H NMR analysis was conducted on a Varian Unity 400 spectrometer. All spectra were obtained from a 10 % solution (w/v) in a DMSO.d_6 solution at room temperature. ATR-FTIR analysis was done in Dura Samp IR instrument. DSC experiment was performed on a TA instrument in presence of N_2. The heating rate was 10 ^{o}C/min.

Intrinsic viscosities were determined in NMP at 25 ^{o}C using a Cannon Ubbelholde viscometer.

2.2.5 Measurement of proton conductivity

Proton conductivity at 30 ^{o}C at full hydration (in liquid water) was determined in a window cell geometry[14] using a Solartron 1252 + 1287 Impedance/Gain-Phase Analyzer over the frequency range of 10 Hz to 1 MHz following procedures reported in the literature.[15] Membranes were equilibrated at 30 °C in DI water for 24 h prior to the determination of proton conductivity in liquid water at 30 ^{o}C.

2.2.6 Determination of water uptake, hydration number, density and effective proton concentration (C_H^+)

The water uptake of all membranes was determined gravimetrically. First, the membranes were soaked in water at 30 °C for 2 days after acidification. Wet membranes were removed from the liquid water, blotted dry to remove surface droplets, and quickly weighed. The membranes were then dried at 120 °C under vacuum for at least 24 h and weighed again. The water uptake of the membranes was calculated according to Equation (2-1) where mass_{dry} and mass_{wet} refer to the mass of the dry membrane and the wet membrane, respectively.

$$\text{water uptake}\% = \frac{\text{mass}_{\text{wet}} - \text{mass}_{\text{dry}}}{\text{mass}_{\text{dry}}} \times 100 \qquad \textbf{Equation 2-1}$$

The hydration number (λ), number of water molecules absorbed per sulfonic acid, can be calculated from the mass water uptake and the ion content of the dry copolymer as shown in Equation (2-2), where MW_{H2O} is the molecular weight of water (18.01 g/mol) and IEC is the ion exchange capacity of the dry copolymer in milliequivalents per gram.

$$\lambda = \frac{(\text{mass}_{\text{wet}} - \text{mass}_{\text{dry}})/\text{MW}_{\text{H}_2\text{O}}}{\text{IEC} \times \text{mass}_{\text{dry}}} \text{.....} \qquad \textbf{Equation 2-2}$$

For density determination, the samples were equilibrated in water. The dried dimensions were obtained by drying the wet membrane at 80 °C in a convection oven for 2 h. Density was calculated from the volume and weight of the dried membranes. An average of 4 samples was taken for each measurement. The effective proton concentration was determined from the water uptake, density and IEC using the following expression

$$C_{H^+} = \frac{IEC \times Density}{(1 + 0.01 \times wateruptake \times Density)} \qquad \textbf{Equation 2-3}$$

2.2.7 Methanol permeability and DMFC performance

Methanol permeability of the membranes was determined by measuring the crossover current in a DMFC under open circuit conditions. The measurement was performed in an identical manner to that of Ren et al.[16]

DMFC performance or the VIR curves were obtained using Fuel Cell Technologies test stand as described earlier.[17] The methanol feed concentration was 0.5 M, air flow rate at cathode was 500 sccm at 90 °C and the cell temperature was 80 °C.

2.3 Results and Discussion

2.3.1 Copolymer synthesis

Hydroquinone based disulfonated poly(arylene ether sulfone)s copolymers were successfully synthesized by a nucleophilic aromatic substitution reaction. A series of copolymers was prepared with varying degrees of disulfonation (SDCDPS content). The high IV values suggest the formation of high molecular weight disulfonated copolymers. The structure of the copolymers was confirmed by ^{1}H NMR spectroscopy. A representative spectrum for HQSH 25 is shown in Figure (2-2). The degree of disulfonation was calculated from the ratio of the protons associated with DCDPS to the protons associated with SDCPDS monomer. The ion exchange capacity (IEC) is a measure of the ionic content, which was calculated from the experimentally determined degree of disulfonation using previously reported procedures.[7] The values matched with the target IEC for all the copolymers, which is shown in Table (2-1). ATR-FTIR analysis (Fig. 2-3) confirmed the successful incorporation of sulfonate groups. The strong characteristic peaks at 1030 cm^{-1} and 1098 cm^{-1} were assigned to symmetric and asymmetric stretching of the sulfonate groups, respectively. Glass transition temperatures were determined from the DSC measurements for the acidified form of the samples. The T_g increased with increasing degree of disulfonation.

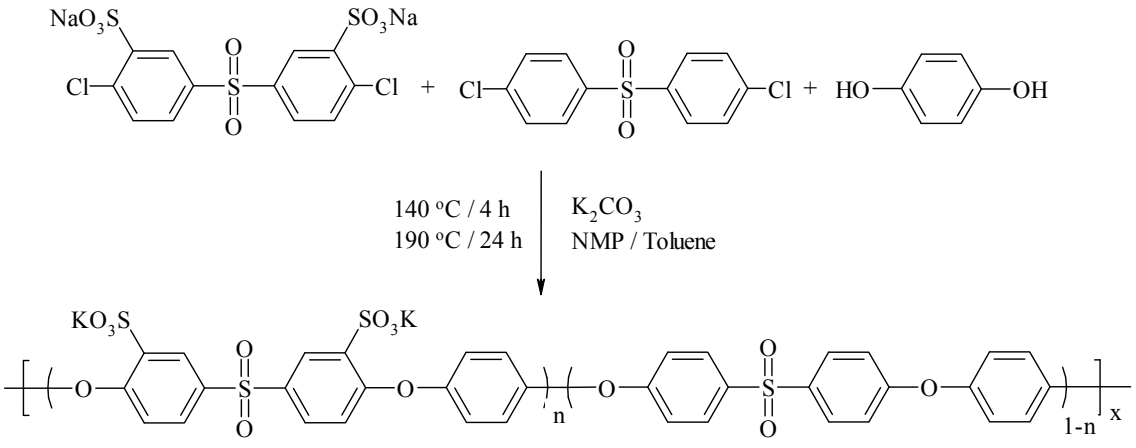

Figure 2-1 Synthetic scheme for HQS-xx random copolymers

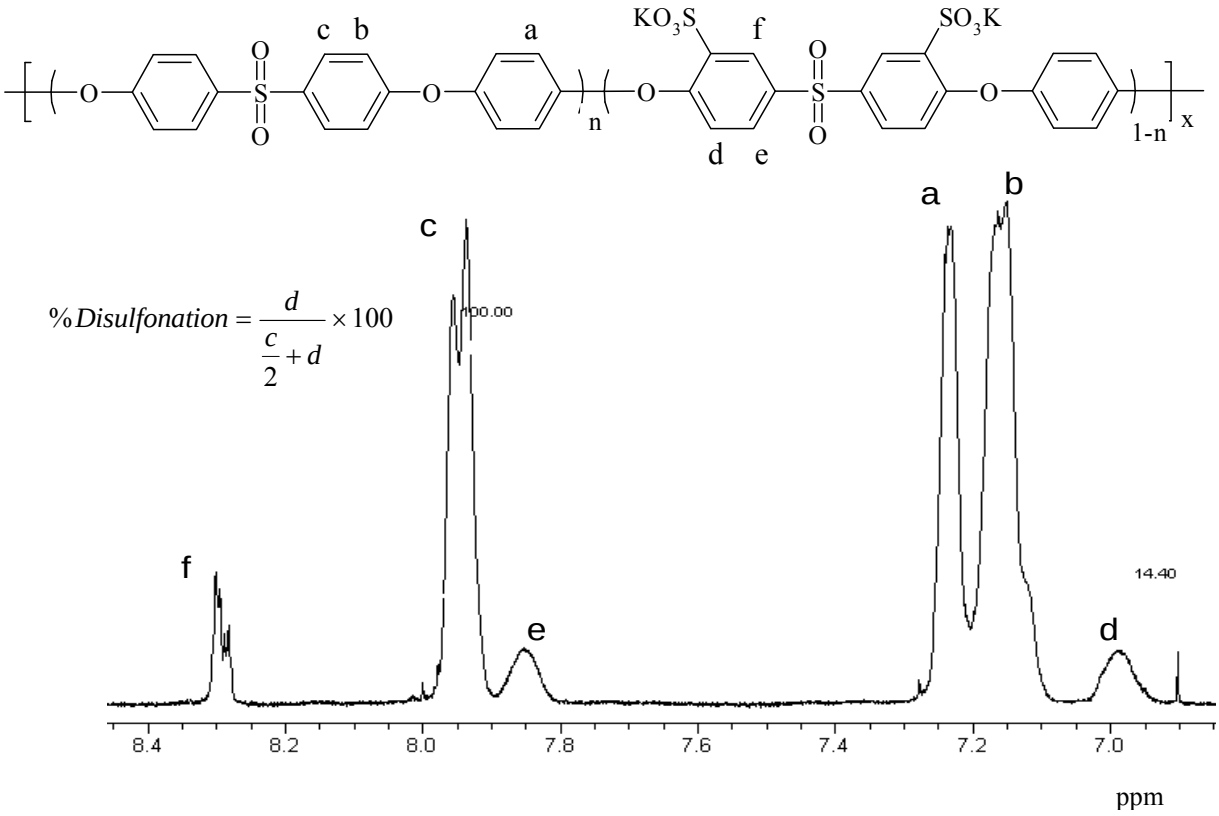

Figure 2-2 ^{1}H NMR spectrum of HQS-25 random copolymer; only the aromatic region is displayed

Table 2-1 Summary of the properties of HQSH-xx copolymers

HQSH-xx sample (xx)	Target IEC (meq/g)	IEC from ^{1}H NMR	IV* (dL/g)	T_g** (^{o}C)
20	1.2	1.1	0.8	220
25	1.4	1.3	1.6	227
30	1.6	1.6	1.1	230
35	1.8	1.8	1.5	237
40	2.0	2.1	1.0	240

* in NMP at 25 ^{o}C

** from DSC, N_2, 10 ^{o}C/min

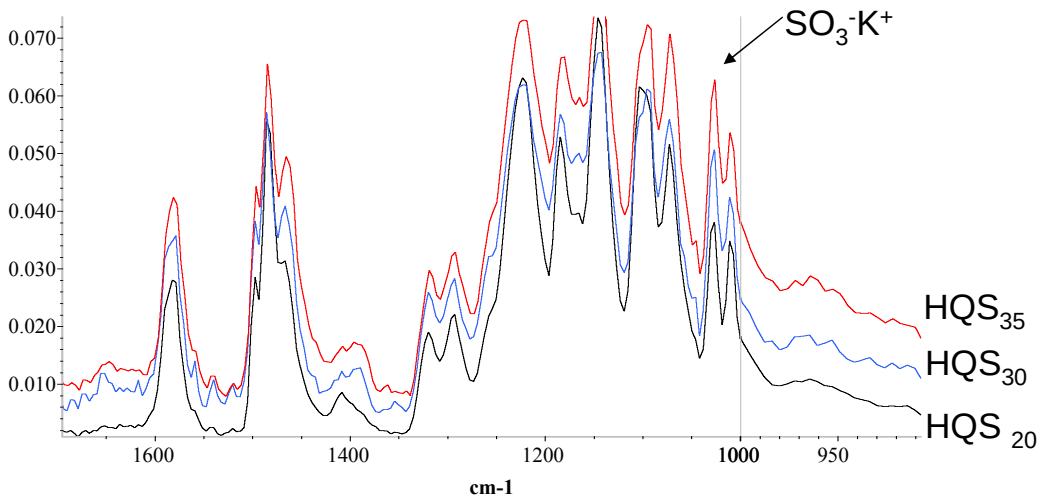

Figure 2-3 ATR-FTIR spectra of HQS-xx copolymers confirming the presence of sulfonate groups

2.3.2 Water uptake

Figure (2-4) depicts two plots for water uptake as a function of IEC for both the HQSH-xx and BPSH-xx[8] copolymers. As shown, water uptake increased with increasing ion exchange capacity. Moreover, a sharp increase in water uptake is observed from IEC 1.6 to 1.8 for the HQSH-xx copolymers. A similar increase was observed for the BPSH-xx copolymer over the IEC range of 1.7 to 2.0. AFM studies of the BPSH-xx systems, associated this sharp increase to a morphological transition from a closed to an open system where the hydrophilic system is the continuous phase.[18] Similar explanations can be drawn for the HQSH-xx copolymers as well. At a given IEC, the HQSH-xx absorbs more water than the BPSH-xx copolymers, which indicates a more open structure for the HQSH-xx copolymers. The rigidity of the backbone influences the water absorption characteristics of these PEMs.

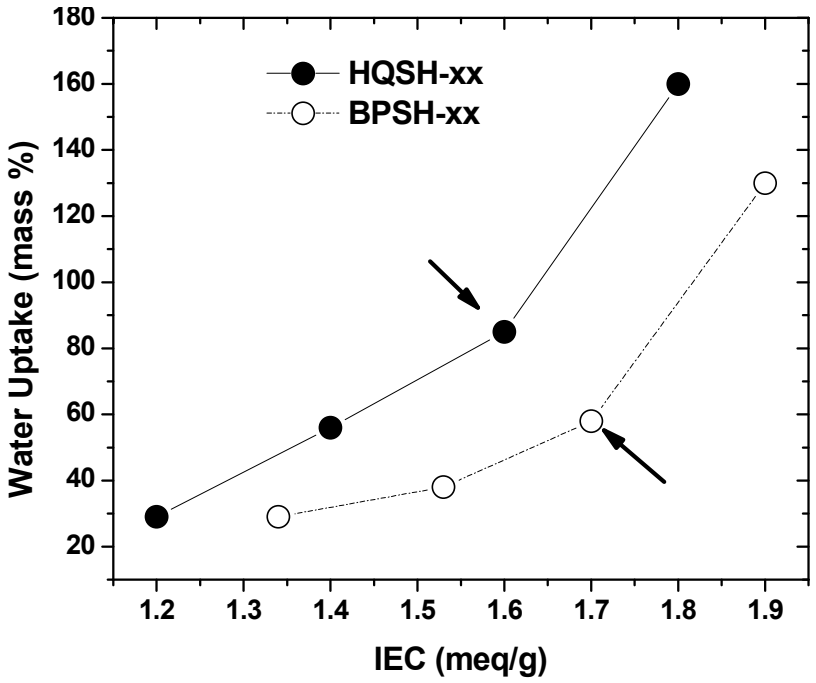

Figure 2-4 Water uptake as a function of IEC for HQSH-xx and BPSH-xx random copolymers

2.3.3 Proton conductivity

Proton conductivity values measured in liquid water at 30 ^{o}C are reported in Table (2-2) along with hydration numbers and IEC results. The BPSH-xx copolymers are included for comparative purposes.[8, 19] Proton conductivity is a function of both proton diffusivity and proton concentration. For most of the random copolymers, proton conductivity scales with IEC. However, the proton conductivity of HQSH-xx copolymers passes through maxima at an IEC of 1.6 meq/g and then decreases. This can be explained in terms of effective proton concentration. Although the proton concentration increases with IEC, the increased water swelling in the membrane decreases the effective charge or proton concentration. The calculated effective proton concentrations (C_H^+) for the HQSH-xx and BPSH-xx copolymers are provided in Table (2-2). The effective C_H^+ remains similar over the IEC range studied for the BPSH-xx copolymers. The increased water uptake for HQSH 35 (1.8 meq/g) significantly decreases the C_H^+ value, which corresponded to a decrease in the overall proton

conductivity for this copolymer. When comparing the two series of copolymers at a given IEC (1.2 to 1.6) meq/g, the HQSH displays higher proton conductivity values over the BPSH-xx copolymers, indicating a much favored and open morphology compared to the BPSH-xx copolymers. In addition to ionic content, the selectivity of proton conductivity over the water absorption is a function of the chemical structure as well.

Table 2-2 Proton exchange membrane properties of HQSH-xx and BPSH-xx[19] copolymers

Sample	IEC (meq/g)	Density (g/cc)	Hydration number (λ)	Proton conductivity* (S/cm)	Effective C_{H^+} (meq/cc)	Methanol permeability (10^{-6} cm^2/s)**
HQSH-35	1.8	1.4	80	0.08	0.54	-
HQSH-30	1.6	1.3	29	0.103	1.00	1.1
HQSH-25	1.4	1.3	23	0.08	1.03	0.46
HQSH-20	1.2	1.3	13	0.06	1.11	0.34
BPSH-40	1.7	1.4	19	0.11	1.30	0.86
BPSH-35	1.5	1.3	14	0.07	1.37	0.56
BPSH-30	1.3	1.3	9	0.04	1.34	0.36

* measured in liquid water, 30 ^oC (± 5%), ** measured at 30 ^oC

2.3.4 DMFC performance and methanol permeability

Membrane electrode assemblies were fabricated for the HQSH-xx random copolymers with varying IEC values using the methodologies outlined in the experimental section. The composition of the electrode and the casting procedures were the same for all the copolymers. Figure (2-5) compares the DMFC performance for the HQSH-xx copolymers. The theoretical open circuit voltage for fuel cell is 1.23 V. A significant decrease in OCV was observed due to the methanol crossover. Specifically,

methanol permeates across the membrane to the cathode where it gets oxidized, thereby reducing its overall potential. HQSH-xx copolymers with higher open circuit voltage values suggest reduced methanol crossover. The membrane properties are known to govern the fuel cell performance over a voltage range of 0.7 to 0.4 V. The lower the slope of the curve, the lower is the membrane resistance. Conversely, electrode viability controls the higher voltage range (1.0-0.7) V, while mass transport characteristics dominate at the lower voltage range (0.4-0.2) V. The membrane fuel cell performance increases with increasing degrees of disulfonation to 30 %. The high water uptake values for HQSH 35 reduces the overall performance for the copolymer.

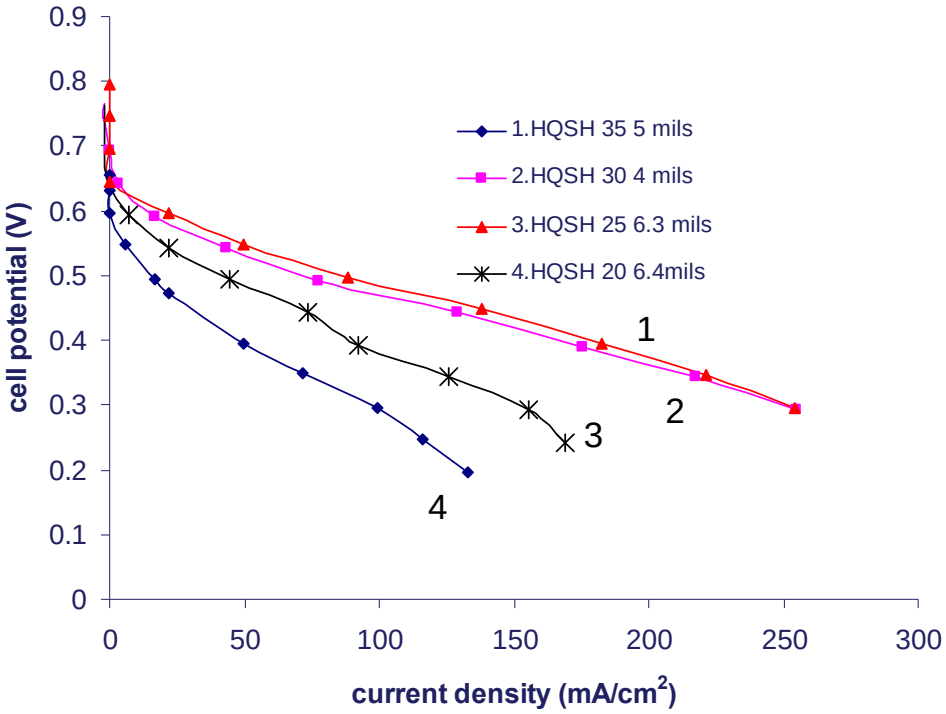

Figure 2-5 DMFC performance of HQSH-xx random copolymers as a function of degree of disulfonation; the thickness of the membranes in mils is provided in the legend

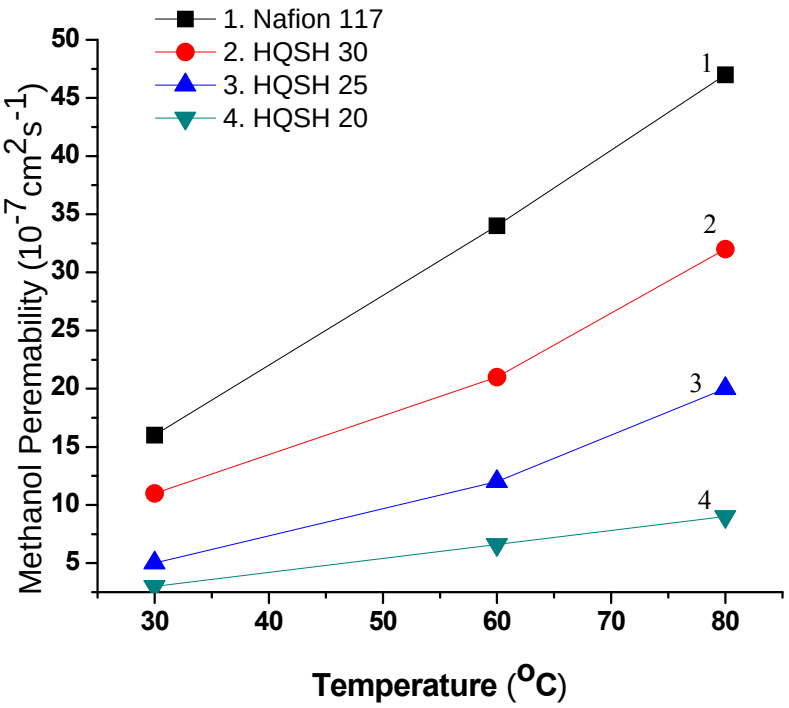

Figure 2-6 Methanol permeability as a function of temperature for the HQSH-xx copolymers

The methanol permeability of the copolymers was determined using crossover current measurements.[17] Methanol permeates across the membrane from anode to cathode and gets oxidized at the cathode. This process is associated with a reduction in the open circuit voltage and decreased fuel efficiency. HQSH-xx copolymers showed significantly lower methanol permeability compared to Nafion® 117 over a wide range of temperature, as shown in Figure (2-6). The aromatic backbone of the copolymers restricts methanol diffusion and reduces methanol permeability. At a lower IEC, the methanol permeability values for the HQSH-xx and BPSH-xx[18] are similar (Table 2-2). However, at a higher IEC (1.6 meq/g), the HQSH-xx has a slightly higher methanol permeability value. A more open morphology at higher degrees of disulfonation for the HQSH-30 facilitates the methanol transport to a small extent over the BPSH-xx copolymers.

In proton exchange membranes, a tradeoff exits between methanol permeability and proton conductivity. In other words, high proton conductivity is often associated

with high methanol permeability. Thus, the key is finding a material with high selectivity and low methanol permeability. Selectivity is defined as the ratio of proton conductivity (in liquid water) to methanol permeability. And while DMFC performance is often a function of the nature of the electrodes and many other variables, methanol selectivity is a critical membrane property.

Figure (2-7) compares the methanol selectivity as a function of the methanol permeability for the HQSH-xx, BPSH-xx and Nafion®117 copolymers. All the measurements were done at 30 ^{o}C. A clear linear relationship exists. Both BPSH-xx and HQSH-xx copolymers display high selectivity at low methanol permeability compared to Naifon® 117. On a comparative basis, both HQSH-xx and BPSH-xx copolymers show a similar relationship between selectivity and methanol permeability. HQSH-20 showed the highest selectivity at low methanol permeability.

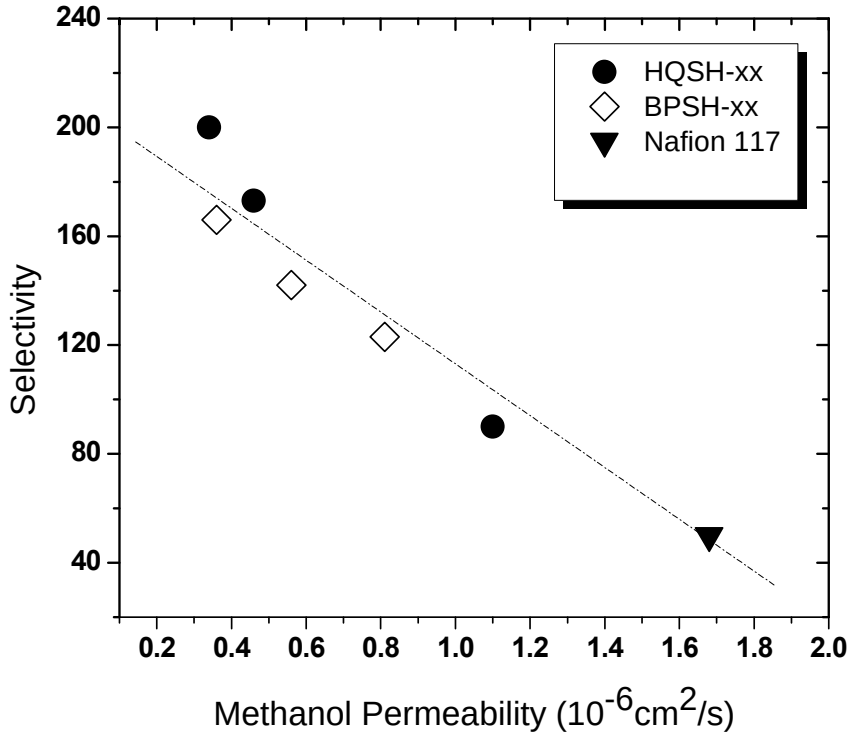

Figure 2-7 Aromatic copolymers display higher selectivity with lower methanol permeability compared to Nafion® 117

2.4 Conclusions

Partially disulfonated hydroquinone based poly(arylene ether sulfone)s copolymers were synthesized for potential application as proton exchange membranes. The copolymers were varied in degree of disulfonation to optimize the balance between the various PEM properties. Both proton conductivity and water absorption increased with increasing IEC. However, higher water uptake at higher IEC decreased the effective proton concentration and, hence, proton conductivity. Copolymers with 25 % degree of disulfonation afforded the best optimized balance between water uptake and proton conductivity. The copolymers exhibited significantly reduced methanol permeability compared to Nafion® and satisfactory DMFC performance.

Another objective of the study was to compare the properties of HQSH-xx copolymers with existing biphenol based disulfonated poly(arylene ether sulfone) (BPSH-xx) random copolymers. Because hydroquinone is less expensive than biphenol, the HQSH-xx system has a distinct economic advantage over the BPSH-xx copolymers. Moreover, the HQSH-xx system has similar IEC values when compared to those of the BPSH-xx system, but with a much lower degree of disulfonation. At a given IEC, the water absorption of HQSH-xx was higher than BPSH-xx, indicating the presence of a more open morphology, which corresponds to higher proton conductivity and slightly higher methanol permeability compared to BPSH-xx. For DMFC applications, a similar relationship between selectivity and methanol permeability was observed for both series of copolymers. The appropriate optimization of electrodes and MEA fabrication process is expected to yield very similar performance results for the HQSH-xx copolymers compared to the existing BPSH-xx copolymers.

The authors would like to thank the National Science Foundation “Partnership for Innovation” Program (HER-0090556) and the Department of Energy (DE-FC36-01G01086) for support of this research effort. The authors would also like to thank UTC Fuel Cell (#PO3561) for their support.

2.5 References

1. Winter, M.; Brodd, R. J., What are batteries, fuel cells, and supercapacitors? *Chemical Reviews* **2004,** 104, (10), 4245-4269.
2. Winter, M.; Brodd, R. J., What are batteries, fuel cells, and supercapacitors? (vol 104, pg 4245, 2003). *Chemical Reviews* **2005,** 105, (3), 1021-1021.
3. Acres, G. J. K., Recent advances in fuel cell technology and its applications. *Journal of Power Sources* **2001,** 100, (1-2), 60-66.
4. Brandon, N. P.; Skinner, S.; Steele, B. C. H., Recent advances in materials for fuel cells. *Annual Review of Materials Research* **2003,** 33, 183-213.
5. Hickner, M. A.; Ghassemi, H.; Kim, Y. S.; Einsla, B. R.; McGrath, J. E., Alternative polymer systems for proton exchange membranes (PEMs). *Chemical Reviews* **2004,** 104, (10), 4587-4611.
6. Kreuer, K.-D.; Paddison, S. J.; Spohr, E.; Schuster, M., Transport in Proton Conductors for Fuel-Cell Applications: Simulations, Elementary Reactions, and Phenomenology. *Chemical Reviews (Washington, DC, United States)* **2004,** 104, (10), 4637-4678.
7. Wang, F.; Hickner, M.; Kim, Y. S.; Zawodzinski, T. A.; McGrath, J. E., Direct polymerization of sulfonated poly(arylene ether sulfone) random (statistical) copolymers: candidates for new proton exchange membranes. *Journal of Membrane Science* **2002,** 197, (1-2), 231-242.
8. Kim, Y. S.; Wang, F.; Hickner, M.; McCartney, S.; Hong, Y. T.; Harrison, W.; Zawodzinski, T. A.; McGrath, J. E., Effect of acidification treatment and morphological stability of sulfonated poly(arylene ether sulfone) copolymer proton-exchange membranes for fuel-cell use above 100 degrees C. *Journal of Polymer Science Part B-Polymer Physics* **2003,** 41, (22), 2816-2828.
9. Kim, Y. S.; Dong, L. M.; Hickner, M. A.; Pivovar, B. S.; McGrath, J. E., Processing induced morphological development in hydrated sulfonated poly(arylene ether sulfone) copolymer membranes. *Polymer* **2003,** 44, (19), 5729-5736.

10. Roy, A.; Einsla, B. R.; Harrison, W. L.; McGrath, J. E., Synthesis and characterization of hydroquinone based disulfonated poly (arylene ether sulfone)s via direct copolymerization. *Preprints of Symposia - American Chemical Society, Division of Fuel Chemistry* **2004,** 49, (2), 614-615.

11. Harrison, W. L.; Wang, F.; Mecham, J. B.; Bhanu, V. A.; Hill, M.; Kim, Y. S.; McGrath, J. E., Influence of the bisphenol structure on the direct synthesis of sulfonated poly(arylene ether) copolymers. I. *Journal of Polymer Science Part a-Polymer Chemistry* **2003,** 41, (14), 2264-2276.

12. Wang, F.; Hickner, M.; Ji, Q.; Harrison, W.; Mecham, J.; Zawodzinski, T. A.; McGrath, J. E., Synthesis of highly sulfonated poly(arylene ether sulfone) random (statistical) copolymers via direct polymerization. *Macromolecular Symposia* **2001,** 175, 387-395.

13. Sankir, M.; Bhanu, V. A.; Harrison, W. L.; Ghassemi, H.; Wiles, K. B.; Glass, T. E.; Brink, A. E.; Brink, M. H.; McGrath, J. E., Synthesis and characterization of 3,3 '-disulfonated-4,4 '-dichlorodiphenyl sulfone (SDCDPS) monomer for proton exchange membranes (PEM) in fuel cell applications. *Journal of Applied Polymer Science* **2006,** 100, (6), 4595-4602.

14. Zawodzinski, T. A.; Neeman, M.; Sillerud, L. O.; Gottesfeld, S., *J. Phys. Chem.* **1991,** 95, 6040.

15. Springer, T. E.; Zawodzinski, T. A.; Wilson, M. S.; Gottesfeld, S., *J. Electrochem. Soc.* **1996,** 143, 587.

16. Ren, X. M.; Springer, T. E.; Zawodzinski, T. A.; Gottesfeld, S., Methanol transport through nafion membranes - Electro-osmotic drag effects on potential step measurements. *Journal of the Electrochemical Society* **2000,** 147, (2), 466-474.

17. Kim, Y. S.; Sumner, M. J.; Harrison, W. L.; Riffle, J. S.; McGrath, J. E.; Pivovar, B. S., Direct methanol fuel cell performance of disulfonated poly-arylene ether benzonitrile) copolymers. *Journal of the Electrochemical Society* **2004,** 151, (12), A2150-a2156.

18. Kim, Y. S.; Hickner, M. A.; Dong, L. M.; Pivovar, B. S.; McGrath, J. E., Sulfonated poly(arylene ether sulfone) copolymer proton exchange membranes:

composition and morphology effects on the methanol permeability. *Journal of Membrane Science* **2004,** 243, (1-2), 317-326.

3.0 Influence of Chemical Composition and Sequence Length on the Transport Properties of Proton Exchange Membranes[1]

Abhishek Roy,[1] Michael A. Hickner,[2] Xiang Yu,[1] Yanxiang Li,[1] Thomas E. Glass,[1] and James E. McGrath[1]

[1] Macromolecules and Interfaces Institute
Virginia Polytechnic Institute and State University, Blacksburg, VA 24061
[2] Present Address: Department of Materials Science and Engineering
The Pennsylvania State University, University Park, PA 16802

Abstract

One of the integral parts of the fuel cell is the proton exchange membrane. Our research group has been engaged in the past few years in the synthesis of several sulfonated poly(arylene ether) random copolymers. The copolymers were varied in both the bisphenol structure as well as in the functional groups in the backbone such as sulfone and ketones. To compare the effect of sequence length, multiblock copolymers based on poly(arylene ether sulfone)s were synthesized. This paper aims to describe our investigation of the effect of chemical composition, morphology, and ion exchange capacity (IEC) on the transport properties of proton conducting membranes. The key properties examined were proton conductivity, methanol permeability, and water self-diffusion coefficient in the membranes. It was observed that under fully hydrated conditions, proton conductivity for both random and block copolymers was a function of IEC and water uptake. However, under partially hydrated conditions, the block copolymers showed improved proton conductivity over the random copolymers. The proton conductivity for the block copolymer series was found to increase with increasing block lengths under partially hydrated conditions.

---

[1] Roy, A.; Hickner, M. A.; Yu, X.; Li, Y.; Glass, T. E.; McGrath, J. E., Influence of chemical composition and sequence length on the transport properties of proton exchange membranes. *Journal of Polymer Science, Part B: Polymer Physics* **2006,** 44, (16), 2226-2239. Reprinted by permission from John Wiley & Sons, Inc

3.1 Introduction

Fuel cells are electrochemical devices that convert chemical energy directly into electrical energy.[1] Proton exchange membrane fuel cells (PEMFC) have shown promise as alternative portable, automotive, and stationary power sources.[1, 2] One of the important components in a PEMFC is the proton exchange membrane (PEM), which serves as the electrolyte that transfers protons from the anode to the cathode and separates the fuel and oxidizer. The current state of the art PEMs are perfluorosulfonic acid membranes such as Nafion® manufactured by DuPont. These membranes show excellent chemical and electrochemical stability as well as high proton conductivity with relatively low water uptake on a mass basis. However, Nafion® suffers from disadvantages including high cost, high methanol permeability (DMFCs), and limited operating temperature (80°C)[3, 4] due to its depressed hydrated α relaxation temperature.[5]

Our research group has been engaged in the past few years in the synthesis and characterization of biphenol based partially disulfonated poly(arylene ether sulfone) random copolymers as potential PEMs.[6-11] This series of polymers are called BPSH-xx [Fig.3-1(a)], where BP stands for biphenol, S is for sulfonated, and H denotes the proton form of the acid where xx represents the degree of disulfonation. Along with the BPSH series, hydroquinone based partially disulfonated poly(arylene ether sulfone)[12] [HQSH-xx – Fig. 3-1(b)] random copolymers and partially disulfonated poly(arylene ether ketone) random copolymers[13] [B-ketone-xx & PB-diketone-xx series – Fig. 3-1(c)] were synthesized. The B-ketone-xx series has a mono ketone functional group per repeat unit and the PB-diketone-xx series has a di-ketone functional group per repeat unit. In addition to the random copolymers, a series of multiblock copolymers [Block BisAF-BPSH(x:y)K series – Fig. 3-1(d)] was also synthesized.[14] In the multiblock copolymer series, BisAF (fluorinated bisphenolA) is the hydrophobic unit and BPSH with 100% degree of disulfonation is the hydrophilic unit. Here x and y represent the block length in g/mole of hydrophobic: hydrophilic units respectively.

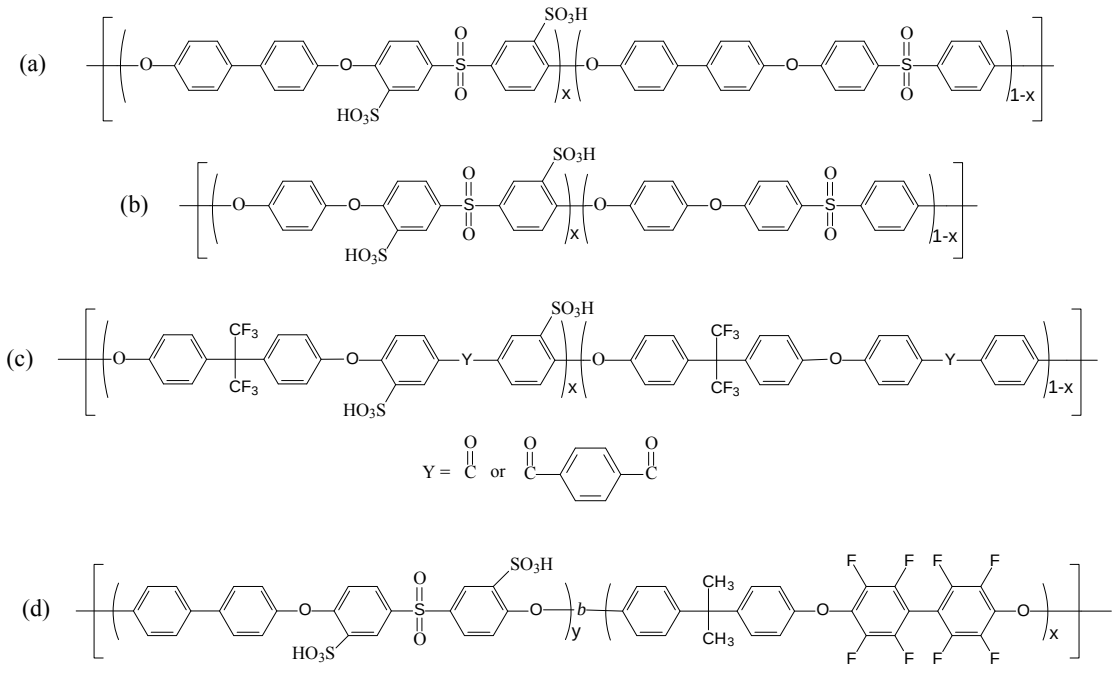

Figure 3-1 Copolymer chemical structures synthesized in this work (a) BPSH-xx; (b) HQSH-xx, (c) B-ketone-xx & PB-diketone-xx, (d) Block BisAF-BPSH(x:y)K

The copolymers were varied in both chemical composition and ion concentration to obtain desirable properties. The transport of water and protons in these systems is both of fundamental interest in terms of structure/property relationships for proton exchange membranes and technological importance in the design of new materials for fuel cells. This paper aims to describe our investigation of the effect of chemical composition, sequence length, morphology and ion concentration on the transport properties for proton conducting membranes. The key properties examined were proton conductivity, methanol permeability and the self-diffusion coefficient of water in the membrane.

3.1.1 Proton conductivity

Proton transport in aqueous environments has been studied extensively and can be described by two principal mechanisms.[15-17] The first is the Grotthuss[18] mechanism

where the protons are transferred down a chain of correlated hydrogen bonds forming, and reforming hydronium cations (H_3O^+). The second mechanism as described by Kreuer[19] is referred to as the vehicle mechanism. It is believed to occur by bulk diffusion of a proton and its associated water molecules or "vehicle" in an H_3O^+, H_5O^{2+}, or other $H_{2n+1}O^{n+}$ cation species. Hence, the self-diffusion coefficient of water is of great importance in understanding the transport behavior of protons as shown by both Kreuer, et al.[16] and Zawodzinski, et al.[20] Both these reports have provided evidence for the vehicle mechanism dominating at low water contents (or hydration number, λ) where the diffusion coefficients of protons and water are similar: water and protons move in concert. At high water contents, the Grotthuss mechanism dominates proton conduction where the computed diffusion coefficient of protons is higher than that of the measured water self-diffusion coefficients: Protons are moving faster across the membrane than the water.

To understand the effect of chemical structure and chemical compositions of the copolymer on proton transport, we have chosen to study proton transport over a range of hydration levels. It has been reported in the literature that for Nafion®, both the water self-diffusion coefficients and proton conductivity increase with increase in hydration levels.[20] Similar observations have been found for the BPSH type random copolymer membranes.[21] As reported earlier, sulfonic acid containing ionomers tend to phase separate into a nano-phase separated hydrophilic and hydrophobic domain morphology with an increase in hydration levels.[7, 10, 22] In other words, the hydrated hydrophilic domains interconnect to form an associated, percolated type morphology. However, at low hydration levels most of the water is tightly associated with sulfonic groups and has a low diffusion coefficient. This tends to form an isolated domain morphology. Thus, although there may be significant concentrations of protons, the transport is limited by the discontinuous morphological structure. With an increase in hydration levels, water assisted percolated structure ensures proper connectivity between the ionic domains. This is marked by the increase in diffusion coefficients of water as transport of water is facilitated though the interconnected channels.

The challenge lies in how to modify the chemistry of the polymers to obtain significant proton conductivity at low hydration levels where the self-diffusion coefficients of the water may still be quite low due to its association to the acid groups. High conductivity at low degrees of disulfonation and low hydration levels may be possible if one can alter the sequential chemical structure of the polymer backbone to produce block copolymers.

Block copolymers[23] consist of two or more chemically dissimilar backbone segments (i.e. blocks) that are chemically conjoined though covalent bonds in the same chain. In many cases where the blocks are immiscible, this leads to improved morphological control by tailoring the chemical composition, molecular weight, and volume fraction of the blocks, and thus the creation of new materials with properties that were not possible in a single phase. In a block ionomer proton exchange membranes, the ionic groups act as proton conducting sites, while the non-ionic component provides dimensional strength and, in the case of DMFCs, may serve as a barrier for methanol transport. Relatively few attempts have been made in the development of block copolymer ionomers having thermally and chemically stable aromatic backbone.[24-26] Synthesis of such systems is made possible by step growth polymerization, i.e. hydrophobic and hydrophilic telechelic macromonomers with appropriate end groups may be copolymerized to obtain multiblock, or segmented, copolymer ionomers. We have recently synthesized a series of multiblock ionomers having highly fluorinated hydrophobic blocks and poly(arylene ether sulfone) hydrophilic blocks with 100% degree of sulfonation [Fig. 3-1(d)].[14, 27] Unlike the BPSH-xx copolymers, where the sulfonic acid groups are randomly distributed in pairs along the chain, the multiblock copolymers will feature an ordered sequence of hydrophilic and hydrophobic segments. If connectivity is established between the hydrophilic domains in these multiblock copolymers, they will not need as much water to form a percolated structure, and hence may show much better proton conductivity than the random copolymers (with similar ionic compositions) under partially hydrated conditions.

3.1.2 Methanol permeability

Methanol permeability is a critical transport property when considering a new proton exchange membrane for use in liquid-fed direct methanol fuel cells. Methanol that is unoxidized at the anode can "cross over" though the membrane and be oxidized at the cathode. This methanol short circuit decreases the fuel efficiency of the system, lowers the cell voltage by causing a mixed potential at the cathode, and increases cell heating. Many novel PEMs have low methanol permeability, but their proton conductivity tends to decrease as well. Membranes with low crossover and high conductivity are sought while still maintaining the ability to form robust junctions at the membrane-electrode interface.

Two common methods for measuring the methanol permeability of PEMs are a membrane separated cell[28] and an open circuit electrochemical crossover measurements in a DMFC.[29] The two methods have been shown to be approximately equivalent.[30]

3.1.3 Self-diffusion coefficient of water

One of the most important techniques for measuring self-diffusion coefficients of water is by pulsed-field gradient spin echo nuclear magnetic resonance (PGSE NMR).[31-35] One of the main advantages of this method is that the measured diffusion coefficients can be related to the mean square displacement of the water molecule, or the effective diffusion length scale[31, 32, 36-38] because the time over which the diffusion measurement is made is known. The displacement is given by Equation (3-1)

$$\langle \Delta r \rangle = \sqrt{2 D_{eff} \Delta} \qquad \textbf{Equation 3-1}$$

for a gradient in one direction. This will provide insight for probing the influence of the restricted morphology on the transport properties.

3.2 Experimental

3.2.1 Materials

Highly purified 4,4'-dichlorodiphenylsulfone (DCDPS) was provided by Solvay Advanced Polymers. Biphenol (BP) and hydroquinone (HQ) was obtained from Eastman Chemical. 4,4'-Hexafluoroisopropylidenediphenol (6F-BPA), received from Ciba, was purified by sublimation. The ketone monomers: 4,4'-difluorobenzophenone (DFBP), and 1,4-Bis(p-fluorobenzoyl)benzene (PBFB) were purchased from Aldrich and used as received. All these monomers were dried under vacuum prior to use. Disulfonated comonomers (SDCDPS, SDFBP, SPBFB) were synthesized according to the modified literature methods[8] and dried under vacuum before copolymerization. The solvent N,N-dimethylacetamide (DMAc, Fisher) and N-methyl-2-pyrrolidinone (NMP, Fisher) was vacuum-distilled from calcium hydride onto molecular sieves. Potassium carbonate (Aldrich) was dried in vacuum before copolymerization. Toluene, sodium chloride, 30% fuming sulfuric acid and methanol were obtained from Aldrich and used as received. The fuming sulfuric acid was further analyzed for active SO_3 concentration.[39] Nafion® 112 and Nafion® 117 were obtained from ElectroChem, Inc.

3.2.2 Synthesis of disulfonated poly(arylene ether) random copolymers (BPSH-xx, HQSH-xx, B-ketone-xx and PB-diketone-xx)

Two series of disulfonated poly (arylene ether sulfone) random copolymers were synthesized via aromatic nucleophilic substitution as reported earlier.[8, 12] One typical copolymerization for a BPSH-32 copolymer was as follows: The 4,4'-biphenol (1.8621g, 10 mmole), 4,4'-dichlorodiphenyl sulfone (1.9528g, 6.8 mmole), and 3,3'-disulfonated 4,4'-dichlorodiphenyl sulfone (1.5721g, 3.2 mmole) were copolymerized in dry DMAc solvent under nitrogen. 1.15 equivalent potassium carbonate was added and toluene (DMAc/toluene = 2/1 v/v) was used as an azeotropic agent to dehydrate the system. The HQSH series copolymers were synthesized with hydroquinone instead of biphenol. The two series disulfonate poly(arylene ether sulfone) copolymers were designated as BPSH-

xx and HQSH-xx (acid form) [Fig. 3-1(a,b)]. The copolymerization procedures for polyketones were similar to those of polysulfones, although the monomers' reactivities are different. The detailed procedure was also introduced in the literature.[13] The PB-diketone-xx series [Fig.3-1(c)] copolymers were based on monomers 6F BPA, PBFB, and SPBFB, while the B-ketone-xx series [Fig. 3-1(c)] copolymers were based on 6F BPA, DFBP, and SDFBP. Because the fluorinated monomers have higher reactivity, high molecular weight copolymers can be achieved within shorter reaction times.

3.2.3 *Synthesis of the hydrophilic/hydrophobic multiblock copolymers*:

The syntheses of hydrophobic and hydrophilic oligomers and multiblock copolymers were carried out as reported earlier.[14] A typical polymerization procedure was as follows: BPA (1.174g, 5.142 mmol) was added to a three neck round bottom flask equipped with a mechanical stirrer, a condenser, a nitrogen inlet and a Dean-Stark trap. NMP (10 mL) was added and the mixture was stirred until dissolved. K_2CO_3 (1.183g, 7.20 mmol) and toluene (5 mL) were added and the system was dehydrated at 150 ^oC. Then the reaction bath was cooled to 50 ^oC and decafluorobiphenyl (2.046g, 6.124mmol) was added. The polymerization was allowed to proceed at 110 ^oC for 5 h. The reaction mixture was isolated by precipitation into a H_2O/methanol (50/50 v/v) mixture. Biphenol (0.412g, 2.213 mmol), SDCDPS (0.912g, 1.856 mmol), and NMP (10 mL) were charged to another three necked round bottomed flask. The mixture was stirred until dissolved, then K_2CO_3 (0.430g, 3.12 mmol) and toluene (5 mL) were added. After dehydration at 150 ^oC the polymerization proceeded at 190 ^oC for 16 h. Then the reaction bath was cooled to 80 ^oC, and the perfluorinated hydrophobic *telechelic* oligomer (1.050g, 0.350 mmol) was dissolved in NMP and added to the same reaction flask. The bath temperature was raised to 95 ^oC and kept at this temperature for 9 h. The reaction mixture was precipitated into isopropanol to obtain a brownish fibrous polymer. A series of block copolymers BisAF-BPSH(x:y)K (Figure 3-1d) were synthesized, differing in IEC and block length. Here x and y are the molecular weights of the hydrophobic and hydrophilic blocks respectively.

3.2.4 Membrane preparation:

The salt form copolymers were redissolved in DMAc to afford transparent 5 wt % solutions, which were then cast onto clean glass substrates. The films were slowly dried for 2 days with infrared heat at gradually increasing temperatures, and then dried under vacuum at 110 ^{o}C for 2 days. The membranes were converted to their acid form by boiling in 0.5M H_2SO_4 for 2 h, and were then boiled in deionized water for 2 h to remove any residual acid. Membranes were stored in deionized water until used for measurements.

3.2.5 Proton conductivity

Proton conductivity at 30°C at full hydration (in liquid water) was determined in a window cell geometry[20] using a Solartron 1252+1287 Impedance/Gain-Phase Analyzer over the frequency range of 10 Hz - 1 MHz following the procedure reported in the literature.[40] In determining proton conductivity in liquid water, membranes were equilibrated at 30 °C in DI water for 24 h prior to the testing. The temperature range chosen for calculation of activation energy for proton transport was from 30-80°C. For determining proton conductivity under partially hydrated conditions, membranes were equilibrated in a humidity- temperature oven (ESPEC Corp., SH-240) at the specified RH and 80°C for 6 h before each measurement.

3.2.6 Water uptake

The water uptake of the membranes was determined gravimetrically.[10] The water uptake of the membranes was calculated according to Equation (3-2) where $mass_{dry}$ and $mass_{wet}$ refer to the mass of the wet membrane and the mass of the dry membrane, respectively:

$$water\ uptake\ \% = \frac{mass_{wet} - mass_{dry}}{mass_{dry}} \times 100 \qquad \textbf{Equation 3-2}$$

The hydration number (λ), number of water molecules absorbed per sulfonic acid, can be calculated from the mass water uptake and the ion content of the dry copolymer as shown in Equation (3-3),

$$\lambda = \frac{mass_{wet} - mass_{dry} / MW_{H_2O}}{IEC \cdot mass_{dry}} \qquad \textbf{Equation 3-3}$$

where MW_{H2O} is the molecular weight of water (18.01 g/mol), and IEC is the ion exchange capacity of the dry copolymer in equivalents per gram.

3.2.7 Methanol permeability

Methanol permeability of the membranes was determined by measuring the crossover current in a DMFC at open circuit. The measurement was performed in an identical manner to Ren et al.[29]

3.2.8 Pulsed-field gradient spin echo nuclear magnetic resonance (PGSE NMR).

Water self-diffusion coefficients were measured using a Varian Inova 400 MHz (for protons) nuclear magnetic resonance spectrometer with a 30 G/cm gradient diffusion probe. A total of 16 points were collected across the range of gradient strength and the signal to noise ratio enhanced by co-adding 4 scans. The standard stimulated-echo NMR pulse sequence is shown in Figure (3-2).

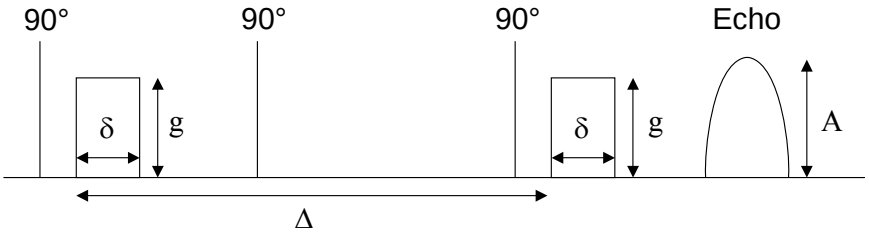

Figure 3-2 Pulse sequence schematic for PGSE NMR experiments

The measurement was conducted by observing the echo signal intensity (A) as a function of the gradient strength. The diffusion coefficient (D) was determined by fitting the data to the Equation (3- 4):[31]

$$A(g) = A(o)\exp[-\gamma^2 D g^2 \delta^2 (\Delta - \delta/3)] \qquad \textbf{Equation 3-4}$$

Where, A is the NMR signal intensity as a function of gradient strength, γ is the gyromagnetic ratio (26752 $radG^{-1}s^{-1}$ for protons), δ is length of the gradient pulse, Δ is the time between gradient pulses.

Membrane samples of approximately 5 mm by 15 mm by 150 μm were equilibrated in liquid water for at least 24 h. The samples were removed from the liquid water, blotted to remove droplets, quickly inserted into the NMR tube, and immediately measured over a span of about 5 minutes. Measurements were repeated by reimmersing the sample in DI water, waiting at least 30 minutes, and then repeating the transfer and measurement process. Separate measurements were collected with different times between the gradient pulses.

3.2.9 NMR spectroscopy, gel permeation chromatography (GPC), intrinsic viscosity and atomic force microscopy characterization (AFM).

^{1}H and ^{19}F NMR analysis were conducted on a Varian Unity 400 spectrometer. All spectra were obtained from a 10% solution (w/v) in a DMSO.d_6 solution at room temperature. GPC experiments were performed on a liquid chromatograph equipped with a Waters 1515 isocratic HPLC pump, Waters Autosampler, Waters 2414 refractive index detector and Viscotek 270 RALLS/ viscometric dual detector. NMP (containing 0.05 M LiBr) was used as the mobile phase. The column temperature was maintained at 60 ^{o}C because of the viscous nature of NMP. Both the mobile phase solvent and sample solution were filtered before introduction to the GPC system. Molecular weights were determined from universal calibration plot using polystyrene as standard. Intrinsic viscosities were determined in 0.05M LiBr NMP at 25 ^{o}C using a Cannon Ubbelholde viscometer. AFM images were taken using Digital Instruments Dimension 3000 with a micro fabricated cantilever. The force constant was 40N/m.

3.3 Results and Discussions

3.3.1 NMR spectroscopy, GPC, intrinsic viscosity and AFM characterization of the multiblock copolymer

Figure 3(a) shows the ^{1}H NMR spectra of the multiblock copolymer BisAF-BPSH(8:8)K and the corresponding sulfonated hydrophilic *telechelic* oligomer.[14] Figure 3-3(b) shows the ^{19}F NMR spectrum of BisAF-BPSH(8:8)K and that of the corresponding fluorinated hydrophobic *telechelic* oligomer. The number average molecular weights of both *telechelic* oligomers can be calculated using end-group analysis in the NMR spectra and were found to be in good agreement with the target values. The end-group peaks that are present in the spectra of *telechelic* oligomers are not observed in those of the multiblock copolymer.

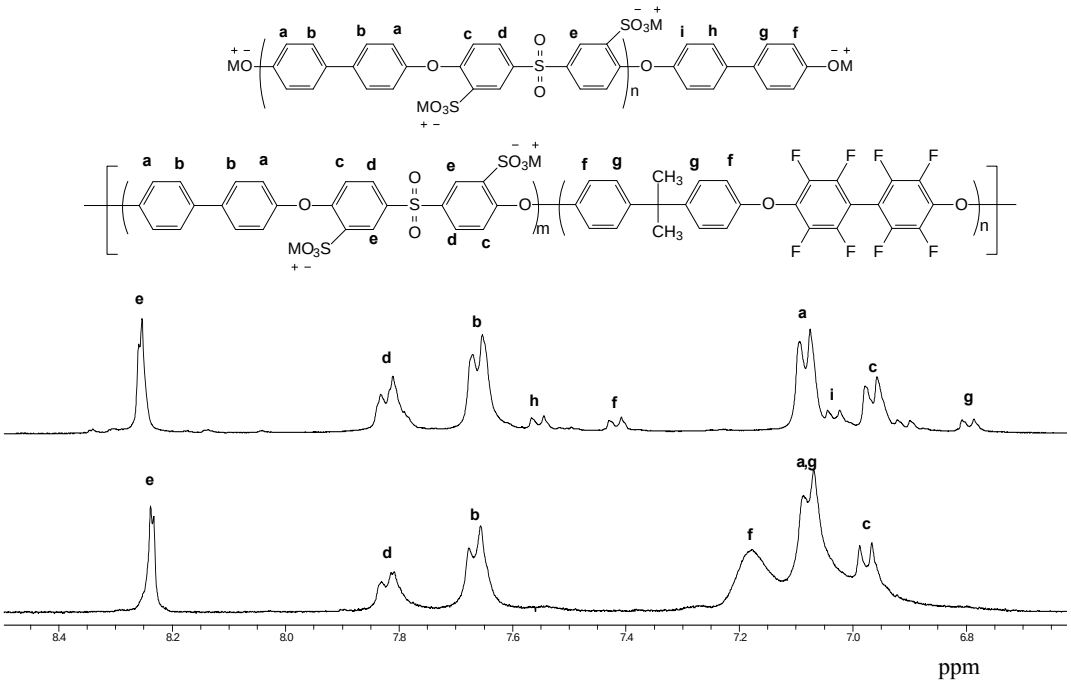

Figure 3-3 a ^{1}H NMR spectra of hydrophilic telechelic oligomer(top) and multiblock (bottom) BisAF-BPSH(8:8)K copolymer

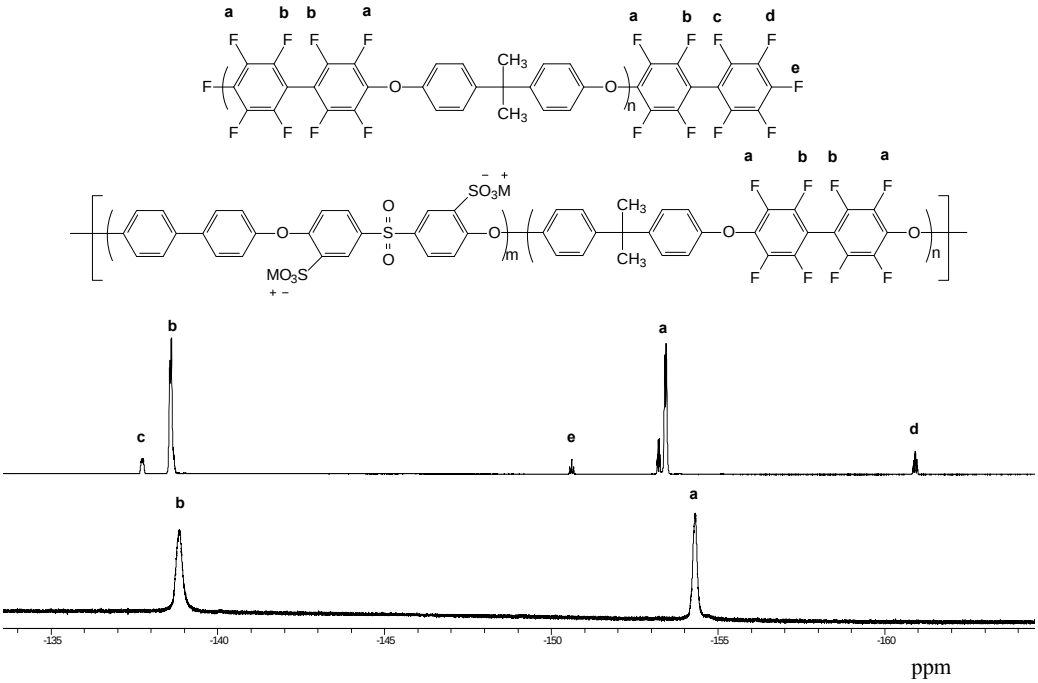

Figure 3-3 b ^{19}F NMR spectra of hydrophobic telechelic oligomer(top) and multiblock BisAF-BPSH(8:8)K (bottom) copolymer

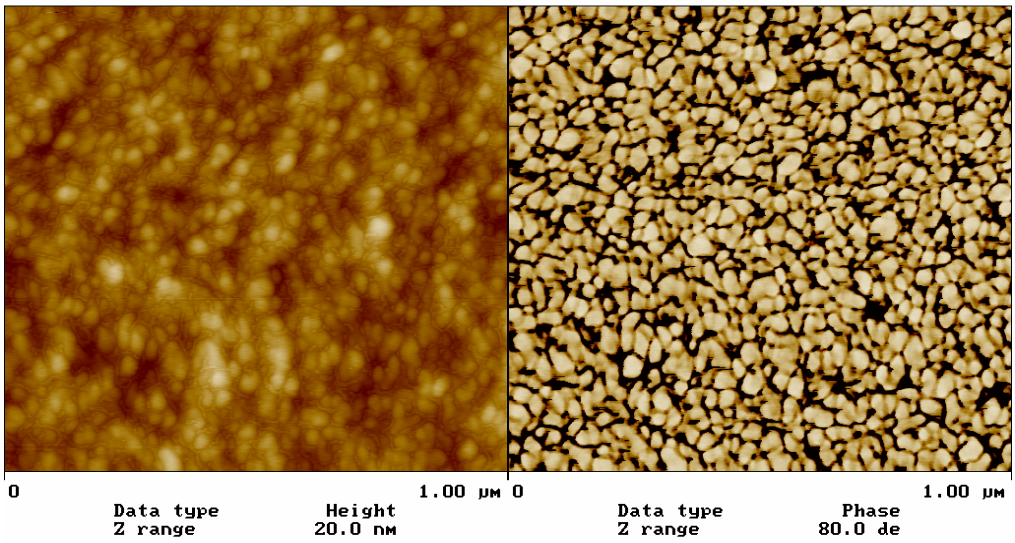

Figure 3-4 Tapping mode AFM height image(left) ,phase image(right)of block BisAF-BPSH(5:5)K indicating nano-phase separation between hydrophilic and hydrophobic domains

Table 3-1 Block lengths, IV, M_n, IEC, water uptake, and proton conductivity of the multiblock BisAF-BPSH(x:y)K copolymers

Polymer	Block lengths[a] (g/mol)	IEC[b]	IV[c]	Mn (g/mole) from GPC	Water uptake (mass %)	Proton[d] conductivity (mS/cm)
BisAF-BPSH(3:3)K	3k:3k	1.6	0.60	30K	71	130
BisAF-BPSH(5:5)K	5k:5k	1.4	0.54	30K	58	104
BisAF-BPSH(8:8)K	8k:8k	1.1	0.53	37K	42	90

[a] Block lengths are expressed in the form hydrophobic: hydrophilic

[b]Measured from ^{1}H NMR, [c]Measured at 25 °C in 0.05M LiBr NMP:

[d]Measured in liquid water at 30 °C

This confirms the high conversion in the block copolymerization. The molecular weights of the multiblock copolymers were confirmed by GPC and intrinsic viscosity data as given in Table (3-1).

Figure (3-4) shows the tapping mode AFM images of BisAF-BPSH(5:5)K multiblock copolymer, with the dark regions representing the hydrophilic domains. Although no orientated morphology can be observed, there exist sharp nanophase separated hydrophilic clusters which may be interconnected by narrow hydrophilic channels.

3.3.2 Proton conductivity and water uptake

It has been widely reported in the literature that proton conductivity for sulfonated polymers depends both on the water uptake and on the ion exchange capacity (IEC) of the material.[7] In addition to IEC, and water uptake on a mass basis, the hydration number (λ) is widely used to compare membranes of different polymer backbone architectures. Previous studies performed in our laboratory indicated that the proton conductivity scales linearly with the IEC for the BPSH-xx copolymers at fully hydrated conditions.[6, 10] Similar trends were observed for HQSH-xx, PB-diketone-xx and B-ketone-xx series as given in Figure (3-5) and Table (3-2).

The increase in proton conductivity can be explained on the basis of an increase in the concentration of protons from the acid sites and corresponding increase in water uptake. In addition to proton conductivity, it has also been reported that water uptake for these sulfonic acid containing copolymers increases with an increase in IEC.[5] It can be argued that at higher water uptake, water facilitates proton transport either by an increase in Grotthuss hopping (dynamic, long-range hydrogen-bonded water molecule chains) or by promoting the formation of percolated structure. This is supported by the decrease in activation energy for proton transport with an increase in IEC and λ as given in Table(3-2) The activation energies were calculated from the temperature dependence of proton conductivity using a simple Arrhenius analysis. The temperature dependence plots of

proton conductivity for the HQSH-xx and PB-diketone-xx series are shown in Figure (3-6) and (3-7) respectively.

Table 3-2 Water uptake, proton conductivity at 30 and 80 °C and activation energies for proton transport for HQSH-xx, PB-diketone-xx, and B-ketone-xx random copolymers

Sample	IEC (meq/g)	Water uptake (λ)	Proton conductivity (mS/cm)@ 30°C	Proton conductivity (mS/cm)@ 80°C	Activation energy E_a (kJ/mole)
HQSH 30	1.6	29	100	170	8.6
HQSH 25	1.4	24	80	140	9.0
HQSH 20	1.2	14	70	122	10.6
PB-diketone 50	1.4	26	76	141	10.4
PB-diketone 40	1.2	12	40	90	14.8
PB-diketone 30	0.9	9	10	24	15.6
B-ketone 50	1.7	32	90	156	8.5
B-ketone 40	1.4	18	73	130	10.3
B-ketone 30	1.1	13	23	40	12.9

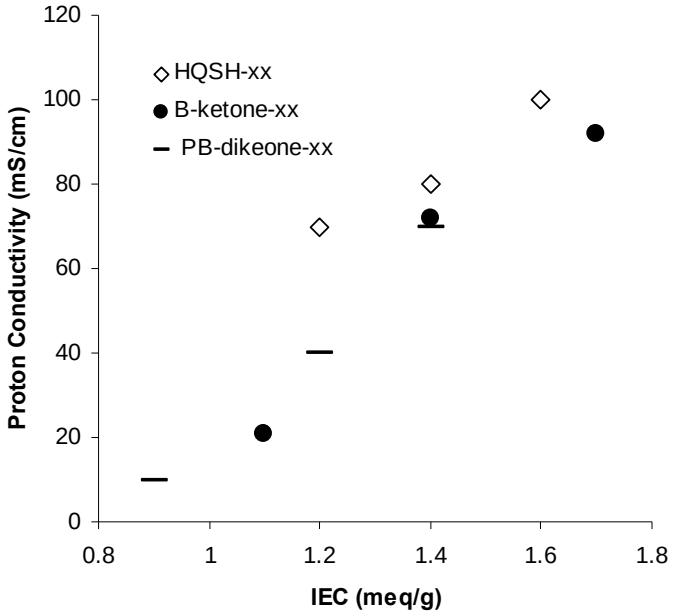

Figure 3-5 Proton conductivity for HQSH-xx, B-ketone-xx and PB-diketone-xx increases with increase in IEC

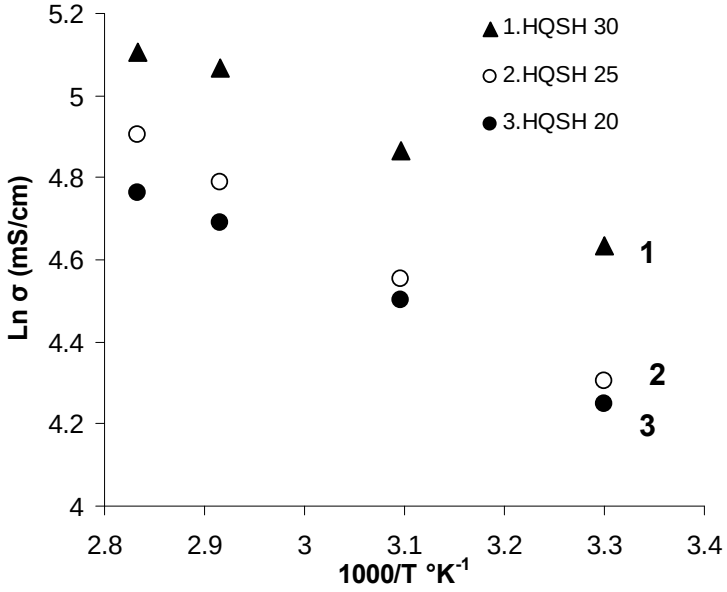

Figure 3-6 Proton conductivity for HQSH –xx random copolymers follows Arrhenius relationship with temperature

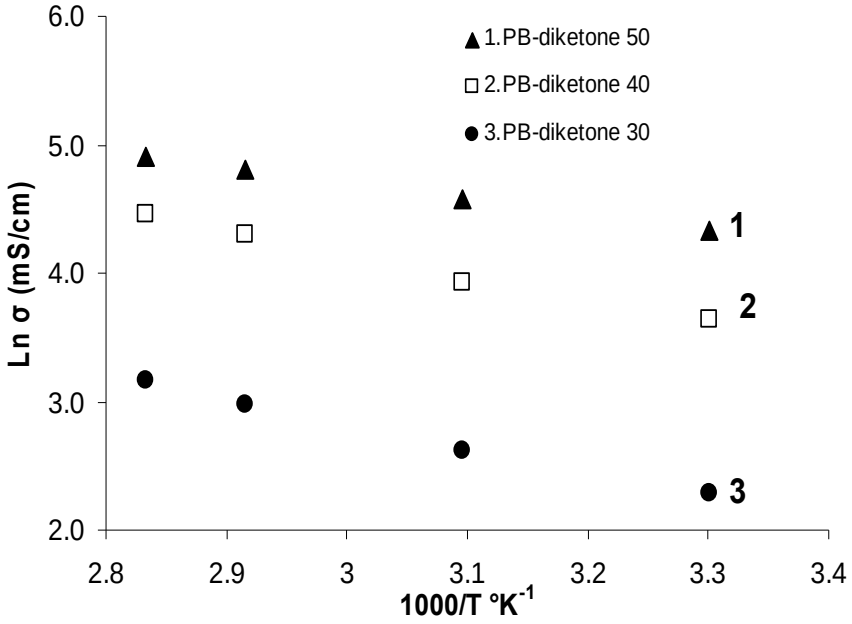

Figure 3-7 Proton conductivity for PB–diketone-xx random copolymers as a function of temperature

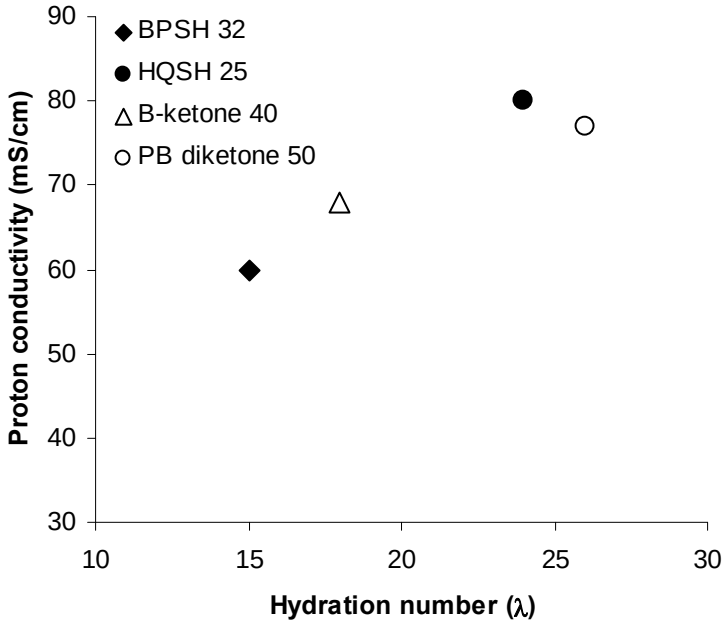

Figure 3-8 Proton conductivity for copolymers scales linearly with hydration number at IEC of 1.4 meq/g

In order to study the effect of the chemical structures on proton conductivity, the proton conductivity for different polymers with the same IEC was compared. The families of copolymers in this study have similar sulfonic acid containing moieties and hence the acidity of these copolymers is assumed to be similar. Figure (3-8) represents the plots of proton conductivity versus hydration number for the BPSH-xx, HQSH-xx, PB-diketone-xx and B-ketone-xx copolymers at an IEC of 1.4 meq/g. It is apparent from the figure that the proton conductivity at fully hydrated conditions for the copolymers with similar acidity is a function of hydration number. With increase in water uptake, proton transport is facilitated irrespective of the IEC value. Thus the chemical structures of these copolymers play a role in controlling the hydration levels which in turn dominates the proton conductivity. Now let us consider the case of the multiblock copolymers. Table (3-1) shows the proton conductivity and water uptake for the multiblock copolymers at different IECs and block lengths. It can be concluded that at fully hydrated conditions, the chemical structure or the block length has little influence on the proton transport. Similar to the random copolymers, proton conductivity increases with increase in IEC and water uptake in a systematic fashion.

Until now, only the proton conductivity under fully hydrated conditions has been discussed and the concentration of the ionic groups and hydration number were found to be the primary effect in this regime. At partially hydrated conditions, proton conductivity for BPSH[11]-xx and other random copolymers was found to be strongly dependent on the hydration levels.

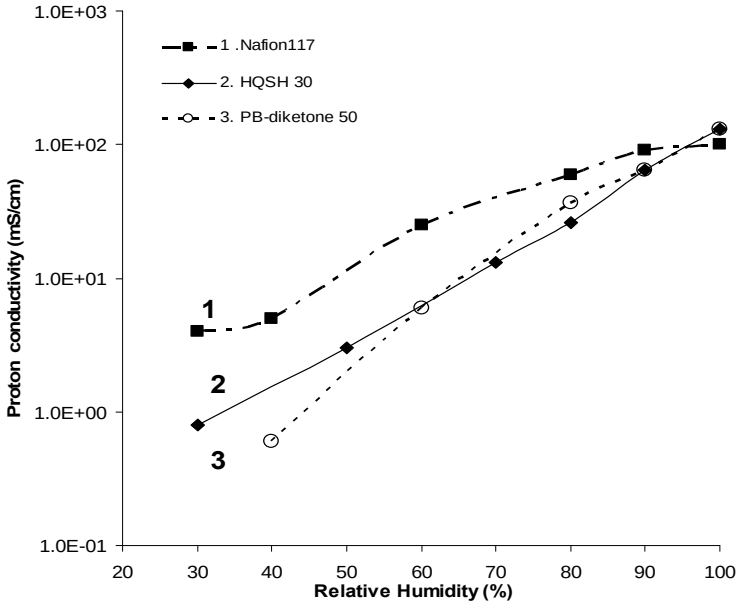

Figure 3-9 Proton conductivity as a function of relative humidity for Nafion® 117, HQSH-30 and PB-diketone-50 at 80 °C

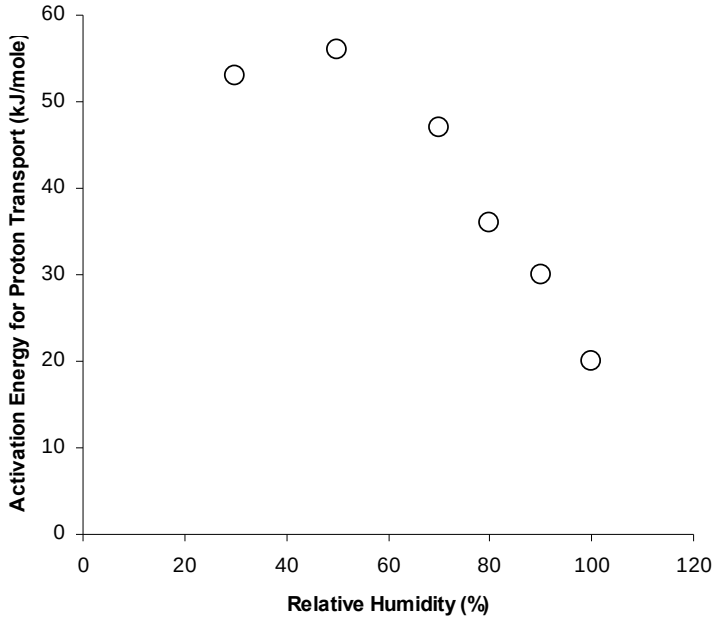

Figure 3-10 Activation energy for proton conduction for HQSH-30 random copolymer decreases with increase in relative humidity over a temperature range of 30-80 °C

Figure (3-9) shows the proton conductivity as a function of relative humidity respectively for HQSH 30, PB-diketone 50 and Nafion® 117. Below 50%RH, the proton conductivity decreases significantly for the random sulfonated aromatic copolymers. The fact is supported by the decrease in activation energy for proton transport with an increase in RH as shown in Figure (3-10) for HQSH 30. For Nafion®, the extent of decrease in conductivity at low RHs is not as severe as that measured for random copolymers. This is related to the unique chemical structure of the Nafion® which consists of highly flexible side chain hydrophilic sulfonic acid groups and a hydrophobic fluorinated flexible backbone. These chemical features apparently promote strong nano-phase separation between distinctly hydrophilic and hydrophobic domains even in random ionomers[3] and allow proton transport between the interconnected hydrophilic domains even at low hydration levels. Hence by synthesizing a predefined nano-phase segregated ionomeric block copolymer using an aromatic backbone; one may obtain improved proton conductivity under partially hydrated conditions.

Figure (3-11) shows the proton conductivity as a function of relative humidity for the block BisAF-BPSH(x:y)K series with differing block lengths and Nafion® 117. The proton conductivity of the block BisAF-BPSH(x:y)K series increases with increasing block lengths under partially hydrated conditions. This is in contrast to fully hydrated conditions where proton conductivity was a function of IEC and hydration number rather than block length. The block BisAF-BPSH(8:8)K sample has the highest proton conductivity among the block BisAF-BPSH(x:y)K copolymers across the range of relative humidity, but the lowest water uptake and IEC as shown in Table (3-1). With an increase in block length, the extent of nano-phase separation and the connectivity between the hydrophilic domains increases. This decreases the morphological barrier for proton transport and as a result, the proton conductivity increased. Under partially hydrated conditions, connectivity between the hydrophilic domains seems to be the driving force for proton transport.

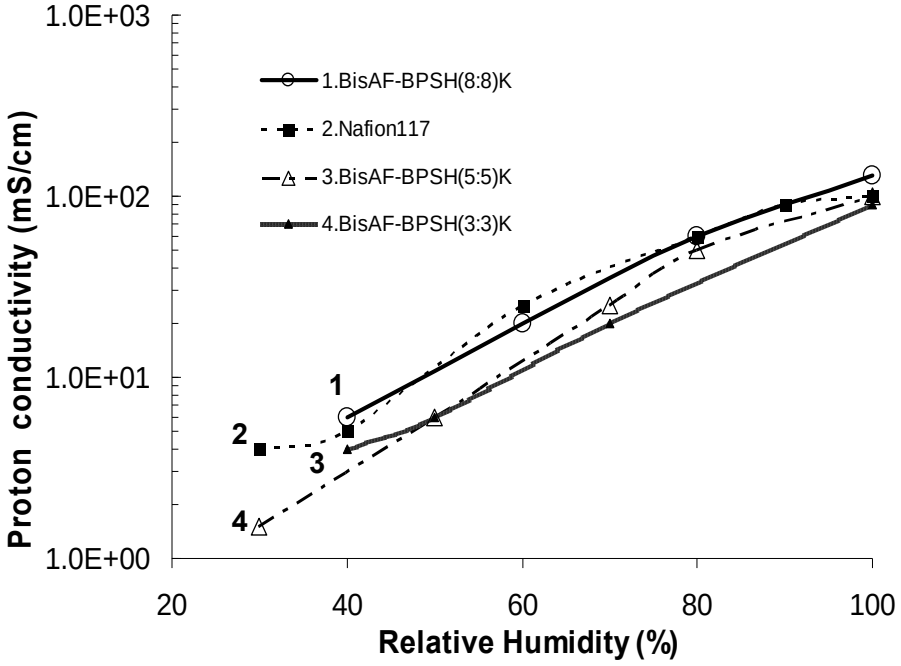

Figure 3-11 Proton conductivity for block BisAF-BPSH(x:y)K under partially hydrated condition increases with increase in block length at 80°C

3.3.3 Self-diffusion coefficient of water

The self-diffusion coefficients for water were measured by PGSE NMR. All of the samples were measured under fully hydrated conditions at 30 °C. Figure (3-12) shows the self-diffusion coefficients of water vs. IEC for the random and the multiblock copolymers. For the random copolymers, particularly for the HQSH-xx series, the diffusion coefficient increases with an increase in ion exchange capacity and so with water uptake. Surprisingly, for the block BisAF-BPSH(x:y)K series, the diffusion coefficient increased with an increase in block length irrespective of the IEC values. This clearly emphasizes the importance of connectivity between the hydrophilic domains on the transport properties.

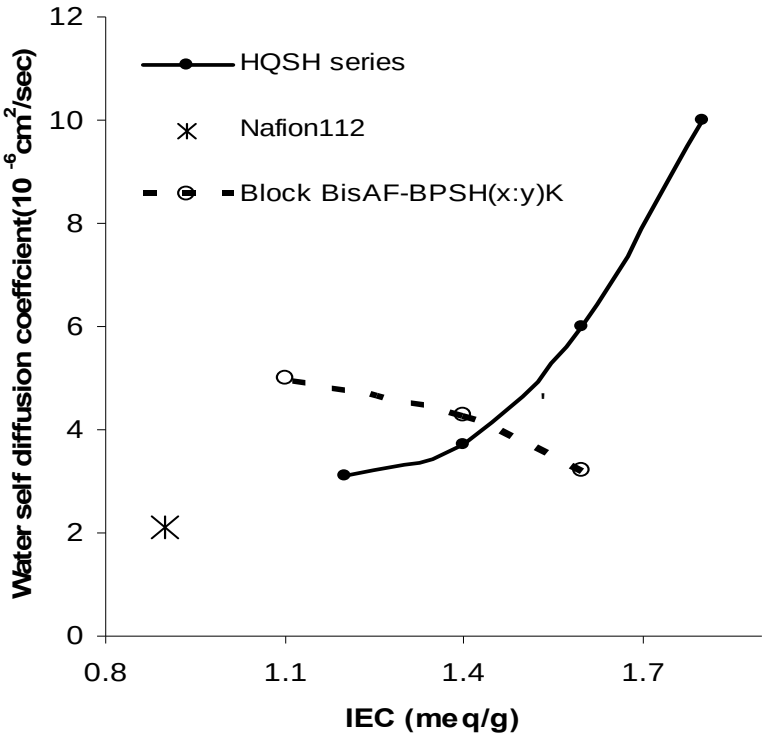

Figure 3-12 Self-diffusion coefficients for water as a function of IEC for the random and block copolymers and Nafion® 112

Probing the morphology of the interconnected channels between the hydrophilic domains will provide a better understanding about the transport mechanism. As mentioned earlier, measuring the self-diffusion coefficients of water by PGSE NMR technique allows relating the self-diffusion coefficients of water to the mean square displacement of the water molecules. The effective diffusion time (and hence the length over which the diffusion coefficient is measured) can be varied by varying the (Δ-δ/3) term in the NMR pulse sequence. It has been reported by Gebel and coauthors[41] that the self-diffusion coefficient of water in ion containing copolymers decreased with diffusion time and became constant after a particular diffusion time. The restricted diffusion can be related to a morphological barrier to the transport of water molecules over a length scale given by Equation (3-1).

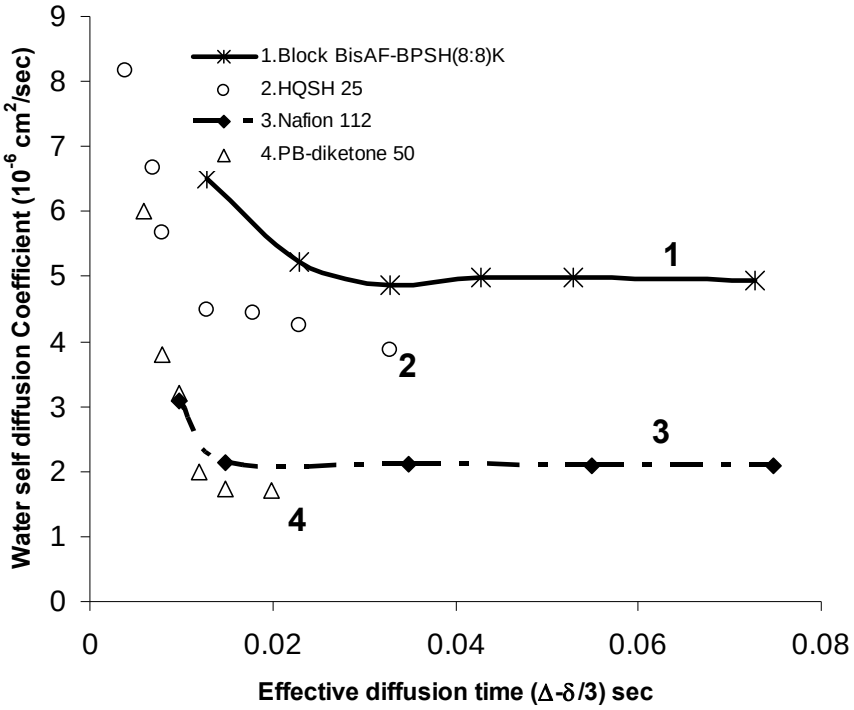

Figure 3-13 Self-diffusion coefficient of water in the polymer samples as a function of effective diffusion time indicating presence of a lower morphological barrier to transport for Nafion®112 and block BisAF-BPSH(8:8)K.

Figure (3-130 shows the self-diffusion coefficients of water versus the effective diffusion time for Nafion®112, block BisAF-BPSH(8:8)K, PB-diketone 50 and HQSH 25. The value for the diffusion coefficient is high at shorter diffusion times. With an increase in diffusion time, the diffusion coefficient decreases. This is more pronounced for the case of random copolymers, HQSH 25 and PB-diketone 50. For Nafion® and block BisAF-BPSH(8:8)K the diffusion coefficient became constant with an increase in diffusion time after a particular timescale. The water experiences less of a morphological barrier to the translational motion for the case in the block copolymers than for random copolymers. Presence of this low morphological barrier eases proton transport under partially hydrated conditions for the block copolymers. It is to be noted that the diffusion coefficient values for the block BisAF-BPSH(8:8)K is significantly higher than that of Nafion® and the random aromatic copolymers.

3.3.4 Methanol permeability

One of the major disadvantages of using Nafion® as a PEM in DMFC type fuel cell is its high methanol permeability. In comparison to Nafion®, BPSH copolymers have shown much lower methanol permeability.[10] This is true in the case for HQSH-xx, B-ketone-xx and PB-diketone-xx series also. Figure (3-14) shows methanol permeability as a function of IEC for Nafion®117, HQSH-xx, B-ketone-xx and block BisAF-BPSH(x:y)K series measured at 80 °C. Similar to conductivity data, the methanol permeability increases with an increase in IEC. Permeability is a function of both the diffusion coefficient for methanol transport and its solubility in the membrane. At higher IECs, greater water self-diffusion coefficients in the membrane may promote higher methanol diffusion and higher methanol permeability. Although a high diffusion coefficient for water is desirable for high proton conductivity, it is not desirable for lowered methanol permeability. There is a tradeoff between proton conductivity and methanol permeability when designing a new PEM for DFMC applications.

The random copolymers with the aromatic backbone and low self-diffusion coefficients of water particularly at lower IECs offer resistance to the diffusion of the methanol. This leads to lower methanol permeability than Nafion®, thus making aromatic hydrocarbon membranes one of the most promising candidates for DMFC applications.[9] As discussed earlier, the block copolymers are found to have higher self-diffusion coefficient of water at higher block lengths. However, this is not reflected in the values for methanol permeability as given in Figure (3-14).

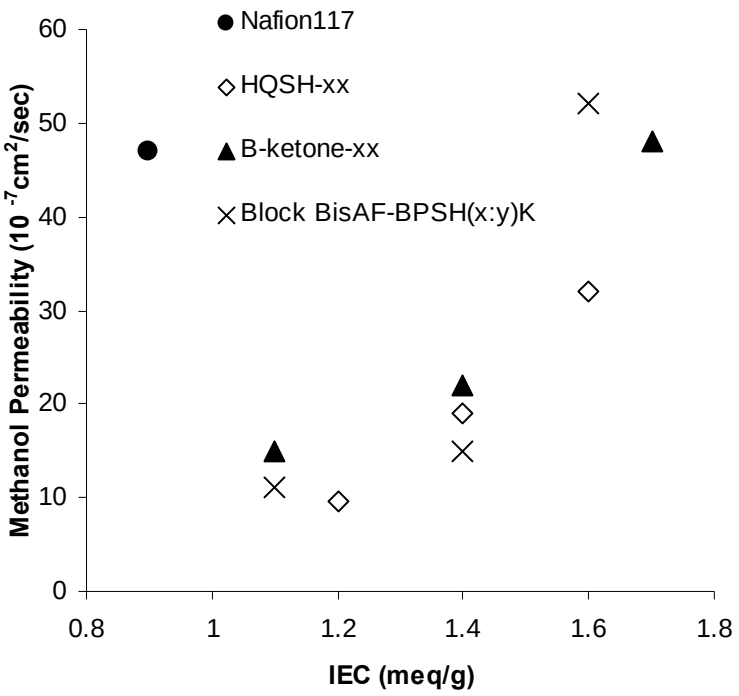

Figure 3-14 Methanol permeability for HQSH-xx, B-ketone-xx, block BisAF-BPSH(x:y)K series and Nafion®117 as a function of IEC at 80 °C

Like random copolymers, methanol permeability of the block copolymers tends to depend more on the IEC and water uptake. Hence, the mechanisms of water and methanol transport may be different in the case for block copolymers. Hydrophobic segments present in the block copolymers offer resistance to the diffusion of methanol and thus decrease the methanol permeability. In ionomeric block copolymers the hard segments may lower the methanol permeability while the soft segments provide pathways for water and proton transport.

3.4 Conclusions

The main objective of the paper was to investigate the influence of the chemical structures and compositions of novel proton exchange membranes on transport properties for fuel cell applications. Disulfonated poly(arylene ether sulfone) and poly(arylene ether ketone) based statistical or random copolymers were synthesized and the copolymers were varied in their ionic content. To compare the effect of chemical structures and sequence lengths, ion containing multiblock poly(arylene ether sulfone)s copolymers were also synthesized. Proton conductivity, methanol permeability and the self-diffusion coefficients of water were determined under different experimental conditions. Proton conductivity when measured under fully hydrated conditions showed that for both the random and block copolymers, the value increased with increase in IEC and water uptake. This is consistent with the theory of vehicle mechanism for proton transport, where water acts as a vehicle for proton transport. The influence of hydration levels in these ion containing copolymers on proton transport is more evident under partially hydrated conditions. For the random copolymers, the proton conductivity was found to decrease drastically with a decrease in hydration level. In the case of multiblock copolymers and for Nafion®, the extent of decrease in proton conductivity with hydration levels is not so severe. It was also observed that the proton conductivity under partially hydrated conditions increased with sequence or block lengths.

Synthesizing ion containing nano phase separated block copolymers, one can develop interconnected hydrophilic domains. This reduces the morphological barrier for proton transport and hence proton transport though these interconnected channels can be possible even in the absence of water. The extent of interconnectivity is expected to increase with an increase in block lengths as evident from the self-diffusion coefficient values of water. Measurements of the self-diffusion coefficients of water showed that for the block copolymers, the value increases with an increase in block lengths irrespective of decrease in IEC and water uptake values. However, for random copolymers, the value increases with IEC and water uptake. Thus, there is a significant difference in proton and water transport between block and random copolymers. Diffusion coefficient values

were also measured as a function of diffusion time. For the random copolymers, the value was found to decrease sharply with time suggesting a strong morphological barrier to transport. Such a dependency was not observed for Nafion® and the blocks. The diffusion coefficient reached a constant value after a particular diffusion time.

Methanol permeability was found to increase with an increase in IEC, water uptake, and self-diffusion coefficients of water for the random copolymers. For multiblock copolymers, the value was not found to depend upon self-diffusion coefficient of water. The hydrophobic segments present in the block copolymers offer resistance to the diffusion of methanol and thus decreases the methanol permeability. Thus in ionomeric block copolymers, the "hard" hydrophobic segments lower the methanol permeability while the "soft" hydrophilic segments provide pathways for water and proton transport.

The authors would like to thank the National Science Foundation "Partnership for Innovation" Program (HER-0090556) and the Department of Energy (DE-FC36-01G01086) for support of this research effort. The authors would also like to thank UTC Fuel Cell (#PO3561) for their support.

3.5 References

1. Winter, M.; Brodd, R. J., What are batteries, fuel cells, and supercapacitors? *Chemical Reviews* **2004,** 104, (10), 4245-4269.

2. Whittingham, M. S.; Savinell, R. F.; Zawodzinski, T., Introduction: Batteries and fuel cells. *Chemical Reviews* **2004,** 104, (10), 4243-4244.

3. Mauritz, K. A.; Moore, R. B., State of understanding of Nafion. *Chemical Reviews* **2004,** 104, (10), 4535-4585.

4. Yeo, R. S., Ion Clustering and Proton Transport in Nafion Membranes and Its Applications as Solid Polymer Electrolyte. *Journal of the Electrochemical Society* **1983,** 130, (3), 533-538.

5. Page, K. A.; Cable, K. M.; Moore, R. B., Molecular Origins of the Thermal Transitions and Dynamic Mechanical Relaxations in Perfluorosulfonate Ionomers. *Macromolecules* **2005,** 38, (15), 6472-6484.

6. Wang, F.; Hickner, M.; Kim, Y. S.; Zawodzinski, T. A.; McGrath, J. E., Direct polymerization of sulfonated poly(arylene ether sulfone) random (statistical) copolymers: candidates for new proton exchange membranes. *Journal of Membrane Science* **2002,** 197, (1-2), 231-242.

7. Hickner, M. A.; Ghassemi, H.; Kim, Y. S.; Einsla, B. R.; McGrath, J. E., Alternative polymer systems for proton exchange membranes (PEMs). *Chemical Reviews* **2004,** 104, (10), 4587-4611.

8. Wang, F.; Hickner, M.; Ji, Q.; Harrison, W.; Mecham, J.; Zawodzinski, T. A.; McGrath, J. E., Synthesis of highly sulfonated poly(arylene ether sulfone) random (statistical) copolymers via direct polymerization. *Macromolecular Symposia* **2001,** 175, 387-395.

9. Kim, Y. S.; Sumner, M. J.; Harrison, W. L.; Riffle, J. S.; McGrath, J. E.; Pivovar, B. S., Direct methanol fuel cell performance of disulfonated poly-arylene ether benzonitrile) copolymers. *Journal of the Electrochemical Society* **2004,** 151, (12), A2150-a2156.

10. Kim, Y. S.; Hickner, M. A.; Dong, L. M.; Pivovar, B. S.; McGrath, J. E., Sulfonated poly(arylene ether sulfone) copolymer proton exchange membranes: composition and morphology effects on the methanol permeability. *Journal of Membrane Science* **2004,** 243, (1-2), 317-326.

11. Kim, Y. S.; Wang, F.; Hickner, M.; McCartney, S.; Hong, Y. T.; Harrison, W.; Zawodzinski, T. A.; McGrath, J. E., Effect of acidification treatment and morphological stability of sulfonated poly(arylene ether sulfone) copolymer proton-exchange membranes for fuel-cell use above 100 degrees C. *Journal of Polymer Science Part B-Polymer Physics* **2003,** 41, (22), 2816-2828.

12. Roy, A.; Einsla, B.; Harrison, W.; McGrath, J. E., Synthesis and characterization of hydroquinone based disulfonated poly(arylene ether sulfone)s via direct copolymerization. *Abstracts of Papers of the American Chemical Society* **2004,** 228, U663-U663.

13. Li, Y. X.; Mukundan, T.; Harrison, W. L.; Hill, M.; Sankir, M.; Yang, J.; McGrath, J. E., Direct synthesis of disulfonated poly(arylene ether ketone)s and investigation of their behavior as proton exchange membrane (PEM). *Abstracts of Papers of the American Chemical Society* **2004,** 228, U657-U657.

14. Xiang, Y. R., Abhishek; McGrath, James E. , Synthesis and characterization of multiblock copolymers for proton exchange membranes. *Preprints of Symposia - American Chemical Society, Division of Fuel Chemistry* **2005**, (50(2)), 577-578.

15. Kreuer, K. D., Proton conductivity: Materials and applications. *Chemistry of Materials* **1996,** 8, (3), 610-641.

16. Kreuer, K. D., On the complexity of proton conduction phenomena. *Solid State Ionics* **2000,** 136, 149-160.

17. Paddison, S. J., Proton conduction mechanisms at low degrees of hydration in sulfonic acid-based polymer electrolyte membranes. *Annual Review of Materials Research* **2003,** 33, 289-319.

18. Van Grotthuss, C. J. D., *Ann. Chim* **1806,** 58, (54).

19. Kreuer, K. D.; Rabenau, A.; Weppner, W., Vehicle Mechanism, a New Model for the Interpretation of the Conductivity of Fast Proton Conductors. *Angewandte Chemie-International Edition in English* **1982,** 21, (3), 208-209.

20. Zawodzinski, T. A.; Neeman, M.; Sillerud, L. O.; Gottesfeld, S., Determination of Water Diffusion-Coefficients in Perfluorosulfonate Ionomeric Membranes. *Journal of Physical Chemistry* **1991,** 95, (15), 6040-6044.

21. Dong, L. M.; Kim, Y. S.; Wang, F.; Hickner, M.; Glass, T. E.; McGrath, J. E., Self-diffusion of water in sulfonated poly(arylene ether sulfone) copolymers by pulse field gradient NMR. *Abstracts of Papers of the American Chemical Society* **2003,** 225, U631-U631.

22. Zawodzinski, T. A.; Davey, J.; Valerio, J.; Gottesfeld, S., Water Transport-Properties of Various Fuel-Cell Ionomers. *Abstracts of Papers of the American Chemical Society* **1993,** 205, 75-Pmse.

23. Noshay, A.; McGrath, J. E., *Block Copolymers: Overview and Critical Survey, Academic Press, New York* **1977**, 91.

24. Ghassemi, H.; McGrath, J. E.; Zawodzinski, T. A., Multiblock sulfonated-fluorinated poly(arylene ether)s for a proton exchange membrane fuel cell. *Polymer* **2006,** 47, (11), 4132-4139.

25. Ghassemi, H.; Ndip, G.; McGrath, J. E., New multiblock copolymers of sulfonated poly(4 '-phenyl-2,5-benzophenone) and poly(arylene ether sulfone) for proton exchange membranes. II. *Polymer* **2004,** 45, (17), 5855-5862.

26. Ghassemi, H.; McGrath, J. E., Synthesis and properties of new sulfonated poly(p-phenylene) derivatives for proton exchange membranes. I. *Polymer* **2004,** 45, (17), 5847-5854.

27. Ghassemi, H.; Zawodzinski, T.; McGrath, J. E., New multiblock copolymers containing hydrophilic-hydrophobic segments for proton exchange membranes. *Polymer,submitted* **2006**.

28. Pivovar, B. S.; Wang, Y. X.; Cussler, E. L., Pervaporation membranes in direct methanol fuel cells. *Journal of Membrane Science* **1999,** 154, (2), 155-162.

29. Ren, X. M.; Springer, T. E.; Zawodzinski, T. A.; Gottesfeld, S., Methanol transport through nafion membranes - Electro-osmotic drag effects on potential step measurements. *Journal of the Electrochemical Society* **2000,** 147, (2), 466-474.

30. Hickner, M. PhD. Thesis, Virginia Polytechnic Institute and State University, Blacksburg, Virginia, August, 2003.

31. Stejskal, E. O.; Tanner, J. E., *J.chem.Phys* **1965**, (42), 288.

32. Zawodzinski, T. A.; Springer, T. E.; Neeman, M.; Sillerud, L. O., Diffusion-Barriers in Pulsed-Gradient Spin-Echo Nmr Microscopy. *Israel Journal of Chemistry* **1992,** 32, (2-3), 281-289.

33. Matsukawa, S.; Yasunaga, H.; Zhao, C.; Kuroki, S.; Kurosu, H.; Ando, I., Diffusion processes in polymer gels as studied by pulsed field-gradient spin-echo NMR spectroscopy. *Progress in Polymer Science* **1999,** 24, (7), 995-1044.

34. Matsukawa, S.; Ando, I., Study of self-diffusion of molecules in polymer gel by pulsed-gradient spin-echo H-1 NMR. 3. Stearyl itaconamide N,N-dimethylacrylamide copolymer gels. *Macromolecules* **1999,** 32, (6), 1865-1871.

35. Zhao, C. H.; Matsukawa, S.; Kurosu, H.; Ando, I., Self-diffusion behavior of solvents in polypeptide gel as studied by pulsed-gradient spin-echo H-1 NMR spectroscopy. *Macromolecules* **1998,** 31, (9), 3139-3141.

36. Ghi, P. Y.; Hill, D. J. T.; Maillet, D.; Whittaker, A. K., Nmr imaging of the diffusion of water into poly(tetrahydrofurfuryl methacrylate-co-hydroxyethyl methacrylate). *Polymer* **1997,** 38, (15), 3985-3989.

37. Ghi, P. Y.; Hill, D. J. T.; Whittaker, A. K., PFG-NMR measurements of the self-diffusion coefficients of water in equilibrium poly(HEMA-co-THFMA) hydrogels. *Biomacromolecules* **2002,** 3, (3), 554-559.

38. Ghi, P. Y.; Hill, D. J. T.; Whittaker, A. K., H-1 NMR study of the states of water in equilibrium Poly(HEMA-co-THFMA) hydrogels. *Biomacromolecules* **2002,** 3, (5), 991-997.

39. Sankir, M.; Bhanu, V. A.; Harrison, W. L.; Ghassemi, H.; Wiles, K. B.; Glass, T. E.; Brink, A. E.; Brink, M. H.; McGrath, J. E., Synthesis and characterization of 3,3 '-disulfonated-4,4 '-dichlorodiphenyl sulfone (SDCDPS) monomer for proton exchange membranes (PEM) in fuel cell applications. *Journal of Applied Polymer Science* **2006,** 100, (6), 4595-4602.

40. Springer, T. E.; Zawodzinski, T. A.; Wilson, M. S.; Gottesfeld, S., Characterization of polymer electrolyte fuel cells using AC impedance spectroscopy. *Journal of the Electrochemical Society* **1996,** 143, (2), 587-599.

41. Rollet, A. L.; Blachot, J.; Delville, A.; Diat, O.; Guillermo, A.; Porion, P.; Rubatat, L.; Gebel, G., Characterization of porous structure through the dynamical properties of ions confined in sulfonated polyimide ionomers films. *European Physical Journal E* **2003,** 12, S131-S134.

4.0 Structure-Property Relationships of Segmented Sulfonated Poly(arylene ether sulfone)-b-Polyimide Multiblock Copolymers for Application in Proton Exchange Membrane Fuel Cells

Abhishek Roy,[1] Hae-Seung Lee,[1] Michael A. Hickner,[2] and James E. McGrath [1]

[1] Macromolecules and Interfaces Institute
Virginia Polytechnic Institute and State University, Blacksburg, VA 24061
[2] Present Address: Department of Materials Science and Engineering
The Pennsylvania State University, University Park, PA 16802

Abstract

Disulfonated poly(arylene ether sulfone) random copolymers have shown promise as potential candidates for proton exchange membranes. The chemical structure of these copolymers has served as a basis for the molecular design of new random and multiblock copolymers. We have recently demonstrated a novel way to make a variety of hydrocarbon hydrophobic-hydrophilic block copolymers. The copolymers are referred to as BPSH-x-PI-y, and detailed synthetic procedures have been reported separately. The major two variables in ionic multiblocks are the ionic content and the individual block length. An increase in block length for a given series of block copolymer under same ionic concentration has been associated with an increase in the self-diffusion coefficient of water and improved proton conduction under partially hydrated conditions. For direct methanol fuel cell (DMFC) applications, the block copolymers were also found to have very low methanol permeability and very high selectivity. A novel structure property relationship between transport properties and the volume fraction of the hydrophilic phase has been achieved.

4.1 Introduction

Over the last few years there has been a substantial amount of research in developing new alternative materials for application as proton exchange membranes (PEMs).[1, 2] Proton exchange membrane fuel cells (PEMFCs) have been shown to be promising for a variety of potential applications, including for use as low power portable device as well as in high power applications.[3] Recently, there has been profound interest in PEMFCs for use in automotive applications to eventually replace the internal combustion engine. One of the major challenges for such an application, however, is to maintain high proton conductivity at low or partially hydrated conditions. In PEMFCs, polymeric membranes with ionic groups (sulfonic) serve the function of proton conduction in the presence of water. The commercially available state-of-the-art PEM, Nafion®, has several advantages such as acceptable proton conduction at low relative humidities (RH).[4] However, Nafion® possesses some disadvantages including very high gas and fuel permeability, reduced stability at high temperatures, and high cost. Alternative aromatic hydrocarbon membranes, in contrast, have reduced gas crossover leading to improved oxidative stability over Nafion®.[5]

The McGrath group has recently been synthesizing wholly aromatic hydrocarbon based disulfonated poly (arylene ether sulfone)s copolymers, known as BPSH-xx,[6] whose structure is shown in Figure (4-1a). The copolymer has excellent oxidative, thermal and chemical stability and significant lower oxygen permeability than Nafion®.[5]

While both Nafion® and BPSH-xx[1, 6] show high proton conductivity under fully hydrated conditions, proton transport is especially limited at low hydration levels for the BPSH-xx random copolymers. Under partially hydrated conditions or low water content, proton transport is believed to take place via the "vehicle mechanism," with water acting as the vehicle for proton transport.[7,8] Under such conditions, the self-diffusion coefficient of water has been reported to be equal to the proton-diffusion coefficient.[9] In the case of random copolymers, at low hydration levels most of the water is tightly associated with sulfonic groups and has a low diffusion coefficient. This tends to encourage an isolated domain morphology. Thus, although there may be significant concentrations of protons,

transport is limited by the discontinuous morphological structure.[10] In contrast, the low β relaxation temperature of Nafion®[11] allows the formation of nanophase separated, well-connected hydrophilic domains, even at low water content. This associated domain morphology decreases the morphological barrier, resulting in increased water and proton transport.

Block copolymers[12] consist of two or more chemically dissimilar backbone segments (i.e., blocks) that are chemically conjoined through covalent bonds in the same chain. In block ionomer proton exchange membranes, the ionic groups act as proton conducting sites, while the non-ionic component provides dimensional strength.[13-16] We have recently demonstrated a novel way to make hydrophobic-hydrophilic block copolymers that are almost completely hydrocarbon in nature. These copolymers are referred to as BPSH-x-PI-y multiblocks, where x represents the block length in kg/mole of the hydrophilic unit, and y represents the block length in kg/mole of the hydrophobic unit.[13, 17] The PI represents a six-membered polyimide hydrophobic unit. The associated structure is provided in Figure (4-1b). Unlike the BPSH-xx random copolymers, where the sulfonic acid groups are randomly distributed in pairs along the chain, the multiblock copolymers feature an ordered sequence of hydrophilic and hydrophobic segments.[17] If connectivity is established between the hydrophilic domains in these multiblock copolymers, it is anticipated that they would not need as much water as random copolymers to form a percolated structure. Hence, they would display much better proton conductivity than the random copolymers (with a similar degree of sulfonation or ionic content) under partially hydrated conditions.

In Part A, the synthesis and preliminary characterization results for the BPSH-x-PI-y multiblock copolymers were discussed.[17] Morphological studies using AFM imagery has demonstrated the formation of a well-ordered, phase separated morphology with increasing block length, particularly for the BPSH-15-PI-15 copolymers. Measurements of the self-diffusion coefficients of water using pulsed gradient spin echo (PGSE) NMR methodology can further assess morphology within the hydrophilic domains. Understanding the extent of connectivity between the hydrophilic domains as a function of block length and morphology will elucidate the relationship between morphology and

proton transport—especially under partially hydrated conditions. This paper will also explore the influence of the differences between block copolymer and random copolymer morphology on water, proton, and methanol transport.

a)

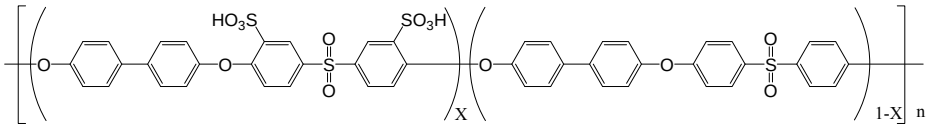

b)

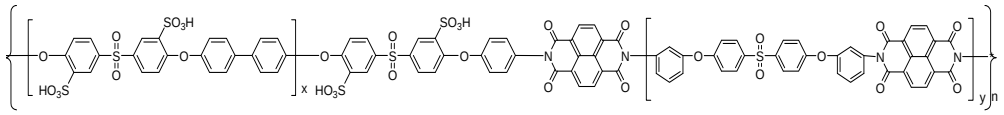

Figure 4-1 Chemical structures of a) BPSH-xx random copolymer, b) BPSH-x-PI-y multiblock copolymer where x and y represent the molecular weight of the hydrophilic and hydrophobic blocks respectively in kg/mole

4.2 Experimental

4.2.1 Materials

N,N-Dimethylacetamide (DMAc), N-methyl-2-pyrrolidinone (NMP), 3-methylphenol (*m*-cresol), and toluene were purchased from Aldrich and distilled from calcium hydride before use. Monomer grade 4,4'-dichlorodiphenyl sulfone (DCDPS) and 4,4'-biphenol (BP) were provided by Solvay Advanced Polymers and Eastman Chemical Company, respectively, and vacuum dried at 110 °C prior to use. 1,4,5,8-Naphthalenetetracarboxylic dianhydride (NDA) and fuming sulfuric acid (SO_3 content ~30%), were used as received from Aldrich. Bis[4-(3-aminophenoxy)phenyl]sulfone (m-BAPS) was purchased from TCI and purified by recrystallization from ethanol. 3-Aminophenol (m-AP) was purchased from Aldrich and sublimed *in vacuo* before use. Potassium carbonate, benzoic acid, ethanol, 2-propanol (IPA), and isoquinoline were purchased from Aldrich and used without further purification. Nafion® 117 and Nafion® 112 were purchased from Electrochem Inc. and used as received. BPSH-35 was synthesized using procedures reported elsewhere[6] and used as a control.

4.2.2 Multiblock copolymer synthesis

A series of segmented disulfonated poly(arylene ether sulfone)-*b*-polyimide copolymers based on hydrophilic and hydrophobic oligomers was synthesized. The disulfonated hydrophilic oligomers were prepared via step growth polymerization using different block lengths ranging from 5 kg/mol to 20 kg/mol. To produce the amine telechelic functionality of the hydrophilic oligomers, *m*-aminophenol (*m*-AP) was used as the endcapping reagent for the reaction. Anhydride-terminated polyimide hydrophobic oligomers with the same molecular weight range as the hydrophilic oligomers were synthesized via a high temperature one-pot imidization. The anhydride end-group functionality was achieved by adding stoichiometrically adjusted amounts of the monomers. Synthesis of the multiblock copolymers was facilitated by an imidization coupling reaction between the amine end-groups on the hydrophilic oligomers and the anhydride end-groups on the hydrophobic oligomers, thereby producing high molecular weight copolymers. A detailed synthesis of the copolymers has been published elsewhere,[13, 17] according to which a series of multiblock copolymers with different block lengths were synthesized and characterized.

4.2.3 Membrane preparation

The salt form copolymers were redissolved in NMP to afford transparent solutions with 5% solids. The solutions were then cast onto clean glass substrates. The films were dried for 2 days with infrared heat at gradually increasing temperatures, and then dried under vacuum at 110 ^{o}C for 2 days. The membranes were converted to their acid form by boiling in 0.5 M H_2SO_4 for 2 h, and were then boiled in deionized water for 2 h.

4.2.4 Measurement of proton conductivity

Proton conductivity at 30 ^{o}C at full hydration (in liquid water) was determined in a window cell geometry[18] using a Solartron 1252 + 1287 Impedance/Gain-Phase

Analyzer over the frequency range of 10 Hz to 1 MHz following the procedure reported in the literature.[19] For determining proton conductivity in liquid water, the membranes were equilibrated at 30 °C in DI water for 24 h prior to testing. For determining proton conductivity under partially hydrated conditions, membranes were equilibrated in a humidity-temperature oven (ESPEC, SH-240) at the specified RH and temperature for 5 h before each measurement.

4.2.5 Determination of water uptake

The water uptake of all membranes was determined gravimetrically. First, the membranes were soaked in water at 30 °C for 2 days after acidification. The wet membranes were removed from the liquid water, blotted dry to remove surface droplets, and quickly weighed. The membranes were then dried at 120 °C under vacuum for at least 24 h and weighed again. The water uptake of the membranes was calculated according to Equation (4-1), where $mass_{dry}$ and $mass_{wet}$ refer to the mass of the dry membrane and the wet membrane, respectively.

$$\text{water uptake}\% = \frac{\text{mass}_{wet} - \text{mass}_{dry}}{\text{mass}_{dry}} \times 100 \qquad \textbf{Equation 4-1}$$

The hydration number (λ), which is the number of water molecules absorbed per sulfonic acid, can be calculated from the mass water uptake and the ion content of the dry copolymer as shown in Equation (4-2), where MW_{H2O} is the molecular weight of water (18.01 g/mol) and IEC is the ion exchange capacity of the dry copolymer in milliequivalents per gram.

$$\lambda = \frac{(\text{mass}_{wet} - \text{mass}_{dry})/\text{MW}_{H_2O}}{\text{IEC} \times \text{mass}_{dry}} \text{.....} \qquad \textbf{Equation 4-2}$$

The volume fraction of water (i.e., the hydrophilic phase) was determined from an established formula[20] (Equation 4-3),

$$\phi = \left(\frac{M_{H_2O} / \rho_{H_2O}}{\left[M_{H_2O} / \rho_{H_2O} + EW / \lambda \rho_{ionomer} \right]} \right) \qquad \textbf{Equation 4-3}$$

where Φ is the volume fraction of water, ρ is the density and EW is the equivalent weight of the ionomer.

4.2.6 Determination of swelling ratio and density

The swelling ratio of all of the membranes was determined from the dimensional changes from wet to dry states, both in-plane and through-plane. Initially, samples were equilibrated in water and wet dimensions were measured. The dried dimensions were obtained by drying the wet membrane at 80 °C in a convection oven for 2 h. Density was also calculated from the volume and weight of the dried membranes. An average of 4 samples was used for each measurement.

4.2.7 Methanol permeability and DMFC performance

The methanol permeability of the membranes was determined by measuring the crossover current in a direct methanol fuel cell (DMFC) under open circuit conditions, in a manner identical to that of Ren et al.[21] DMFC performance or the VIR curves were obtained using a Fuel Cell Technologies test stand as described earlier.[22] The methanol feed concentration was 0.5M, the air flow rate at the cathode was 500 sccm at 90 °C, and the cell temperature was 80 °C.

4.2.8 Pulsed-field gradient spin echo nuclear magnetic resonance (PGSE NMR)

The self-diffusion coefficients of water were measured using a Varian Inova 400 MHz (for protons) nuclear magnetic resonance spectrometer with a 60 G/cm gradient

diffusion probe. A total of 16 points was collected across a range of gradient strengths and the signal–to-noise ratio was enhanced by co-adding 4 scans. The standard stimulated-echo NMR pulse sequence is shown in Figure (4-2).

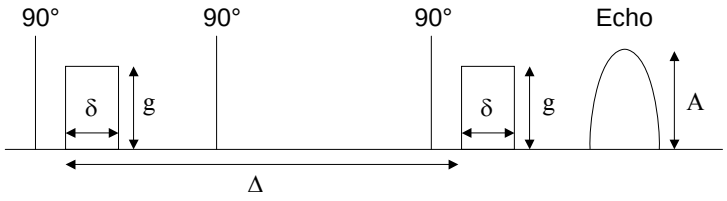

Figure 4-2 Stimulated echo pulse sequence schematic for PGSE NMR experiments

The measurement was calculated by observing the echo signal intensity (A) as a function of gradient strength. The diffusion coefficient (D) was determined by fitting the data to Equation (4-4): [23]

$$A(g) = A(o)\exp[-\gamma^2 D g^2 \delta^2 (\Delta - \delta/3)] \qquad \textbf{Equation 4-4}$$

where, A is the NMR signal intensity as a function of gradient strength(g), γ is the gyromagnetic ratio (26752 radG^{-1}s^{-1} for protons), δ is length of the gradient pulse, Δ is the time between gradient pulses. The experimental procedures used were similar to earlier reported procedures.[24] The membranes were at a fully hydrated state and the temperature of the experiment was 25 ^{o}C.

4.3 Results and Discussion

4.3.1 Multiblock copolymer synthesis

A series of multiblock copolymers was synthesized as described in Part A of a previously reported article.[17] These copolymers can be divided into subgroups on the basis of their hydrophilic block lengths. For example, in the first series of BPSH-5-PI-y copolymers, the hydrophilic block length (x) was kept fixed at 5 kg/mole and the hydrophobic block length (y) was varied from (5, 10, 15 & 20) kg/mole. Similarly for

the BPSH-10-PI-y, BPSH-15-PI-y & BPSH-20-PI-y copolymers, the hydrophilic block lengths were kept constant at (10, 15 & 20) kg/mole, respectively. For each of these multiblock copolymer series, the ion exchange capacity decreased with increasing hydrophobic block length. The equal block length materials (5-5, 10-10, 15-15 & 20-20) would theoretically have the same IEC. Therefore, studying the equal block length materials would be appropriate in understanding the effect of block lengths on the properties of copolymers at the same ionic content. The properties of the all copolymers were evaluated under both fully hydrated conditions and partially hydrated conditions.

Fully Hydrated State

4.3.2 Water uptake, volume fraction, swelling and IEC

The water uptake, corresponding water volume fractions, and the titrated IEC values are summarized in Table (4-1). The multiblock copolymers with high IECs (around 2.0 meq/g) had extremely high water uptake and could not measured accurately. Thus, those copolymers were not evaluated for this study. Water volume fractions were calculated from density and water uptake measurements.

The relationship between water uptake and IEC for the three series of multiblock copolymers (BPSH-5-BPS-y, BPSH-10-BPS-y and BPSH-15-BPS-y) is plotted in Figure (4-3). The water uptake increased with increasing IEC values for the all the three series of multiblock copolymers. This is in agreement with earlier findings for the ionic random copolymers, where water uptake is known to be a function of ionic content.[24] However, at a given IEC water uptake was found to also be a function of hydrophilic block length for the multiblocks. When compared at similar IECs, BPSH-15-BPS-y multiblock copolymers swelled the most. More interestingly, for the equal block length materials (5-5, 10-10 & 15-15) an increase in water uptake was observed with increasing block length.

Table 4-1 Summary of the properties of the BPSH-x-PI-y multiblocks

Copolymers	Target IEC (meq g^{-1})	Experimental IEC (meq g^{-1})[a]	Density (g/cc)	Water uptake (%)	Water volume fraction	Conductivity (S cm^{-1})[b]
BPSH5 – PI5	1.63	1.65	1.6	55	0.46	0.090
BPSH5 – PI10	1.13	1.09	1.6	22	0.26	0.018
BPSH5 – PI15	0.80	0.78	1.6	15	0.19	0.010
BPSH5 – PI20	0.62	0.53	1.5	12	0.15	0.006
BPSH10 – PI5	2.10	1.98	-	-[c]	-	-[c]
BPSH10 – PI10	1.59	1.57	1.6	70	0.53	0.100
BPSH10 – PI15	1.20	1.17	1.6	40	0.39	0.073
BPSH10 – PI20	0.96	0.86	1.5	24	0.27	0.030
BPSH15 – PI5	2.38	2.12	-	-[c]	-	-[c]
BPSH15 – PI10	1.91	1.83	1.5	156	0.70	0.161
BPSH15 – PI15	1.51	1.55	1.5	85	0.56	0.110
BPSH15 – PI20	1.25	1.12	1.5	38	0.37	0.055
BPSH20 – PI5	2.58	2.20	-	-[c]	-	-[c]
BPSH20 – PI10	2.17	2.02	-	-[c]	-	-[c]
BPSH20 – PI15	1.78	1.71	1.4	97	0.58	0.092
BPSH20 – PI20	1.51	1.20	1.4	56	0.44	0.100

[a] Determined by titration with NaOH.[17]

[b] Measured in deionized water at 30 ºC (± 5%).

[c] Not available due to poor mechanical strength of the hydrated film.

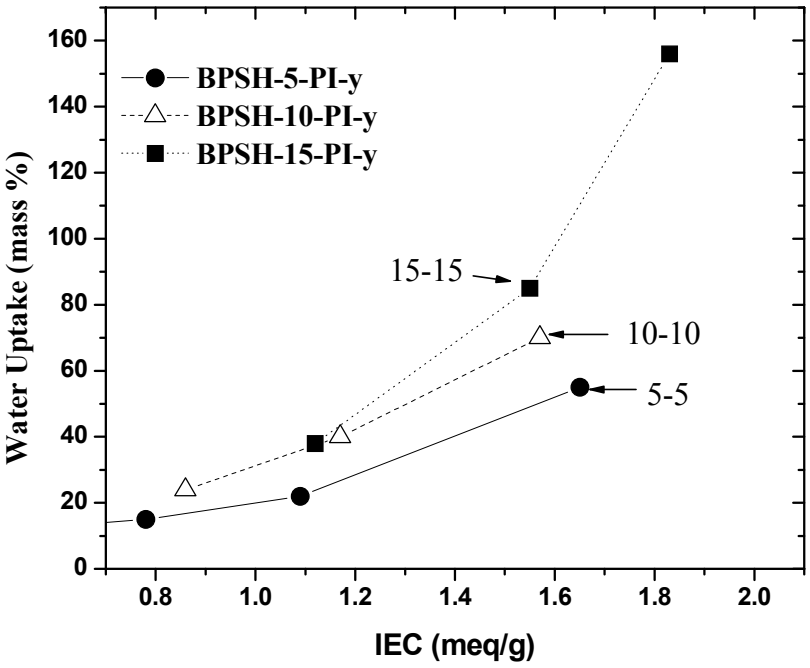

Figure 4-3 Influence of block length and IEC on water uptake

To further investigate these important relationships, three-dimensional water swelling behavior was determined (Fig. 4-4b) for the three equal block length materials, along with an analysis of the associated atomic force microscopy images[13, 17, 25] (Fig. 4-4a). The x, y represents the in-plane swelling and the z represents the through-plane swelling. The dark region in the AFM images corresponds to the hydrophilic portions and the lighter region the hydrophobic portions. An anisotropic increase in swelling along the through-plane was observed with increasing block length. This, along with the AFM images (Fig. 4-4 a),[25] suggest the formation of an "associated," well "ordered" hydrophilic domain morphology with increasing block length. This associated hydrophilic domain morphology would be expected to absorb more water than an isolated domain morphology.

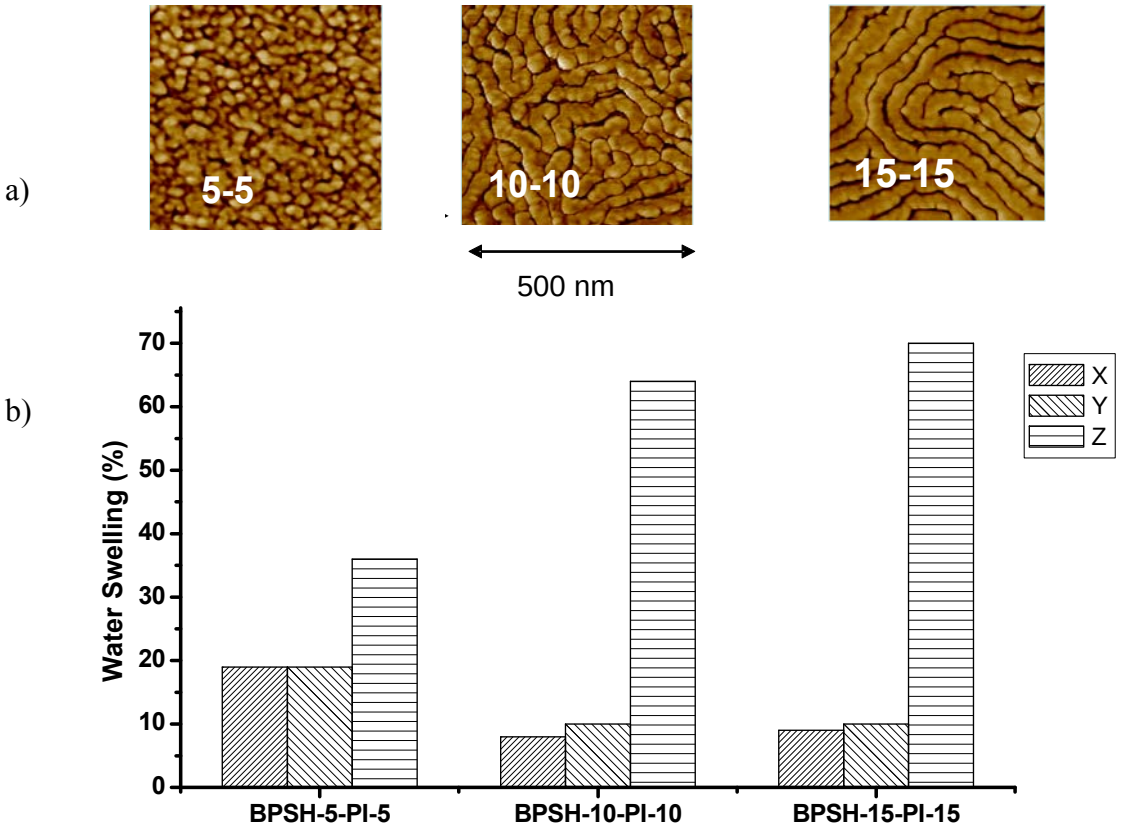

Figure 4-4 a) Tapping mode AFM images of the multiblocks. Reprinted with permission from John Wiley & Sons, Inc.[17] b) Water swelling in both in-plane and through-plane as a function of the block lengths

4.3.3 Self-diffusion coefficient of water

The water absorption and AFM images indicate the formation of a phase separated hydrophobic – hydrophilic domain morphology with increasing block lengths at a given IEC. However, it is also important to investigate the extent of connectivity within the hydrophilic domains as a function of block copolymer morphology. Well-connected hydrophilic domains may reduce morphological barriers, thereby enhancing proton transport under partially hydrated conditions. We propose that measuring the self-diffusion coefficients of water through the hydrophilic domains will further elucidate the impact of block copolymer morphology on transport properties. The self-diffusion

coefficient of water as measured by PGSE-NMR techniques is a weighted average of the diffusion of the H^+ ion and the associated water within a polymer. Theoretically, the diffusion coefficient of a species is related exponentially to the free volume fraction of the copolymer.[9, 26] Free volume can be approximated to the volume fraction of the solvent that a polymer absorbs—or in this case, the water volume fractions. A semi-log plot showing the self-diffusion coefficients of water (25 ^oC) and the inverse of the volume fractions of water for the multiblocks represented by a linear fit demonstrates a similar principle (Fig. 4-5). At a given water volume fraction, copolymers with higher self-diffusion coefficients of water demonstrate better facilitated water transport within hydrophilic domains. When comparing the three series, values are higher for the higher block length materials at similar water contents.

The multiblock copolymers were also compared with the commercially available Nafion® and the BPSH 35 random disulfonated copolymers. At similar water content, the random copolymers showed a much lower diffusion coefficient value than both the Nafion® and the multiblocks. This may indicate the presence of an isolated morphology for the random copolymers. The equal block length materials (5-5, 10-10, 15-15) under similar ionic and water content more clearly demonstrated the influence of block length on water transport. A sharp increase in the water self-diffusion coefficient was associated with the BPSH-15-PI-15 sample as compared to the 5-5 or 10-10 copolymer. The observed phase separated morphology with increasing block length increased the connectivity within the hydrophilic domains, thereby enhancing water transport.

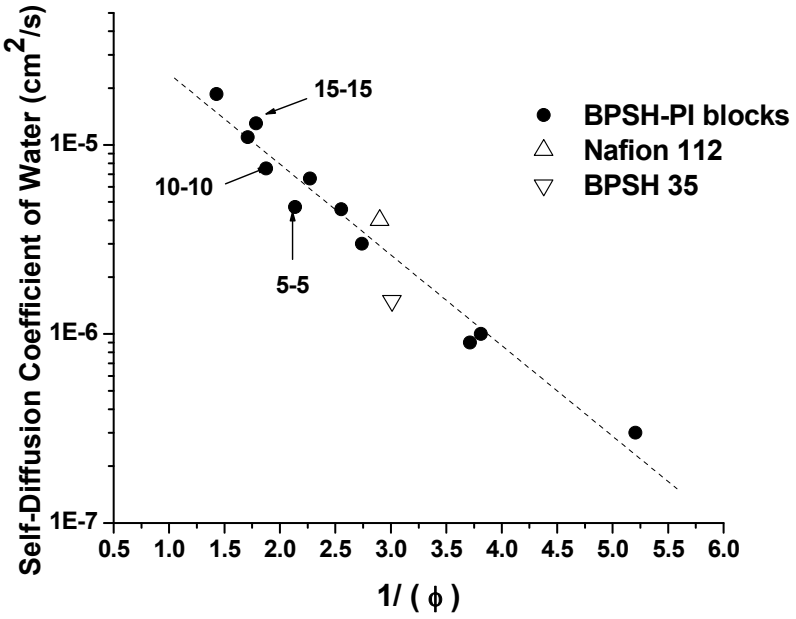

Figure 4-5 Self-diffusion coefficients of water scale with the water volume fractions for the multiblocks, Nafion® and BPSH 35 at 25 °C

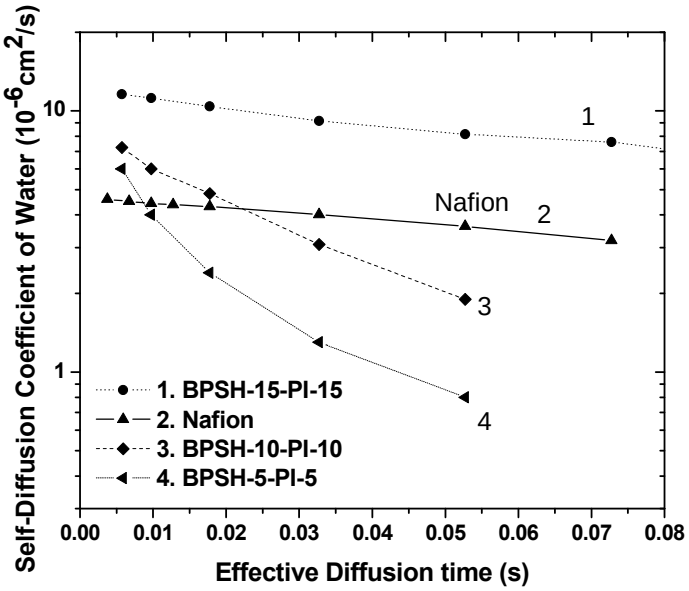

Figure 4-6 Self-diffusion coefficients of water as a function of the effective diffusion time scale with the morphology of the block copolymer

PGSE-NMR enables one to measure the diffusion coefficient as a function of the effective diffusion time by varying the time between the two gradient pulses. This technique facilitates a better understanding of the morphology within the hydrophilic domains as a function of block lengths. Water diffusion within the hydrophilic domain as a function of diffusion time can be modeled using Einstein random walk theory. The distance traveled (Δ r) during diffusion transport at a given time (Δ) is represented by the following Equation (4-5).[27]

$$\langle \Delta r \rangle = \sqrt{2 D_{eff} \Delta} \qquad \textbf{Equation 4-5}$$

As noted above, Figure (4-6) represents plots of the self-diffusion coefficients of water as a function of effective diffusion time for the three equal block length materials with similar IEC values. Nafion® 112 is used as a control. The self-diffusion coefficient values decreased with increasing diffusion time for the BPSH-5-PI-5 and BPSH-10-PI-10 samples. This indicates that the water encounters a morphological barrier within the hydrophilic domain. Interestingly, for the Nafion® and BPSH-15-PI-15 samples, the measured diffusion coefficient value was independent of diffusion time. The co-continuous channel morphology of the BPSH-15-PI-15 sample resulted in lowering of the morphological barrier within the hydrophilic domains.

These experimental results can be modeled to Equation (4-5), as shown in Figure (4-7). Figure (4-7) plots the distance traveled by a water molecule within a hydrophilic domain as a function of time traveled. For the BPSH-5-PI-5 and BPSH-10-PI-10 multiblock copolymers, the distance traveled becomes constant after a specific point in time, indicating the restricted diffusion phenomenon.[27] However, for the BPSH-10-PI-10 sample, the distance traveled was greater than documented for the BPSH-5-PI-5 sample. For both Nafion® and the BPSH-15-PI-15, the distance traveled by the water molecule increased and plateaued with increasing time of travel. This phenomenon represents classical tortuous or facilitated diffusion. Hence, with increasing block length it is possible to induce a morphology that alters the nature of water transport from a restricted to a tortuous type.

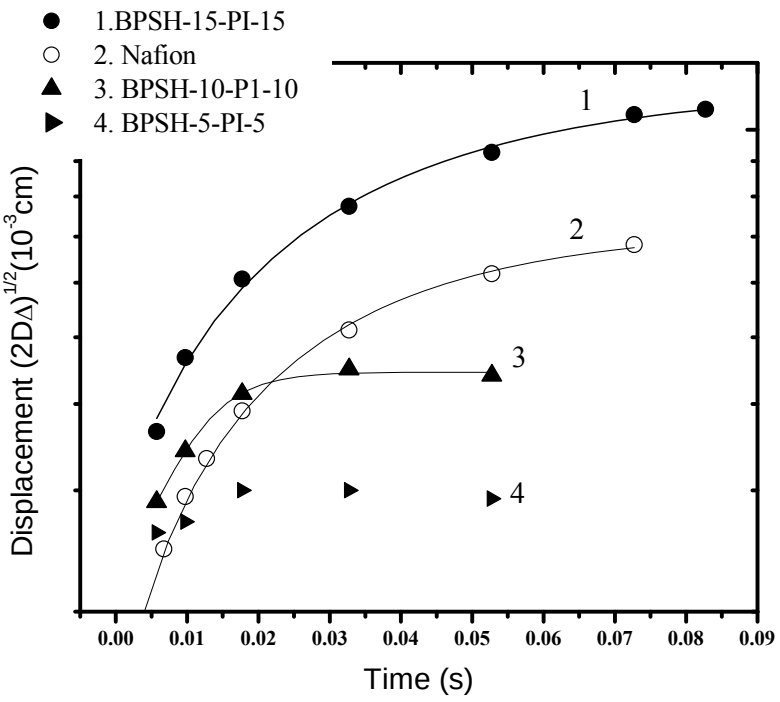

Figure 4-7 Water diffusion changes from restricted to tortuous in nature with increasing block length

4.3.4 Proton Conductivity

Proton flux for ion containing copolymers can be described by the Nernst Plank equation [28]

$$-j_p = D_p C_p \left(\frac{\nabla C_p}{C_p} + z_p \frac{F \nabla \psi}{RT} \right) \qquad \textbf{Equation 4-6}$$

where j_p is the proton flux, C_p is the concentration of the protons, D_p is the diffusion coefficient of the protons, z_p the proton charge, Ψ the electrostatic potential, R the gas constant, and F the Faraday constant. For a membrane with constant thickness and a proton charge of +1, proton flux can be related to proton conductivity (σ) via the following Equation (4-7).

$$\sigma \propto j_p \propto D_p C_p \qquad \textbf{Equation 4-7}$$

Thus, proton conductivity is a function of both the concentration and diffusion coefficients of the protons (Eq^{n}. 4-8).

$$\sigma = f(C, D) \qquad \textbf{Equation 4-8}$$

The concentration value is governed by the ionic composition of the copolymer, whereas the diffusion component depends more on the structure or the morphology. In the case of random copolymers, proton conductivity under fully hydrated conditions scales linearly with the concentration of protons or the IEC of the copolymer. However, for multiblock copolymers no such linear relationship can be obtained between proton conductivity and IEC. For example, for equal block length materials with the same IEC, proton conductivity increases from 80 to 110 mS/cm. The diffusion value, which depends upon the morphology of the copolymer, may play a bigger role than the concentration value. As discussed earlier, the diffusion of a species tends to scale more with the volume fraction of water.

Earlier, Elabd et al.[28] explained the relationship between proton transport and water volume fraction using a percolated model theory. The percolated model, which was applied to the BPSH-x-PI-y multiblocks, demonstrates a power law dependence of the proton conductivity (liq. water, 30 ^{o}C) on the water volume fraction, as shown in Figure (4-8). A better phase separated morphology results in a higher fraction of the associated hydrophilic phase, thereby increasing proton conductivity. In contrast to random copolymers, morphology plays the dominant role in explaining proton transport behavior in multiblock copolymers. One should note that at higher volume fractions of water, significantly higher proton conductivity (up to ~160 mS/cm) can be achieved in the multiblocks. By comparison, proton conductivity for Nafion® copolymers is 90 mS/cm in liquid water at 30 °C.

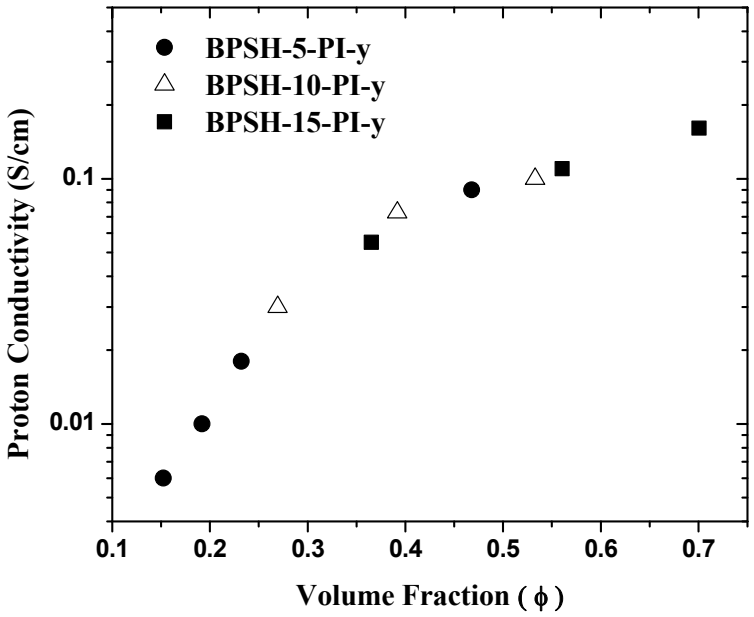

Figure 4-8 Proton conduction under fully hydrated conditions at 30 ^{o}C is a function of the water or hydrophilic volume fractions

4.3.5 Partially hydrated conditions: water absorption and proton conduction

One of the major objectives of this research was to investigate the influence of the morphology of ion containing copolymers for improving proton transport under partially hydrated conditions. Among the multiblock copolymers synthesized, three equal block length materials with similar IEC values were evaluated in order to eliminate the possible influence of ionic concentration on proton transport at low RH.

Water absorption

Water sorption as a function of water activity was studied for the three block copolymers; water uptake was normalized in terms of hydration number (λ) (Fig.4-9). The hydration number is defined as the number of water molecules per sulfonic acid group in a copolymer. At low water activity or at low RH, the hydration numbers for the

three block copolymers were similar irrespective of the nature of the block length. As observed, most of the water at low RH was tightly bound and depended more on the nature of the sulfonic group or the chemical structure. However, at higher water activity levels, the hydration number increased with increasing block length. This difference in behavior indicates a change in the distribution of the different states of water in the copolymer.[29] The distinct phase separated morphology of BPSH-15-PI-15 copolymer encouraged the formation of free water at high RH in the system, resulting in an overall increase in the hydration number.

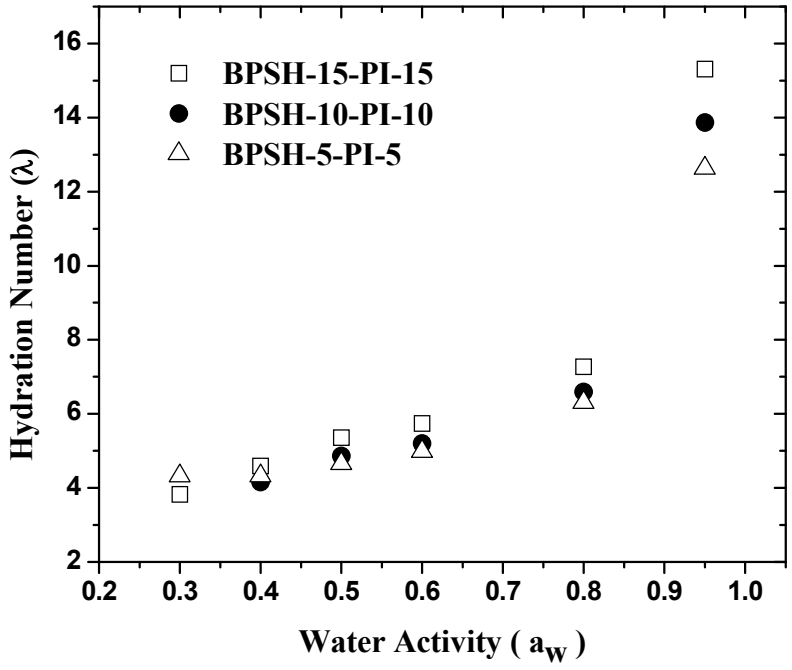

Figure 4-9 Water absorption under partially hydrated conditions as a function of the block length

Proton conduction

Proton conduction of the block copolymers under fully hydrated conditions was found to be a function of the water volume fraction of the system. Comparing proton conductivity for the multiblocks at a similar hydration level and ionic content normalizes the influence of water content and ionic content on proton conductivity. This should

highlight the true influence of morphology on proton transport. Hence proton conductivity was measured for the three equal block length materials over a wide range of water volume fractions (Fig.4-10). The copolymers were equilibrated with different water content and proton conductivity was measured at those hydration levels at 30 °C. At a given water volume fraction, proton conductivity increased with increasing block length. This effect was more pronounced at low water content or under partially hydrated conditions.

At higher hydration levels, proton transport can be facilitated through water assisted percolated hydrophilic domains. Under partially hydrated conditions, however, there is an insufficient amount of water for developing essential connectivity between these domains, resulting in an increase in the morphological barrier for proton transport. Earlier diffusion coefficient experiments suggested the presence of low morphological barriers for higher block length materials. In the present study, because IEC and water content values were fixed, improved morphological connectivity between the hydrophilic domains with increasing block lengths increased proton conductivity at low water content.

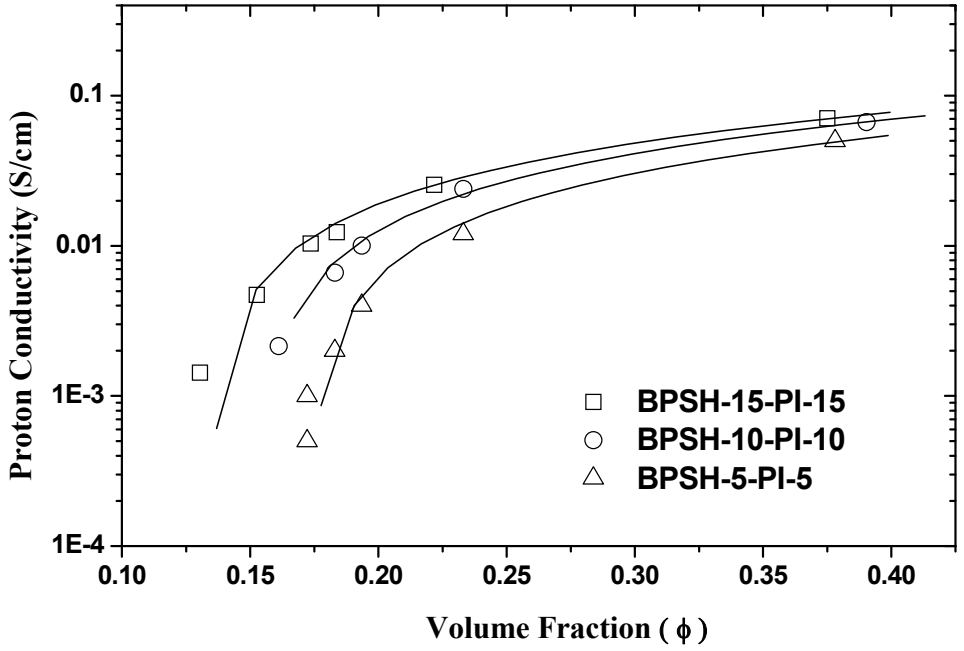

Figure 4-10 Proton conduction vs. volume fraction of water as a function of block length

Proton conductivity performance as a function of relative humidity was evaluated at 80 °C for the three equal block length materials, the Nafion® 112, and the BPSH 35 random copolymers (Fig.4-11). At higher RH, proton conductivity was similar for all the copolymers; however, with decreasing RH, proton conductivity decreased sharply for the BPSH 35 random copolymers. Among the block copolymers, the less phase separated BPSH-5-PI-5 copolymers exhibited behaviors similar to the random copolymers, indicating the presence of an isolated domain morphology. Performance under low RH improved with increasing block length. The well-connected phase separated morphology improved proton transport for the BPSH-15-PI-15 copolymers, which was comparable to the state-of-the-art Nafion® 112, even at low RH.

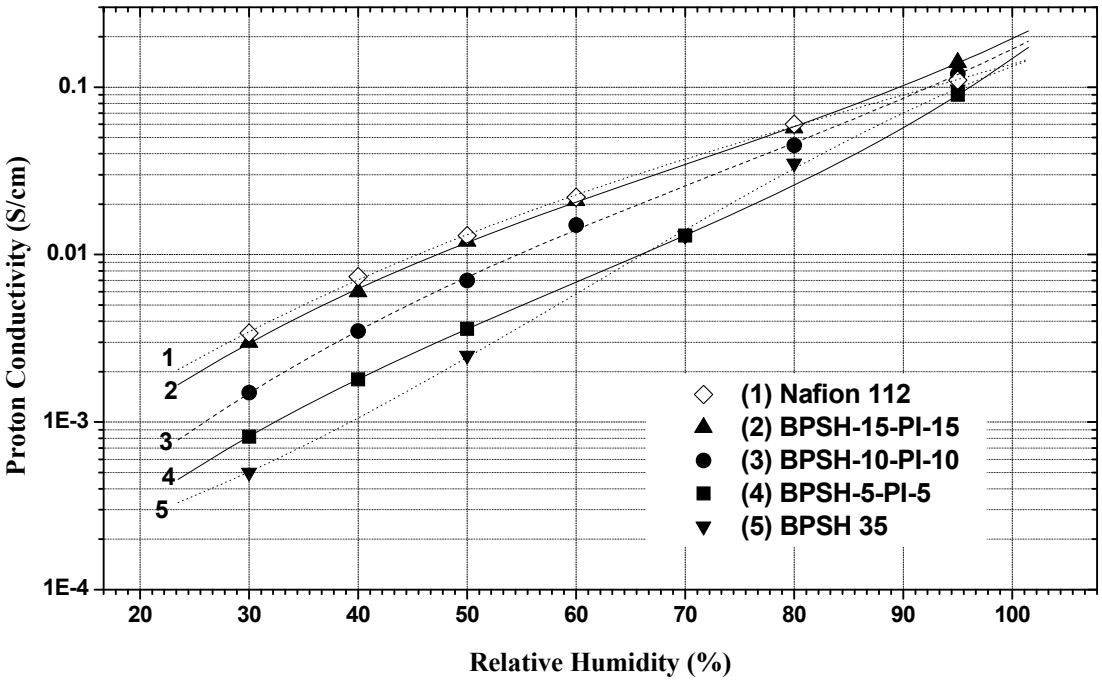

Figure 4-11 Proton conduction under partially hydrated conditions at 80 °C increases with increasing block length or with the extent of phase separation in multiblocks

4.3.6 Methanol permeability and DMFC performance

Methanol permeability is one of the key factors controlling overall performance in DMFC applications. An ion containing proton exchange membrane allows the permeation of methanol from anode to cathode. Methanol that is unoxidized at the anode can "cross over" through the membrane and be oxidized at the cathode, thereby decreasing fuel efficiency. And in fact, one of the major disadvantages of Nafion® as a PEM in a DMFC-type fuel cell is its high methanol permeability. In comparison to Nafion®117, BPSH-xx and the other aromatic random copolymers have shown much lower methanol permeability.[30] Similar to the random copolymers, the BPSH-x-PI-y multiblock copolymer has also demonstrated significantly reduced methanol permeability. Methanol permeability as a function of ion exchange capacity measured at 80 ^{o}C is shown in Figure (4-12) for Nafion®117, HQSH-xx, PB-xx and the BPSH-x-PI-y multiblock copolymers.[25] As depicted, the increase in methanol permeability with increasing IEC was quite significant for the random copolymers in contrast to the multiblock copolymers.

One of the challenges in designing a new PEM for DFMC applications is the tradeoff between proton conductivity and methanol permeability. At low IECs, random copolymers are associated with both low methanol permeability and low proton conductivity. For the multiblock copolymer systems, however, the higher block length materials—even those with low ion exchange capacities—are associated with both high proton conductivity and low methanol permeability. This combination increases a multiblock copolymer's selectivity, which is defined as the ratio of proton conductivity to methanol permeability, over the selectivity of a random copolymer.

Figure (4-13) shows the selectivity of the PEMs as a function of methanol permeability at 30 ^{o}C. Among the various copolymers studied, the BPSH-20-PI-20 demonstrated the highest selectivity. This result can be interpreted to the preferential selectivity of the hydrophobic and hydrophilic blocks towards methanol and water. In other words, the hydrophobic segments present in the block copolymers offered resistance to the diffusion of methanol and thus decreased methanol permeability. Thus,

in ionomeric block copolymers, it is suggested that the "hard" segments are capable of lowering methanol permeability, while the "soft" hydrophilic segments provide enhanced pathways for water and proton transport.

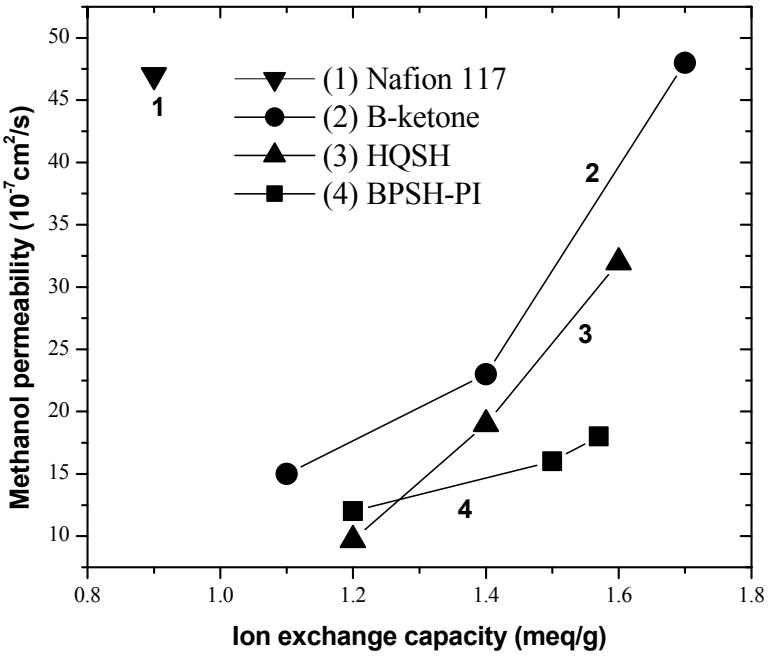

Figure 4-12 Methanol permeability as a function of ion exchange capacity for several systems at 80 °C Reproduced with permissions from ECS Transactions.[25] Copyright [2007], The Electrochemical Society

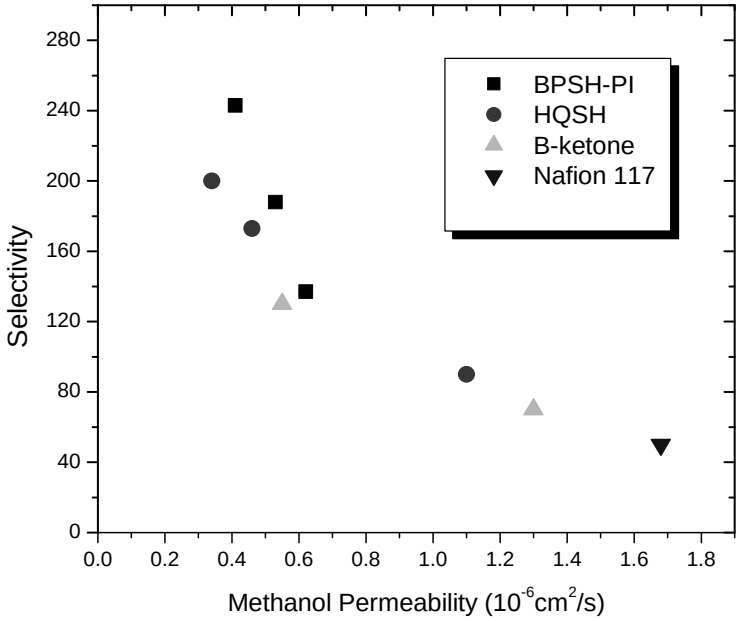

Figure 4-13 Phase separated morphology of multiblocks allows to achieve high selectivity at low methanol permeability. Reproduced with permissions from ECS Transactions.[25] Copyright [2007], The Electrochemical Society

The DMFC performance characteristics of the BPSH-PI multiblock copolymers were assessed using the fuel cell operating conditions provided in the experimental section. Representative plots for the multiblocks and Nafion® 117 are given in Figure (4-14). Both the BPSH-10-PI-10 and BPSH-20-PI-20 copolymers showed comparable DMFC performance to Nafion® 117, but at less than 33% of the thickness.

DMFC performance results for the two multiblock copolymers and Nafion® 117 are reported in Table (4-2). The open circuit voltage (OCV) value in a DMFC is one of the key factors in assessing the fuel efficiency of a cell. A major portion of OCV loss is generally attributed to methanol crossover. Materials with low methanol permeability are expected to have much higher OCV values. Hence, the multiblock copolymers showed much higher open circuit voltage characteristics compared to Nafion®. High frequency resistance (HFR), which is the sum of the resistances originating from the membrane, the interfacial resistance between the electrodes and the membrane, as well as the resistance of the gas diffusion layers, was also determined for the PEMs. For an identical set of

electrodes and gas diffusion layers, HFR can be considered to be a membrane property. Materials with higher HFR values offer higher resistance to proton transport across the membrane and may also cause poor bonding with the electrodes. These two factors affect both the overall and long-term performance of a PEM. One way to decrease HFR is to use a thinner membrane. However, the disadvantage of using a thinner membrane is higher methanol crossover, which is typically reported as the $\zeta_{\text{lim, ocv}}$ value. The open circuit limiting crossover current ($\zeta_{\text{lim, ocv}}$) is a measure of the amount of methanol crossover from anode to cathode under open circuit voltage. This value increases with decreasing membrane thickness, thereby lowering the OCV and fuel efficiency of a cell. Hence, there is a tradeoff between the HFR and the crossover current. Fuel cell selectivity can be defined by Equation (4-9).

$$Selectivity = \frac{1}{HFR * \zeta_{\text{lim},ocv}} \qquad \textbf{Equation 4-9}$$

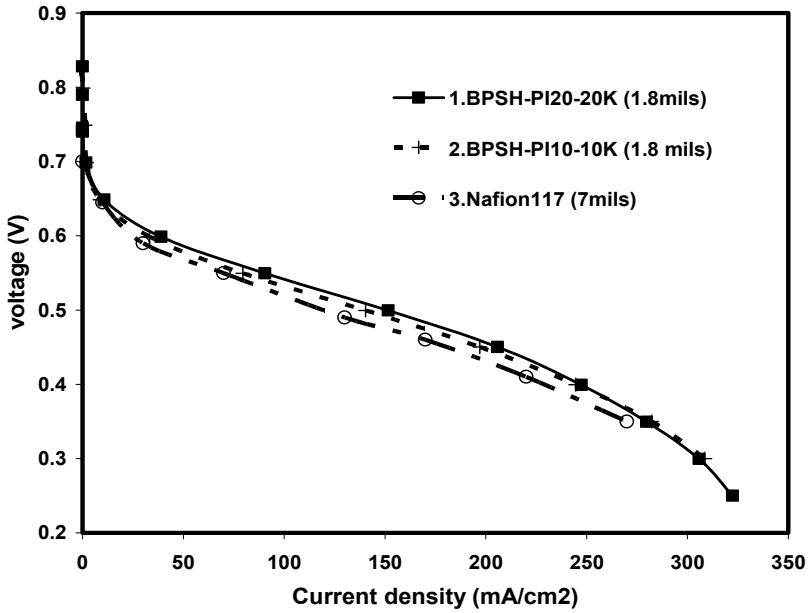

Figure 4-14 DMFC performances of Nafion®117 and BPSH-PI multiblock copolymers, the membrane thicknesses (dried) are given along with the copolymer names in the legend. Reproduced with permissions from ECS Transactions.[31] Copyright [2007], The Electrochemical Society.

Table 4-2 Summary of DMFC performance results for the copolymers studied. Reproduced with permissions from ECS Transactions.[31] Copyright [2007], The Electrochemical Society.

Sample	Thickness (dried) (mils)	OCV (V)	HFR (Ω cm^2)	$\zeta_{lim, ocv}$ (mA/cm^2)	MEA relative* selectivity
Nafion® 117	7	0.70	0.17	68	1.00
BPSH-10-PI-10	1.8	0.79	0.11	58	1.78
BPSH-20-PI-20	1.8	0.80	0.10	57	2.28

* Relative to Nafion® 117

For Nafion®, its 7 mils thickness is normally found to afford the best selectivity between HFR and limiting crossover current. Membranes of greater thickness have higher HFR values, as documented in Table (4-2). This study confirms that it is possible to synthesize much thinner multiblock copolymers while maintaining lower HFR values. Even for a BPSH-PI multiblock of 1.8 mils, its crossover limiting current was well within acceptable limits. It is suggested that on one hand, the connectivity between hydrophobic units restricts the diffusion of methanol while maintaining dimensional stability, even at lower thicknesses. On the other hand, the hydrophilic domains provide a pathway for proton transport and decrease membrane resistance. The overall result is a membrane with improved selectivity over Nafion® 117.

4.4 Conclusions

Novel proton exchange membranes based upon disulfonated poly (arylene ether sulfone) copolymers were synthesized, and their chemical structures were varied to produce random and multiblock copolymers. The transport properties of the BPSH-x-PI-y multiblock copolymers were studied over a range of different block lengths and IECs.

Novel structure–property relationships were achieved by modifying transport properties, as well as the volume fraction of water of these materials. Under fully hydrated conditions, proton conductivity was related more closely to the volume fraction of water than to ion exchange capacity. This highlights the morphological relationship with transport properties. Under partially hydrated conditions, proton conductivity was found to be a function of block length. This was attributed to the decreasing morphological barrier for transport with increasing block length, which was verified by water diffusion coefficients experiments. Multiblock copolymers displayed reduced methanol permeability and very high selectivity. Similar DMFC performance to Nafion® 117 was achieved with a three-fold reduction in thickness for the multiblocks over Nafion®. Thus, for the multiblock copolymers studied, the hydrophilic domains provided a better pathway for water and proton transport, while the hydrophobic domains apparently acted as a barrier for methanol transport.

The authors wish to acknowledge Nissan Motor Company and Department of Energy (DOE Contract # DE-FG36-06G016038) for support of this research.

4.5 References

1. Hickner, M. A.; Ghassemi, H.; Kim, Y. S.; Einsla, B. R.; McGrath, J. E., Alternative polymer systems for proton exchange membranes (PEMs). *Chemical Reviews* **2004,** 104, (10), 4587-4611.

2. Roziere, J.; Jones, D. J., Non-fluorinated polymer materials for proton exchange membrane fuel cells. *Annual Review of Materials Research* **2003,** 33, 503-555.

3. Zalbowitz, M.; S, T., Green Power. *Fuel Cells* **1999**.

4. Mauritz, K. A.; Moore, R. B., State of understanding of Nafion. *Chemical Reviews (Washington, DC, United States)* **2004,** 104, (10), 4535-4585.

5. *DOE Program Review* **2005,** May 23-26, (Arlington,VA).

6. Wang, F.; Hickner, M.; Kim, Y. S.; Zawodzinski, T. A.; McGrath, J. E., Direct polymerization of sulfonated poly(arylene ether sulfone) random (statistical) copolymers

candidates for new proton exchange membranes. *Journal of Membrane Science* **2002,** 197, (1-2), 231-242.

7. Kreuer, K.-D.; Paddison, S. J.; Spohr, E.; Schuster, M., Transport in Proton Conductors for Fuel-Cell Applications: Simulations, Elementary Reactions, and Phenomenology. *Chemical Reviews (Washington, DC, United States)* **2004,** 104, (10), 4637-4678.

8. Kreuer, K. D., On the complexity of proton conduction phenomena. *Solid State Ionics* **2000,** 136-137, 149-160.

9. Zawodzinski, T. A.; Neeman, M.; Sillerud, L. O.; Gottesfeld, S., Determination of Water Diffusion-Coefficients in Perfluorosulfonate Ionomeric Membranes. *Journal of Physical Chemistry* **1991,** 95, (15), 6040-6044.

10. Roy, A.; Hickner, M. A.; Yu, X.; Li, Y. X.; Glass, T. E.; McGrath, J. E., Influence of chemical composition and sequence length on the transport properties of proton exchange membranes. *Journal of Polymer Science Part B-Polymer Physics* **2006,** 44, (16), 2226-2239.

11. Page, K. A.; Cable, K. M.; Moore, R. B., Molecular Origins of the Thermal Transitions and Dynamic Mechanical Relaxations in Perfluorosulfonate Ionomers. *Macromolecules* **2005,** 38, (15), 6472-6484.

12. Noshay, A.; McGrath, J. E., *Block Copolymers: Overview and Critical Survey, Academic Press, New York* **1977**, 91.

13. Lee, H.-S.; Roy, A.; Badami, A. S.; McGrath, J. E., Synthesis and characterization of sulfonated poly(arylene ether) polyimide multiblock copolymers for proton exchange membranes. *Macromolecular Research* **2007,** 15, (2), 160-166.

14. Yu, X.; Roy, A.; Dunn, S.; Yang, J.; McGrath, J. E., Synthesis and characterization of sulfonated-fluorinated, hydrophilic-hydrophobic multiblock copolymers for proton exchange membranes. *Macromolecular Symposia* **2006,** 245/246, (World Polymer Congress--MACRO 2006), 439-449.

15. Wang, H.; Badami, A. S.; Roy, A.; McGrath, J. E., Multiblock copolymers of poly(2,5-benzophenone) and disulfonated poly(arylene ether sulfone) for proton-exchange membranes. I. Synthesis and characterization. *Journal of Polymer Science, Part A: Polymer Chemistry* **2006,** 45, (2), 284-294.

16. Roy, A.; Lee, H.-S.; Badami, A. S.; Yu, X.; Li, Y.; Glass, T. E.; McGrath, J. E., Transport properties of multiblock hydrophilic-hydrophobic proton exchange membranes for fuel cells. *Abstracts of Papers, 232nd ACS National Meeting, San Francisco, CA, United States, Sept. 10-14, 2006*, FUEL-173.

17. Lee, H.-S.; Badami, A. S.; Roy, A.; McGrath, J. E., Segmented sulfonated poly(arylene ether sulfone)-b-polyimide copolymers for proton exchange membrane fuel cells. I. Copolymer synthesis and fundamental properties. *Journal of Polymer Science, Part A: Polymer Chemistry* **2007,** 45, (21), 4879-4890.

18. Zawodzinski, T. A.; Neeman, M.; Sillerud, L. O.; Gottesfeld, S., *J. Phys. Chem.* **1991,** 95, 6040.

19. Springer, T. E.; Zawodzinski, T. A.; Wilson, M. S.; Gottesfeld, S., *J. Electrochem. Soc.* **1996,** 143, 587.

20. Schuster, M.; Kreuer, K.-D.; Andersen, H. T.; Maier, J., Sulfonated poly(phenylene sulfone) polymers as hydrolytically and thermooxidatively stable proton conducting ionomers. *Macromolecules* **2007,** 40, (3), 598-607.

21. Ren, X. M.; Springer, T. E.; Zawodzinski, T. A.; Gottesfeld, S., Methanol transport through nafion membranes - Electro-osmotic drag effects on potential step measurements. *Journal of the Electrochemical Society* **2000,** 147, (2), 466-474.

22. Kim, Y. S.; Sumner, M. J.; Harrison, W. L.; Riffle, J. S.; McGrath, J. E.; Pivovar, B. S., Direct methanol fuel cell performance of disulfonated poly-arylene ether benzonitrile) copolymers. *Journal of the Electrochemical Society* **2004,** 151, (12), A2150-a2156.

23. Stejskal, E. O.; Tanner, J. E., *J.chem.Phys* **1965**, (42), 288.

24. Roy, A.; Hickner, M. A.; Yu, X.; Li, Y.; Glass, T. E.; McGrath, J. E., Influence of chemical composition and sequence length on the transport properties of proton exchange membranes. *Journal of Polymer Science, Part B: Polymer Physics* **2006,** 44, (16), 2226-2239.

25. Roy, A.; Hickner, M. A.; Lee, H.-S.; Badami, A.; Yu, X.; Li, Y.; Glass, T.; McGrath, J. E., Transport properties of proton exchange membranes. *ECS Transactions* **2007,** 2, (24, Direct Methanol Fuel Cells), 45-54.

26. Yasuda, H.; Lamaze, C. E.; Ikenberry, L. D., Permeability of Solutes Through Hydrated Polymer Membranes. *Die Makromoleculare Chemie* **1968,** 118, (NR-2858), 19-35.

27. Cussler, E. L., Diffusion Mass Transfer in Fluid Systems. *2nd Ed. Cambridge University Press, New York,* **1997**.

28. Elabd, Y. A.; Napadensky, E.; Sloan, J. M.; Crawford, D. M.; Walker, C. W., Triblock copolymer ionomer membranes Part I. Methanol and proton transport. *Journal of Membrane Science* **2003,** 217, (1-2), 227-242.

29. Roy, A.; Hickner, M. A.; Lee, H.-S.; Glass, T. E.; McGrath, J. E., States of Water of Proton Exchange Membranes Part-A- Influence of Chemical Structure and Compositions. *To be Submitted* **2008**.

30. Kim, Y. S.; Hickner, M. A.; Dong, L. M.; Pivovar, B. S.; McGrath, J. E., Sulfonated poly(arylene ether sulfone) copolymer proton exchange membranes: composition and morphology effects on the methanol permeability. *Journal of Membrane Science* **2004,** 243, (1-2), 317-326.

31. McGrath, J. E.; Roy, A.; Lee, H.-S.; Yu, X.; Badami, A.; Li, Y.; Wang, H., Multiblock hydrophilic-hydrophobic proton exchange membranes for direct methanol based fuel cell. *ECS Transactions* **2007,** 2, (24, Direct Methanol Fuel Cells), 55-62.

5.0 States of Water of Proton Exchange Membranes Part-A- Influence of Chemical Structures and Compositions

Abhishek Roy,[1] Michael A. Hickner,[2] Hae-Seung-Lee,[1] Tom Glass,[1]
Yanxiang Li,[1] and James E. McGrath[1]

[1] Macromolecules and Interfaces Institute
Virginia Polytechnic Institute and State University, Blacksburg, VA 24061
[2] Department of Materials Science and Engineering
The Pennsylvania State University, University Park, PA 16802

Abstract

Sulfonated copolymers studied in our laboratory phase separate to form nano-scale hydrophilic and hydrophobic domain morphology. Water existing in these domains exits in three different states, tightly bound, loosely bound and free water. The states of water were characterized using DSC, NMR relaxation and TGA measurement techniques. The chemical structure of the proton exchange membranes was varied in chemical compositions, microstructures (random and block) and also the functional groups in the polymeric backbone. A strong dependence of the types of water on the ion content and morphology was observed. For the random copolymers, the formation of free water in the system occurs after reaching a certain ionic content. For the blocks, in addition to the ionic content, free water also develops with increasing block lengths. The formation of continuous morphology in the copolymers was correlated to the onset of free water. The influence of states of water on PEM properties will be reported separately in Part-B.

5.1 Introduction

Fuel cells are electrochemical devices that convert chemical energy to electrical energy.[1] Among various types of fuel cells, proton exchange membrane fuel cells (PEMFCs) are of major importance. PEMFCs have a diverse field of applications ranging from stationary, automotive to even portable power systems. Hydrogen air fuel cells and direct methanol fuel cells (DMFC) are the two main types used for these applications.[2, 3] A typical operating principle for a PEMFC involve oxidations of the fuel H_2 at the anode to positively charged hydrogen ions and electrons. The hydrogen ions or the protons are transported across the proton exchange membrane (PEM) to the cathode and react with oxygen to form water. The integral part of the fuel cell is considered to be the PEM and its primary demands are high proton conductivity and low water uptake. In addition, the membrane should have both thermal and oxidative stability, good mechanical properties, low permeability to fuels and dimensional stability under hydrated conditions.[4, 5] The current state of the art PEMs are perfluorosulfonic acid membranes such as Nafion® manufactured by DuPont. These membranes show excellent chemical and electrochemical stability as well as high proton conductivity with relatively low water uptake on a mass basis. However, Nafion® suffers from disadvantages including high cost, high methanol permeability (DMFCs), and limited operating temperature (80°C)[5, 6] due to its low hydrated α relaxation temeprature.[7] Our research group has been engaged in the past few years in the synthesis and characterization of biphenol based partially disulfonated poly(arylene ether sulfone) (BPSH) random copolymers as potential PEMs.[4, 8-12]

All of these sulfonated copolymers phase separate to form nano scale hydrophilic and hydrophobic morphological domains. The hydrophilic phase containing the sulfonic acid moieties causes the copolymer to absorb water. Water confined in hydrophilic pores in concert with the sulfonic acid groups serve the critical function of proton (ion) conduction in these systems.[13] The transport of water and protons in these confined systems are both of fundamental interest and technological importance in the design of new materials. There are at least three states of water that have been associated with

water residing in hydrophilic phases of polymers.[14-17] The presence of these three states can be defined by thermal properties. *Non-freezing bound water* is strongly associated with the polymer and depresses its T_g, but the water shows no melting endotherm by differential scanning calorimetry (DSC). *Freezable bound water* is weakly bound to the polymer (or weakly bound to the non-freezing water), and displays broad melting behavior around 0° C. *Free water* exhibits a sharp melting point at 0° C.

States of water for hydrophilic polymers have been characterized by various methods including DSC and NMR relaxation measurements.[14, 15, 18-21] Previous work has shown that DSC thermograms are a function of water content for polymers, showing melting endotherms of loosely bound water and free water.[15] Tightly bound water can be correlated to the maximum amount of water for which there is no melting endotherm. Quinn et al.[14] have proposed a better mathematical technique to estimate the distribution of each type of water. They showed that if the integrated change in enthalpy (per gram of dry polymer) from the DSC thermogram is plotted against water content, the intercept gives the tightly bound water content. By subtracting the tightly bound water from the total water, the combined content of the loosely bound water and free water can be obtained. However, it is difficult to quantify the loosely bound and free water separately using DSC as the two melting endotherms of free and loosely bound water overlap with each other. Hence other experimental techniques in conjunction with DSC are needed for proper quantification.

NMR relaxation (T_2) experiments can provide improved quantification of three states of water as reported by Whittaker et al.[18] They showed that for a hydrophilic polymer with three states of water, the decay in transverse relaxation magnetization of water can be modeled to a tri- exponential function. The shortest component of the decay with the fastest relaxation time corresponds to the tightly bound water having the shortest diffusive path length. The intermediate component represents the loosely bound water and the long component of T_2 can be related to the bulk or free water. The relative fractions of the coefficients of the exponential terms are proportional to the respective types of water, allowing quantification of each.

This paper (Part-A) proposes to quantify and characterize the states of water for PEMs by DSC and NMR relaxation measurements. The influence of the distribution of the three types of water on various transport and electrochemical properties of PEMs will be discussed in Part-B.

Synthesis of controlled series of materials varying in ion content, chemical composition and sequence lengths, structure/property relationships between the functionality of the polymer backbone, the states of water, and the membrane transport has been achieved. The chemical microstructure was varied from random morphology to a phase separated multiblock morphology. It is hypothesized that this will have a large influence on the states of water through the phase separation characteristics of the polymers as well as direct interaction between the functional groups and water molecules.

5.2 Experimental

5.2.1 Materials

Highly purified 4,4'-dichlorodiphenylsulfone (DCDPS) was provided by Solvay Advanced Polymers. Hydroquinone (HQ) was obtained from Eastman Chemical Company. 4,4'-Hexafluoroisopropylidenediphenol (6F-BPA), received from Ciba, was purified by sublimation. The ketone monomer, 4,4'-difluorobenzophenone (DFBP) was purchased from Aldrich and used as received. All these monomers were dried under vacuum prior to use. Disulfonated comonomers (SDCDPS, SDFBP) were synthesized according to the modified literature methods[8] and dried under vacuum before copolymerization. The solvent N,N-dimethylacetamide (DMAc, Fisher) and N-methyl-2-pyrrolidinone (NMP, Fisher) were vacuum-distilled from calcium hydride onto molecular sieves. Potassium carbonate (Aldrich) was dried in vacuum before copolymerization. Toluene, sodium chloride, 30% fuming sulfuric acid and methanol were obtained from

Aldrich and used as received. The fuming sulfuric acid was further analyzed for active SO_3 concentration.[22] Nafion® 112 and 117 were obtained from ElectroChem, Inc.

5.2.2 Synthesis of partially disulfonated poly(arylene ether) random copolymers (HQSH-xx and B-ketone-xx)

Synthesis of disulfonated poly(arylene ether sulfone) copolymers was successfully achieved via aromatic nucleophilic substitution as described previously.[8, 23] One typical copolymerization for a HQSH-40 copolymer was as follows. Hydroquinone (10 mmole), 4,4'-dichlorodiphenylsulfone (6 mmole), and 3,3'-disulfonated-4,4'-dichlorodiphenylsulfone (4 mmole) were charged to the flame dried 3-neck flask, which was equipped with a mechanical stirrer, nitrogen inlet and a Dean-Stark trap. Potassium carbonate (11.5 mmole) was added to the system. Dry NMP was introduced to afford about a 20% solids concentration and toluene (NMP/toluene = 2/1 v/v) was used as an azeotropic agent. The reaction mixture was heated under reflux at 150 ºC for 4 h to remove the water. Then, the bath temperature was raised slowly to 180 ºC and reacted for an additional 24 h. The viscous solution was cooled to room temperature, and then diluted with NMP. The copolymer solution was filtered to remove the byproduct salt and then isolated by precipitation in deionized water. The copolymer was separated by filtration and dried in a vacuum oven at 120 °C for 24 h.

The copolymerization procedures for polyketones were similar to those of polysulfones, although the monomers' reactivities are different. The detailed procedure was also introduced in the literature.[24] The B-ketone-xx series [Fig. 5-1(c)] copolymers were based on 6F BPA, DFBP, and SDFBP. Because the fluorinated monomers have higher reactivity, high molecular weight copolymers can be achieved within shorter reaction times.

5.2.3 Synthesis of disulfonated poly(arylene ether sulfone)-b-polyimide (BPSH-x-PI-y) multiblock copolymers

A series of segmented disulfonated poly(arylene ether sulfone)-*b*-polyimide copolymers based on hydrophilic and hydrophobic oligomers was synthesized. The disulfonated hydrophilic oligomers were prepared via step growth polymerization using different block lengths ranging from 5 kg/mol to 20 kg/mol. To produce the amine telechelic functionality of the hydrophilic oligomers, *m*-aminophenol (*m*-AP) was used as the endcapping reagent for the reaction. Anhydride-terminated polyimide hydrophobic oligomers with the same molecular weight range as the hydrophilic oligomers were synthesized via a high temperature one-pot imidization. The anhydride end-group functionality was achieved by adding stoichiometrically adjusted amounts of the monomers. Synthesis of the multiblock copolymers was facilitated by an imidization coupling reaction between the amine end-groups on the hydrophilic oligomers and the anhydride end-groups on the hydrophobic oligomers, thereby producing high molecular weight copolymers. A detailed synthesis of the copolymers has been published elsewhere,[25, 26] according to which a series of multiblock copolymers with different block lengths were synthesized and characterized.

5.2.4 *Membrane preparation*

The salt form copolymers were redissolved in DMAc to afford transparent 5 wt % solutions, which were then cast onto clean glass substrates. The films were slowly dried for 2 days with infrared heat at gradually increasing temperatures, and then dried under vacuum at 110 ^{o}C for 2 days. The membranes were converted to their acid form by boiling in 0.5 M H_2SO_4 for 2 h, and were then boiled in deionized water for 2 h to remove any residual acid. Membranes were stored in deionized water until used for measurement.

5.2.5 Differential scanning calorimetry (DSC) and nuclear magnetic resonance (NMR) and thermo gravimetric Analyzer (TGA)

The DSC experiments were performed in a TA DSC instrument using liquid nitrogen as cooling medium for subambient operation. The samples were equilibrated in a relative humidity oven (ESPEC SH240) to achieve desired hydration levels. The samples were placed in thermally sealed pans capable of withstanding pressure of 100 atm. Samples were cooled to -70 °C and then heated at a rate of 5 °C per min under a N_2 atmosphere.

The proton spin relaxation time, T_2, was measured in a Varian Inova 400 spectrometer using Carr-Purcell-Meiboom-Gill (CPMG) pulse sequence. The 90° pulse was of 13.8 μs and the 180° pulse of 27.6 μs. A total of 200 decay points was collected over 8 ms. Samples were equilibrated at room temperature in water. Just before the experiment, they were removed from water, blotted to remove the surface water and placed in the NMR probe. The fitting procedure was performed using a non-negative least square analysis by Matlab software. The goodness of the fits was determined by comparing the statistical parameters (RMSE and SSE). The relative fractions of the coefficients of the exponential terms are proportional to the weighed average of the respective types of water, allowing quantification of each. The spin lattice relaxation time, T_1 was measured using the inversion recovery method and sequence. The 90° pulse was of 13.8 μs and the 180° pulse of 27.6 μs. A total of 14 points was collected and the d1 was kept 3 s.

TGA experiments were conducted on a TA instrument for the fully hydrated sample. Just before the experiment, they were removed from water, blotted to remove the surface water and placed in the TGA sample pan. Air was the atmosphere and 10 ^{o}C/min was the heating rate.

5.3 Results

5.3.1 Model copolymers

Our research group has been engaged in the past few years in the synthesis and characterization of wholly aromatic, biphenol based partially disulfonated poly(arylene ether sulfone) random copolymers as potential PEMs.[4, 8-12] This series of copolymers are called BPSH-xx [Fig. 5-1(a)], where BP stands for biphenol, S is for sulfonated, and H denotes the protonated form of the acid where xx represents the degree of disulfonation. Similar to the BPSH series, hydroquinone based partially disulfonated poly(arylene ether sulfone)[23] [HQSH-xx – Fig. 5-1(b)] random copolymers and partially disulfonated poly(arylene ether ketone) random copolymers[24] [B-ketone-xx Fig. 5-1(c)] were synthesized. In addition to the random copolymers, a series of multiblock copolymers [BPSH-x-PI-y – Fig. 5-1(d)] was also synthesized. In the multiblock copolymers, x and y represent the block lengths in kg/mol of hydrophilic:hydrophobic units, respectively. The IECs of the multiblocks were kept similar (1.5~1.6 meq/g). The individual molecular weights of the hydrophobic and hydrophilic blocks were kept similar to each other and the molecular weight was varied from 5000, 10000 to 15000 g/mole.

a)

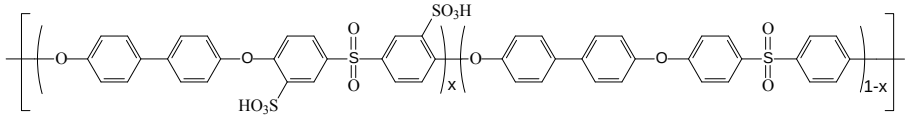

b)

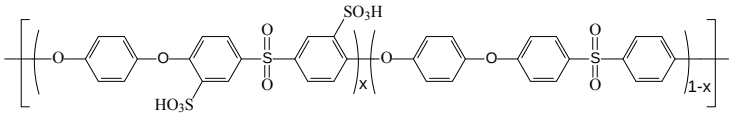

c)

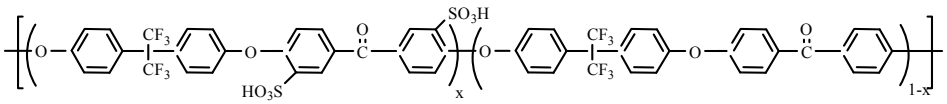

d)

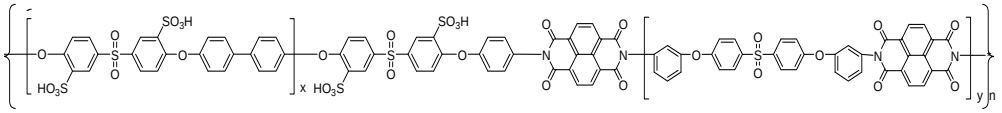

Figure 5-1 Copolymer chemical structures: (a) BPSH-xx; (b) HQSH-xx, (c) B-ketone-xx, (d) BPSH-x-PI-y multiblocks

5.3.2 Water uptake

Water uptake in proton exchange membranes is considered to be one of the most important properties. On one hand, proton conductivity is a strong function of the water content of the polymer and increases with increasing water content.[27] On the other hand, a low water swelling for the membrane is desired for improved fuel cell performance and durability. Figure (5-2) represents the water uptake values as a function of IEC for the random, multiblock and Nafion® 117 copolymers. A sharp increase in the water uptake is observed after reaching a particular IEC for the random copolymers. Previous reports from our laboratories have related this IEC to the percolation limit for the water uptake.[12] A morphological transition from closed to open structure is believed to be the reason as supported by AFM studies.[28]

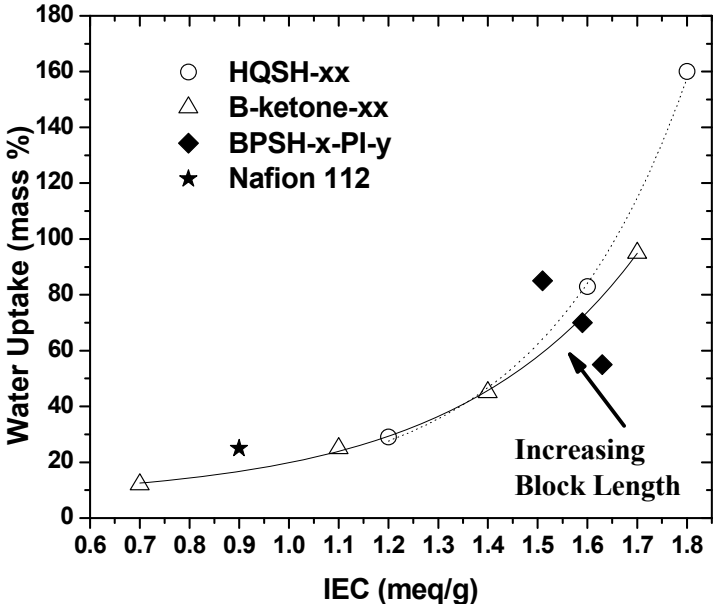

Figure 5-2 Influence of IEC and block lengths on water uptake at fully hydrated conditions

The three multiblock copolymers had similar IECs. Therefore, studying the equal block length materials would be appropriate in understanding the effect of block lengths on the properties of copolymers at the same ionic content. A sharp increase in water

uptake is associated with increasing block lengths from 5-5, 10-10 to 15-15. Unlike the random copolymers, where the isolated sulfonic acid groups are randomly distributed in pairs along the chain, the multiblock copolymers feature a sequence of hydrophilic and hydrophobic segments. Although the ionic content for the three multiblocks is similar, the chemical incompatibility between the individual blocks results in increasing phase separation with increasing block length. AFM studies revealed the formation of a co-continuous morphology with increasing block length, particularly for the BPSH-15-PI-15.[25] The morphological transition induced sharp water absorption.

The above study was conducted under fully hydrated conditions. It is also important to investigate the influence of IEC and morphology on the water uptake over a wide range of water activity. Here the water activity is defined by the Equation (5-1). Also, to normalize the effect of IEC, water uptake values for the copolymers are hereafter reported as hydration numbers. The hydration number (λ) is defined as the number of water molecules present per sulfonic acid group (Eq^{n}. 5-2).

$$\text{Water Activity} = \%\ RH/100 \qquad \textbf{Equation 5-1}$$

$$\lambda = \frac{(mass_{wet} - mass_{dry}) / MW_{H_2O}}{IEC * mass_{dry}} \qquad \textbf{Equation 5-2}$$

Figure (5-3a) shows the influence of water activity on water uptake for the random HQSH-xx copolymers with varying IEC and Figure (5-3b) shows the same for BPSH-x-PI-y multiblocks with increasing block lengths. At low water activity levels, the hydration numbers for all of the random copolymers were similar. This is true for the multiblocks also. At low water activity, the nature of the water tends to depend more on the nature of the sulfonic groups and the chemical backbone. A sudden increase in hydration number after a certain water activity (~0.8) is observed for both random and multiblock copolymers. This effect is more pronounced for random copolymers with higher IEC and for multiblocks with higher block lengths. The increasing ionic content

in random copolymers and the increasing block lengths for multiblock copolymers are inducing morphological changes within the copolymers altering the types of water. This phenomenon will be examined in depth using DSC and NMR relaxation measurements.

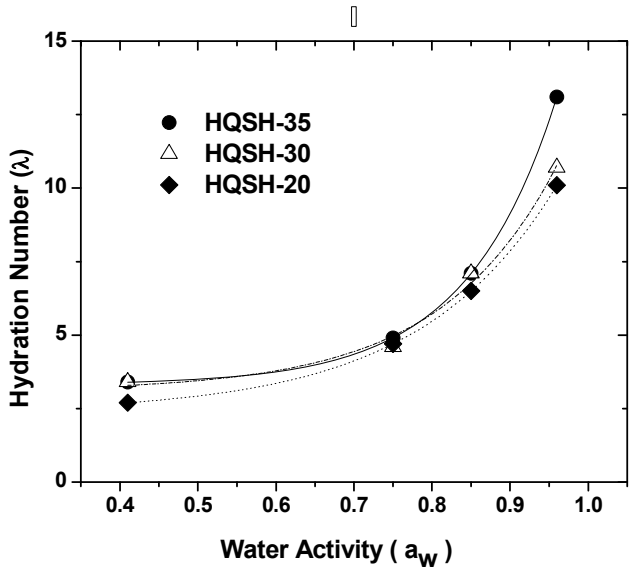

Figure 5-3 a) Water absorption under partially hydrated conditions for the random HQSH-xx copolymers as a function of IEC

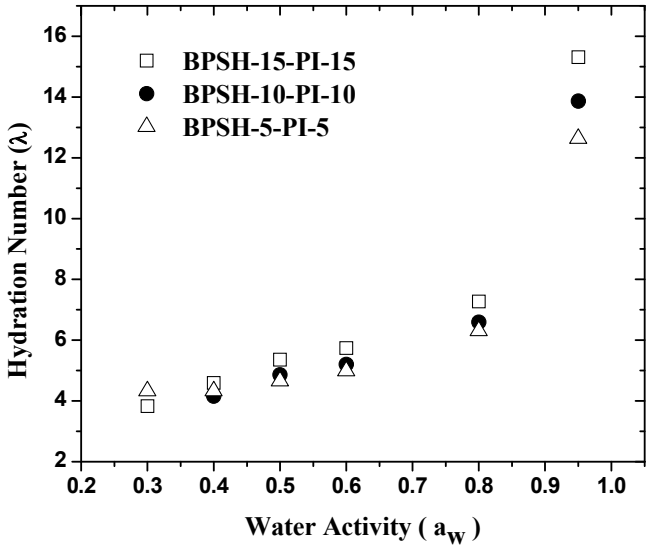

Figure 5-3 b) Water absorption under partially hydrated conditions for the block copolymers BPSH-x-PI-y as a function of the block length

5.3.3 DSC results

The influence of degree of disulfonation on the melting endotherms of the *freezing water* present in the HQSH-xx copolymers under fully hydrated conditions is shown in Figure (5-4a). The DSC thermograms show an overlapping set of peaks for free water (expected at 0 °C) and loosely bound water from -30 to 10 °C. The areas under the peaks increased with increasing degrees of disulfonation. The increasing area under the peak suggests the presence of increased amount of freezing water with increasing ionic content. Similar results were obtained for the other copolymers. Studies conducted on the multiblocks indicated a strong influence of morphology or the block lengths on the melting endotherm peaks. In spite of having similar ionic concentrations, the area under the peak increased with increasing block lengths as shown in Figure (5-4b). Hence in addition to ionic content, morphology of the copolymer is also influencing the freezing water content.

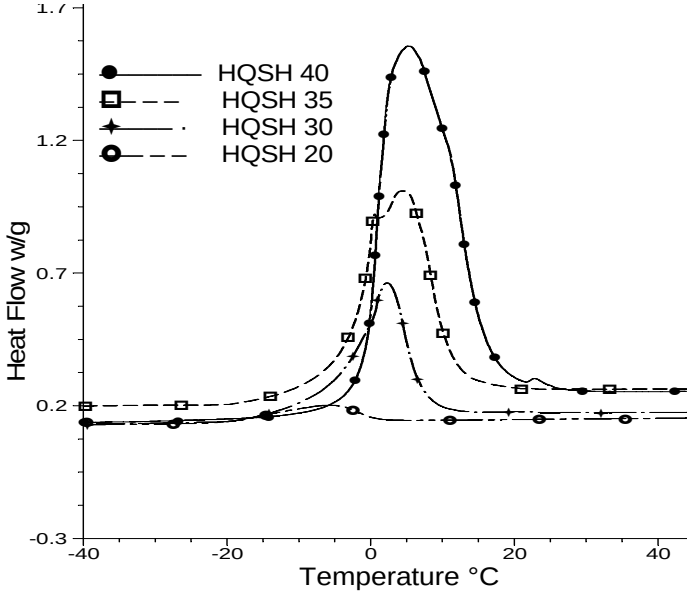

Figure 5-4 a) Melting endotherms of the freezing water in HQSH-xx copolymers as a function of degree of disulfonation under fully hydrated condition

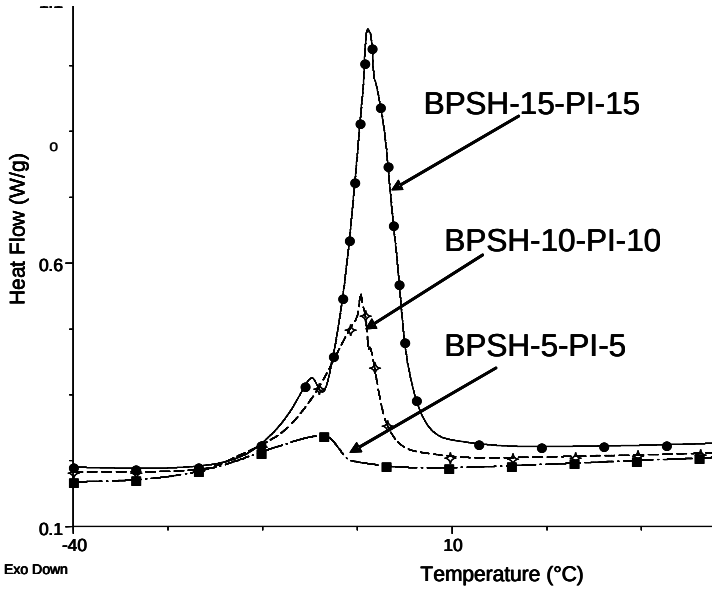

Figure 5-4 b) Melting endotherms of the freezing water in BPSH-x-PI-y multiblock copolymers as a function of block length under fully hydrated condition

The influence of water content on the endothermic peaks and glass transition temperatures (T_g) for the HQSH 35 and BPSH-15-PI-15 copolymers is shown in Figure (5-5a) and (5-5b). At fully hydrated conditions, the sharp melting endotherm of water is observed at around 0 °C (T_m). The measured T_m of freezing water for the copolymers is provided in Table (5-1). The area under the melting endotherm peak broadens and decreases with a decrease in water content (represented within parenthesis) in the membranes for both HQSH 35 (42%) and BPSH-15-PI-15 (56%) copolymers. This indicates a presence of higher fraction of loosely bound freezable water over the free water at this hydration level for each of the two copolymers. However, with further decrease in water content, no endothermic peak was seen in the DSC traces. The amount of water present at this hydration level in the copolymers is non freezable and can be correlated to the amount of tightly bound water in the membranes. In order to get a more accurate estimation of the tightly bound water content, a quantitative analysis described earlier in this paper is followed. The integrated change in enthalpy (per dry g of polymer) is plotted as a function of hydration number in Figure (5-6) for the HQSH-xx series.

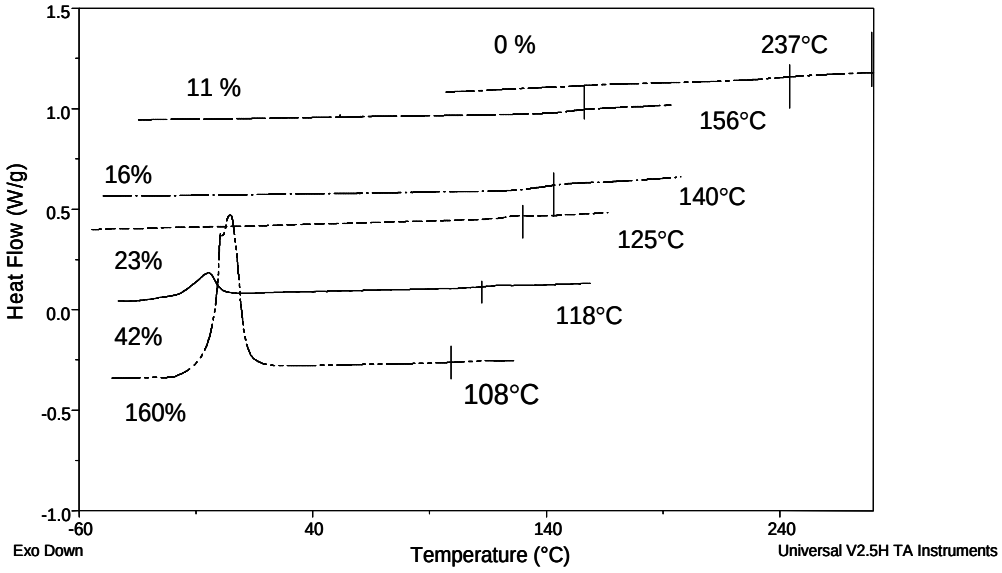

Figure 5-5 a) Influence of water content on endothermic peaks and T_gs of HQSH 35

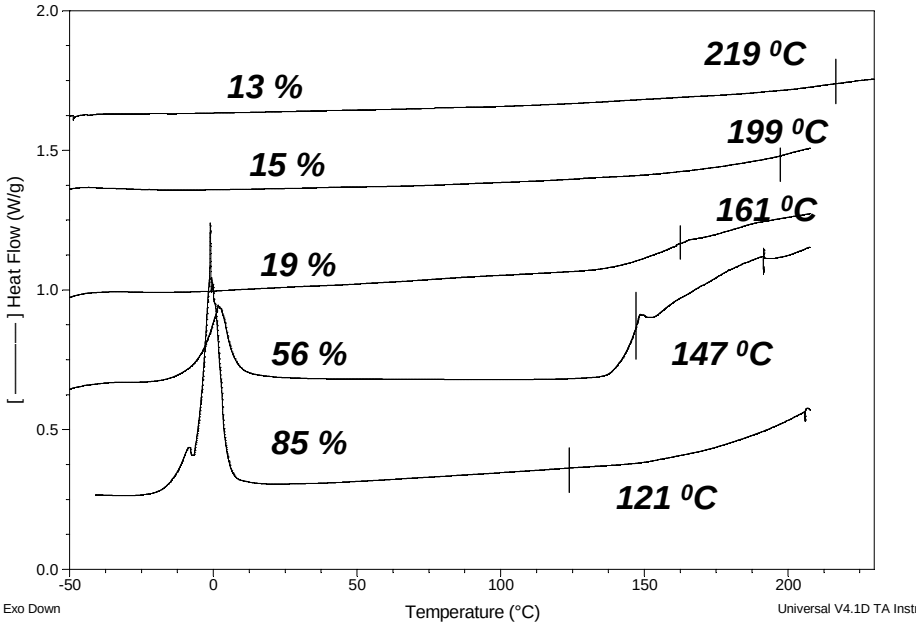

Figure 5-5 b) Influence of water content on endothermic peaks and T_gs of BPSH-15-PI-15. The numbers in the left side represent water uptake and on right T_gs respectively

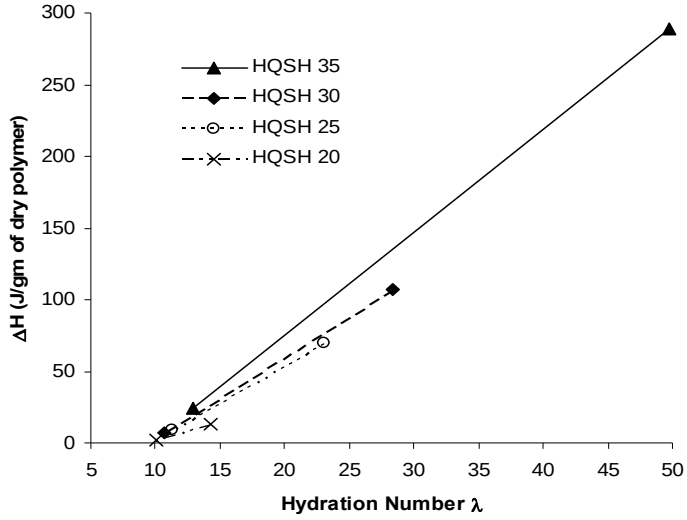

Figure 5-6 Normalized enthalpy changes of water as a function of the hydration number for HQSH-xx random copolymers; the intercepts are the tightly bound water contents

All the HQSH copolymers irrespective of the degree of disulfonation showed a similar intercept or an identical nonfreezing, tightly bound water content. Subtracting the value from the total water content gives the respective freezing and nonfreezing (tightly bound) water content in the membranes. Similar analyses for all the copolymers were conducted. NMR relaxation measurements were used to quantify the freezing water to loosely bound and free water, as discussed later on.

Water, known to act as a plasticizer with T_g around -139 ^oC, depresses the T_g of the copolymer. The hydrated T_g of all the copolymers measured under fully hydrated conditions are reported in Table (5-1). The hydrated T_g restricts the upper use temperature for fuel cell operations. The depression in T_g with increasing water content within the copolymer is seen from Figure (5-5a and 5-5b) for the HQSH 35 and the BPSH-15-PI-15 respectively. Kim et al.[15] were able to scale this depression in T_g more precisely with the tightly water content than with the total water content in the

membranes.[15] The areas under the melting endotherms were normalized to obtain the ΔH_{fus} / g of the freezing water. ΔH_{fus} / g increased with increasing ionic concentration for the random copolymers and with block lengths for the multiblocks. Nafion® has the highest ΔH_{fus} / g among the studied copolymers. Qualitatively the ΔH_{fus} / g can be related to the nature of the water–water interaction. Higher value represents better water-water interactions or decreased water –polymer interactions, indicating presence of more free water concentration in the system.

Table 5-1 Summary of copolymer properties

Sample	IEC (meq/g)	Water uptake (mass %)	Hydration number (λ)	ΔH (J/g of water)	Hydrated T_g (°C)	T_m (°C) (fully hydrated)
Nafion 117	0.9	27	17	210	99	2.0
HQSH-35	1.8	160	50	180	108	4.6
HQSH-30	1.6	83	29	128	107	2.2
HQSH-25	1.4	60	23	110	107	1.9
HQSH-20	1.2	29	14	45	110	-6.0
B-ketone-50	1.7	95	32	120	104	3.3
B-ketone-40	1.4	45	18	90	118	1.1
B-ketone-30	1.1	25	13	5	99	-1.4
BPSH-5-PI-5	1.6	55	18	33	110	-10.0
BPSH-10-PI-10	1.6	70	24	81	118	1.0
BPSH-15-PI-15	1.5	85	31	172	121	2.0

5.3.4 NMR relaxation measurements (T_2 and T_1)

To quantify the freezing water content to loosely bound and free water content, T_2 NMR relaxation experiments were conducted for all the copolymers. The mechanism for the T_2 relaxation in sulfonic acid containing polymers is believed to be an exchange

process between the water molecules and the exchangeable protons in sulfonic acid groups.[19] The water molecules (tightly and loosely bound) associated with the sulfonic acid groups relax faster than the ones (free water) which are not. However for the copolymers studied, T_2 data cannot distinguish the shortest and the intermediate components from each other. Loosely bound and tightly bound water are believed to exist in the same hydrophilic domain and fast exchange occurs in between the two environments. Specifically, for the copolymers having water absorption below the sharp inflection point or the percolation threshold (Fig. 5-2), the relaxation nature fits well with monoexponential decay function. In those cases, it was hard to distinguish the loosely and tightly bound water separately from NMR only and DSC was utilized to quantify the two types of water. Only for the copolymers with open or co-continuous morphology i.e. high IEC random copolymers and higher block length multiblocks, a distinct longer relaxation component was detected and was assigned to the free water. The free water content was quantified from NMR, tightly bound from DSC. Subtracting the free and tightly bound from total water content, allows to properly estimating the loosely bound water content. Thus the NMR in conjunction with DSC experiments allowed proper quantification of the states of water in the copolymers as shown in Table (5-2).

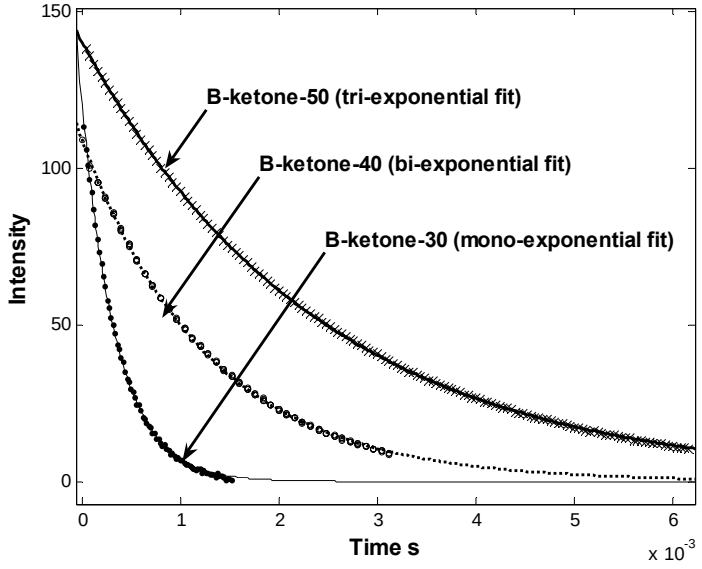

Figure 5-7 Influence of disulfonic acid concentrations on ^1H T_2 decays for the B-ketone-xx copolymers. The markers represent actual experimental data and the lines represent the fitted functions

The mechanism for T_1 relaxation is known to be different than T_2 relaxations.[19] T_1 or the longitudinal NMR relaxation provides an idea of the nano-viscosity of the sulfonic acid domains and the state of water present in those domains. The inverse of the T_1 relaxation times can be related to the correlation time (τ_c) for molecular motion. A high $1/T_1$ value indicates a fast exchange process and restricted molecular mobility for the water molecules. $1/T_1$ relaxation times for the copolymers are reported Table (5-2). The water molecules associated with low IEC random copolymers have very high $1/T_1$ or low T_1 relaxation values. This fast exchange process between the water molecules and the sulfonic acid groups indicates high water–polymer interactions and presence of mostly tightly bound water. At a given IEC, the poly(arylene ether ketone) copolymers have higher $1/T_1$ values for water in compared to poly(arylene ether sulfone) copolymers. The ketone group being more polarizable interacts more with the water than sulfone and is more tightly bound. The $1/T_1$ value decreased with increasing IEC for the random copolymers and at high IECs, the value approaches similar to Nafion®. The low $1/T_1$ value corresponds to an increased water molecular mobility or better rotational dynamics, suggesting appearance of free and loosely bound water in these copolymers. In addition to IEC, the rotational dynamics of water is also influenced by the morphology of the copolymers. The $1/T_1$ value decreased with increasing block length for the multiblocks. The co-continuous hydrophobic-hydrophilic domain morphology influenced the rotational dynamics of water and would expect to influence the translational dynamics or the diffusion coefficients of water also.

Table 5-2 Quantification of the different states of water and the $1/T_1$ relaxation time

Sample	IEC (meq/g)	Total water (λ)	Non freezing water (λ)	Freezing water		$1/T_1$ (s^{-1})
				Loosely bound (λ)	Free (λ)	
Nafion 117	0.9	17	3	9	5	4.7
HQSH-35	1.8	50	9	27	14	3.6
HQSH-30	1.6	29	9	11	8	6.6
HQSH-25	1.4	23	9	10	4	47.6
HQSH-20	1.2	14	9	5	0	-
B-ketone-50	2.1	32	8	21	3	95.2
B-ketone-40	1.7	18	8	10	0	250.0
B-ketone-30	1.3	13	8	5	0	333.3
BPSH-5-PI-5	1.6	18	14	4	0	166.0
BPSH-10-PI-10	1.6	24	14	8	2	111.0
BPSH-15-PI-15	1.5	31	15	11	5	25.0

Quantification of the three states of water was successfully achieved from a combination of DSC and NMR relaxation measurements. Apart from these two, an independent type of measurement will broaden the scope for this paper. This paper proposes to study the different states of water using thermo gravimetric analysis (TGA). In the light of the DSC and the NMR relaxation experiments, a difference in water – polymer interaction can be predicted for the different states of water. Hence the retention of water as a function of temperature may be different for different types of water. Figure (5-8) represents the weight loss or retention of water as a function of temperature

for the HQSH-xx and Nafion® copolymers. An initial quick loss in hydration number is seen for all the copolymers upto 50 to 60 °C. The water lost in this temperature regime can be related to the type of water which has the lowest interaction with the copolymer. After this temperature regime, the rate of loss of water is found to be very slow over a wide temperature range. Hence the residual water in the membrane seems to resemble the tightly bound water content and can be easily calculated from the ordinate value. Both for the HQSH-xx series and Nafion®, the tightly bound water content, calculated from TGA (9 and 2 respectively) are found to be similar to the DSC and NMR results.

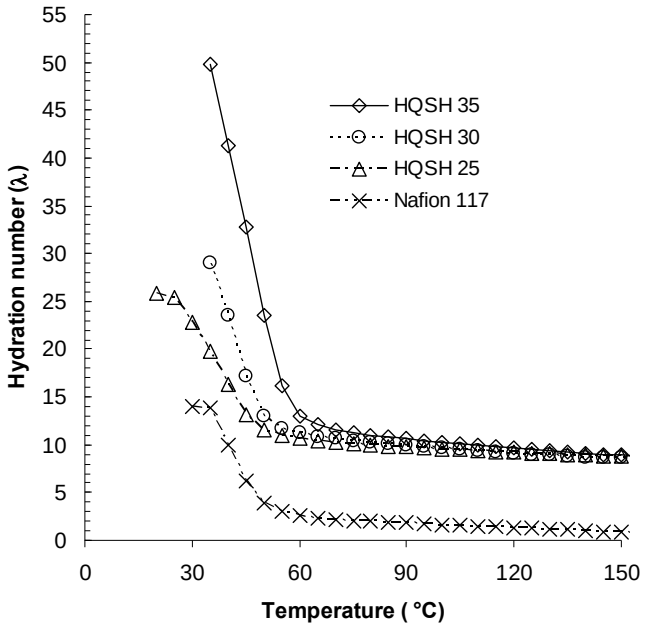

Figure 5-8 Retention of water as a function of temperature for the HQSH-xx and Nafion® copolymers

5.4 Discussion and Conclusions

The quantified values of the three types of water as a function of IEC and block lengths are given in Table (5-2). For the random copolymers, the loosely bound water and free water comprising the freezing water increase with increasing IEC. The increasing free water content influenced the thermodynamic and rotational properties of

water in PEMs. This is in agreement with the increasing ΔH_{fus} and decreasing $1/T_1$ relaxation trends with IECs, as seen from the DSC and NMR measurements. It is important to note that the free water develops in random copolymers only after reaching a particular IEC. This particular IEC also corresponds to the characteristic non linear increase in water uptake (Figure 5-2).

The question arises that what is the reason behind the origination of free water in these copolymers. The random copolymers containing sulfonic acid groups are also known to also phase separate into hydrophobic and hydrophilic domains with increasing ion exchange capacity and water uptake.[11] In other words, at a higher sulfonic acid concentrations, the hydrated hydrophilic domains interconnect with each other to form associated, percolated type morphology. At this point it is debatable that whether the percolated phase separated morphology or the higher ionic content is responsible for the origin of free water. Keeping the IEC similar, varying the morphology and understanding its effect on free water content will elucidate the reason behind the origin of free water. Multiblock copolymers studied are of ideal choice. The IEC being similar, morphology is the function of the block lengths only. Both loosely bound and free water content increase with increasing block lengths or with the extent of microphase separation. The sharp increase in the area under the melting endotherm correlates with the origin of the free water inside co-continuous ordered hydrophilic domains for the BPSH-15-PI-15 copolymer. Thus microphase separation between hydrophilic and hydrophobic domains or the connectivity between hydrophilic domains seems to be one of the major factors behind the origin of free water.

The tightly bound water content determined from DSC measurements depends more on the nature of the sulfonic acid groups or the strength of the conjugate base and the chemical back bone. On a quantitative basis, the Nafion® has the least amount of tightly bound water followed by the random copolymers and then the block copolymers. The unique chemical structure of the Nafion® consists of highly flexible side chains bearing the hydrophilic sulfonic acid groups and a highly hydrophobic fluorinated flexible backbone. The perflurosulfonic acid being a very strong acid, the conjugate base

is much weaker with reduced effective charge density. The weak conjugate base and the presence of highly hydrophobic back bone lowers the water coordination number or precisely the tightly bound water content in Nafion®.

In contrast, for the random copolymers, the sulfonic acid groups are directly attached to the main polymer chain backbone. This results in a restricted morphological structure. Also compared to Nafion®, the sulfonic acid groups are of lower acidity or alternatively, the conjugate base is stronger. A stronger conjugate base increases the negative charge density and hence increases the tightly bound water content. The normalized tightly bound water content per sulfonic groups was independent of the overall ionic content in the copolymers.

In the multiblock copolymers, the nature of the sulfonic group is similar with the aromatic random copolymers studied. However unlike the random copolymers, where the sulfonic acid groups are distributed through out the copolymer, in multiblocks, sulfonic acid groups are arranged in a concerted array network. As a result, the local effective negative charge density is higher in multiblocks compared to that of random copolymers. This increased the tightly bound water content in multiblocks.

The study revealed a strong relationship of the morphology, chemical structure and compositions with the different types of water. In part-B, the distribution of these states of water in the copolymer will be related to the fundamental transport properties. The states of water investigation coupled with transport property measurements will be instrumental in developing a novel structure property relationship for PEMs.

The authors would like to thank the National Science Foundation “Partnership for Innovation” Program (HER-0090556) and the Department of Energy (DE-FC36-01G01086) for support of this research effort. The authors would also like to thank Sandia National Laboratories for their support.

5.5 References

1. Winter, M.; Brodd, R. J., What are batteries, fuel cells, and supercapacitors? *Chemical Reviews* **2004,** 104, (10), 4245-4269.

2. Zalbowitz, M.; S, T., Green Power. *Fuel Cells* **1999**.

3. Carrette, L.; Friedrich, K. A.; Stimming, U., Fuel cells: Principles, types, fuels, and applications. *Chemphyschem* **2000,** 1, (4), 162-193.

4. Hickner, M. A.; Ghassemi, H.; Kim, Y. S.; Einsla, B. R.; McGrath, J. E., Alternative polymer systems for proton exchange membranes (PEMs). *Chemical Reviews* **2004,** 104, (10), 4587-4611.

5. Mauritz, K. A.; Moore, R. B., State of understanding of Nafion. *Chemical Reviews* **2004,** 104, (10), 4535-4585.

6. Yeo, R. S., Ion Clustering and Proton Transport in Nafion Membranes and Its Applications as Solid Polymer Electrolyte. *Journal of the Electrochemical Society* **1983,** 130, (3), 533-538.

7. Page, K. A.; Cable, K. M.; Moore, R. B., Molecular Origins of the Thermal Transitions and Dynamic Mechanical Relaxations in Perfluorosulfonate Ionomers. *Macromolecules* **2005,** 38, (15), 6472-6484.

8. Wang, F.; Hickner, M.; Ji, Q.; Harrison, W.; Mecham, J.; Zawodzinski, T. A.; McGrath, J. E., Synthesis of highly sulfonated poly(arylene ether sulfone) random (statistical) copolymers via direct polymerization. *Macromolecular Symposia* **2001,** 175, 387-395.

9. Wang, F.; Hickner, M.; Kim, Y. S.; Zawodzinski, T. A.; McGrath, J. E., Direct polymerization of sulfonated poly(arylene ether sulfone) random (statistical) copolymers: candidates for new proton exchange membranes. *Journal of Membrane Science* **2002,** 197, (1-2), 231-242.

10. Kim, Y. S.; Sumner, M. J.; Harrison, W. L.; Riffle, J. S.; McGrath, J. E.; Pivovar, B. S., Direct methanol fuel cell performance of disulfonated poly-arylene ether benzonitrile) copolymers. *Journal of the Electrochemical Society* **2004,** 151, (12), A2150-a2156.

11. Kim, Y. S.; Hickner, M. A.; Dong, L. M.; Pivovar, B. S.; McGrath, J. E., Sulfonated poly(arylene ether sulfone) copolymer proton exchange membranes: composition and morphology effects on the methanol permeability. *Journal of Membrane Science* **2004,** 243, (1-2), 317-326.

12. Kim, Y. S.; Wang, F.; Hickner, M.; McCartney, S.; Hong, Y. T.; Harrison, W.; Zawodzinski, T. A.; McGrath, J. E., Effect of acidification treatment and morphological stability of sulfonated poly(arylene ether sulfone) copolymer proton-exchange membranes for fuel-cell use above 100 degrees C. *Journal of Polymer Science Part B-Polymer Physics* **2003,** 41, (22), 2816-2828.

13. Zawodzinski, T. A.; Neeman, M.; Sillerud, L. O.; Gottesfeld, S., Determination of Water Diffusion-Coefficients in Perfluorosulfonate Ionomeric Membranes. *Journal of Physical Chemistry* **1991,** 95, (15), 6040-6044.

14. Quinn, F. X.; Kampff, E.; Smyth, G.; Mcbrierty, V. J., Water in Hydrogels .1. A Study of Water in Poly(N-Vinyl-2-Pyrrolidone Methyl-Methacrylate) Copolymer. *Macromolecules* **1988,** 21, (11), 3191-3198.

15. Kim, Y. S.; Dong, L. M.; Hickner, M. A.; Glass, T. E.; Webb, V.; McGrath, J. E., State of water in disulfonated poly(arylene ether sulfone) copolymers and a perfluorosulfonic acid copolymer (nafion) and its effect on physical and electrochemical properties. *Macromolecules* **2003,** 36, (17), 6281-6285.

16. Hodge, R. M.; Edward, G. H.; Simon, G. P., Water absorption and states of water in semicrystalline poly(vinyl alcohol) films. *Polymer* **1996,** 37, (8), 1371-1376.

17. Hodge, R. M.; Bastow, T. J.; Edward, G. H.; Simon, G. P.; Hill, A. J., Free volume and the mechanism of plasticization in water-swollen poly(vinyl alcohol). *Macromolecules* **1996,** 29, (25), 8137-8143.

18. Ghi, P. Y.; Hill, D. J. T.; Whittaker, A. K., H-1 NMR study of the states of water in equilibrium Poly(HEMA-co-THFMA) hydrogels. *Biomacromolecules* **2002,** 3, (5), 991-997.

19. Barbieri, R.; Quaglia, M.; Delfini, M.; Brosio, E., Investigation of water dynamic behaviour in poly(HEMA) and poly(HEMA-co-DHPMA) hydrogels by proton T-2 relaxation time and self-diffusion coefficient nmr measurements. *Polymer* **1998,** 39, (5), 1059-1066.

20. Quinn, F. X.; Mcbrierty, V. J.; Wilson, A. C.; Friends, G. D., Water in Hydrogels .3. Poly(Hydroxyethyl Methacrylate) Saline Solution Systems. *Macromolecules* **1990,** 23, (21), 4576-4581.

21. McConville, P.; Pope, J. M., H-1 NMR T-2 relaxation in contact lens hydrogels as a probe of water mobility. *Polymer* **2001,** 42, (8), 3559-3568.

22. Sankir, M.; Bhanu, V. A.; Harrison, W. L.; Ghassemi, H.; Wiles, K. B.; Glass, T. E.; Brink, A. E.; Brink, M. H.; McGrath, J. E., Synthesis and characterization of 3,3 '-disulfonated-4,4 '-dichlorodiphenyl sulfone (SDCDPS) monomer for proton exchange membranes (PEM) in fuel cell applications. *Journal of Applied Polymer Science* **2006,** 100, (6), 4595-4602.

23. Roy, A.; Einsla, B.; Harrison, W.; McGrath, J. E., Synthesis and characterization of hydroquinone based disulfonated poly(arylene ether sulfone)s via direct copolymerization. *Abstracts of Papers of the American Chemical Society* **2004,** 228, U663-U663.

24. Li, Y. X.; Mukundan, T.; Harrison, W. L.; Hill, M.; Sankir, M.; Yang, J.; McGrath, J. E., Direct synthesis of disulfonated poly(arylene ether ketone)s and investigation of their behavior as proton exchange membrane (PEM). *Abstracts of Papers of the American Chemical Society* **2004,** 228, U657-U657.

25. Lee, H.-S.; Badami, A. S.; Roy, A.; McGrath, J. E., Segmented sulfonated poly(arylene ether sulfone)-b-polyimide copolymers for proton exchange membrane fuel cells. I. Copolymer synthesis and fundamental properties. *Journal of Polymer Science, Part A: Polymer Chemistry* **2007,** 45, (21), 4879-4890.

26. Lee, H.-S.; Roy, A.; Badami, A. S.; McGrath, J. E., Synthesis and characterization of sulfonated poly(arylene ether) polyimide multiblock copolymers for proton exchange membranes. *Macromolecular Research* **2007,** 15, (2), 160-166.

27. Roy, A.; Hickner, M. A.; Yu, X.; Li, Y.; Glass, T. E.; McGrath, J. E., Influence of chemical composition and sequence length on the transport properties of proton exchange membranes. *Journal of Polymer Science, Part B: Polymer Physics* **2006,** 44, (16), 2226-2239.

28. Kim, Y. S.; Dong, L. M.; Hickner, M. A.; Pivovar, B. S.; McGrath, J. E., Processing induced morphological development in hydrated sulfonated poly(arylene ether sulfone) copolymer membranes. *Polymer* **2003,** 44, (19), 5729-5736.

6.0 States of Water in Proton Exchange Membranes-Part-B-Influence on Transport Properties

Abhishek Roy,[1] Michael A. Hickner,[2] Hae-Seung-Lee,[1] Tom Glass,[1]
Yanxiang Li,[1] and James E. McGrath[1]

[1]Macromolecules and Interfaces Institute
Virginia Polytechnic Institute and State University, Blacksburg, VA 24061
[2] Present Address: Department of Materials Science and Engineering
The Pennsylvania State University, University Park, PA 16802

Abstract

The influence of chemical composition and morphology on states of water in PEMs was investigated in Part A. A relationship between transport properties and different types of water was established. Transport properties, which include proton conductivity, the self-diffusion coefficient of water and methanol permeability, scaled well with the free water content. Although the presence of free water was required to achieve high proton conductivity, high free water content in random copolymers reduced methanol permeability and the selectivity of the membrane. In contrast, the multiblock copolymers showed lower methanol permeability even with higher free water content. Aromatic copolymers with higher amounts of non-freezing water demonstrated promise for improved transport at both high and freezing temperatures. The relationship of morphology to different states of water was reinvestigated.

6.1 Introduction

Water in hydrophilic polymers exists in three different states; tightly bound, loosely bound and free.[1, 2] The nature and the distribution of these types of water are all influenced by the chemical structure, microstructure and chemical composition of the membranes.[3, 4] In proton exchange membranes, the membranes are hydrophilic in nature due to the presence of sulfonic acid groups. Water confined in hydrophilic pores, in concert with the sulfonic acid groups, are critical for proton (ion) conduction in these systems.[5] In Part A, the different states of water in different copolymers were characterized and quantified using DSC, NMR relaxation and TGA analytical techniques. The chemical architecture of the copolymers was varied from random to phase separated multiblocks. A relationship between morphology and the nature of the water was revealed. A distinct phase separated hydrophobic-hydrophilic domain morphology in a polymer was responsible for the development of the free water in the system. The strength of the acid or the effective charge density of the copolymer controlled the content of the tightly bound water. The objective of this paper, therefore, is to investigate the influence of the states of water on different transport properties for proton exchange membranes.

Among the various transport properties for proton exchange membranes, proton conductivity, methanol permeability and the self-diffusion coefficient of water are of greatest importance. Earlier research from our laboratories has confirmed the importance of states of water on the various transport properties of proton exchange membranes. Kim et al.[4] reported the importance of free water with respect to proton transport. The nature of water at different hydration states for PEMs and their influence on transport properties are of great relevance to this study. As discussed in Part A, at low hydration states most water molecules associated with sulfonic acid groups are tightly bound. As a result, very low self-diffusion coefficients of water and reduced proton conductivity are reported for PEMS at low hydration levels.[6] At higher hydration levels, loosely bound water appears first, followed by free water. This corresponds to the increase in both proton conductivity and the diffusion coefficients of water, as observed for Nafion® by

Kreuer et al.[7] and Zawodzinski et al.[5] Hence, a strong relationship exists between the nature of water and transport properties over a wide range of water activity. This study will also highlight the influence of chemical structure on proton transport at low hydration levels.

Methanol permeability is another important transport property to be considered when liquid methanol is the fuel of choice. Ren et al.[8] reported that for DMFCs, unoxidized methanol at the anode tends to cross over through the membrane and undergo oxidation at the cathode. This causes the generation of mixed potentials at the cathode, which lowers the voltage and fuel efficiency of the cell. Methanol permeability has also been associated with increasing free water, facilitating methanol diffusion through the membrane. Although high proton conductivity is always desirable, high methanol permeability is unwanted. Thus, to achieve better selectivity of proton conductivity over methanol permeability, a clearer understanding of the relationship between chemical structure and states of water in hydrophilic membranes is critical. This knowledge, coupled with states of water experiments, essential transport measurements, and chemical structure of the copolymers, will provide a fundamental picture of how the chemical nature of a phase separated copolymer influences transport properties.

6.2 Experimental

6.2.1 Materials

The synthesis of the copolymers used in this study was discussed in Part A of this paper. The random copolymers studied include biphenol-based partially disulfonated poly(arylene ether sulfone)[9] [BPSH-xx – Fig. 6-1(a)], hydroquinone-based partially disulfonated poly(arylene ether sulfone) [HQSH-xx – Fig. 6-1(b)][4, 10, 11] and partially disulfonated poly(arylene ether ketone) random copolymers[12] [B-ketone-xx Fig. 6-1(c)]. In addition to the random copolymers, a series of multiblock copolymers [BPSH-x-PI-y – Fig. 6-1(d)] was also investigated.[13, 14] In the multiblock copolymers, x and y represent the block lengths in kg/mol of hydrophobic and hydrophilic units, respectively. The ion exchange capacity of the multiblocks was the same (1.5~1.6 meq/g), and the individual

molecular weights of the hydrophobic and hydrophilic blocks were similar to each other. The molecular weights of the individual blocks were varied from 5000, 10000 and 15000 g/mole. Nafion® 112 and 117, which were purchased from Electrochem Inc., were used as controls and used as received. The proton conductivity, self-diffusion coefficient of water and methanol permeability data for the copolymers were obtained from earlier publications.[4, 10, 14-19]

6.2.2 Pulsed-field gradient spin echo nuclear magnetic resonance (PGSE NMR).

The self-diffusion coefficients of water were measured using a Varian Inova 400 MHz (for protons) nuclear magnetic resonance spectrometer with a 30 G/cm gradient diffusion probe. A total of 16 points was collected across a range of gradient strengths and the signal-to-noise ratio was enhanced by co-adding 4 scans. Measurements were obtained by observing the echo signal intensity (A) as a function of the gradient strength(g). The diffusion coefficient (D) was determined by fitting the data to Equation (6-1):[20]

$$A(g) = A(o)\exp[-\gamma^2 D g^2 \delta^2 (\Delta - \delta/3)] \qquad \textbf{Equation 6-1}$$

where, A is the NMR signal intensity as a function of gradient strength, γ is the gyromagnetic ratio (26752 $radG^{-1}s^{-1}$ for protons), δ is length of the gradient pulse, and Δ is the time between gradient pulses. Membrane samples of approximately 5 mm by 15 mm by 150 μm were equilibrated in liquid water for at least 24 h. The samples were then removed, blotted to eliminate droplets, quickly inserted into an NMR tube, and immediately imaged over a span of about 5 minutes. For measurements done under sub-zero conditions, the sample was first cooled to -80 °C. The temperature was then raised to a specific point (e.g., -60 °C), and then held there for an optimized time period, which was determined by the time needed for the diffusion coefficient to become constant (usually 15-30 min). Similar methods were followed at other temperatures.

6.2.3 Thermogravimetric analysis (TGA)

Prior to conducting TGA experiments on the fully hydrated samples, they were removed from the water, blotted to remove any surface water, and placed in the TGA pan. Experimental conditions featured an air atmosphere and a heating rate of 10 °C/min.

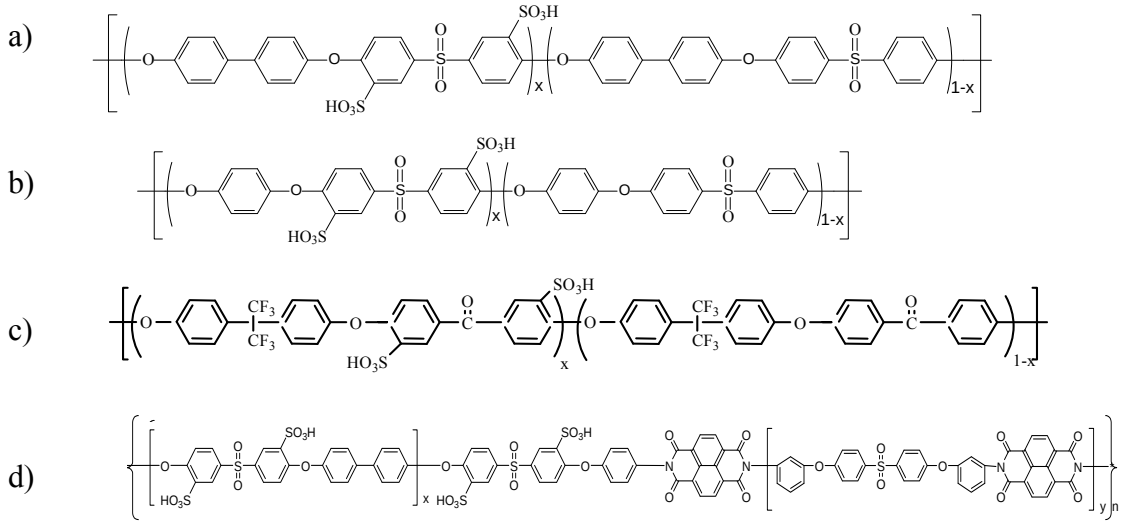

Figure 6-1 Copolymer chemical structures: (a) BPSH-xx; (b) HQSH-xx, (c) B-ketone-xx, (d) BPSH-x-PI-y multiblocks

6.3 Results and Discussion

6.3.1 Proton conductivity

The single most important requirement for a proton exchange membranes is high proton conductivity. Proton transport, particularly under hydrated condition, is primarily a function of water content and the acidity of the membrane. The current study aims to go in more details in establishing the relationship between the proton transport with individual types of water. Earlier studies from our group identified a qualitative relationship between the free water and the proton conduction for the BPSH-xx random

copolymers with varying ionic content.[10, 19] In this paper, the study is extended to other copolymers varying in chemical compositions, structure and sequence length distribution covering a wide range of structural and morphological variables. It should be noted that for the following discussion, proton conductivities were determined in liquid water at 30 °C.

The plot displayed in Figure (6-2) represents proton conductivity as a function of free water content for the HQSH-xx, ketone-B-xx, BPSH-xx, multiblock BPSH-x-PI-y and Nafion® copolymers (The free water content for each of these copolymers was obtained as described in Part A). Regardless of the nature of the copolymer and ionic compositions, the onset of free water was found to be extremely important in achieving high conductivity over 80 mS/cm. This highlights the importance of the presence of free water on proton transport for the PEMs. However, with further increasing free water content, proton conductivity increases modestly. Higher free water content reduces the effective proton concentration and levels off the increasing trend for proton conductivity.

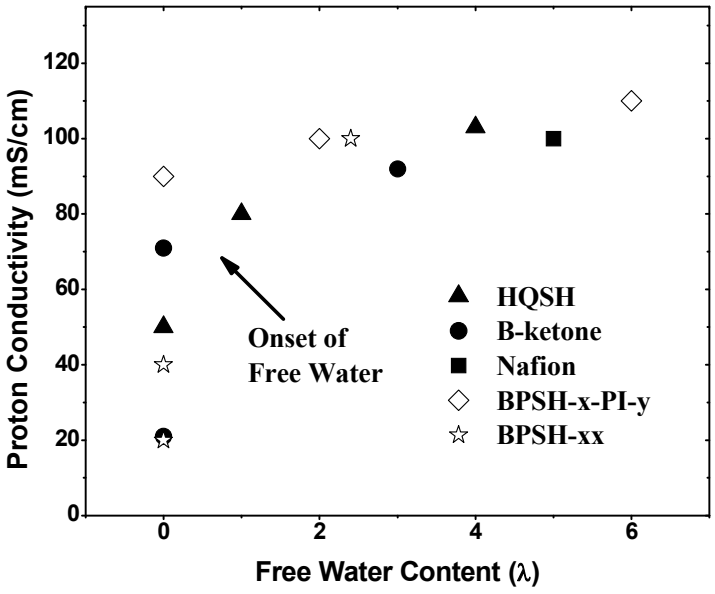

Figure 6-2 Influence of free water content on proton conductivity in liquid water at 30 °C

The effect of free water content on the activation energy for proton transport under fully hydrated conditions is shown in Figure (6-3). Activation energy is related to the ease of the transport process and/or a measure of the associated morphological barrier. The activation energy decreased with increasing free water content for all the copolymers. Hence, the presence of free water in the system reduced the barriers associated with proton transport, indicating a strong relationship between the presence of free water and the morphology of the copolymer.

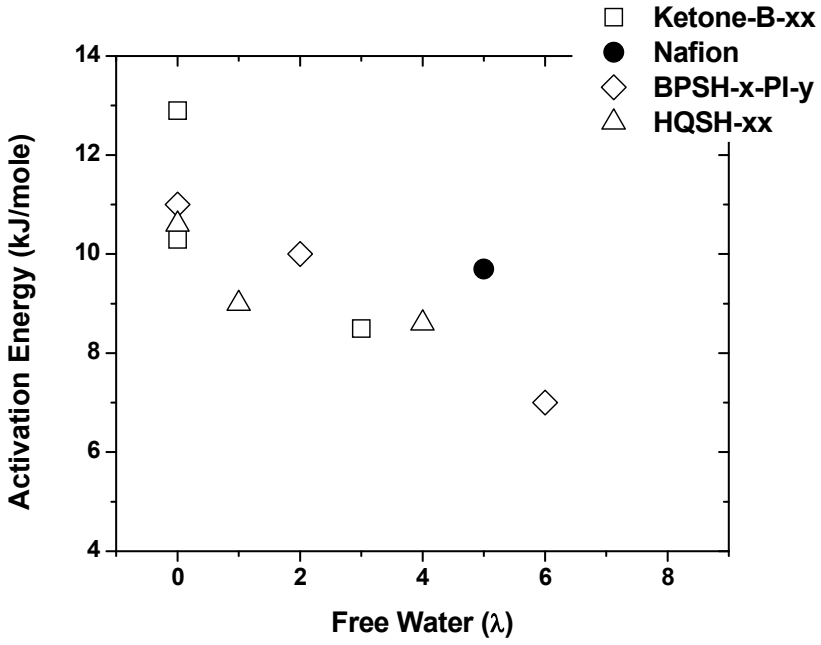

Figure 6-3 Activation energy for proton transport decreases with increasing free water content

As noted in Part A, the origin of the free water is related to the formation of co-continuous, phase separated hydrophilic-hydrophobic domain network within the membrane. The presence of free water improves the connectivity between the sulfonic acid groups through the formation of a water-assisted percolated hydrophilic domain morphology. This is more prominent for the random copolymers. Thus, the onset of free water can be considered as a morphological transition from an isolated to an associated hydrophilic domain morphology. This associated domain morphology in the presence of free water reduces the morphological barrier for transport and improves proton

conductivity. This explains why proton conductivity increases significantly with the onset of free water in the system.

However, free water develops only at higher water activities. Thus, the absence of free water under partially hydrated conditions results in the formation of isolated domains and a loss of connectivity. This is especially true for random copolymer, as reflected by a sharp fall in proton conductivity under partially hydrated conditions. In contrast, the multiblock BPSH-15-PI-15 copolymers, with a similar IEC to the random HQSH 35 copolymers, demonstrate better performance under partially hydrated conditions at 80 ^{o}C, as shown in Figure (6-4). Unlike random copolymers, phase separation in multiblocks is a function of the chemical incompatibility between the two individual blocks and their molecular weights. Connectivity between the hydrophilic domains can exist even at low water content, which facilitates proton transport at partially hydrated conditions.

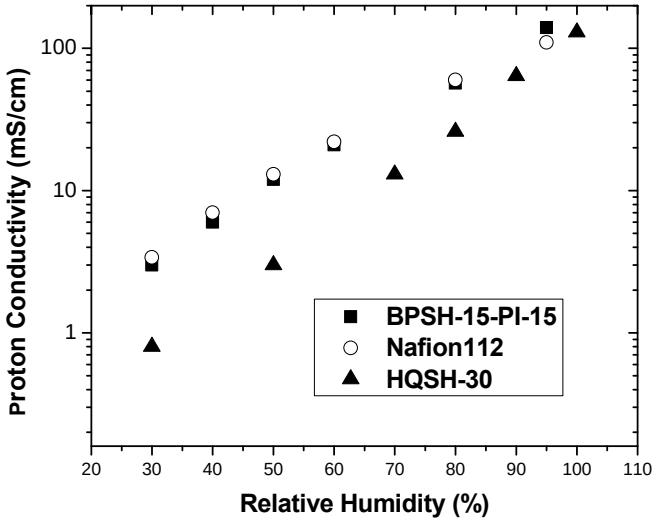

Figure 6-4 Proton conductivity as a function of the relative humidity for multiblock and random copolymers at 80 ^{o}C

6.3.2 Self-diffusion coefficient of water

The self-diffusion coefficient of water is an important property in understanding water transport behavior within PEMs, and is indicative of the morphology of the copolymer.

Classically the diffusion of a species within a polymer scales with the free volume or the volume fraction of the solvent (water) in the polymer. Although DSC and other methods can detect the presence of the three types of water, the diffusion coefficient of water measured by PGSE is expected to be a weighted average of the three types. The free water with the longest relaxation time contributes significantly to the signal at longer time scales. Representative plots of the intensity of NMR signal vs. gradient strength were shown to be mono-exponential, as depicted in Figure (6-5) and Figure (6-6). The self-diffusion coefficients of water measured at 25 ^{o}C under fully hydrated conditions was correlated with the free water content in the copolymers (Fig. 6-7). Moreover, it was observed that the morphology of the copolymer significantly influenced transport properties. At a given free water content, the water self-diffusion coefficient of the multiblock BPSH-15-PI-15 was significantly higher than that of the random copolymers. The co-continuous phase separated morphology for the BPSH-15-PI-15 copolymer more efficiently facilitated water transport within the hydrophilic domains compared to the random copolymers. With increasing free water content, however, the self-diffusion coefficient of water leveled off. This is attributed to the fact that confining a large volume fraction of water molecules within a fixed volume of the hydrophilic domains restricted overall transport.

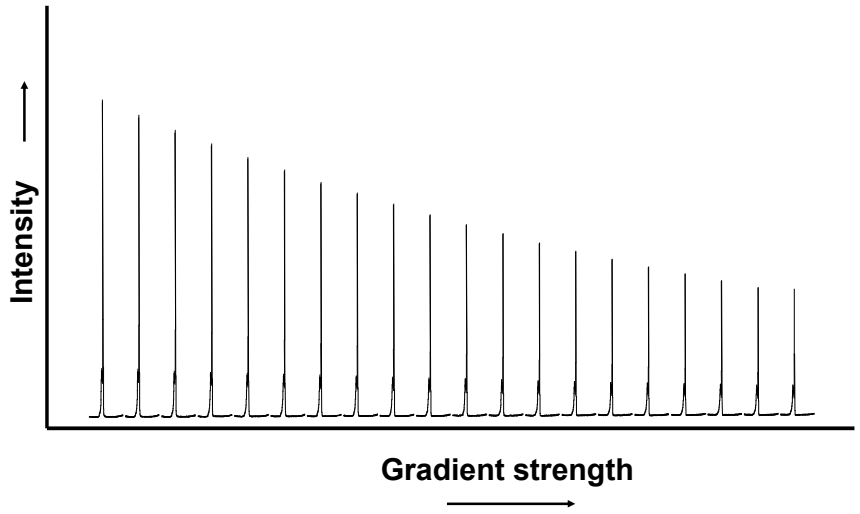

Figure 6-5 Intensity of the water signal as a function of gradient strength in an ideal PGSE experiment; a mono exponential relationship was observed

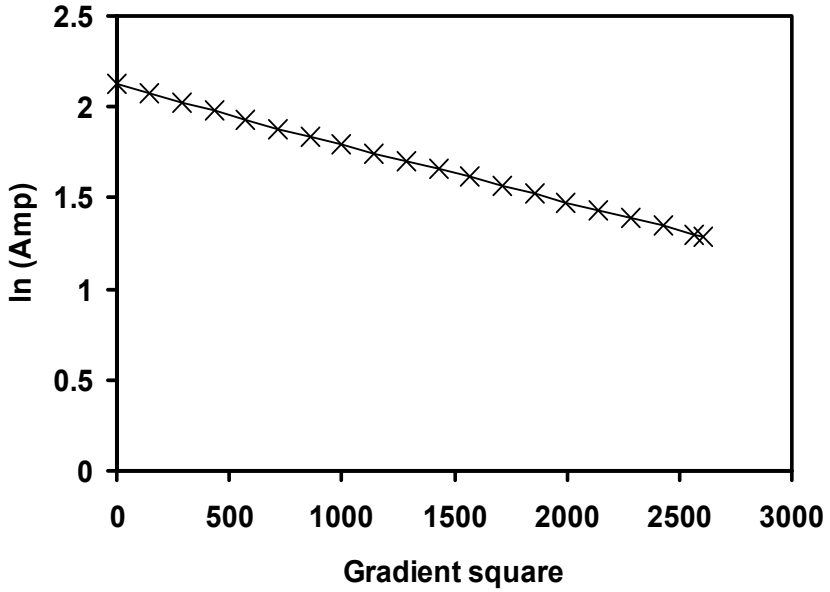

Figure 6-6 Linear curve fitting of the PGSE experimental results

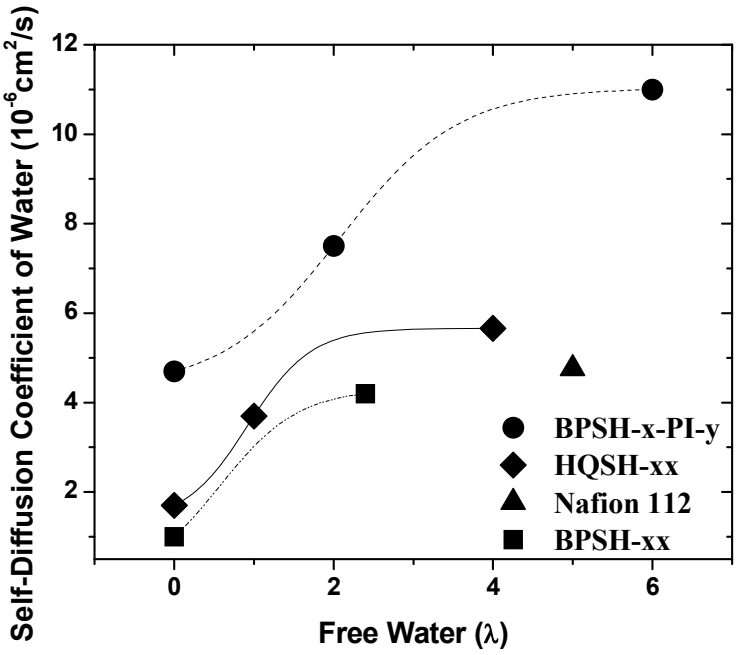

Figure 6-7 Self-diffusion coefficients of water as a function of free water content; multiblock copolymers at 25 ^{o}C show better water transport than random copolymers at a given free water content

6.3.3 Methanol permeability

Similar to proton and water transport, methanol transport within hydrophilic domains can be modeled with the free water content. Methanol permeability (P) is defined by the following Equation (6-2), where D is the methanol diffusion coefficient and H is the solubility or the partition coefficient.

$$P = DH \qquad \textbf{Equation 6-2}$$

While D (methanol diffusion coefficient) is a morphology-related term, H (solubility/partition coefficient) is a structure-related term. Figure (6-8) represents the plot of methanol permeability with free water content for the copolymers studied. Unlike proton transport, methanol permeability increased linearly—particularly for the random copolymers. For DMFC applications, however, very low methanol permeability is desired. To have the best selectivity between the proton conductivity and methanol permeability, a random copolymer with 1-3 free water content per sulfonic acid group is desired.

The multiblock copolymers studied showed significantly reduced methanol permeability at 30 ^{o}C at given free water content compared to random copolymers. The following possible explanations are suggested. Multiblock copolymers, particularly the BPSH-15-PI-15, phase separate distinctly into hydrophobic and hydrophilic phases. Each of the blocks retains their individual properties. The hydrophobic unit is a rigid six-member polyimide and has a very low interaction parameter with the methanol. The hydrophobic unit acts as a barrier to methanol transport, while the hydrophilic unit provides a pathway for proton transport. In addition to this, the difference in the morphological structures of the multiblock and random copolymers at high free water content may play a significant role. The random copolymers with higher free water content represent a more open morphological structure. Because the hydrophilic phase is the continuous phase, methanol can easily diffuse through, resulting in increased methanol permeability. In contrast, because the morphological structure of the BPSH-15-PI-15 copolymer is a co-continuous hydrophilic and hydrophobic structure, the

hydrophilic units are constrained by the hydrophobic blocks, thereby reducing methanol permeability.

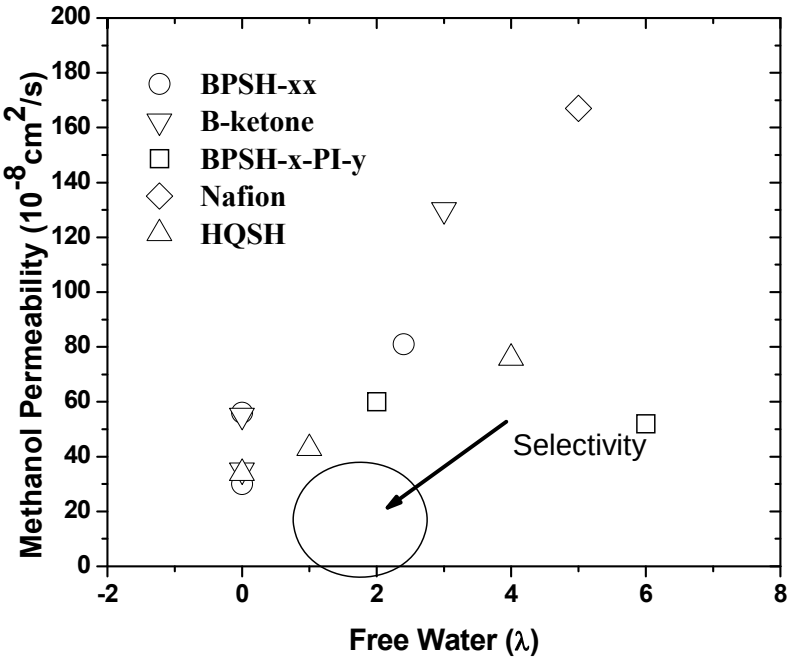

Figure 6-8 Methanol permeability at 30 ^{o}C increases with increasing free water content

6.3.4 Importance of bound water on freezing and high temperature transport processes

Over the last several years, there has been significant interest in using PEMs for automotive applications. One of the major challenges of using PEMs in this way is to maintain sufficient proton transport at both high and sub-ambient temperatures. Unless externally humidified, water loss from the membrane as a result of evaporation at high temperatures reduces overall performance. Conversely, under freezing conditions, most of the water inside the PEM will freeze and proton transport will be restricted. Moreover, the ice-water transitions during freezing-thaw cycles will generate structural stresses within the polymeric membrane.

As discussed earlier, water in a hydrophilic polymer can exist in three different states: free, loosely bound, and tightly bound. Tightly bound water is nonfreezing water which shows no melting endotherm of water, as characterized from DSC. Thermodynamically, tightly bound water has the strongest interaction with sulfonic acid groups and represents the first shell of hydration. Unless the glass transition temperature of the copolymer is exceeded, it is difficult to remove tightly bound water from the polymeric network. Thus, it can be hypothesized that presence of tightly bound water inside a membrane at both low and high temperatures is possible and will contribute to proton transport.

In Part A of this paper, TGA was used to measure the retention of water as a function of temperature. All the copolymers studied retained their tightly bound water even at higher temperatures. Random and the multiblock copolymers with higher tightly bound water content retained higher amounts of water at elevated temperature compared to Nafion® (Fig.6-9). This is expected to improve their performance compared to Nafion® at elevated temperatures.

The self-diffusion coefficients of water were measured at sub-ambient temperatures to probe the transport behavior of non-freezing water. As plotted in Figure (6-10), the self-diffusion coefficients of water were measured for both HQSH 30 and Nafion®112 over a temperature range of -40 to 40 °C. For the HQHS 30 sample featuring 9 tightly bound water units per sulfonic acid group, it was possible to obtain diffusion coefficient values even at -40 °C. Because the water was non-freezing, it was able to contribute to the transport process. A sharp increase in diffusion coefficient values was observed near 0 °C, which corresponds to the contribution from the free and loosely bound water as it melted from the ice form. Under similar experimental procedures and NMR pulse sequences, no signal intensity was obtained for Nafion®112. By designing a new pulse sequence, it may be possible to obtain diffusion coefficients value for Nafion®112, even at low temperature. However, at this point, this is beyond the scope of our study. Nafion®112 with very low tightly bound water content (3) is expected to have significantly lower water transport capabilities at freezing temperatures compared to the copolymers with higher tightly bound water content.

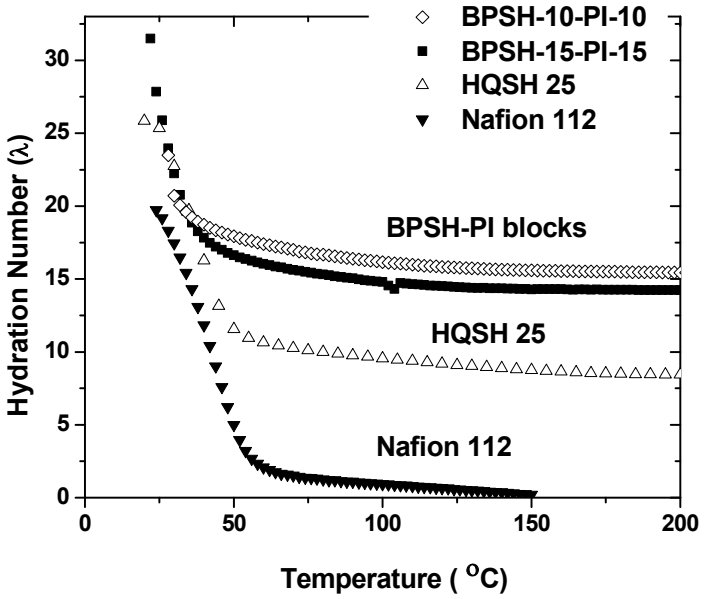

Figure 6-9 Water retention as a function of temperature depends on the morphology of the PEMs

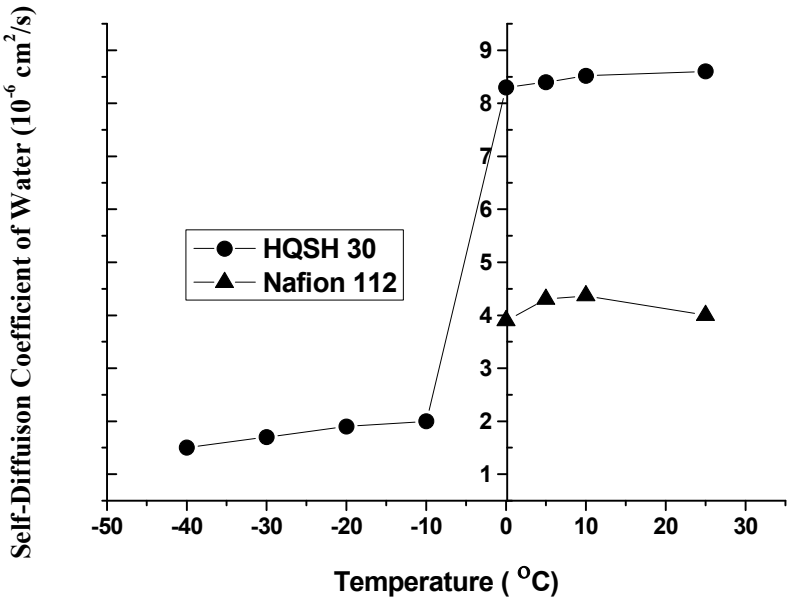

Figure 6-10 Water transport under freezing conditions is a function of the non-freezing water content

6.4 Conclusions

In Part A of this study, the different states of water was quantified as a function of the chemical structure and morphology of proton exchange membranes. In this segment, the quantified results have been related to the various transport processes in PEMs. The onset of free water, which was correlated to the formation of phase separated morphology, is extremely important in achieving high proton conductivity. The activation energy for proton transport decreased with increasing free water content. For most of the aromatic random copolymers, water-assisted phase separation occurred after reaching a certain increase in IEC. Hence, high proton conductivity was only achieved at high IECs for the random copolymers. In contrast, phase separation in multiblock copolymers was observed to be a function of the individual molecular weight and the chemical structure of the individual blocks. Therefore, by tailoring the chemistry, it is possible to achieve phase separation at very low IECs with increased free water content and proton conductivity. A strong influence of morphology on water transport was also observed. At a given free water content, the multiblock morphology resulted in much higher water self-diffusion coefficients values over both Nafion®112 and the random copolymers. Similar to proton conductivity, the self-diffusion coefficient of water leveled off at high free water content. Further investigations on this restricted transport phenomena at high free water content would be desirable for designing new generation membranes with improved performance. This study also proved that methanol transport was facilitated with increasing free water content for the random copolymers. For DMFC applications, random copolymers having two to three free water molecules per sulfonic groups are expected to afford the best selectivity between proton and methanol transport. In contrast, the multiblock copolymers showed lower methanol permeability even with higher free water content.

A strong influence of the non-freezing water content on both high and freezing temperatures was observed. Specifically, the aromatic sulfonic acid groups containing backbones for the multiblock and the random copolymers retained significant amounts of tightly bound water at high temperature (>140 ^{o}C). Investigation of the proton conductivity at this temperature for the copolymers is ongoing. At freezing temperatures,

the presence of tightly bound or the non-freezing water contributed to the water transport process for the HQSH 30 random copolymers. Similar studies are ongoing for the multiblocks and other copolymers. This study was proof of the importance of non-freezing water content for PEM applications at freezing and high temperatures.

In summary, the states of water experiments, coupled with transport property measurements, reinforce the critical influence of chemical structure, composition, and microstructure on resulting PEM properties.

The authors would like to thank the National Science Foundation "Partnership for Innovation" Program (HER-0090556) and the Department of Energy (DE-FC36-01G01086) for support of this research effort. The authors would also like to thank UTC Fuel Cell (#PO3561) for their support.

6.5 References

1. Quinn, F. X.; Kampff, E.; Smyth, G.; Mcbrierty, V. J., Water in Hydrogels .1. A Study of Water in Poly(N-Vinyl-2-Pyrrolidone Methyl-Methacrylate) Copolymer. *Macromolecules* **1988,** 21, (11), 3191-3198.

2. Hodge, R. M.; Edward, G. H.; Simon, G. P.; Hill, A. J., The States of Water within Poly(Vinyl Alcohol) Thin-Films .1. Investigation by Positron-Annihilation Lifetime Spectroscopy. *Abstracts of Papers of the American Chemical Society* **1993,** 205, 447-POLY.

3. Roy, A.; Hickner, M.; Glass, T.; Li, Y.; Einsla, B.; Wiles, K. B.; Yu, X.; McGrath, J. E., States of water- investigating the water-polymer interactions and transport phenomenon in proton exchange membranes. *Preprints of Symposia - American Chemical Society, Division of Fuel Chemistry* **2005,** 50, (2), 699-700.

4. Kim, Y. S.; Dong, L. M.; Hickner, M. A.; Glass, T. E.; Webb, V.; McGrath, J. E., State of water in disulfonated poly(arylene ether sulfone) copolymers and a perfluorosulfonic acid copolymer (nafion) and its effect on physical and electrochemical properties. *Macromolecules* **2003,** 36, (17), 6281-6285.

5. Zawodzinski, T. A.; Neeman, M.; Sillerud, L. O.; Gottesfeld, S., Determination of Water Diffusion-Coefficients in Perfluorosulfonate Ionomeric Membranes. *Journal of Physical Chemistry* **1991,** 95, (15), 6040-6044.

6. Kreuer, K. D.; Paddison, S. J.; Spohr, E.; Schuster, M., Transport in proton conductors for fuel-cell applications: Simulations, elementary reactions, and phenomenology. *Chemical Reviews* **2004,** 104, (10), 4637-4678.

7. Kreuer, K. D., On the complexity of proton conduction phenomena. *Solid State Ionics* **2000,** 136, 149-160.

8. Ren, X. M.; Springer, T. E.; Zawodzinski, T. A.; Gottesfeld, S., Methanol transport through nafion membranes - Electro-osmotic drag effects on potential step measurements. *Journal of the Electrochemical Society* **2000,** 147, (2), 466-474.

9. Roy, A.; Einsla, B.; Harrison, W.; McGrath, J. E., Synthesis and characterization of hydroquinone based disulfonated poly(arylene ether sulfone)s via direct copolymerization. *Abstracts of Papers of the American Chemical Society* **2004,** 228, U663-U663.

10. Kim, Y. S.; Wang, F.; Hickner, M.; McCartney, S.; Hong, Y. T.; Harrison, W.; Zawodzinski, T. A.; McGrath, J. E., Effect of acidification treatment and morphological stability of sulfonated poly(arylene ether sulfone) copolymer proton-exchange membranes for fuel-cell use above 100 degrees C. *Journal of Polymer Science Part B-Polymer Physics* **2003,** 41, (22), 2816-2828.

11. Wang, F.; Hickner, M.; Kim, Y. S.; Zawodzinski, T. A.; McGrath, J. E., Direct polymerization of sulfonated poly(arylene ether sulfone) random (statistical) copolymers: candidates for new proton exchange membranes. *Journal of Membrane Science* **2002,** 197, (1-2), 231-242.

12. Li, Y. X.; Mukundan, T.; Harrison, W. L.; Hill, M.; Sankir, M.; Yang, J.; McGrath, J. E., Direct synthesis of disulfonated poly(arylene ether ketone)s and investigation of their behavior as proton exchange membrane (PEM). *Abstracts of Papers of the American Chemical Society* **2004,** 228, U657-U657.

13. Lee, H.-S.; Badami, A. S.; Roy, A.; McGrath, J. E., Segmented sulfonated poly(arylene ether sulfone)-b-polyimide copolymers for proton exchange membrane fuel

cells. I. Copolymer synthesis and fundamental properties. *Journal of Polymer Science, Part A: Polymer Chemistry* **2007,** 45, (21), 4879-4890.

14. Lee, H.-S.; Roy, A.; Badami, A. S.; McGrath, J. E., Synthesis and characterization of sulfonated poly(arylene ether) polyimide multiblock copolymers for proton exchange membranes. *Macromolecular Research* **2007,** 15, (2), 160-166.

15. Roy, A.; Hickner, M. A.; Lee, H.-S.; Badami, A.; Yu, X.; Li, Y.; Glass, T.; McGrath, J. E., Transport properties of proton exchange membranes. *ECS Transactions* **2007,** 2, (24, Direct Methanol Fuel Cells), 45-54.

16. McGrath, J. E.; Roy, A.; Lee, H.-S.; Yu, X.; Badami, A.; Li, Y.; Wang, H., Multiblock hydrophilic-hydrophobic proton exchange membranes for direct methanol based fuel cell. *ECS Transactions* **2007,** 2, (24, Direct Methanol Fuel Cells), 55-62.

17. Roy, A.; Hickner, M. A.; Yu, X.; Li, Y.; Glass, T. E.; McGrath, J. E., Influence of chemical composition and sequence length on the transport properties of proton exchange membranes. *Journal of Polymer Science, Part B: Polymer Physics* **2006,** 44, (16), 2226-2239.

18. Kim, Y. S.; Einsla, B.; Sankir, M.; Harrison, W.; Pivovar, B. S., Structure-property-performance relationships of sulfonated poly(arylene ether sulfone)s as a polymer electrolyte for fuel cell applications. *Polymer* **2006,** 47, (11), 4026-4035.

19. Kim, Y. S.; Dong, L. M.; Hickner, M. A.; Pivovar, B. S.; McGrath, J. E., Processing induced morphological development in hydrated sulfonated poly(arylene ether sulfone) copolymer membranes. *Polymer* **2003,** 44, (19), 5729-5736.

20. Stejskal, E. O.; Tanner, J. E., *J.chem.Phys* **1965**, (42), 288.

7.0 Hydrophilic-Hydrophobic Multiblock Copolymers based on Poly(arylene ether sulfone)s as Novel Proton Exchange Membranes-Part-B

Abhishek Roy, Hae-Seung Lee & James E. McGrath

Macromolecules and Interfaces Institute
Virginia Polytechnic Institute and State University, Blacksburg, VA 24061

Abstract

There has been growing evidence, both experimental and theoretical, that block copolymer systems with well-defined sulfonated regions may provide enhanced proton transport, especially at low relative humidity. We have recently demonstrated a novel way to make hydrocarbon hydrophobic-hydrophilic block copolymers. While the chemical structure and chemical compositions are very similar to random BPSH copolymers, the microstructure and the morphology are very different. The self-diffusion coefficients of water, as measured by PGSE NMR techniques, have indicated a significant improvement in water transport after reaching a particular block length. At that block length, the multiblocks display better proton conductivity under partially hydrated conditions than the random copolymers. The presence of increased free water content in the multiblocks with increasing block lengths was confirmed by states of water analysis. A significant change in the distribution of three types of water was also observed compared to the random copolymers. This paper will discuss the structure property relationships of these multiblock copolymers for potential application as proton exchange membranes.

7.1 Introduction

Ions containing polymeric membranes have been widely used as proton exchange membranes in fuel cells. The nature of the ionic groups, chemical composition, and copolymer microstructure all play important roles in controlling the desired properties. One important criterion for a PEM is to have sufficient proton conductivity under partially hydrated conditions. Nafion®, a commercially available PEM developed by DuPont, has met that criterion to a certain extent. However, it has several disadvantages such as high cost, reduced performance at elevated temperatures. More importantly, Nafion® displays high gas and methanol cross-over rates.[1] Sulfonic acid group containing hydrocarbon based random copolymers have been proposed as alternative membranes.[2] Our research group had been engaged over the past several years in synthesizing and characterizing biphenol based partially disulfonated poly(arylene ether sulfone) (BPSH) random copolymers as potential PEMs.[2-5] The copolymers have demonstrated superior performance at elevated temperatures and higher hydration levels when compared to Nafion®. However, the random architecture results in the formation of isolated domains which significantly restricts proton transport at low hydration levels.

Ion containing block copolymers with better phase separated microstructures are reported to have better performance than random copolymers at low hydration levels. Recently, our group has synthesized thermally stable multiblock copolymers with varying chemical structures and compositions.[6-10] These have included highly fluorinated and partially fluorinated systems, as well as hydrocarbon based copolymers—all of which feature the same hydrophilic units. Transport properties have scaled with the block lengths of the copolymers, irrespective of the nature of the backbone. An increase in block length for a given series of block copolymers under the same ionic concentration has been associated with an increase in the self-diffusion coefficients of water, as well as improved proton conduction under partially hydrated conditions, especially when compared to BPSH-xx random copolymers. Nanophase separation or the extent of connectivity between the hydrophilic domains, which has been shown to be a function of

block lengths, lowers the morphological barrier for transport.[10] However, the chemical structure of the multiblock copolymers studied was different from the random BPSH-xx copolymer. Hence a true understanding of the influence of block copolymer microstructure on the properties is yet to be achieved.

We have recently demonstrated a novel way to make hydrocarbon hydrophobic-hydrophilic block copolymers. The detailed synthesis and fundamental polymer characterization studies have been reported separately.[11] In contrast to random copolymers, the block copolymer chemistry involves decaflurobiphenol as a coupling agent to facilitate a low temperature coupling reaction between the hydrophilic and hydrophobic blocks. The decaflurobiphenol unit is present in very small amounts, only about 1-2 % on a weight basis; hence, the chemical structure will be very similar to BPSH-xx[3] random copolymers. However, the microstructure and the morphology are very different. In this paper, BPSH-xx random copolymers of varying ionic compositions will be compared with BPSH block copolymers of varying block lengths and ionic compositions. This will provide a better understanding of the effect of the differences in random and block copolymer morphology on the transport properties under both fully and partially hydrated conditions.

The McGrath group established earlier that the nature of water, i.e., the different states of water existing in the hydrophilic domains, is of great fundamental importance in understanding the influence of chemical structure on transport properties.[12, 13] As has been documented, there are at least three states of water that have been associated with water residing in the hydrophilic phases of polymers.[13-16] The presence and nature of these three states are defined by the thermal properties. *Non-freezing bound water,* also referred to as *tightly bound water*, is firmly bound to the polymer and depresses its T_g, but the water shows no melting endotherm by differential scanning calorimetry (DSC). *Freezable bound water* is weakly bound to the polymer (or loosely bound to the non-freezing water), and displays a broad melting behavior around 0 °C. *Free water* exhibits a sharp melting point at 0 °C. A strong relationship between the states of water and transport properties is known to exist. In this paper, the characterization and

quantification of the different types of water will be reported as a function of block and random copolymer morphology. A fuller understanding of the relationships between chemical composition, microstructure, states of water, and transport properties will lead to synthesizing tailored PEMs with improved performance capabilities.

7.2 Experimental

7.2.1 Materials

Highly purified 4,4'-dichlorodiphenyl sulfone (DCDPS) was provided by Solvay Advanced Polymers. Biphenol (BP) was obtained from Eastman Chemical. All these monomers were well dried under vacuum prior to use and dried under *vacuo* before copolymerization. Decaflurobiphenyl (DFBP) was obtained from Lancaster and used as received. Disulfonated derivatized comonomer (SDCDPS) was synthesized according to modified literature methods[17] and dried under *vacuo* before copolymerization. The solvent N, N-Dimethylacetamide (DMAc, Fisher) and N- Methyl-2-pyrrolidinone (NMP; Fisher) were vacuum-distilled from calcium hydride onto molecular sieves. Potassium carbonate (Aldrich) was dried *in vacuo* before copolymerization. Toluene, sodium chloride, 30% fuming sulfuric acid and methanol were obtained from Aldrich and used as received. The fuming sulfuric acid was further analyzed for active SO_3 concentration.[18] Nafion® 112 and Nafion® 117 were obtained from ElectroChem, Inc.

7.2.2 Multiblock and random copolymer synthesis

A series of segmented disulfonated multiblock copolymers based on poly(arylene ether sulfone) were synthesized. The multiblock copolymers were prepared by a coupling reaction between phenoxide terminated fully disulfonated poly(arylene ether sulfone) (BPSH100) and decafluorobiphenyl (DFBP) end-capped unsulfonated poly(arylene ether sulfone) (BPS00) as hydrophilic and hydrophobic blocks, respectively. BPSH100 hydrophilic oligomers with phenoxide end-groups were prepared with varying block lengths ranging from 3 kg/mol to 20 kg/mol via step growth polymerization.

DFBP end-capped unsulfonated BPS00 hydrophobic oligomers were prepared via a two-step reaction. First, phenoxide terminated BPS00 oligomers with the same molecular weight range of the hydrophilic oligomers were synthesized. Second, the oligomers were end-capped with DFBP. Synthesis of the multiblock copolymers was facilitated by a nucleophilic substitution coupling reaction between the phenoxide end-groups on the hydrophilic oligomers and the fluorine containing end-groups on the hydrophobic oligomers, producing high molecular weight multiblock copolymers. A detailed synthesis for producing these copolymers has been published elsewhere.[11] Random BPSH-xx copolymers were synthesized using the procedures described earlier.[3]

7.2.3. Membrane preparation

Salt form copolymers were redissolved in NMP to afford transparent solutions with 5% solids, then the solutions were cast onto clean glass substrates. The films were dried for 2 days with infrared heat at gradually increasing temperatures, and then dried under vacuum at 110 ^{o}C for 2 days. The membranes were converted to their acid form by boiling in 0.5 M H_2SO_4 for 2 h, and were then boiled in deionized water for 2 h.

7.2.4. Measurement of proton conductivity

Proton conductivity at 30 ^{o}C and at full hydration (in liquid water) was determined in a window cell geometry[19] using a Solartron 1252 + 1287 Impedance/Gain-Phase Analyzer over the frequency range of 10 Hz to 1 MHz following literature procedures.[20] For determining proton conductivity in liquid water, membranes were equilibrated at 30 ^{o}C in DI water for 24 h prior to testing. In order to determine proton conductivity under partially hydrated conditions, membranes were equilibrated in a humidity-temperature oven (ESPEC, SH-240) at the specified RH and temperature for 5 h before each measurement.

7.2.5. Determination of water uptake

The water uptake of all membranes was determined gravimetrically. First, the membranes were soaked in water at 30 °C for 2 days after acidification. Wet membranes were removed from the liquid water, blotted dry to remove surface droplets, and quickly weighed. The membranes were then dried at 120 ^{o}C under vacuum for at least 24 h and weighed again. The water uptake of the membranes was calculated according to Equation (7-1) where $mass_{dry}$ and $mass_{wet}$ refer to the mass of the dry membrane and the wet membrane, respectively.

$$\text{water uptake}\% = \frac{\text{mass}_{\text{wet}} - \text{mass}_{\text{dry}}}{\text{mass}_{\text{dry}}} \times 100 \text{ .....} \qquad \textbf{Equation 7-1}$$

The hydration number (λ), namely, the number of water molecules absorbed per sulfonic acid group, can be calculated from the mass water uptake and the ion content of the dry copolymer. This is shown in Equation (7-2), where MW_{H2O} is the molecular weight of water (18.01 g/mol) and IEC is the ion exchange capacity of the dry copolymer in equivalents per gram.

$$\lambda = \frac{(\text{mass}_{\text{wet}} - \text{mass}_{\text{dry}})/\text{MW}_{\text{H}_2\text{O}}}{\text{IEC} \times \text{mass}_{\text{dry}}} \text{ .....} \qquad \textbf{Equation 7-2}$$

The volume fraction of water or the hydrophilic phase was determined from the given expression,[21]

$$\phi = \left(\frac{M_{H_2O} / \rho_{H_2O}}{\left[M_{H_2O} / \rho_{H_2O} + EW / \lambda \rho_{ionomer} \right]} \right) \qquad \textbf{Equation 7-3}$$

where Φ is the volume fraction of water, ρ is the density, and EW is the equivalent weight of the ionomer.

7.2.6. Determination of swelling ratio and density

The water swelling ratio of all of the membranes was determined from the dimensional changes from wet to dry states both in-plane and through-plane. Initially, samples were equilibrated in water and the wet dimensions were measured. The dried dimensions were obtained by drying the wet membrane at 80 ^{o}C in a convection oven for 2 h. Density was also calculated from the volume and weight of the dried membranes. An average of 4 samples was obtained for each measurement.

7.2.7. Determination of self-diffusion coefficient of water

The self-diffusion coefficients of water were measured using a Varian Inova 400 MHz (for protons) nuclear magnetic resonance spectrometer with a 60 G/cm gradient diffusion probe. Corresponding experimental procedures were reported earlier.[10]

7.2.8. Differential scanning calorimetry (DSC) and nuclear magnetic resonance (NMR)

The DSC experiments were performed in a TA DSC instrument using liquid nitrogen as cooling medium for subambient operation. The samples were equilibrated in a relative humidity oven (ESPEC SH240) to achieve desired hydration levels. The samples were placed in thermally sealed pans capable of withstanding pressure of 100 atm. Samples were cooled to -70 °C and then heated at a rate of 5 °C per min under a N_2 atmosphere.

The proton spin relaxation time, $T_{2,}$ was measured in a Varian Inova 400 spectrometer using Carr-Purcell-Meiboom-Gill (CPMG) pulse sequence. The 90° pulse was of 13.8 μs and the 180° pulse of 27.6 μs. A total of 200 decay points was collected over 8 ms. Samples were equilibrated at room temperature in water. Just before the

experiment, they were removed from water, blotted to remove the surface water and placed in the NMR probe.

7.3. Results and discussion

7.3.1 Summary of the copolymers synthesized

The multiblock copolymers examined in this study are listed in Table 7-1. The copolymers are identified as BPSH-BPS(A:B) multiblocks, where A represents the hydrophilic (BPSH) block lengths in kg/mole, and B represents the hydrophobic (BPS) block length in kg/mole. The hydrophilic block is a 100 % disulfonated system. The multiblock copolymers are classified in two different categories. The first one represents an equal block length series with lower and similar IEC values as shown in Table (7-1). The second category represents multiblocks of unequal block lengths. The hydrophilic block lengths were purposefully synthesized to be longer than the hydrophobic segments in order to achieve higher IEC values. The multiblocks were then compared to the random copolymers with very similar chemical structures represented by BPSH-xx, where xx stands for the degree of disulfonation. The random copolymers were varied in terms of ionic compositions. Nafion® 112 was used as a control for the study. The structures of the BPSH-BPS (A:B) and BPSH-xx are given in Figure (7-1).

a)

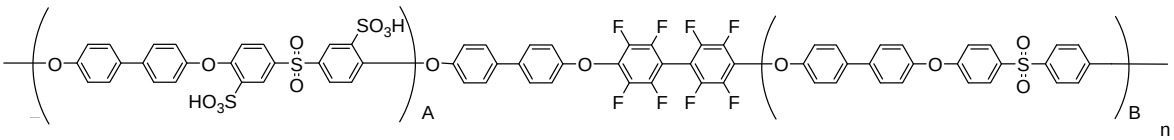

b)

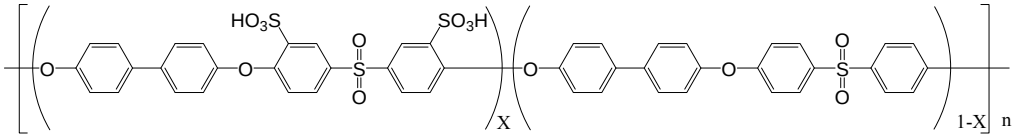

Figure 7-1 Chemical Structure of a) BPSH-BPS (A:B) multiblock and b) BPSH-xx random copolymers

Table 7-1 Summary of the properties of copolymers

Copolymer	Ion exchange capacity (IEC) (meq/g)	Water uptake (%)	Water volume fraction	Self-diffusion coefficients of water ($10^{-6}cm^2s^{-1}$)[a]	Proton conductivity [b] (S/cm)	Density (g/cc)
Nafion® 112	0.90	25	0.30	4.0	0.09	2.1
BPSH-BPS(3:3)	1.33	30	0.28	1.9	0.065	1.3
BPSH-BPS(5:5)	1.39	33	0.32	2.2	0.088	1.4
BPSH-BPS(10:10)	1.28	60	0.45	9.1	0.095	1.4
BPSH-BPS (10:5)	1.83	100	0.60	-	0.160	1.5
BPSH-BPS(15:10)	1.71	90	0.57	-	0.140	1.5
BPSH-BPS(20:15)	1.71	70	0.49	-	0.120	1.4
BPSH40	1.73	60	0.45	5.1	0.100	1.3
BPSH35	1.50	36	0.33	3.1	0.070	1.3
BPSH30	1.34	29	0.22	1.6	0.04	1.2

a. Measurements were conducted in fully hydrated state at 25 °C, ± 10%

b. Measurements were conducted in water at 30 ºC, ± 5%

7.3.2 Physical properties: IEC, density, water uptake and water volume fraction

The titrated ion exchange capacity (Table 7-1) values were similar for each of the three equal block length materials. Because the ionic compositions were similar, any change in properties with increasing block length would inevitably result from either the extent of phase separation or the morphology. Water uptake values increased with increasing block length. The observed increase in the water volume fraction with increasing block length indicates the formation of distinct phase separated and associated hydrophilic domains. This is consistent with TEM findings which revealed the formation

of an ordered co-continuous lamella-like morphology with increasing block length—BPSH-BPS (10:10).[22] The multiblock copolymers with unequal blocks and higher IECs showed significantly higher water uptake. In addition to the morphology effect, higher IEC values corresponded to increased water uptake. For the random copolymers, water uptake was mainly a function of the ion exchange capacity as shown in Table (7-1). In comparing the random copolymers and the multiblocks at similar IEC values, the multiblocks with higher block lengths absorbed more water than the random copolymers. The higher water uptake and volume fraction for the multiblocks as compared to the random copolymers indicate a better phase separated and associated hydrophilic-hydrophobic domain microstructure for the multiblocks.

Distinct anisotropic swelling was observed for the multiblock copolymers in comparison to the random BPSH 35 copolymers, as shown in Figure (7-2). The x,y represents in-plane swelling and z represents through-plane swelling. All the multiblock copolymers showed similar in-plane swelling. However, the through-plane swelling increased significantly for the BPSH-BPS (10:10) copolymers.[11] The increase in water uptake and through-plane swelling with increasing block lengths again supports the formation of ordered hydrophilic domains within the copolymer. This is consistent with our earlier findings in other multiblock systems.

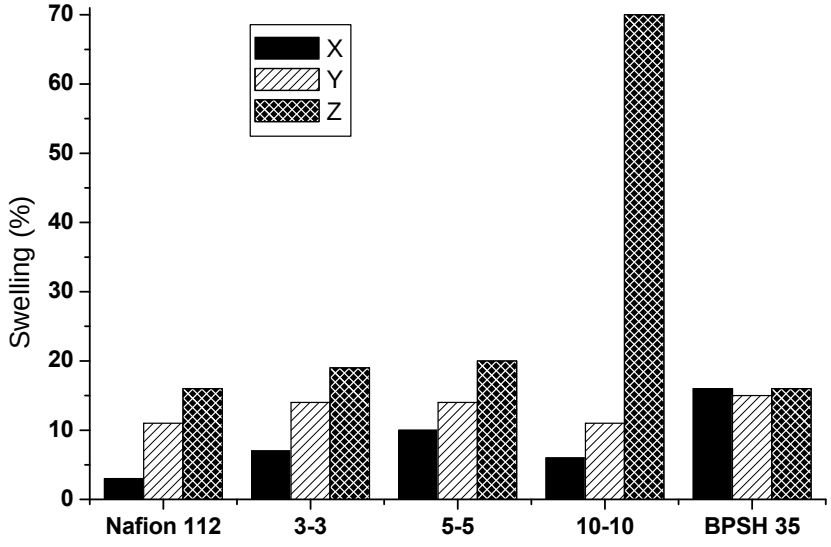

Figure 7-2 In-plane and through plane swelling ratios for the copolymers; multiblock copolymers show anisotropic swelling after a certain block length

Microstructural difference were clearly observed from the self-diffusion coefficient of water values measured at 25 ^{o}C under fully hydrated conditions between the multiblocks with equal block lengths and the random copolymers (Table 7-1). Specifically, for the multiblocks, a significant five-fold increase in diffusion values was observed with increasing block lengths. In addition to the TEM study, the higher diffusion coefficient value for the BPSH-BPS(10:10) copolymer confirms the presence of co-continuous hydrophobic-hydrophilic morphological network with a lower morphological barrier for transport. In contrast, at similar IECs, the random copolymers with significantly lowered water transport values represent an isolated morphological structure with higher a morphological barrier for transport. Understanding these microstructural differences is important in addressing the proton transport issue under partially hydrated conditions.

Proton conductivity for the multiblocks in liquid water at 30 ^{o}C was determined and the resulting values are listed in Table (7-1). For the random copolymers, proton conductivity normally scales with ion exchange capacity. For the multiblocks, however, an increase in conductivity values with both block lengths and IEC was observed. The increased phase separated morphology with increasing block lengths is expected to increase the available volume fraction for transport. As a result, proton transport in multiblock copolymers seems to be dependent on the volume fraction of the water or the hydrophilic phase (Figure7-3). This clearly emphasizes the importance of morphology on proton transport. In addition, the BPSH-BPS (5:5) multiblock copolymers showed much higher proton conductivity at lower water uptake than the random BPSH 35 copolymers. Although the chemical structures and compositions are fairly similar, the differences in the microstructure and morphology make the multiblock copolymers more selective.

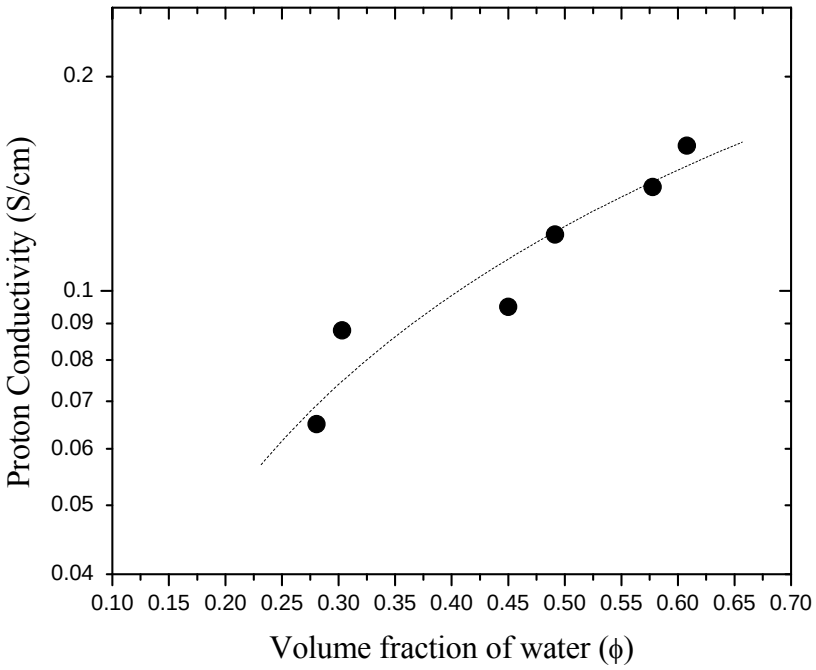

Figure 7-3 Proton conductivity scales with the volume fraction of water

The activation energy for proton transport in liquid water was studied over a temperature range of 30-80 ^{o}C for the equal block length materials. Because the equal block length materials all had similar IEC values, any change in the activation energy would essentially be a function of morphology. Figure (7-4) depicts plots of temperature vs. conductivity for the three equal block length copolymers and the random BPSH 35 copolymer. The slopes represent activation energy and value is given within the box as units of kJ/mole. A significant decrease in activation energy was observed as block lengths increased from 5000g/mole to 10,000 g/mole. The activation energy of the BPSH-BPS (10:10) multiblock copolymer was significantly lower than the BPSH 35 random multiblock copolymer. The morphological transition taking place over that particular block length regime decreased the morphological barrier, thereby lowering the activation energy for proton transport.

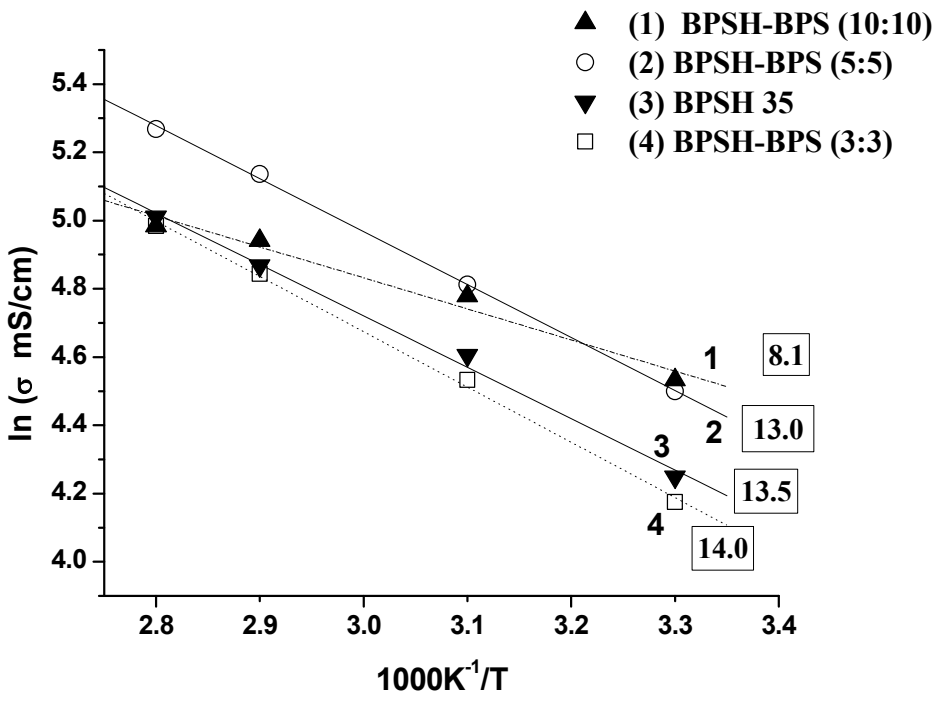

Figure 7-4 Influence of temperature on proton conductivity as a function of block length; activation energy in kJ/mole represented within boxes decreases with increasing block length

Proton conductivity as a function of relative humidity (RH) at 80 ^{o}C was studied and the results are displayed in Figure (7-5). As shown, proton conductivity dropped significantly at lower RH values for the BPSH-35 random copolymers. Random copolymers show acceptable performance under fully hydrated conditions since there are sufficient water molecules to provide proton transport. Due to the scattered hydrophilic domains in the copolymer, however, they lack the connectivity among sulfonic acid groups for proton transport under partially hydrated conditions. In contrast, the performance of the multiblock copolymers under partially hydrated condition improved with increasing block lengths. The performance of the BPSH-BPS(10:10) was comparable to that of commercially available Nafion® 112. This performance improvement is related to the formation of long, co-continuous channels at higher block lengths, through which protons can be transported along with the sulfonic acid groups

and water molecules. The distinct phase separated co-continuous hydrophilic domain morphology, as supported by the diffusion coefficient, TEM and water sorption studies, lowers the morphological barrier for proton transport and improves the proton transport at low water content. Although the multiblocks and random copolymers have identical chemical structures, the difference in their chemical microstructures, particularly at higher block lengths, improves proton transport under partially hydrated conditions.

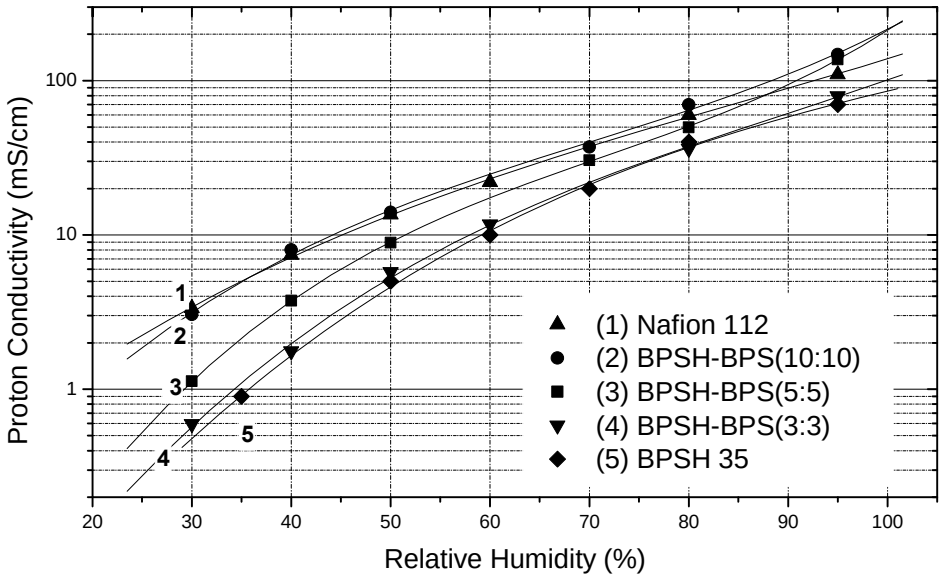

Figure 7-5 Proton conductivity under partially hydrated conditions increases with increasing block lengths at 80 ^{o}C

Proton conductivity was measured for the unequal block length materials as a function of relative humidity as shown in Figure (7-6). Both the higher IEC values and the higher volume fraction of hydrophilic units were expected to improve connectivity within the hydrophilic domains compared to the lower IEC materials. Performance was improved significantly and was shown to be better than the benchmark Nafion®112. However, the copolymers exhibited higher water uptake.

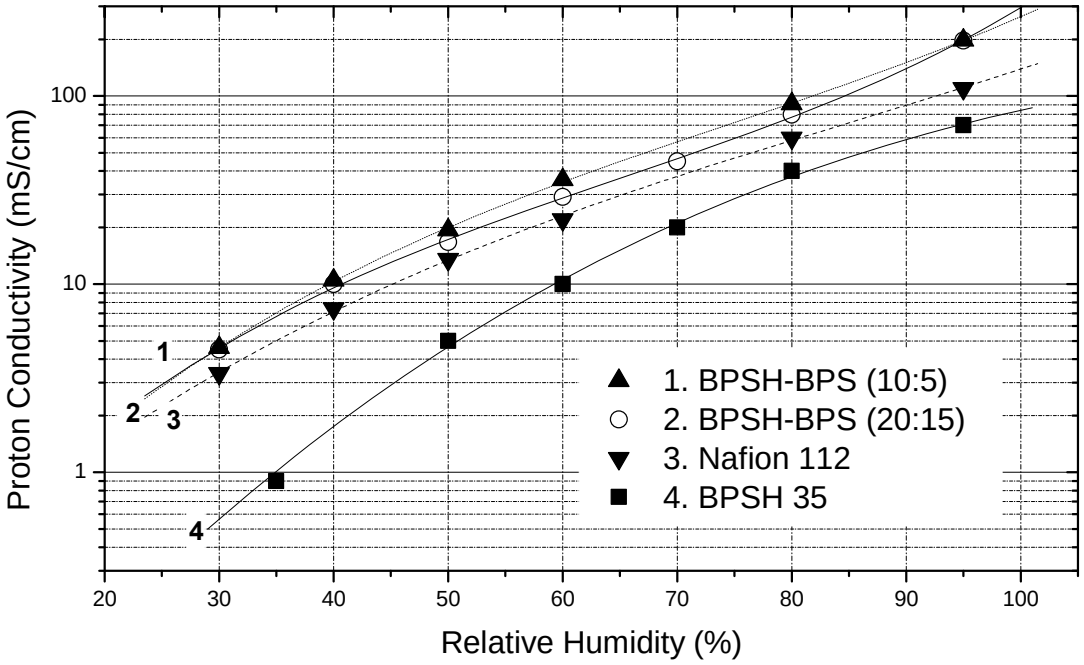

Figure 7-6 Proton conductivity as a function of relative humidity for the multiblocks with higher IECs at 80 ^{o}C

This study confirmed that although morphology is a highly significant factor for performance, the other important variable is water content. To normalize the water content effect, the proton conductivity values of the multiblocks and the random BPSH 35 copolymers were compared over a wide range of water volume fractions. The copolymers were equilibrated with different water contents, after which proton conductivity was measured at 30 °C.

It follows that even under similar water content level; proton transport is a function of block length, which is confirmed in Figure (7-7). Although the multiblock copolymers showed improved proton conductivity over a wide range of water content compared to the BPSH 35 random copolymers, the effect was more pronounced in lower water content regions. Interestingly, the BPSH-BPS (10:10) with the best phase separated morphology required the least amount of water to achieve similar proton

conductivity results. Hence, the microstructural difference between the block and random copolymer is the primary factor for controlling proton transport at low water content.

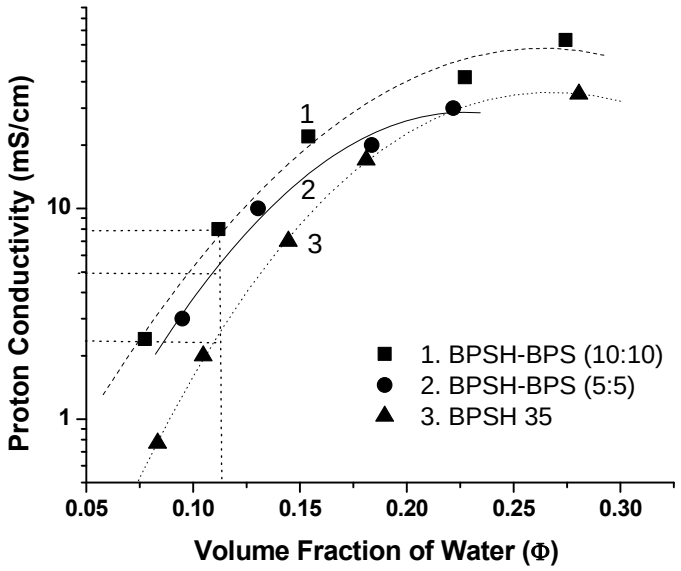

Figure 7-7 Proton conductivity as a function of volume fraction of water in the copolymers at 30 ^{o}C; morphology dominates transport at low water content

7.3.3 States of water

The states of water of the BPSH-BPS (A:B) multiblock copolymers were characterized and quantified using DSC and NMR T_2 relaxation methods. Our earlier investigations of the states of water of BPSH random copolymers indicated a strong relationship between ionic content and the nature of water.[13] Free water was found to develop within the BPSH random copolymers after attaining a particular IEC value. In case of the ion containing multiblock copolymers studied so far, the nature of water has been found to be a function of morphology as well. Specifically, an increase in block length has been associated with increasing free water.[12] This paper will extend this analysis to the BPSH-BPS block copolymers.

7.3.3.1 Water absorption

Water uptake values expressed in terms of a hydration number were measured over a wide range of water activity levels for the multiblocks with equal block lengths. Nafion®112 and BPSH 35 were included for comparison (Fig.7-8). At low water activity, the BPSH-BPS (10:10) and the random BPSH 35 showed similar absorption characteristics. However, after 0.7 water activity, a sharp increase in water absorption was observed for the BPSH-BPS (10:10) in contrast to the random copolymers. This suggests that the observed change in the type or state of water for the multiblock was influenced by the morphology of the copolymer. The higher hydration value for the BPSH-BPS (10:10) compared to all the other copolymers at higher water activity levels indicates the presence of more free water. The multiblock copolymers with lower block lengths, i.e. BPSH-BPS (5:5) and BPSH-BPS (3:3), showed very similar water absorption tendencies compared to the random copolymers. Hence, the distribution of the types of water is thought to be similar in these systems.

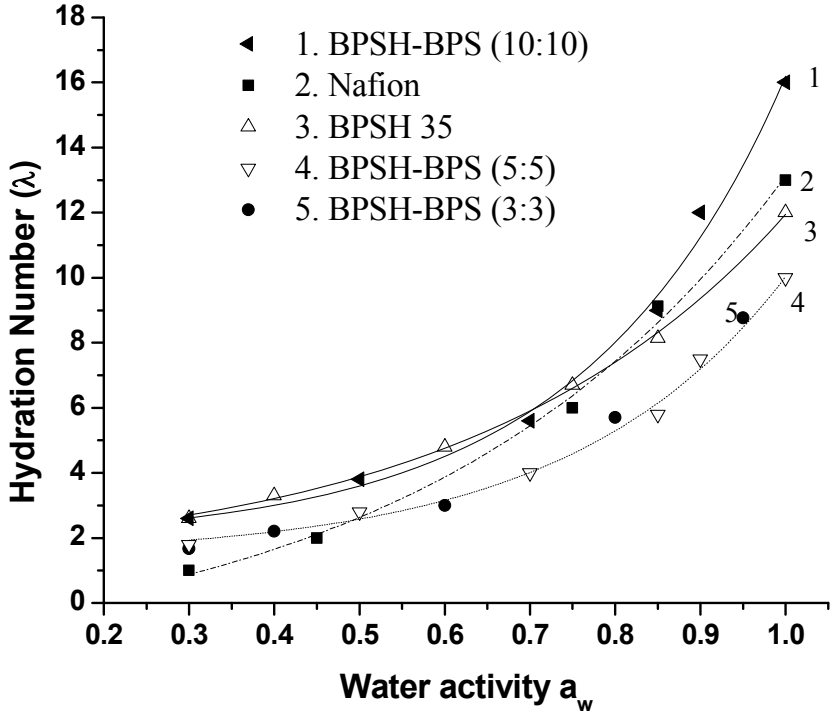

Figure 7-8 Water absorption of copolymers under partially hydrated conditions

7.3.3.2 DSC studies

The melting endotherm of water as a function of block length was characterized from DSC experiments as shown in Figure (7-9). A significant increase in the area under the curve was observed for the BPSH-BPS (10:10) multiblock as block lengths were increased from 5000 g/mole to 10,000 g/mole. It should be noted that the IEC values of the multiblocks were comparable. A similar effect of block length on the melting endotherm of water was observed earlier for the BPSH-PI multiblocks.[12] The increased area under the peak with increasing block lengths corresponds to increased freezing water (free and loosely bound water) content. The co-continuous, ordered, phase separated morphology for the BPSH-BPS (10:10) multiblocks allows the retention of more loosely bound water and, more importantly, the retention of free water in the system. The calculated ΔH_{fus} values from the melting endotherm peaks are given in Table (7-2). A higher ΔH_{fus} value represents better water–water interactions. This increased value complements a similar water/proton transport trend with increasing block length. However, with decreasing block length—particularly for the BPSH-BPS (3:3) sample—the melting endotherm peak shifted towards to the left or to a lower temperature. This indicates the water is more bound to the sulfonic groups, as evidenced by the significantly decreased ΔH_{fus} values.

As discussed earlier, DSC can be used to quantify the types of water present in copolymers.[12] For example, tightly bound water content can be determined quite accurately in this way. Previous work has shown that DSC thermograms are a function of water content for polymers, showing the melting endotherms of both loosely bound water and free water. Tightly bound water can be correlated to the maximum amount of water for which there is no melting endotherm.[13] Quinn et al.[15] proposed a better mathematical technique to estimate the distribution of each type of water. They showed that if the integrated change in enthalpy (per gram of dry polymer) from the DSC thermogram is plotted against total water content, the intercept corresponds to the amount

of tightly bound water. By subtracting the tightly bound water from the total water, the combined content of the loosely bound water and free water can be obtained.

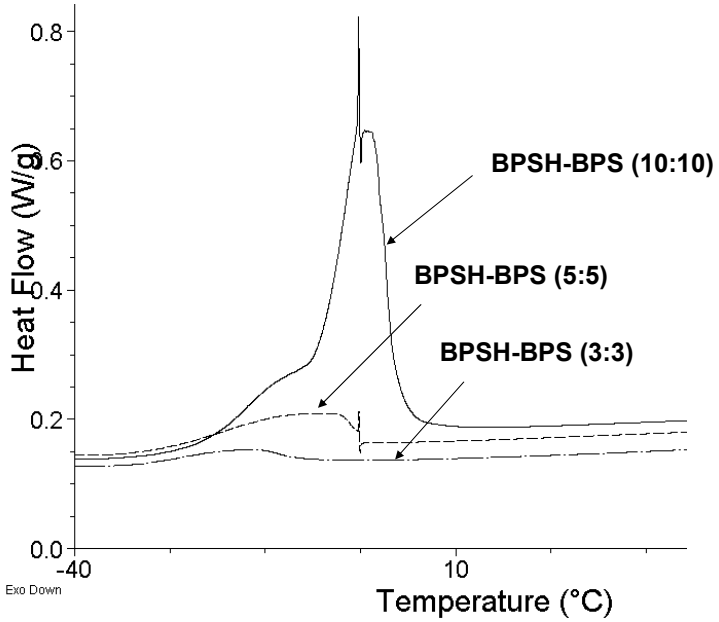

Figure 7-9 DSC thermograms of the melting endotherm of water as a function of block lengths

Figure (7-10) depicts representative plots of DSC thermograms for BPSH-BPS(10:10) multiblocks with increasing water content. The percentages in the figure represent the respective water uptake on a mass basis. The thermogram corresponding to maximum water uptake represents the fully hydrated state. A sharp and broad melting endotherm was observed, indicating the presence of both loosely and free water content. When the water uptake was decreased to 27%, the area under the peak decreased, as did the percentage of free water content. However, no melting endotherm was observed when water uptake was decreased to 18 %. This corresponds to the presence of only tightly bound water in the system and can be quantify easily. It should be noted that it was difficult to quantify the loosely bound and free water separately only using DSC. This is due to the fact that the two melting endotherms of free and loosely bound water

overlapped with each other. Hence, other experimental techniques should be used in conjunction with DSC to properly quantify the states of water.

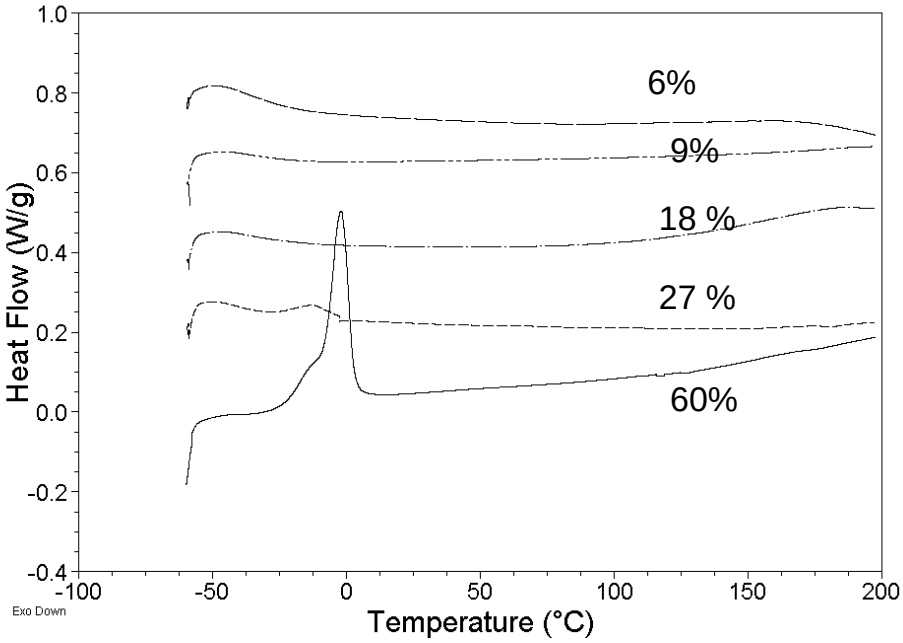

Figure 7-10 DSC thermograms of BPSH-BPS (10:10) multiblock at various water content, the numbers represent the water uptake on mass basis

7.3.3.3 NMR relaxation measurements

In order to quantify the loosely bound and free water content, T_2 NMR relaxation experiments were conducted. The mechanism for the T_2 relaxation in sulfonic acid containing copolymers is believed to be an exchange process between the water molecules and the exchangeable protons in the sulfonic acid groups.[23] Hence, the water molecules (tightly and loosely bound) associated with the sulfonic groups will relax faster than the ones (free water) which are not associated. However, for the copolymers studied, T_2 data could not distinguish between the shortest and the intermediate components. Loosely bound and tightly bound water are believed to exist in the same hydrophilic domain, and a rapid exchange can occur in between the two environments. For the BPSH-BPS (3:3) and BPSH-BPS (5:5) multiblock copolymers, the T_2 relaxation

was found to follow a mono exponential decay function. No free water was detected in these materials. By subtracting the tightly bound water content from the total water content, it was possible to determine the content of loosely bound water.

However, for the BPSH-BPS (10:10) multiblocks, the T_2 relaxation was triexponential in nature (Fig.7-11). A unique, longer relaxation time was associated with the presence of free water in the system. The relative proportion of the corresponding coefficient of the exponent term allowed the quantification of the free water component. The sharp peak observed in the melting endotherm of the BPSH-BPS (10:10), multiblock as evidenced by DSC also supports the presence of free water. The free water content was then quantified by NMR, while the tightly bound water was quantified by DSC. Subtracting the free and tightly bound water from total water content allows proper estimation of loosely bound water content. Hence, the use of NMR in conjunction with DSC allows one to accurately quantify the states of water, as shown in Table (7-2).

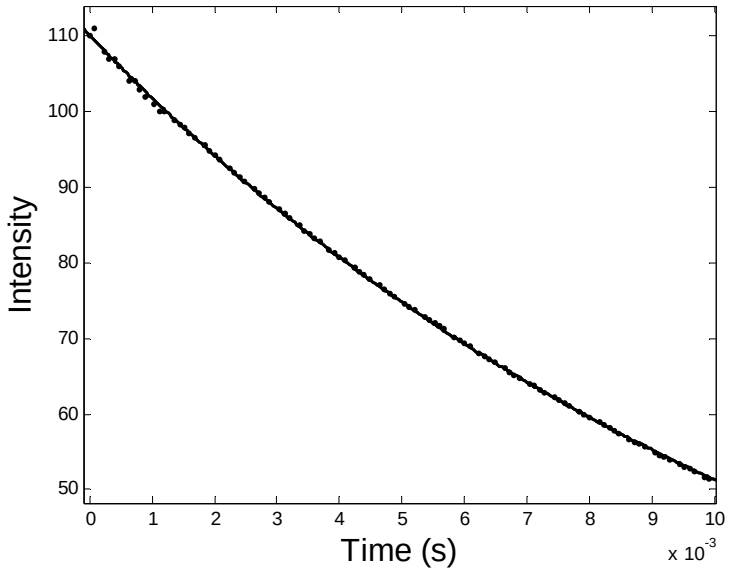

Figure 7-11 ^{1}H NMR T_2 relaxation (tri-exponential fit) behavior of BPSH-BPS (10:10) multiblock copolymer

The three different types of water quantified for the multiblocks, along with the ΔH_{fus} of water, are given in Table 7-2. The data for BPSH-xx were obtained from our

earlier publications. [13] The method used to quantify the states of water was similar to the methods described in this paper. Nafion® 112 was used as the control.

Table 7-2 States of water quantification for the BPSH-BPS (A:B) multiblocks and BPSH- xx random[13] copolymers

Sample	IEC (meq/g)	Total water content (λ)	Tightly bound water (λ)	Loosely bound water (λ)	Free water (λ)	Δ H_{fus} water (J/g of water)
Nafion® 112	0.90	17	3	9	5	210
BPSH-BPS(3:3)	1.33	12	7	5	0	151
BPSH-BPS(5:5)	1.39	13	8	5	0	42
BPSH-BPS(10:10)	1.28	26	10	8	8	14
BPSH 50	2.18	33	5	24	4	-
BPSH 40	1.73	18	5	11	2	-
BPSH 30	1.34	12	4	8	0	-

The content of tightly bound water was found to be higher in the multiblocks than in the random copolymers. And while free water content developed after reaching a particular IEC for the random copolymers, for the multiblock copolymers it developed with increasing block length without having any increase in the IEC. In comparing the multiblock copolymers to the random copolymers at a given IEC (1.3), the BPSH-BPS(10:10) multiblock copolymer displayed significantly higher free water content than the random copolymer. As reported earlier, free water content impacts transport properties. Hence, in spite of their lower IEC values, the presence of free water in the BPSH-BPS (10:10) copolymers enhanced their performance as compared to the random copolymers. Earlier investigations have associated the origins of free water with the formation of a phase separated, co-continuous hydrophilic-hydrophobic domain morphology.[12] The higher ionic content in the random copolymers induced

microstructural changes, leading to the formation of water-assisted phase separated morphology. Hence free water develops in random copolymers only at higher IECs. In contrast, the chemically phase separated morphology of the multiblocks is responsible for the formation of free water even at a low IEC. As a comparison, Nafion® also has higher free water content at low IEC, indicating a similar phase separation characteristic to the multiblock copolymers.

7.4 Conclusions

The influence of microstructure/sequence distribution on the performance properties of proton exchange membranes was investigated. The BPSH-xx random copolymers and the BPSH-BPS (A:B) multiblock copolymers have a similar chemical structure. At a same IEC, the acidity and the concentration of sulfonic groups are similar in these two systems. They differ only in microstructure or sequence distribution. The microstructure of the multiblocks was varied by changing the molecular weights of the individual blocks. The random copolymer morphology resulted in lower water uptake and reduced proton and water transport. The lower block length multiblocks displayed properties similar to the random copolymers at a given IEC. However, proton and water transport increased significantly with increasing block length as observed for the BPSH-BPS (10:10) multiblock copolymers. The observed transition behavior corresponds to the formation of a co-continuous hydrophilic-hydrophobic morphology with enhanced phase separation as seen from TEM and swelling studies.

The enhanced phase separated morphology of the multiblocks improved the desired proton conductivity under partially hydrated conditions. Thus, one can conclude that under partially hydrated conditions proton transport is controlled by the morphology and not by the acidity of the system. Hence, by changing the chemical architecture from a random to a phase separated domain network, significant improvements in PEM properties can be achieved.

Fundamental morphological differences between the random and multiblock architectures were also investigated by states of water analysis. Significant differences were observed between the two systems in the distribution of the three types of water. Specifically, a random morphology resulted in lower free water content, suggesting a closed, isolated morphological structure. Phase separated morphology in the block copolymer encouraged the formation of free water, even at lower IEC values. Free water content and the ΔH_{fus} of water increased with increasing block length under similar ionic concentrations. All these facts support the presence of a "favored or facilitated" morphology in the multiblocks, which is conducive to improved proton and water transport.

The authors wish to acknowledge Nissan Motor Company and Department of Energy (DOE Contract # DE-FG36-06G016038) for support of this research.

7.5 References

1. Mauritz, K. A.; Moore, R. B., State of understanding of Nafion. *Chemical Reviews (Washington, DC, United States)* **2004,** 104, (10), 4535-4585.

2. Hickner, M. A.; Ghassemi, H.; Kim, Y. S.; Einsla, B. R.; McGrath, J. E., Alternative polymer systems for proton exchange membranes (PEMs). *Chemical Reviews* **2004,** 104, (10), 4587-4611.

3. Wang, F.; Hickner, M.; Kim, Y. S.; Zawodzinski, T. A.; McGrath, J. E., Direct polymerization of sulfonated poly(arylene ether sulfone) random (statistical) copolymers: candidates for new proton exchange membranes. *Journal of Membrane Science* **2002,** 197, (1-2), 231-242.

4. Kim, Y. S.; Wang, F.; Hickner, M.; McCartney, S.; Hong, Y. T.; Harrison, W.; Zawodzinski, T. A.; McGrath, J. E., Effect of acidification treatment and morphological stability of sulfonated poly(arylene ether sulfone) copolymer proton-exchange membranes for fuel-cell use above 100 degrees C. *Journal of Polymer Science Part B-Polymer Physics* **2003,** 41, (22), 2816-2828.

5. Kim, Y. S.; Dong, L. M.; Hickner, M. A.; Pivovar, B. S.; McGrath, J. E., Processing induced morphological development in hydrated sulfonated poly(arylene ether sulfone) copolymer membranes. *Polymer* **2003,** 44, (19), 5729-5736.

6. Li, Y.; Roy, A.; Badami, A. S.; Hill, M.; Yang, J.; Dunn, S.; McGrath, J. E., Synthesis and characterization of partially fluorinated hydrophobic-hydrophilic multiblock copolymers containing sulfonate groups for proton exchange membrane. *Journal of Power Sources* **2007,** 172, (1), 30-38.

7. Lee, H.-S.; Roy, A.; Badami, A. S.; McGrath, J. E., Synthesis and characterization of sulfonated poly(arylene ether) polyimide multiblock copolymers for proton exchange membranes. *Macromolecular Research* **2007,** 15, (2), 160-166.

8. Lee, H.-S.; Badami, A. S.; Roy, A.; McGrath, J. E., Segmented sulfonated poly(arylene ether sulfone)-b-polyimide copolymers for proton exchange membrane fuel cells. I. Copolymer synthesis and fundamental properties. *Journal of Polymer Science, Part A: Polymer Chemistry* **2007,** 45, (21), 4879-4890.

9. Yu, X.; Roy, A.; Dunn, S.; Yang, J.; McGrath, J. E., Synthesis and characterization of sulfonated-fluorinated, hydrophilic-hydrophobic multiblock copolymers for proton exchange membranes. *Macromolecular Symposia* **2006,** 245/246, (World Polymer Congress--MACRO 2006), 439-449.

10. Roy, A.; Hickner, M. A.; Yu, X.; Li, Y.; Glass, T. E.; McGrath, J. E., Influence of chemical composition and sequence length on the transport properties of proton exchange membranes. *Journal of Polymer Science, Part B: Polymer Physics* **2006,** 44, (16), 2226-2239.

11. Lee, H.-S.; Roy, A.; Lane, O.; Dunn, S.; McGrath, J. E., Hydrophilic-hydrophobic multiblock copolymers based on poly(arylene ether sulfone) via low-temperature coupling reactions for proton exchange membrane fuel cells. *Polymer* **2008,** 49, (3), 715-723.

12. Roy, A.; Hickner, M. A.; Lee, H.-S.; Glass, T. E.; McGrath, J. E., States of Water of Proton Exchange Membranes Part-A- Influence of Chemical Structure and Compositions. *To be Submitted* **2008**.

13. Kim, Y. S.; Dong, L. M.; Hickner, M. A.; Glass, T. E.; Webb, V.; McGrath, J. E., State of water in disulfonated poly(arylene ether sulfone) copolymers and a

perfluorosulfonic acid copolymer (nafion) and its effect on physical and electrochemical properties. *Macromolecules* **2003,** 36, (17), 6281-6285.

14. Boyle, N. G.; Mcbrierty, V. J.; Douglass, D. C., A Study of the Behavior of Water in Nafion Membranes. *Macromolecules* **1983,** 16, (1), 75-80.

15. Quinn, F. X.; Kampff, E.; Smyth, G.; Mcbrierty, V. J., Water in Hydrogels .1. A Study of Water in Poly(N-Vinyl-2-Pyrrolidone Methyl-Methacrylate) Copolymer. *Macromolecules* **1988,** 21, (11), 3191-3198.

16. Hodge, R. M.; Edward, G. H.; Simon, G. P.; Hill, A. J., The States of Water within Poly(Vinyl Alcohol) Thin-Films .1. Investigation by Positron-Annihilation Lifetime Spectroscopy. *Abstracts of Papers of the American Chemical Society* **1993,** 205, 447-POLY.

17. Wang, F.; Hickner, M.; Ji, Q.; Harrison, W.; Mecham, J.; Zawodzinski, T. A.; McGrath, J. E., Synthesis of highly sulfonated poly(arylene ether sulfone) random (statistical) copolymers via direct polymerization. *Macromolecular Symposia* **2001,** 175, 387-395.

18. Sankir, M.; Bhanu, V. A.; Harrison, W. L.; Ghassemi, H.; Wiles, K. B.; Glass, T. E.; Brink, A. E.; Brink, M. H.; McGrath, J. E., Synthesis and characterization of 3,3 '-disulfonated-4,4 '-dichlorodiphenyl sulfone (SDCDPS) monomer for proton exchange membranes (PEM) in fuel cell applications. *Journal of Applied Polymer Science* **2006,** 100, (6), 4595-4602.

19. Zawodzinski, T. A.; Neeman, M.; Sillerud, L. O.; Gottesfeld, S., *J. Phys. Chem.* **1991,** 95, 6040.

20. Springer, T. E.; Zawodzinski, T. A.; Wilson, M. S.; Gottesfeld, S., *J. Electrochem. Soc.* **1996,** 143, 587.

21. Schuster, M.; Kreuer, K.-D.; Andersen, H. T.; Maier, J., Sulfonated poly(phenylene sulfone) polymers as hydrolytically and thermooxidatively stable proton conducting ionomers. *Macromolecules* **2007,** 40, (3), 598-607.

22. Badami, A., Ph.D Thesis. *ETD, Virginia Tech* **2007**.

23. Barbieri, R.; Quaglia, M.; Delfini, M.; Brosio, E., Investigation of water dynamic behaviour in poly(HEMA) and poly(HEMA-co-DHPMA) hydrogels by proton T-2

relaxation time and self-diffusion coefficient nmr measurements. *Polymer* **1998,** 39, (5), 1059-1066.

8.0 Influence of Microstructure and Chemical Composition on Proton Exchange Membrane Properties of Sulfonated-Fluorinated, Hydrophilic-Hydrophobic Multiblock Copolymers

Abhishek Roy, Xiang Yu, Stuart Dunn & James E. McGrath

Macromolecules and Interfaces Institute, Virginia Polytechnic Institute and State University, Blacksburg, Virginia, 24061

Abstract

Nanophase separated ionic-hydrophobic block copolymers have shown promise as proton exchange membranes than random copolymers. A series of multiblock copolymers composed of alternating segments of fully disulfonated poly(arylene ether sulfone)s and highly fluorinated poly(arylene ether sulfone)s were evaluated for their potential as proton exchange membranes. Block length and chemical composition were the two major structural variables influencing the properties. Significantly, higher water and proton transport were observed for the higher block length materials. Water uptake was controlled by controlling the ratio between the hydrophobic and hydrophilic block lengths. These ion containing multiblock copolymers showed promise as some of the more selective PEMs in terms of achieving both high proton conductivity and low water uptake. Detailed structure-property relationships are provided in the paper.

8.1 Introduction

Sulfonic acid containing polymeric membranes are known to phase separate into hydrophilic and hydrophobic domain morphologies. The extent of phase separation has been identified as one of the major factors for achieving proton conduction, particularly under partially hydrated conditions.[1] In aromatic random copolymers the extent of phase separation, and thus membrane performance, is primarily a function of water content. As a result, the proton conductivity decreases significantly under partially hydrated conditions, as seen for the random copolymers. Therefore, the challenge lies in altering the chemical architecture for synthesizing copolymers such that phase separation will mainly be a function of copolymer microstructure. One such approach is to synthesize nanophase separated ion containing block copolymers.

Block copolymers consist of two or more chemically dissimilar backbone segments (i.e. blocks) that are chemically joined through covalent bonds in the same chain.[10] When one of the blocks is fully or partially modified with ion containing groups, ion containing block copolymers can be obtained. Over the last few years our group has synthesized thermally stable multiblock copolymers with varying chemical structures and compositions.[1-8] Irrespective of the nature of the backbone, the transport properties scaled with the block lengths of the copolymers. An increase in block length for a series of block copolymers with the same ionic concentration was associated with an increase in the self-diffusion coefficients of water, as well as with improved proton conduction under partially hydrated conditions over the random copolymers.[1, 9] While the hydrophilic segments of these materials were identical, the chemical structure of the hydrophobic unit was varied from highly fluorinated to partially fluorinated to hydrocarbon based multiblock copolymers. It is anticipated that the difference in hydrophobicity would also influence overall phase separation. The higher the hydrophobicity of the hydrophobic blocks, the sharper is the phase separation. Because hydrophobicity is a function of the nature of the repeat units in the hydrophobic block, a fully hydrocarbon block would be less hydrophobic than a partially fluorinated block.

We have been engaged in the synthesis of ion containing multiblock copolymer with partially fluorinated hydrophobic block. The structures of these blocks are shown in (Figure 8-1), where X represents an isopropylidene unit (Figure 8-1 a), a hexafluoroisopropylidene unit (Figure 8-1 b), or a sulfone group (Figure 8-1 c). The corresponding copolymers are termed BisAF-BPSH(x:y), 6FBisAF-BPSH(x:y), and BisSF-BPSH(x:y), respectively. We have previously published some work on the first two types of multiblock copolymers.[10-12] The synthesis details of the BisSF-BPSH multiblocks are reported separately.[13] In this work, the characterization of the BisSF-BPSH(x:y) series copolymers will be reported. The presence of fluorine in a hydrophobic block is expected to impact the extent of phase separation, and therefore PEM properties.

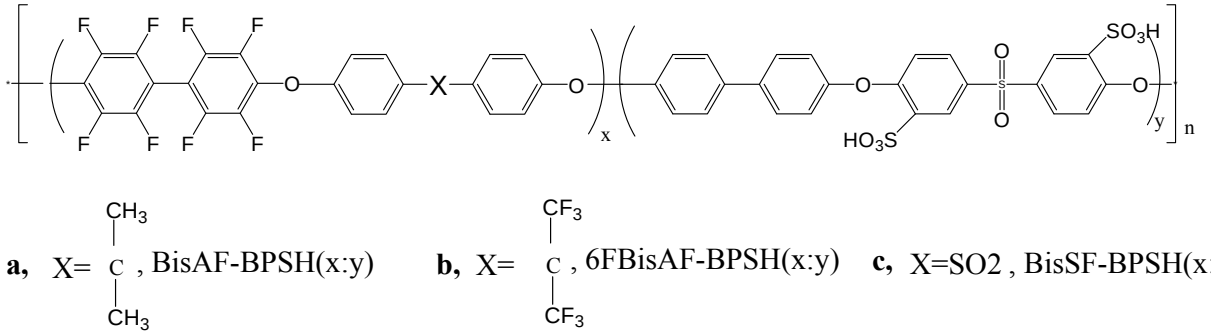

Figure 8-1 Structures of sulfonated-fluorinated multiblock copolymers

One of the major challenges in optimizing structure-property relationships for PEMs is to design a system with high proton conductivity and low water uptake. Theoretically, proton conductivity is a function of both diffusion (i.e., the ionic mobility of the protons) and the concentration of the available protons. Because increased swelling in the membrane lowers the effective proton concentration and therefore proton conductivity, maximizing proton concentration is essential. In addition to this, high swelling in the membrane results in significant cathode flooding and a loss of both dimensional and mechanical properties at higher hydration levels. In the typical fuel cell environment, membranes often are subjected to significant RH cycles, subjecting the

membrane to repeated swelling-deswelling. A very low swelling deswelling ratio, particularly along the in-plane direction, is desired for better mechanical durability.

Several strategies for reducing water uptake in membranes have been attempted in the past. For random copolymers, reducing ionic content is associated with both reduced water uptake and proton conductivity, but with only nominal improvements in selectivity. The addition of inorganic materials to polymeric membranes has shown great promise in significantly reducing water uptake. The mechanical properties of these inorganic polymeric composites also improved substantially.[14] However, because proton conduction depends strongly on water content, maintaining proton conduction at low water contents has been a significant challenge. The addition of inorganic particles has also been shown to decrease the available volume fraction for transport and hence reducing the proton conductivity. Alberty et. al.[15] reported the use of ionic inorganic fillers to counter the loss in proton conductivity. Crosslinking materials with higher ion exchange capacity (IEC) values is another viable approach. Introducing thermally stable crosslinks within high IEC materials is expected to reduce the swelling of the membrane. At the same time, the high IEC of the copolymer may provide a way of maintaining reasonable proton conductivity. However, synthesizing thermally stable crosslinked ionic polymeric networks while maintaining the ductility of the membrane have been a serious challenge. Recently, Riffle et al.[16] have reported the synthesis of thermally stable epoxy–crossslinked disulfonated poly(arylene ether sulfone) copolymers which have shown promise.

In our study of various multiblocks, a strong relationship between water uptake and block length has been observed.[1,9] Particularly for the equal block length materials having similar IECs, water uptake increased with increasing block length or in association with the extent of phase separation. Hence altering the morphology can also change the water uptake property. In random copolymers, morphology is mainly a function of ion exchange capacity. In the case of multiblock copolymers, however, morphology depends both on IEC and block length, which can be equal or unequal. In this paper, the influence of these three major variables (IEC, equal block lengths, and

unequal block lengths) on block copolymer properties will be investigated with the goal of improving the selectivity between the water uptake and proton conductivity.

8.2 Experimental

8.2.1 Materials

4,4'-Dihydroxydiphenyl sulfone (Bisphenol-S) and decafluorobiphenyl were obtained from Aldrich and dried under vacuum before use. 4,4'-Dichlorodiphenylsulfone (DCDPS) was obtained from Solvay Advanced Polymers and used as received. 3,3'-Disulfonated-4,4'-dichlorodiphenylsulfone (SDCDPS) was synthesized from DCDPS according to a process reported elsewhere.[17] 4,4'-Biphenol was obtained from Eastman Chemical and used as received. *N*-methyl-2-pyrrolidone (NMP), purchased from Aldrich, was vacuum-distilled from calcium hydride and stored under nitrogen. Nafion®112 was purchased from Electrochem Inc and used as recieved. NRE® 211 was donated by Nissan Motor Company.

8.2.2 Synthesis

BisSF-BPSH(x:y) multiblock copolymers were synthesized by procedures similar to those reported earlier.[12] Fluorinated BisSF oligomers were prepared by polymerizing decafluorobiphenyl and 4,4′-dihydroxy diphenyl sulfone (bisphenol-S). 3,3′-Disulfonated-4,4′-dichlorodiphenyl-sulfone (SDCDPS) was polymerized with biphenol to synthesize the BPS100 hydrophilic oligomers. Calculated amounts of BisSF oligomer were added to BPS100 to initiate the block copolymerization. The salt form of the BisSF-BPS100 multiblock copolymer was obtained and cast according to reported procedures.[12] Acidifying the film in 0.5 M boiling sulfuric acid for 2 h and then in boiling deionized water for 2 h yielded the BisSF-BPSH(x:y) multiblock copolymer. A series of block copolymers BisSF-BPSH(x:y) was synthesized, which varied in ion exchange capacity (IEC) and block length.

8.2.3 NMR spectroscopy

^{1}H NMR analysis was conducted on a Varian Unity 400 spectrometer. All spectra were obtained from 10% solutions (w/v) in DMSO d_6 solution at room temperature.

8.2.4 Proton conductivity

Proton conductivity at 30 °C at full hydration (in liquid water) was determined in a window cell geometry[18] using a Solartron 1252+1287 Impedance/Gain-Phase Analyzer over the frequency range of 10 Hz -1 MHz following procedures reported in the literature.[19] Membranes were equilibrated at 30 °C in DI water for 24 h prior to testing. The temperature range chosen for calculating activation energy for proton transport was from 30-80 °C. For determining proton conductivity under partially hydrated conditions, the membranes were equilibrated in a humidity-temperature oven (ESPEC Corp., SH-240) at a specified RH and at 80 °C for 5 h before each measurement.

8.2.5 Water uptake

The water uptake of the membranes was calculated gravimetrically,[10] according to Equation(8-1) where $mass_{dry}$ and $mass_{wet}$ refer to the mass of the wet membrane and the mass of the dry membrane, respectively.

$$water\ uptake\ \% = \frac{mass_{wet} - mass_{dry}}{mass_{dry}} \times 100 \qquad \textbf{Equation 8-1}$$

The hydration number (λ), which is the number of water molecules absorbed per sulfonic acid group, can be calculated from the mass water uptake and the ion content of the dry copolymer as shown in Equation (8-2),

$$\lambda = \frac{(\mathrm{mass}_{\mathrm{wet}} - \mathrm{mass}_{\mathrm{dry}})/\mathrm{MW}_{\mathrm{H_2O}}}{\mathrm{IEC} \times \mathrm{mass}_{\mathrm{dry}}} \qquad \textbf{Equation 8-2}$$

where MW_{H2O} is the molecular weight of water (18.01 g/mol), and IEC is the ion exchange capacity of the dry copolymer in milliequivalents per gram.

The volume fraction of water or the hydrophilic phase was determined from the given expression[20] (Equation 8-3),

$$\phi = \left(\frac{M_{H_2O} / \rho_{H_2O}}{\left[M_{H_2O} / \rho_{H_2O} + EW / \lambda \rho_{ionomer} \right]} \right) \qquad \textbf{Equation 8-3}$$

where Φ is the volume fraction of water, ρ is the density and EW is the equivalent weight of the ionomer.

8.2.6 Determination of swelling ratio and density

The swelling ratio of all the membranes was determined from dimensional changes observed from wet to dry states, both in-plane and through-plane. Initially, samples were equilibrated in water and wet dimensions were measured. The dry dimensions were obtained by drying the wet membrane at 80 °C in a convection oven for 2 h. Density was also calculated from the volume and weight of the dried membranes. An average of 4 samples was taken for each measurement.

8.2.7 Pulsed-field gradient spin echo nuclear magnetic resonance (PGSE NMR)

The self-diffusion coefficients of water were measured using a Varian Inova 400 MHz (for protons) nuclear magnetic resonance spectrometer with a 60 G/cm gradient diffusion probe. A total of 16 points was collected across the range of gradient strength, and the signal-to-noise ratio was enhanced by co-adding 4 scans. The standard stimulated-echo NMR pulse sequence is shown in Figure (8-2).

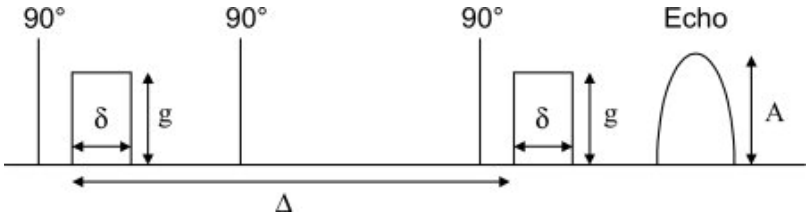

Figure 8-2 Pulse sequence schematic for PGSE NMR experiments

Measurements were obtained by observing the echo signal intensity (A) as a function of the gradient strength. The diffusion coefficient (D) was determined by fitting the data to Equation (8-4), [21]

$$A(g) = A(o)\exp[-\gamma^2 D g^2 \delta^2 (\Delta - \delta/3)] \qquad \textbf{Equation 8-4}$$

where, A is the NMR signal intensity as a function of gradient strength, γ is the gyromagnetic ratio (26752 $radG^{-1}s^{-1}$ for protons), δ is length of the gradient pulse, Δ is the time between gradient pulses. The experiment and sample preparation were similar to earlier reported methods.[1]

8.3 Results and discussion

8.3.1 Multiblock synthesis and structural variables

As described earlier,[22] BisSF-BPSH(x:y) multiblock copolymers were synthesized, where x refers to the molecular weight of the hydrophobic (BisSF) blocks in kg/mole, and y refers to the hydrophilic (BPSH) blocks in kg/mole. The hydrophilic unit was 100% disulfonated. The structural variables, i.e., IEC and block length (both equal and unequal) were varied to synthesize a wide range of multiblocks varying in chemical composition. For all the unequal block length materials, the hydrophobic unit was kept longer.

For our systematic study, the synthesized multiblocks were categorized into two different series. In the first one, the IEC was kept fixed at a value close to 1.3 meq/g, and the block length was varied from equal (5-5, 10-8 and 15-15) to unequal (15-10, 17-12 and 25-12). In the second series, the block length (17-12 and 25-16) was kept constant, and the IEC was varied from 1.1 to 1.5 meq/g. BPSH 35 random copolymers and Nafion® 112 were used as controls. The block length, molar feed ratio, density and ion exchange capacity of the BisSF-BPSH(x:y) copolymers are summarized in Table (8-1). As reflected in the molar ratios, an excess of the BisSF hydrophobic oligomer was used in the syntheses of all the multiblock copolymers. Thus, both feed ratio and block length are variables that can be tailored to a certain extent to control IEC.

Influence of block lengths at constant IEC

8.3.2 Water uptake and hydration number

The multiblock copolymers were characterized on the basis of water uptake, volume fraction of water, proton conductivity and self-diffusion coefficients of water. Table (8-1) summarizes these properties as a function of block length. For the first series of multiblocks studied, the IEC was similar for all the copolymers. Thus, any property change reflects the effects of block length.

For the equal block length materials, the water uptake increased with increasing block length, which is comparable to our previous observations.[9, 23] The water volume fractions, calculated from water uptake and density of the copolymers, can be approximated with the volume fraction of the associated hydrophilic phase. The increased volume fraction of water (i.e., the hydrophilic phase) indicated a sharper phase separation with increasing block length. The sharpness of the phase separation or the morphology controls the water absorption in the multiblocks. It is possible to alter the sharpness of the phase separation by altering the individual block length ratio. In this case, by increasing the hydrophobic block length over the hydrophilic block length, one can constrain the hydrophilic phase and restrict swelling. The unequal block length

multiblocks showed significant reduction in water uptake. The extent of reduction was empirically related to the ratio of the hydrophobic to hydrophilic block lengths. In other words, the higher the difference between the hydrophobic and hydrophilic block lengths, the greater the reduction in swelling. The BisSF-BPSH (25:12) materials showed the lowest water uptake among all the multiblocks with similar IECs. Hence, it is possible to reduce water uptake by controlling the morphology while keeping the IEC constant.

Table 8-1 Summary of properties for BisSF-BPSH (x:y) copolymers with IEC 1.3 meq/g

Hydrophobic: Hydrophilic Block Length (g/mol)	IEC ^{1}H NMR[22]	Molar charge ratio[22]	Density (g/cc)	Water uptake (%)	Water volume fraction	Proton conductivity (mS/cm)*	Self-Diffusion coefficient of water ($10^{-6}cm^2s^{-1}$)**
Nafion 112	--	-	2.1	25	0.30	90	4.0
5K : 5K	1.3	1:0.59	1.6	31	0.33	90	2.9
10K : 8K	1.3	1:0.74	1.6	52	0.45	120	8.6
15K : 15K	1.4	1:0.63	1.5	78	0.54	140	12.0
15K : 10K	1.3	1:0.82	1.6	47	0.42	130	8.0
17K : 12K	1.3	1:0.77	1.7	38	0.39	130	7.0
25K : 16K	1.3	1:0.85	1.7	40	0.39	120	6.4
25K: 12K	1.3	-	1.7	25	0.26	42	-

* liq. water, 30 ^{o}C, ±5%, ** fully hydrated 25 ^{o}C, ±5%,

8.3.3 Self-diffusion coefficient of water and proton conductivity

Ion-containing copolymers are known to phase separate into hydrophilic and hydrophobic domains. The degree of phase separation governs proton transport, which increases with increasing block length as observed in the case of other ionic block copolymers.[5, 7, 22] Higher water self-diffusion coefficient values indicate a more distinct phase separated morphology and presence of lower morphological barrier.[1] Under partially hydrated conditions, the self-diffusion coefficients of water scales with the diffusion coefficients of proton for Nafion®112.[24, 25] This underlines the importance of water self-diffusion coefficient on proton transport particularly under partially hydrated conditions. For the copolymers studied in this research, the self-diffusion coefficients of water measured at 25 ^{o}C were found to increase with increasing block length—with the BisSF-BPSH (15:15) sample showing the highest value (Table 8-1). A significant three-fold increase in this value was observed when compared to Nafion®112.

Varying the (Δ–δ/3) term in the NMR pulse sequence demonstrated the dependence of D_{eff} on effective diffusion time, which is directly related to the length over which D_{eff} is measured. Figure (8-3) depicts the plots of self-diffusion coefficients of water vs. effective diffusion time for the multiblock copolymers, the BPSH 35 random copolymer, and Nafion®112. Due to the confinement of water molecules within the isolated hydrophilic domains, water transport in polymers normally decreases with increasing time, as has been observed for the BPSH 35 random copolymers. The lower block length materials demonstrated similar behaviors, which represents a morphology close to that of the random copolymers. However, for the higher block length materials, the diffusion is independent on the time scale of the experiment. Particularly for the BisSF-BPSH (15:15) materials, the nature of diffusion was similar to that of normal liquid diffusion. This indicates the presence of a co-continuous channel morphology through which water can be easily transported without encountering any morphological barriers. By synthesizing ion containing multiblock copolymers with improved phase separation, the connectivity within hydrophilic domains can be established.

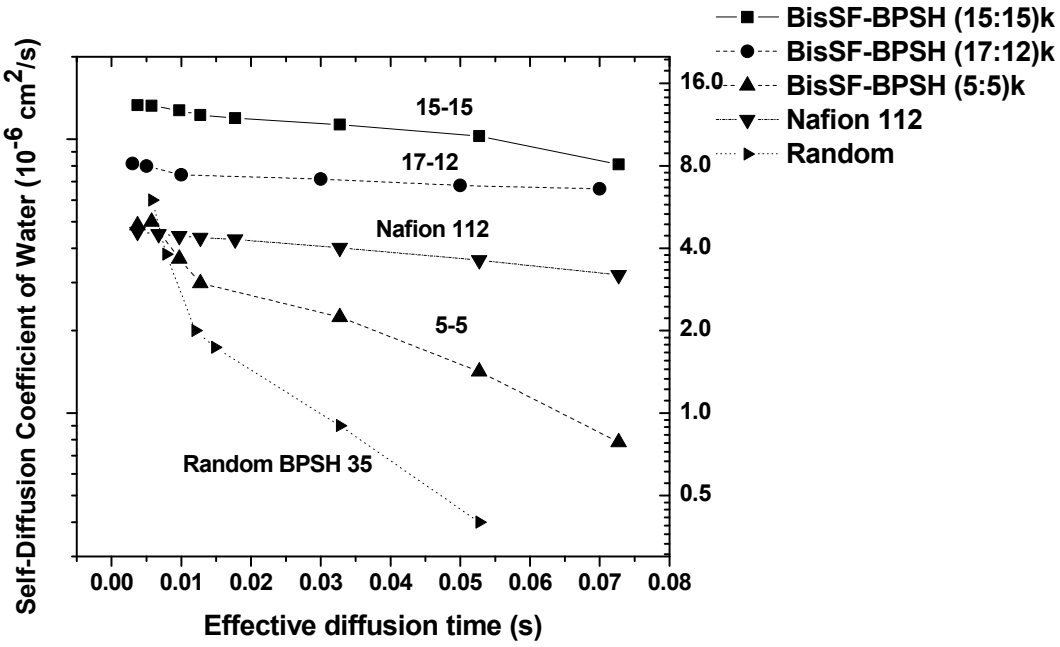

Figure 8-3 Self-diffusion coefficients of water vs. the effective diffusion time

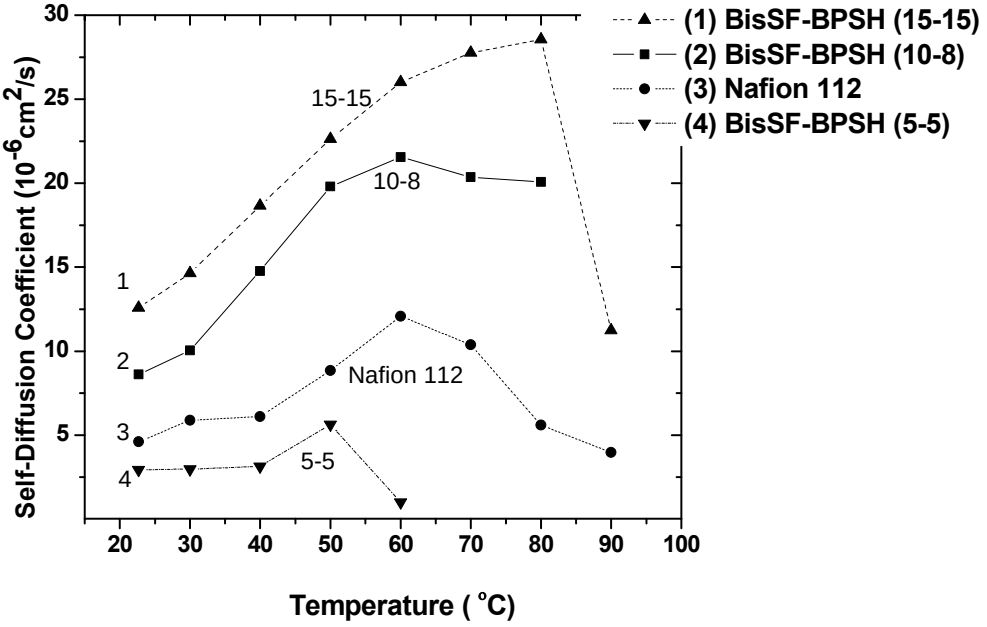

Figure 8-4 Influence of temperature on self-diffusion coefficients of water

The self-diffusion coefficient of water was studied as a function of temperature for the multiblock copolymers (Figure 8-4). As expected, water transport initially increased with increasing temperature. However, the diffusion coefficient dropped significantly after a particular temperature which was unique to each copolymer. This drop is related to the loss of water from the system. The temperature at which water loss occurs depends on the morphology of the proton exchange membrane. For example, the onset of water loss for the BisSF-BPSH (15:15) and BisSF-BPSH (15:10) samples occurred at 80 ºC, while for the BisSF-BPSH (5:5) materials, water loss began at 60 ºC. This can be attributed to the high volume fraction of the hydrophilic phase in the BisSF-BPSH (15:15) copolymers, wherein the sulfonic acid groups along the channels attracted and retained water molecules.

Proton conductivity measured in liquid water at 30 ^{o}C (Table 8-1) showed a comparable trend when compared to water uptake. Although the ionic concentration was kept constant, proton conductivity increased with increasing block length, and scaled with the volume fraction of water. The enhanced nanophase separation in higher block length materials resulted in higher proton conductivity than Nafion®112 and BPSH 35. It was interesting, however, to observe the effects of unequal block length on proton conduction. Specifically, no significant loss in conductivity was detected for the multiblocks as long as the difference between block length was maintained within 10 kg/mole. A further increase may offset the continuity among the hydrophilic domains as seen for the BisSF-BPSH (25:12) sample. Although water uptake was reduced significantly for BisSF-BPSH (25:12), proton conductivity also went down. The effect of temperature on proton conductivity for the BisSF-BPSH (x:y) multiblocks was studied, as shown in Figure (8-5). The BisSF-BPSH (x:y) multiblock copolymers exhibited higher proton conductivity than Nafion®112 in liquid water, with the BisSF-BPSH (15:15) showing the highest proton conductivity at 80 ºC. The activation energy (represented within the boxes) decreased with increasing block length. This in addition to the diffusion coefficient experiments also suggests the formation of a co-continuous hydrophilic channel morphology at higher block length, which decreases the barrier for proton transport.

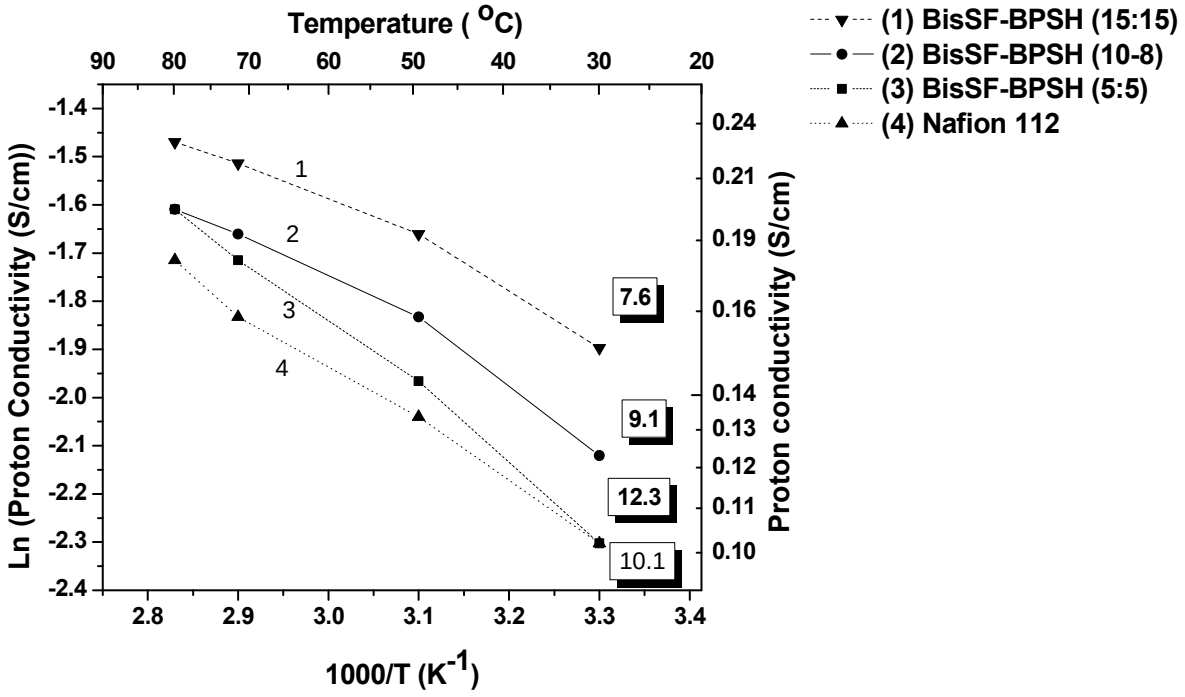

Figure 8-5 Influence of temperature on proton conductivity as a function of block lengths; activation energy in kJ/mole represented within boxes decreases with increasing block length

The proton conductivity of BisSF-BPSH (x:y) multiblock copolymers as a function of relative humidity (RH) is shown in Figure (8-6). This figure depicts the effects of morphology on proton conductivity under partially hydrated conditions. For the random copolymer BPSH-35, proton conductivity drops significantly at lower RH values. Random copolymers show decent performance under fully hydrated conditions since there are sufficient water molecules to provide proton transport. However, due to the scattered hydrophilic domains in the membranes, they lack the connectivity among sulfonic acid groups for proton transport under partially hydrated conditions. In contrast, the performance of the multiblocks under partially hydrated conditions increases with increasing block lengths, particularly for the equal block length materials. The increased connectivity at higher block lengths as supported by the diffusion coefficient experiments, improves the proton conduction under partially hydrated conditions. The

BisSF-BPSH (15:15) multiblock copolymers exhibited higher proton conductivity than Nafion®112 at all RH values. Although proton conductivity improved significantly under partially hydrated conditions for the BisSF-BPSH (15:15) sample, the water uptake of the membrane was much higher. In contrast, the unequal block length materials had much lower water uptake and similar proton conductivity under fully hydrated conditions. However, under partially hydrated conditions, the performance of the BisSF-BPSH (17:12) material was reduced compared to the BisSF-BPSH (15:15) copolymer. As confirmed, the connectivity between hydrophilic domains is an important factor controlling proton transport under partially hydrated conditions. The increased hydrophobic block lengths may have constrained the hydrophilic domains resulting in a reduction in the connectivity and the performance under low RH.

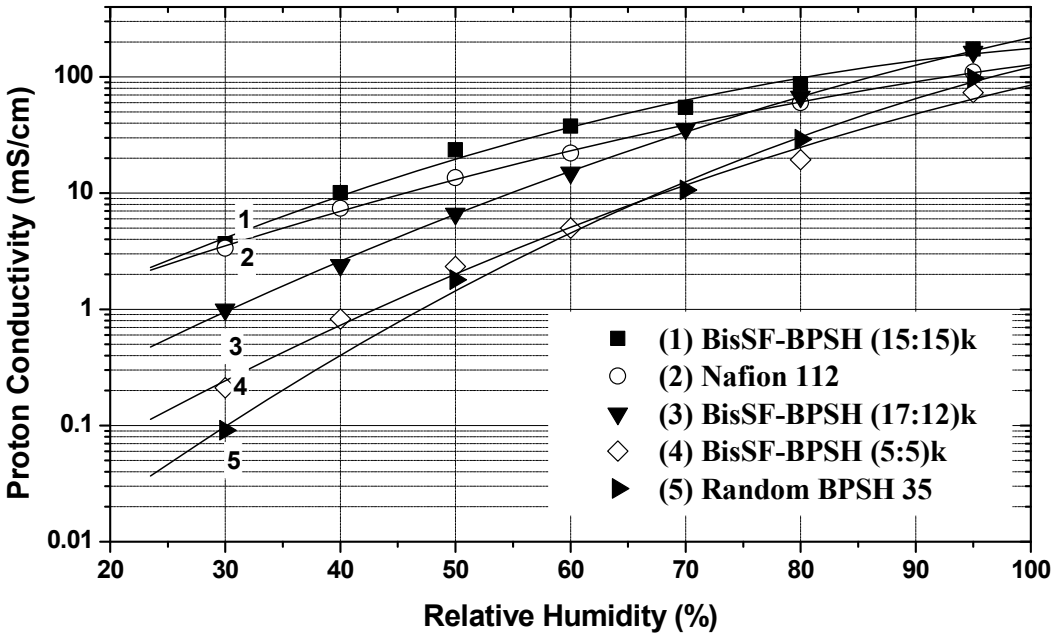

Figure 8-6 Influence of block length on proton conduction under partially hydrated conditions at 80 °C for the BisSF-BPSH multiblocks at similar IECs

Influence of IEC

The connectivity between hydrophilic domains is related to the extent of phase separation between the hydrophilic and hydrophilic domains. Phase separation for ionic

multiblock copolymers is a function of both block length and the ionic content. Unequal block length materials, BisSF-BPSH (17:12) and BisSF-BPSH (25:16), were synthesized with varying IEC values ranging from 1.1 to 1.5 meq/g. The effect of IEC on the multiblock properties can be well understood from these two series of multiblock copolymers with constant block lengths. It is hypothesized that increasing the hydrophilic content may improve the connectivity between the domains, improving the performance under low RH while the higher hydrophobic block length will keep the water uptake controlled. The water uptake, water volume fraction, proton conductivity under fully hydrated conditions, and self-diffusion coefficients of water for BisSF-BPSH (x:y) multiblock copolymers with varying IECs are shown in Table (8-2). As the IEC was increased from 1.1 to 1.3, an increase in water uptake was observed both for the BisSF-BPSH (17:12) and BisSF-BPSH (25:16) materials. However after going from 1.3 to 1.5 IEC, no further significant increase was observed.

Table 8-2 Summary of the properties for BisSF-BPSH (x:y) multiblocks with varying IECs

Hydrophobic : Hydrophilic Block Length (g/mol)	IEC by ^{1}H NMR	Molar charge ratio	Density (g/cc)	Water uptake (%)	Water volume fraction	Proton conductivity (mS/cm)*	Self-Diffusion coefficient of water ($10^{-6}cm^2s^{-1}$)**
17K-12K	1.5	1:1.02	1.6	42	0.38	120	7.0
17K-12K	1.3	1:0.77	1.7	38	0.40	130	7.0
17K-12K	1.1	1:0.64	1.7	25	0.30	70	2.0
25K-16K	1.5	1:1.04	1.6	48	0.43	130	7.0
25K-16K	1.3	1:0.85	1.6	40	0.39	120	6.4
25K-16K	1.1	1:0.65	1.6	24	0.28	40	2.0

* liq. water, 30 ^{o}C, ±5%, ** fully hydrated 25 ^{o}C, ±5%,

The influence of unequal block length on water absorption was further investigated using water swelling measurements across the two planes of the membranes (Fig. 8-7). The x and y represent the in-plane swelling and z represents the through-plane swelling. NRE211 is the commercially available Nafion®112 membrane, which was used as the control. Significant anisotropic swelling was observed for the multiblocks, and through-plane swelling increased with increasing IECs. However, the in-plane swelling was shown to be only modestly impacted by ion exchange capacity, which was significantly lower than both NRE211 and BPSH35. The higher block length hydrophobic blocks constrained the hydrophilic domains along the in-plane direction, reducing water swelling.

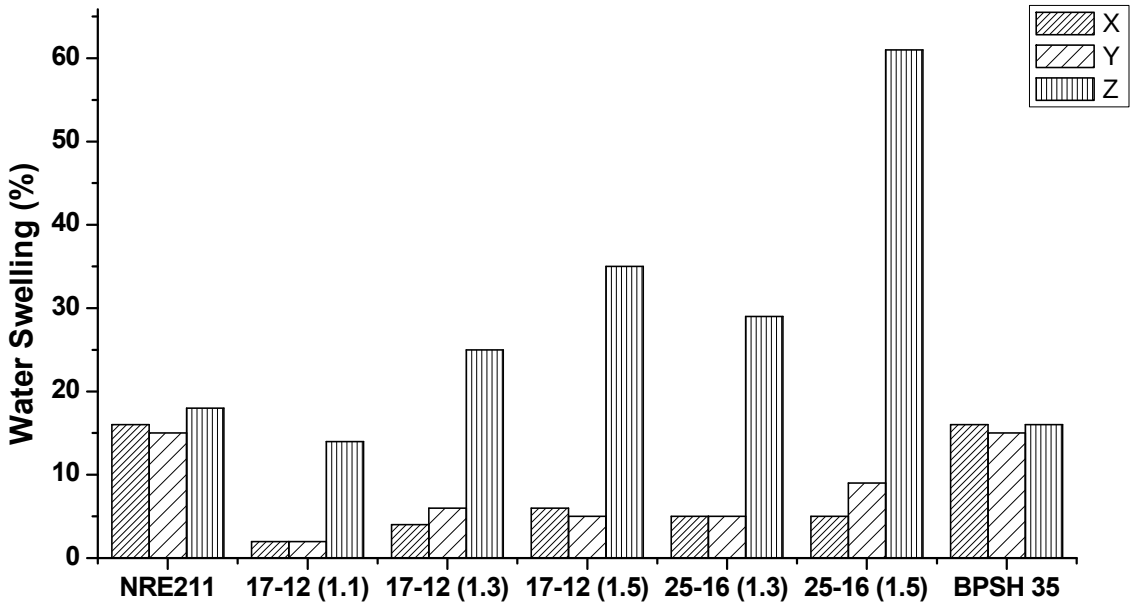

Figure 8-7 Multiblock copolymers display reduced in-plane swelling; the numbers in the parenthesis represent IEC in meq/g

More recently, in-plane swelling has been identified as a factor impacting the mechanical durability of a membrane during low relative humidity cycling operations. In general, very low in-plane swelling is desirable for extended membrane lifetime. Multiblock copolymers show significant promise in that regard.

Both proton conductivity and self-diffusion coefficient of water showed similar dependency on IEC. The increase in the property was more significant from IEC 1.1 to 1.3 (meq/g) than from IEC 1.3 to 1.5 (meq/g). As under fully hydrated conditions proton conduction is mainly a function of the water content, it scaled with the water content in the copolymers.

The influence of IEC on proton transport under partially hydrated conditions was investigated. As shown in Figures (8-8) and (8-9), proton conductivity under partially hydrated conditions improved significantly with increasing IEC for both the BisSF-BPSH (17:12) and BisSF-BPSH (25:16) multiblocks. The increased hydrophilic segments associated with the increase in ion exchange capacity serve to reestablish the connectivity between the hydrophilic domains for the unequal block length copolymers. This reduces the morphological barrier and allowed improved proton conduction at low water contents. The performance characteristics of BisSF-BPSH (17:12) with an IEC of 1.5 meq/g were comparable to those of the equal block length BisSF-BPSH (15:15) material—but with a significantly lower water uptake (45 %) compared to BisSF-BPSH (15:15) (70%). By creating the correct balance between ionic content and block length, one can tailor the morphology of PEMs for improved performance at low RH with reduced water uptake.

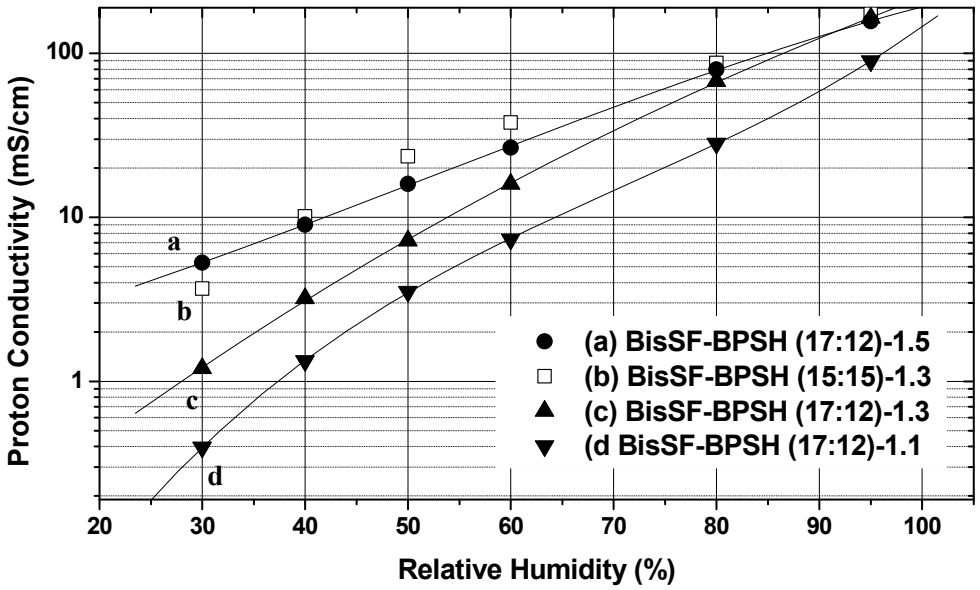

Figure 8-8 Proton conductivity as a function of relative humidity for the BisSF-BPSH (17:12) with varying IECs; the number after the parenthesis represents IEC in meq/g

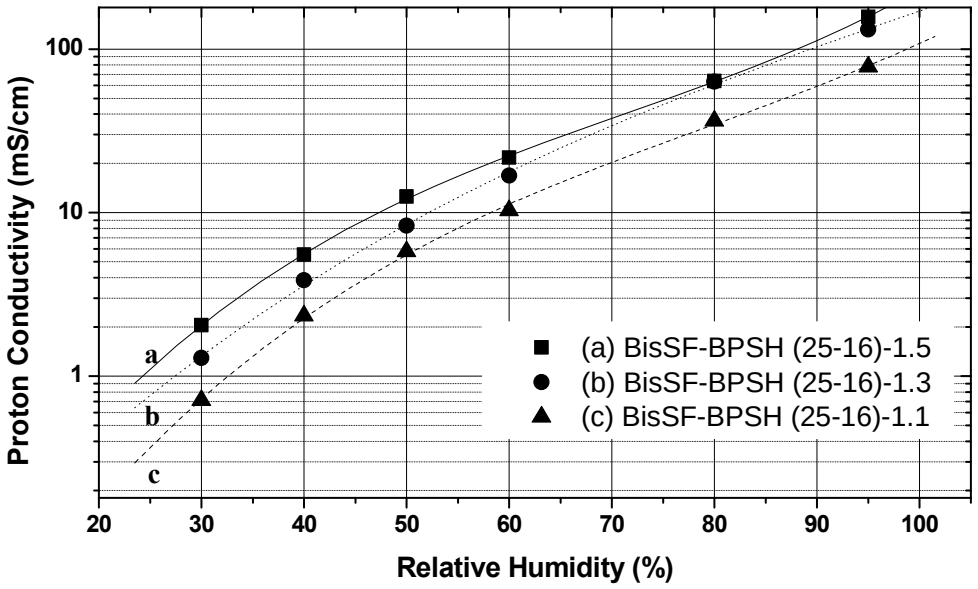

Figure 8-9 Proton conductivity as a function of relative humidity for the BisSF-BPSH (25:16) with varying IECs; the number after the parenthesis represents IEC in meq/g

8.3.4 Selectivity

.

As discussed earlier, one of the major challenges in designing a proton exchange membrane is to achieve both high proton conductivity and low water uptake. Normally there is a trade off between the two properties and can be explained mathematically in terms of selectivity (Ψ), as shown in the following Equation (8-5).

$$\Psi = \sigma / \lambda \qquad \textbf{Equation 8-5}$$

Here, σ is proton conductivity measured in liquid water at 30 ^{o}C, and λ is the hydration number. High selectivity at low hydration number is desired. A plot of selectivity vs. hydration (Figure 8-10) illustrates the various structure-property relationships for the BisSF-BPSH (x:y) copolymers, BPSH-35 and Nafion®112. In spite of having the same hydration number, the BPSH 35 random copolymers showed less selectivity than Nafion®112 due to lower proton conductivity. At a similar hydration number, the multiblock BisSF-BPSH (17:12) sample with an IEC of 1.5 meq/g demonstrated the highest selectivity—even higher than the state-of-the-art material, Nafion®112. The high hydrophilic block length provides higher proton conductivity, while the increased hydrophobic/hydrophilic block length ratio (17:12) may have contributed to its low water uptake. Changing the hydrophobic/hydrophilic block length balance from equal to unequal increased the selectivity of the multiblock copolymers.

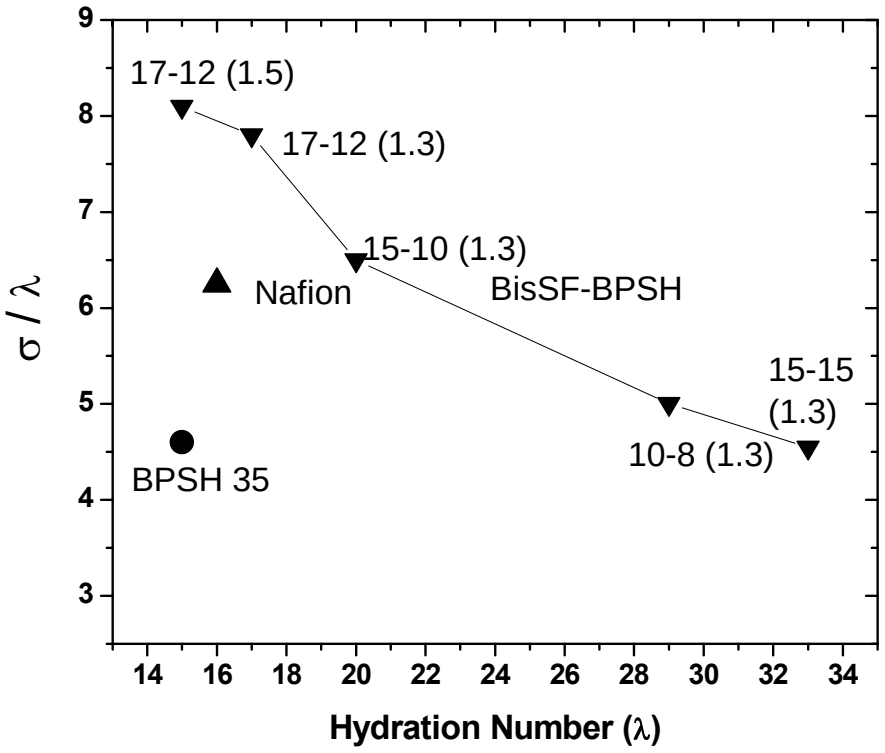

Figure 8-10 Selectivity of PEMs as a function of hydration number

8.4 Conclusions

The structure property relationships for the BisSF-BPSH (x:y) multiblock was achieved. To summarize, the sequence length of the copolymers appears to dominate proton conductivity both in liquid water and under partially hydrated conditions. Water uptake generally increased with increasing block length, but at similar IECs, the ratio of hydrophobic to hydrophilic block length, besides the absolute values, can also play a role. Keeping the hydrophobic block length longer than the hydrophilic block, significant reduction in water uptake and in-plane swelling was achieved. Importantly, no noticeable changes in proton conductivity under fully hydrated conditions were observed. Various optimized combinations of IEC, hydrophilic and hydrophobic sequence lengths, all of which can be readily controlled by synthesis, have yielded materials that are more selective than Nafion®112.

Under partially hydrated conditions, multiblock copolymers with higher block lengths showed better performance with regard to proton conductivity as a function of relative humidity, presumably due to their more distinct nanophase separation and better connectivity among the ionic domains. The self-diffusion coefficient of water followed the same trend as the conductivity and is a measure of proton transport under partially hydrated conditions.

One of the major challenges was to develop a system with both low water uptake and improved proton conductivity at low RH. In ion containing multiblock copolymers, however, there is often a trade off between these two factors. Nonetheless, by tailoring block length and IEC values, these two important properties were achieved. A longer hydrophobic block length than the hydrophilic one reduced the water uptake. At the same time, by only modestly increasing the ion exchange capacity, connectivity was improved between the hydrophilic domains, which enhanced proton conductivity at low RH.

The authors wish to acknowledge Nissan Motor Company and Department of Energy (DOE Contract # DE-FG36-06G016038)) for support of this research.

8.5 References

1. Roy, A.; Hickner, M. A.; Yu, X.; Li, Y.; Glass, T. E.; McGrath, J. E., Influence of chemical composition and sequence length on the transport properties of proton exchange membranes. *Journal of Polymer Science, Part B: Polymer Physics* **2006,** 44, (16), 2226-2239.

2. Ghassemi, H.; McGrath, J. E.; Zawodzinski, J. T. A., Multiblock sulfonated-fluorinated poly(arylene ether)s for a proton exchange membrane fuel cell. *Polymer* **2006,** 47, (11), 4132-4139.

3. Ghassemi, H.; Ndip, G.; McGrath, J. E., New multiblock copolymers of sulfonated poly(4 '-phenyl-2,5-benzophenone) and poly(arylene ether sulfone) for proton exchange membranes. II. *Polymer* **2004,** 45, (17), 5855-5862.

4. Ghassemi, H.; McGrath, J. E., Synthesis and properties of new sulfonated poly(p-phenylene) derivatives for proton exchange membranes. I. *Polymer* **2004,** 45, (17), 5847-5854.

5. Li, Y.; Roy, A.; Badami, A. S.; Hill, M.; Yang, J.; Dunn, S.; McGrath, J. E., Synthesis and characterization of partially fluorinated hydrophobic-hydrophilic multiblock copolymers containing sulfonate groups for proton exchange membrane. *Journal of Power Sources* **2007,** 172, (1), 30-38.

6. Lee, H.-S.; Roy, A.; Badami, A. S.; McGrath, J. E., Synthesis and characterization of sulfonated poly(arylene ether) polyimide multiblock copolymers for proton exchange membranes. *Macromolecular Research* **2007,** 15, (2), 160-166.

7. Lee, H.-S.; Badami, A. S.; Roy, A.; McGrath, J. E., Segmented sulfonated poly(arylene ether sulfone)-b-polyimide copolymers for proton exchange membrane fuel cells. I. Copolymer synthesis and fundamental properties. *Journal of Polymer Science, Part A: Polymer Chemistry* **2007,** 45, (21), 4879-4890.

8. Wang, H.; Badami, A. S.; Roy, A.; McGrath, J. E., Multiblock copolymers of poly(2,5-benzophenone) and disulfonated poly(arylene ether sulfone) for proton-exchange membranes. I. Synthesis and characterization. *Journal of Polymer Science, Part A: Polymer Chemistry* **2006,** 45, (2), 284-294.

9. Roy, A.; Lee, H.-S.; McGrath, J. E., Structure-Property Relationships of BPSH-PI Multiblock Copolymers for Application in Proton Exchange Membrane Fuel Cells. *To be Submitted* **2008**.

10. Yu, X.; Roy, A.; McGrath, J. E., *Div. Fuel Chem.* **2005,** 50(2), 577.

11. Roy, A.; Hickner, M. A.; Yu, X.; Li, Y. X.; Glass, T. E.; McGrath, J. E., Influence of chemical composition and sequence length on the transport properties of proton exchange membranes. *Journal of Polymer Science Part B-Polymer Physics* **2006,** 44, (16), 2226-2239.

12. Roy, A.; Hickner, M. A.; Yu, X.; Li, Y.; Glass, T.; McGrath, J. E., *J. Polym. Sci. Part B: Polym. Phys.* **2006,** 44, 2226.

13. Yu, X.; Roy, A.; McGrath, J. E., Perfluorinated-sulfonated hydrophobic-hydrophilic multiblock copolymers for proton exchange membranes (PEMs). *PMSE Preprints* **2006,** 95, 141-142.

14. Alberti, G.; Casciola, M., Composite membranes for medium-temperature PEM fuel cells. *Annual Review of Materials Research* **2003,** 33, 129-154.

15. Casciola, M.; Alberti, G.; Ciarletta, A.; Cruccolini, A.; Piaggio, P.; Pica, M., Nanocomposite membranes made of zirconium phosphate sulfophenylenphosphonate dispersed in polyvinylidene fluoride: Preparation and proton conductivity. *Solid State Ionics* **2005,** 176, (39-40), 2985-2989.

16. Paul, M.; Park, H. B.; Freeman, B. D.; Roy, A.; McGrath, J. E.; Riffle, J. S., Synthesis and crosslinking of partially disulfonated poly(arylene ether sulfone) random copolymers as candidates for chlorine resistant reverse osmosis membranes. available online, doi:10.1016/j.polymer.2008.02.039, **2008**.

17. Sankir, M.; Bhanu, V. A.; Harrison, W. L.; Ghassemi, H.; Wiles, K. B.; Glass, T. E.; Brink, A. E.; Brink, M. H.; McGrath, J. E., *J. Appl. Polym. Sci.* **2006,** 100, 4595.

18. Zawodzinski, T. A.; Neeman, M.; Sillerud, L. O.; Gottesfeld, S., Determination of Water Diffusion-Coefficients in Perfluorosulfonate Ionomeric Membranes. *Journal of Physical Chemistry* **1991,** 95, (15), 6040-6044.

19. Springer, T. E.; Zawodzinski, T. A.; Wilson, M. S.; Gottesfeld, S., Characterization of polymer electrolyte fuel cells using AC impedance spectroscopy. *Journal of the Electrochemical Society* **1996,** 143, (2), 587-599.

20. Schuster, M.; Kreuer, K.-D.; Andersen, H. T.; Maier, J., Sulfonated poly(phenylene sulfone) polymers as hydrolytically and thermooxidatively stable proton conducting ionomers. *Macromolecules* **2007,** 40, (3), 598-607.

21. Stejskal, E. O.; Tanner, J. E., *J.chem.Phys* **1965**, (42), 288.

22. Yu, X.; Roy, A.; Dunn, S.; Yang, J.; McGrath, J. E., Synthesis and characterization of sulfonated-fluorinated, hydrophilic-hydrophobic multiblock copolymers for proton exchange membranes. *Macromolecular Symposia* **2006,** 245/246, (World Polymer Congress--MACRO 2006), 439-449.

23. Roy, A.; Lee, H.-S.; McGrath, J. E., Hydrocarbon based BPSH-BPS Multiblock Copolymers as Novel Proton Exchange Membranes Part-B. *To be Submitted* **2008**.

24. Kreuer, K. D., On the complexity of proton conduction phenomena. Solid State Ionics 2000, 136, 149-160., *Solid State Ionics* **2000,** 136, 149.

25. Zawodzinski, T. A.; Neeman, M.; Sillerud, L. O.; Gottesfeld, S., *J. Phys. Chem.* **1991,** 95, 6040.

9.0 Investigation of Proton Transport Phenomenon in Phosphoric Acid Doped Poly(arylene ether sulfone)-*b*-polybenzimidazole Copolymers

Abhishek Roy, Hae-Seung Lee, and James E. McGrath

Macromolecules and Interfaces Institute,
Virginia Polytechnic Institute and State University, Blacksburg, Virginia 24061

Abstract

A series of phosphoric acid doped multiblock copolymers based on poly(arylene ether sulfone) and polybenzimidazole (PBI) with different block lengths were studied and evaluated as a high temperature proton exchange membrane (PEM). The proton conductivity performance was evaluated over a wide temperature range of 100-200 ^{o}C. The proton conductivity of the doped samples showed significant dependency on temperature, doping level, water content and more importantly the microstructure of the copolymers. Activation energy decreased with increasing doping levels. Proton conductivity was found to increase with increasing block lengths at a given doping level. The effect was more prominent at a low doping level of 6-7. The proton conductivity evaluated under partially hydrated condition at 80 ^{o}C showed significantly higher value than the commercial available Nafion® copolymer. The developed phosphoric acid doped multiblock copolymer system is a strong candidate for high temperature and low relative humidity PEM applications.

9.1 Introduction

The current operating temperature for proton exchange membrane fuel cells is between 80-120 ^{o}C. However there has been a growing demand to raise the operating temperature. A higher temperature operation is expected to have several advantages over the current technology. Among the notable ones are the a) improved oxygen reduction kinetics, b) improved electrode performance, c) reduced fuel impurities like CO and d) improved heat and water management.[1, 2] However the major challenge lies in achieving high proton conductivity from the polymeric membranes at elevated temperature. The commercially available Nafion® shows reduced performance at elevated temperature as it passes through its α relaxation temperature.[3] Aromatic copolymers with higher α relaxation temperature have shown better promise than the perflurosulfonic acid Nafion® copolymer.[4] However, all these sulfonic acid containing copolymers require presence of water for proton transport. Unless adequate external humidification is applied, the performance drops significantly at high temperatures. The biggest challenge is to maintain a high proton transport both at high temperature and at low relative humidity.

Several approaches have been taken to develop new systems with the improved high temperature properties. Our group is involved with the synthesis and characterization of thermally stable sulfonic acid containing multiblocks. The enhanced phase separated morphology has resulted in much improved performance, particularly under partially hydrated conditions over the existing PEMs.[5] Although the morphology is ideal for enhanced proton transport, the thermal stability of the sulfonic acid group limits high temperature application.

The inorganic acid doped polymeric membranes have also been studied for long time.[6-8] In these systems, inorganic acids act as proton conducting materials while polymers, which typically possess basic moieties, immobilize the acid. Among various inorganic acids, phosphoric acid (H_3PO_4) has been widely studied due to its excellent thermal stability, low vapor pressure, and high proton conductivity even at anhydrous conditions.[9-13] For the matrix polymer, the polybenzimidazole (PBI) family, especially

poly 2,2'-*m*-(phenylene)-5,5'-bibenzimidazole has been intensively studied due to the ease of synthesis and commercial availability. Phosphoric acid doped PBI membranes can be easily fabricated by immersing solvent cast PBI membranes in phosphoric acid solution. The doping level which can be defined as the number of moles of phosphoric acid per one repeat unit of PBI is controlled by using different concentrations of the doping solution.[14]

In contrast to sulfonic acid based PEMs, the proton transport in phosphoric acid doped systems under anhydrous conditions is believed to follow a proton hopping or Grotthus mechanism.[15] The mechanism is reported to depend strongly on acid doping level, water content and temperature. At low doping levels, the proton transport is reported to take place between the N-H sites of the polymer and phosphate anion.[16, 17] The doping level is defined as the number of phosphoric acid per PBI unit. At higher doping levels, the presence of "free" acid facilitates the enhanced transport from the more rapid diffusion of additional phosphate anions. In the presence of water, H_3O^+ is also involved as an additional proton carrier. [16, 17] At high temperatures in the condensed phosphoric acid state, proton transport involving proton bodily diffusion via the vehicle mechanism is also proposed.[16] Generally, the proton conductivity of phosphoric acid doped PBI increases along with the increased doping level and temperature. However, doping levels higher than 5 are not desirable due to high swelling and deterioration of mechanical properties.[18]

The morphology of the studied phosphoric acid based PBI was mostly similar to random copolymer morphology. Little has been known on the effect of the morphology on the proton transport for this system. It can be hypothesized that significant improvement in proton conductivity can be achieved from phosphoric acid doped PBI having phase separated multiblock morphology. The enhanced phase separated, well connected PBI network will improve the proton conduction and phosphoric acids will allow proton conduction in absence of water at high temperature.

In the present work, a series of multiblock copolymers was synthesized by a coupling reaction between diamine terminated PBI oligomers and benzoic acid terminated poly(arylene ether sulfone) oligomers.[19] The PBI segments in the system will facilitate proton conduction with doped H_3PO_4 while poly(arylene ether sulfone)(BPS) segments maintain the dimensional and mechanical stability. The acronym of the multiblock is BPS-PBI(x-y) where x is the molecular weight of the polysulfone block (BPS) and y is the molecular weight of the PBI block. This paper investigates the proton transport mechanism and the influence of morphology, temperature, phosphoric acid and water content on the proton conductivity for the phosphoric acid doped BPS-PBI multiblocks.

9.2 Experimental

9.2.1 Materials

N,N-Dimethylacetamide (DMAc), N-methyl-2-pyrrolidinone (NMP) and toluene were purchased from Aldrich and distilled from calcium hydride before use. Monomer grade 4,4'-dichlorodiphenyl sulfone (DCDPS) and 4,4'-biphenol (BP) were provided by Solvay Advanced Polymers and Eastman Chemical Company, respectively, and vacuum dried at 110 °C prior to use. Potassium carbonate, 3-hydroxybenzoic acid (3-HBA), isophthalic acid (99%), 3,3'-diaminobenzidine (99%) (DAB), phosphoric acid (85%) and polyphosphoric acid (115%) were purchased from Aldrich and used without further purification.

9.2.2 Multiblock Copolymer Synthesis

The multiblock copolymers were synthesized via a coupling reaction between benzoic acid terminated poly(arylene ether sulfone) (BPS) and diamine terminated polybenzimidazole (PBI) by forming benzimidazole moieties (Fig.9-1). The molecular weights of the BPS and PBI oligomers for the copolymer synthesis were 5, 10 and 15 kg/mol. The control of molecular weight and end-group functionality of both of the oligomers was achieved by using stoichiometrically adjusted amounts of the monomers for the synthesis. By the described synthetic route, three multiblock copolymers with equal block lengths of BPS and PBI oligomers were synthesized in NMP (e.g., 5k-5k, 10k-10k, 15k-15k).

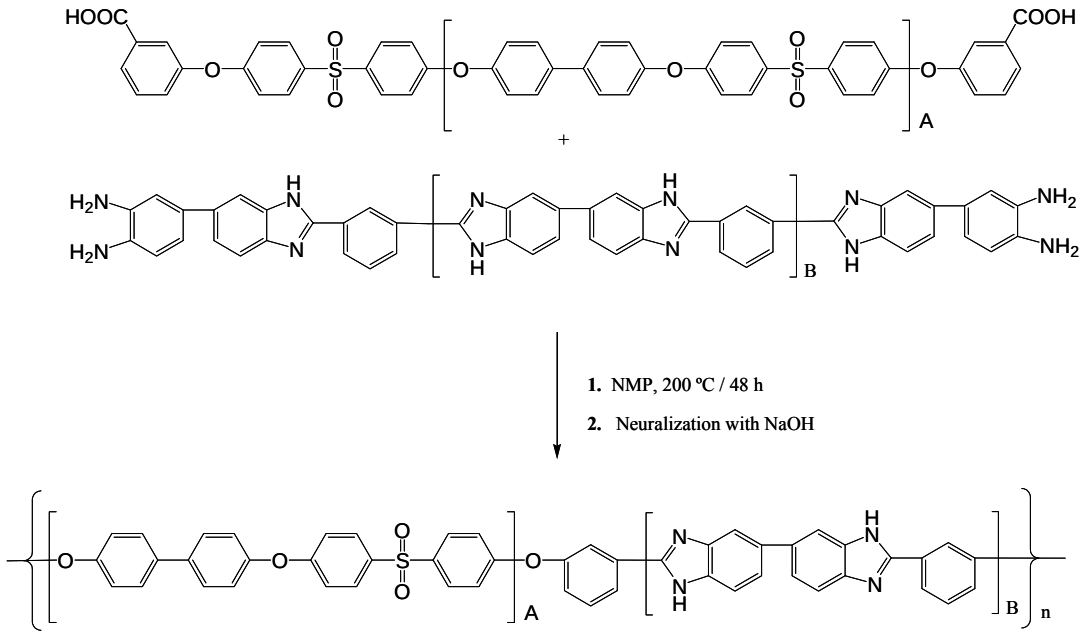

Figure 9-1 Synthesis scheme of Poly(arylene ether sulfone)-*b*-polybenzimidazole copolymers

9.2.3 Film casting and H_3PO_4 doping

Multiblock copolymer membranes were prepared by solution casting from DMAc. The copolymers were dissolved in DMAc (10% w/v), filtered through 0.45 μm Teflon® syringe filters, and cast onto clean glass substrates. The solvent was evaporated under an infrared lamp for 48 h at 50-70 °C, resulting in transparent, tough and flexible films. The films were further dried *in vacuo* at 110 °C for 24 h to remove residual solvent. The H_3PO_4 doped membranes were prepared by immersing the cast membranes in various concentrations (3-14.6 M) of aqueous H_3PO_4 solution for 72 h at room temperature.

9.2.4 Determination of proton conductivity

All conductivity measurements were made using a Solartron (1252A +1287) impedance/gain-phase analyzer over the frequency range of 10 Hz - 1 MHz. The conductivity of the membrane was determined from the geometry of the cell and resistance of the film which was taken at the frequency that produced the minimum imaginary response. For the temperature sweep experiments, the conductivity cells with the membranes were equilibrated at 100 °C for 4-5 h before the start of the experiment. This was done to remove the excess water from the membranes. In situ measurements were taken as a function of increasing temperature with the cells equilibrated in a convection oven. Equilibration time at each temperature was kept fixed for 3 h. For determining proton conductivity under partially hydrated conditions, membranes were equilibrated in a humidity-temperature oven (ESPEC, SH-240) at the specified RH and 80 ^{o}C for 5 h before each measurement.

9.3 Results and Discussion

9.3.1 Proton conductivity

Influence of temperature and doping levels of phosphoric acid on proton conductivity

The proton conductivities of the BPS-PBI copolymers were determined as a function of temperature without any external humidification supply. The temperature range was 100 to 200 °C. Figure (9-2) represents the temperature vs. conductivity plots for BPS-PBI(15-15) doped with different concentrations of phosphoric acid (e.g., 3, 9, 12, and 14.6 M). A similar study was conducted for the BPS-PBI(5-5) and BPS-PBI(10-10) samples as shown in Figures (9-3) and (9-4). The numbers within the brackets in the legends refer to the doping levels of phosphoric acid in the samples.

In all cases, the proton conductivities increased with increasing temperature and doping levels. However, the proton conductivities of the copolymers doped at higher concentrations (e.g., 12 and 14.6 M) increased more rapidly with temperature than the samples doped with lower concentrations (e.g., 3 and 9 M). For the membranes doped with lower acid concentrations (3 and 9 M), the doping levels ranged from 4 to 5. As the theoretical number of "bound" phosphoric acid units is 4, proton conduction at this doping level can occur only through proton hopping between the N-H site and the phosphate anion. However when the membranes were doped with higher acid concentrations (12 and 14.6 M), the doping levels were in between 6-12. The presence of "free" phosphoric acid or the quickly diffusing $H_2PO_4^-$ anions increased the proton conductivity significantly.

As discussed, proton conductivity measured as a function of temperature showed an increasing trend for all samples. A change in slope, specifically for the higher doped samples, was observed above 150 °C, which may be attributed to a change in the conduction mechanism.

It is known that "fused" phosphoric acid can be formed from the "free" phosphoric acid at high temperatures and so the slope change may indicate a transition from a hopping mechanism to a vehicle mechanism involving bodily diffusion of protons as proposed by Hayamizu et al.[16] The activation energy for proton transport was determined for all samples over the temperature range from 100 °C to 150 °C. The activation energy calculated showed a strong dependence on doping level as shown in Figure (9-5). A significant drop in activation energy from 60 to 20 kJ/mole was observed for the BPS-PBI(15-15) sample as the doping level was increased from 2 to 6. A similar trend was also observed in the BPS-PBI(5-5) and BPS-PBI(10-10) samples. This sharp decrease can be attributed to the involvement of the free phosphoric acid or the phosphate anion in the transport process. A further increase in phosphoric acid content resulted in a nominal decrease in the activation energy value. Among the copolymers, the highest conductivity at 200 °C was 47 mS/cm from BPS-PBI(15-15) with a doping level of 11.5. It is to be noted that the doping level of 11.5 of the BPS-PBI(15-15) did not cause any dramatic swelling or softening behavior. This implies that the BPS-PBI samples can utilize higher doping levels (e.g., >5) to attain higher proton conductivity. These levels were previously impractical for the conventional phosphoric acid doped PBI systems due to significant deterioration of their mechanical properties.[17]

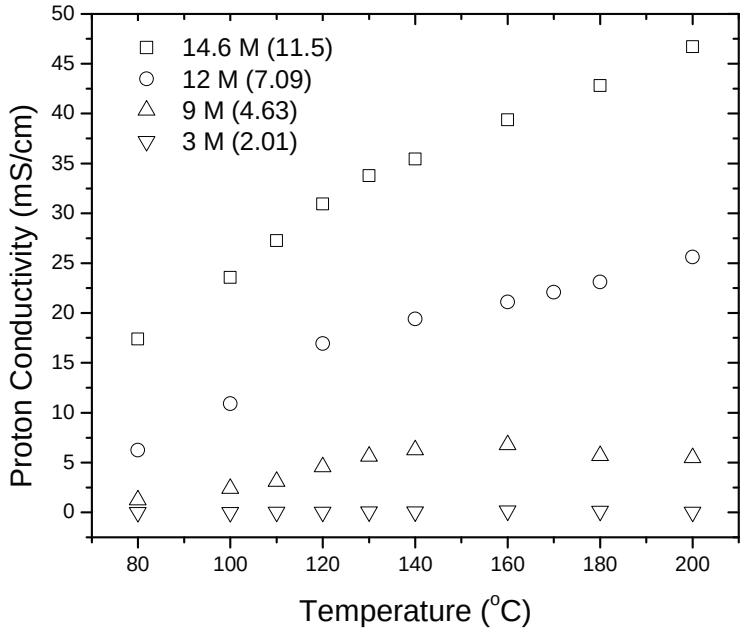

Figure 9-2 Influence of temperature on proton conductivity for BPS-PBI(15-15) samples at varying phosphoric acid doping levels

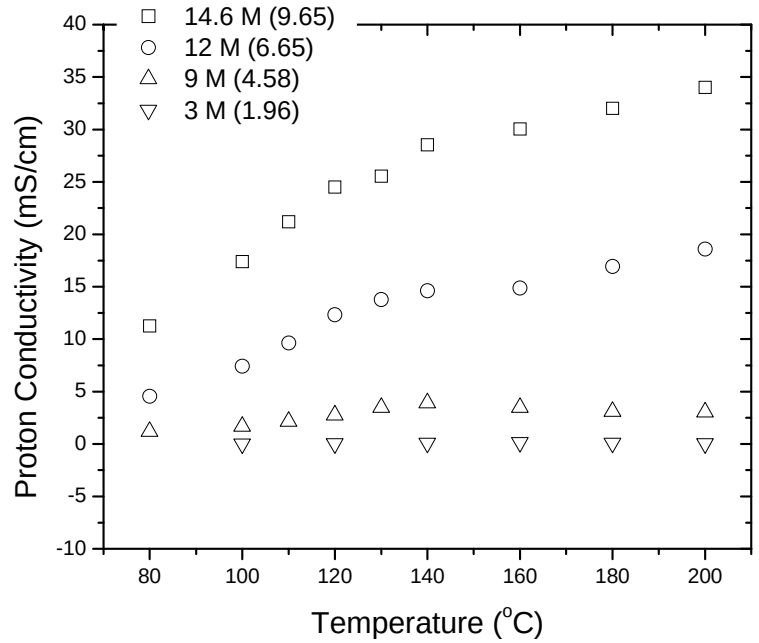

Figure 9-3 Influence of temperature on proton conductivity for BPS-PBI(10-10) samples at varying phosphoric acid doping levels

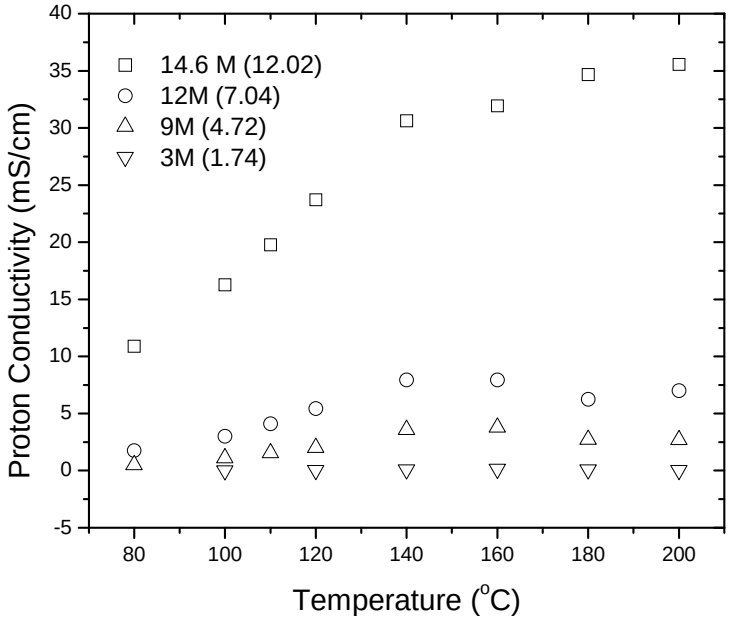

Figure 9-4 Influence of temperature on proton conductivity for BPS-PBI(5-5) samples at varying phosphoric acid doping levels

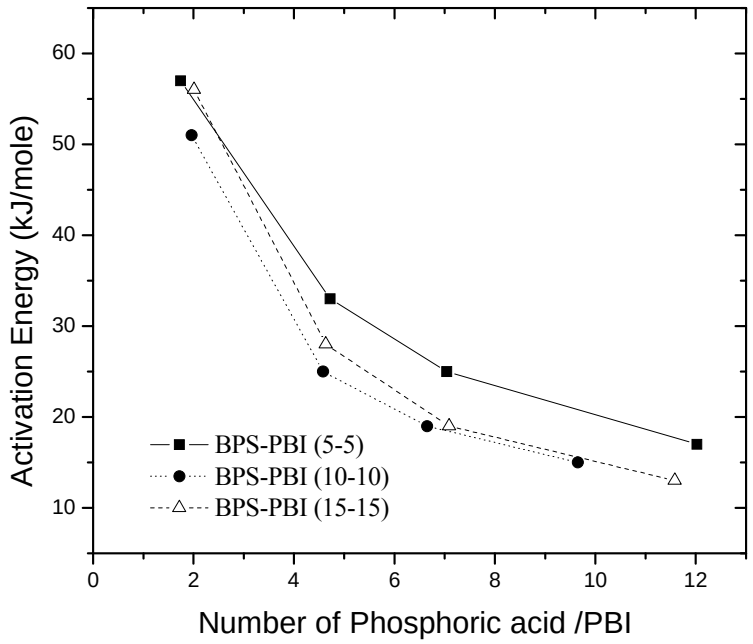

Figure 9-5 Influence of phosphoric acid content on activation energy for proton conduction

Influence of the microstructure of the multiblocks on the proton transport

Over the last few years, our group has been investigating the influence of morphology on proton transport of sulfonic acid containing multiblock copolymers as a function of relative humidity (RH).[20-23] The proton conductivity under partially hydrated conditions was found to increase with increasing block length or with the extent of phase separation. In the current investigation with the BPS-PBI system, proton conductivity was studied as a function of doping level at 140 °C. The three copolymers with varying block lengths were compared as shown in Figure (9-6). Among the copolymers, the conductivities of BPS-PBI(15-15) and BPS-PBI(10-10) showed a similar trend with doping level in contrast to the BPS-PBI(5-5) sample. This suggests a morphological change from the BPS-PBI(5-5) sample to the BPS-PBI(10-10) sample. At a given doping level, the proton conductivity was found to increase with increasing block length. The effect was more pronounced at lower doping levels (6-7). This can be attributed to the formation of phase separated morphology with increasing block lengths as indicated by the DMA study.[19] The phase separated morphology resulted in improved connectivity within the PBI units. This is consistent with our earlier findings with the sulfonic acid containing multiblock copolymers. The increased connectivity with increasing block length is expected to lower the morphological barrier for proton transport. Thus by synthesizing phase separated multiblock copolymers, improved proton conductivity can be achieved even with lower phosphoric acid doping levels.

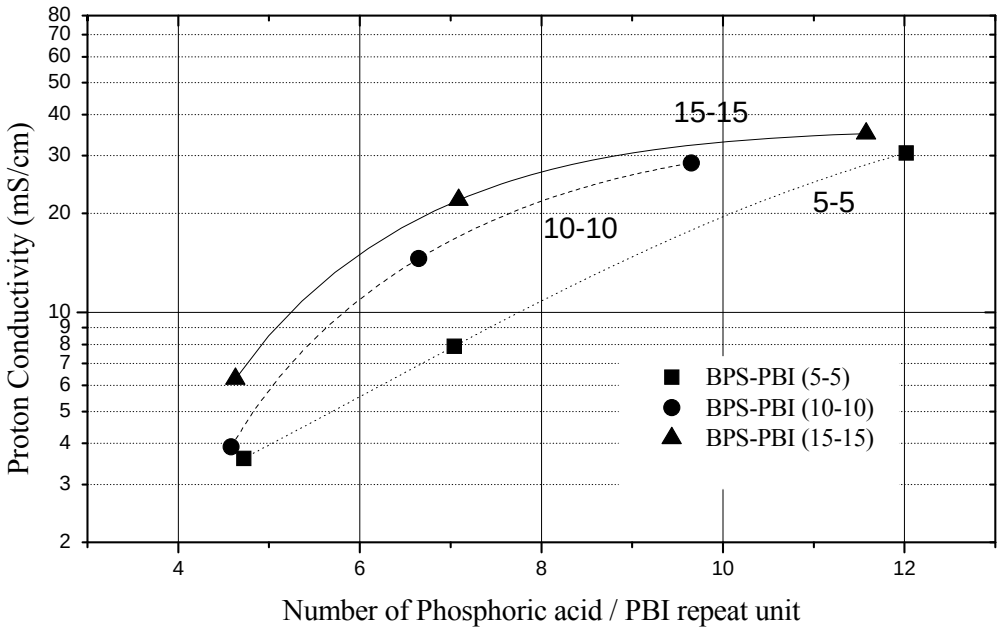

Figure 9-6 Influence of block length on proton conduction at varying phosphoric acid doping levels at 140 °C

Influence of water content on the proton transport

The effect of the relative humidity on the proton conductivity for the BPSH-PBI(10-10) multiblocks was studied at 80 °C. Nafion® 112 was used as control (Fig.9-7). Both water and phosphoric acid contribute as the vehicle for the proton transport. Significant improvement in the proton conductivity for the multiblock was observed compared to Nafion® under low relative humidity. The conductivity increased with increasing hydration level. Although the temperature is much lower to allow sufficient proton transport via phosphoric acid, water acts as the major vehicle for the transport. This widens the applicability of these systems for both low temperature and low RH applications.

However the major drawback of phosphoric acid systems is the leaching of phosphoric acid from the system. The process is catalyzed in the presence of water. The leaching results in loss in phosphoric acid content and poisoning of the Pt electrodes. It is proposed that the presence of the poly sulfone block may restrict the phosphoric acid

leaching by constraining the PBI unit. Ongoing study in optimizing the morphology to reduce phosphoric acid leaching is encouraging and will be reported separately.

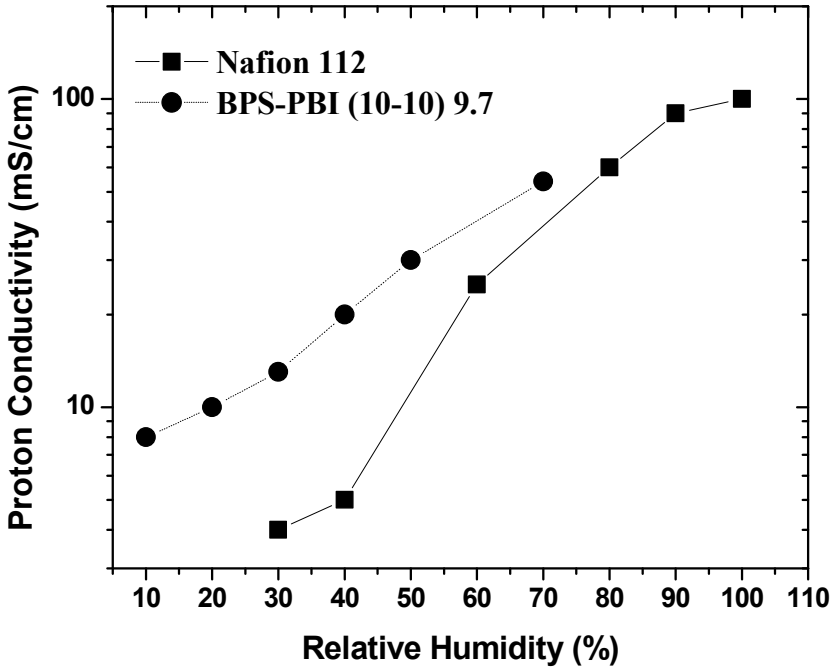

Figure 9-7 Influence of relative humidity on proton transport for the phosphoric acid doped BPS-PBI (10-10) multiblock at 80 ^{o}C; the number after the parenthesis in the legend represents the doping level

9.4 Conclusions

A novel multiblock copolymer system was developed and characterized for high temperature PEM applications. The copolymers showed satisfactory proton conductivity over a wide range of temperature (100-200 ^{o}C) in absence of water. The proton transport mechanism involved both hopping and vehicle mechanism. The significant increase in proton conductivity after a particular doping level was attributed to the presence of "free" phosphoric acid or the quickly diffusing $H_2PO_4^-$ contributing to the proton conduction mechanism. However at high temperatures, the formation of fused phosphoric reduced that contribution.

Similar to sulfonic acid multiblock systems, proton conduction was improved by the phase separated morphology of the BPS-PBI multiblocks. At a given doping level, the proton conductivity was found to increase with increasing block length. The effect was more prominent in low doping levels. At low doping level, most of the phosphoric acids are bound and proton diffusion occurs only through the hopping mechanism between the N-H sites and the phosphate anions. The formation of well connected PBI domains improved the proton transport.

The above study was done in absence of water. Proton conductivity measured as a function of the water content or under partially hydrated at 80 ^{o}C conditions was significantly higher than the benchmark Nafion®112. In addition to the $H_2PO_4^-$ anion, water contributes to the vehicle mechanism. The developed phosphoric acid doped multiblock copolymer system is strong candidate for both high temperature and low relative humidity PEM applications.

The authors wish to acknowledge the support of the Nissan Motor Company and Department of Energy (DOE Contract # DE-FG36-06G016038) for support of this research.

9.5 References

1. Carrette, L.; Friedrich, K. A.; Stimming, U., Fuel cells: Principles, types, fuels, and applications. *Chemphyschem* **2000,** 1, (4), 162-193.

2. Zalbowitz, M.; S, T., Green Power. *Fuel Cells* **1999**.

3. Page, K. A.; Cable, K. M.; Moore, R. B., Molecular Origins of the Thermal Transitions and Dynamic Mechanical Relaxations in Perfluorosulfonate Ionomers. *Macromolecules* **2005,** 38, (15), 6472-6484.

4. Hickner, M. A.; Ghassemi, H.; Kim, Y. S.; Einsla, B. R.; McGrath, J. E., Alternative polymer systems for proton exchange membranes (PEMs). *Chemical Reviews* **2004,** 104, (10), 4587-4611.

5. Roy, A.; Hickner, M. A.; Yu, X.; Li, Y.; Glass, T. E.; McGrath, J. E., Influence of chemical composition and sequence length on the transport properties of proton exchange membranes. *Journal of Polymer Science, Part B: Polymer Physics* **2006,** 44, (16), 2226-2239.

6. Kim, Y. S.; Wang, F.; Hickner, M.; Zawodzinski, T. A.; McGrath, J. E., Fabrication and characterization of heteropoly acid (H3PW12O40)/directly polymerized sulfonated poly(arylene ether sulfone) copolymer composite membranes for higher temperature fuel cell applications. *Journal of Membrane Science* **2003,** 212, (1-2), 263-282.

7. Hill, M. L.; Kim, Y. S.; Einsla, B. R.; McGrath, J. E., Zirconium hydrogen phosphate/disulfonated poly(arylene ether sulfone) copolymer composite membranes for proton exchange membrane fuel cells. *Journal of Membrane Science* **2006,** 283, (1+2), 102-108.

8. Costamagna, P.; Yang, C.; Bocarsly, A. B.; Srinivasan, S., Nafion115/zirconium phosphate composite membranes for operation of PEMFCs above 100 DegC. *Electrochimica Acta* **2002,** 47, (7), 1023-1033.

9. He, R.; Li, Q.; Xiao, G.; Bjerrum, N. J., Proton conductivity of phosphoric acid doped polybenzimidazole and its composites with inorganic proton conductors. *Journal of Membrane Science* **2003,** 226, (1-2), 169-184.

10. Steininger, H.; Schuster, M.; Kreuer, K. D.; Kaltbeitzel, A.; Bingoel, B.; Meyer, W. H.; Schauff, S.; Brunklaus, G.; Maier, J.; Spiess, H. W., Intermediate temperature proton conductors for PEM fuel cells based on phosphonic acid as protogenic group: A progress report. *Physical Chemistry Chemical Physics* **2007,** 9, (15), 1764-1773.

11. Sammes, N.; Bove, R.; Stahl, K., Phosphoric acid fuel cells: fundamentals and applications. *Current Opinion in Solid State & Materials Science* **2005,** 8, (5), 372-378.

12. Kongstein, O. E.; Berning, T.; Borresen, B.; Seland, F.; Tunold, R., Polymer electrolyte fuel cells based on phosphoric acid doped polybenzimidazole (PBI) membranes. *Energy (Oxford, United Kingdom)* **2006,** 32, (4), 418-422.

13. Lobato, J.; Canizares, P.; Rodrigo, M. A.; Linares, J. J., PBI-based polymer electrolyte membranes fuel cells. *Electrochimica Acta* **2007,** 52, (12), 3910-3920.

14. Li, Q.; He, R.; Berg, R. W.; Hjuler, H. A.; Bjerrum, N. J., Water uptake and acid doping of polybenzimidazoles as electrolyte membranes for fuel cells. *Solid State Ionics* **2004,** 168, (1-2), 177-185.

15. Van Grotthuss, C. J. D., *Ann. Chim* **1806,** 58, (54).

16. Aihara, Y.; Sonai, A.; Hattori, M.; Hayamizu, K., Ion Conduction Mechanisms and Thermal Properties of Hydrated and Anhydrous Phosphoric Acids Studied with 1H, 2H, and 31P NMR. *Journal of Physical Chemistry B* **2006,** 110, (49), 24999-25006.

17. Jayakody, J. R. P.; Chung, S. H.; Durantino, L.; Zhang, H.; Xiao, L.; Benicewicz, B. C.; Greenbaum, S. G., NMR studies of mass transport in high-acid-content fuel cell membranes based on phosphoric acid and polybenzimidazole. *Journal of the Electrochemical Society* **2007,** 154, (2), B242-B246.

18. Li, Q.; He, R.; Jensen, J. O.; Bjerrum, N. J., PBI-based polymer membranes for high temperature fuel cells - preparation, characterization and fuel cell demonstration. *Fuel Cells (Weinheim, Germany)* **2004,** 4, (3), 147-159.

19. Lee, H.-S.; Roy, A.; Lane, O.; McGrath, J. E., Synthesis and Characterization of Poly(arylene ether sulfone)-b-polybenzimidazole Copolymers for High Temperature Proton Exchange Membrane Fuel Cells. *Unpublished Result* **2008**.

20. Li, Y.; Roy, A.; Badami, A. S.; Hill, M.; Yang, J.; Dunn, S.; McGrath, J. E., Synthesis and characterization of partially fluorinated hydrophobic-hydrophilic multiblock copolymers containing sulfonate groups for proton exchange membrane. *Journal of Power Sources* **2007,** 172, (1), 30-38.

21. Lee, H.-S.; Roy, A.; Badami, A. S.; McGrath, J. E., Synthesis and characterization of sulfonated poly(arylene ether) polyimide multiblock copolymers for proton exchange membranes. *Macromolecular Research* **2007,** 15, (2), 160-166.

22. Yu, X.; Roy, A.; Dunn, S.; Yang, J.; McGrath, J. E., Synthesis and characterization of sulfonated-fluorinated, hydrophilic-hydrophobic multiblock copolymers for proton exchange membranes. *Macromolecular Symposia* **2006,** 245/246, (World Polymer Congress--MACRO 2006), 439-449.

23. Lee, H.-S.; Roy, A.; Badami, A. S.; McGrath, J. E., Synthesis of multiblock copolymers based on sulfonated segmented hydrophilic-hydrophobic blocks for proton

exchange membranes. *Abstracts of Papers, 232nd ACS National Meeting, San Francisco, CA, United States, Sept. 10-14, 2006* , PMSE-124.

10.0 Optimization of MEA Processing Parameters

Abhishek Roy, Linda Harris and J.E. McGrath

Macromolecular Science and Engineering Program
Macromolecules and Interfaces Institute
Virginia Polytechnic Institute and State University, Blacksburg, VA 24061

Abstract

The membrane electrode assembly (MEA) is a critical component of a proton exchange membrane fuel cell. The interface between the membrane and the electrodes plays a significant role in controlling overall performance and durability. Moreover, the processing parameters of an MEA control the interface. In this paper, the parameters influencing processing conditions were investigated, and optimized processing parameters are suggested. As documented herein, the water content present in the polymers at the time of MEA fabrication significantly influences fuel cell performance. The optimized fabrication temperature is close to the hydrated glass transition temperature of the copolymer and is a function of both water content and molecular weight of the copolymer.

10.1 Introduction

The integral part of a fuel cell is the membrane electrode assembly (MEA). The MEA consists of a proton exchange membrane (PEM) bonded to two electrodes (Figure 10-1). The electrodes are carbon supported platinum particles dispersed in a polymer matrix.[1, 2] The proton exchange membranes contain sulfonic acid groups responsible for proton transport.

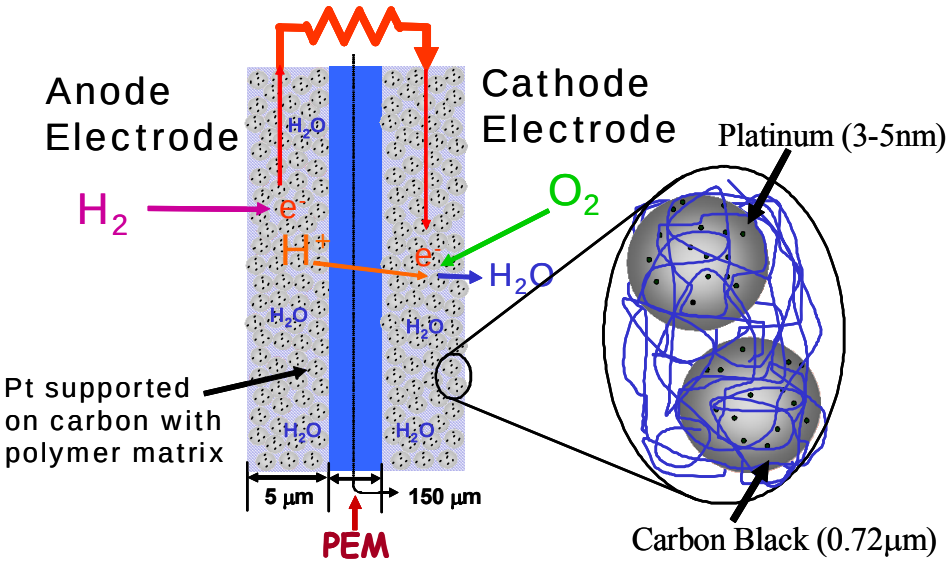

Figure 10-1 Membrane electrode assembly. Reprinted with permission.[1] Copyright 2004 American Chemical Society

The MEA manufacturing process initially involves the preparation of a Nafion platinum (Pt) dispersion, also referred to as the "ink," which is painted onto decals to obtain 0.2-0.4 mg/cm^2 of Pt loadings. The decals are then hot pressed onto the PEM to form the MEA.[3] The whole process is schematically represented in Figure (10-2).

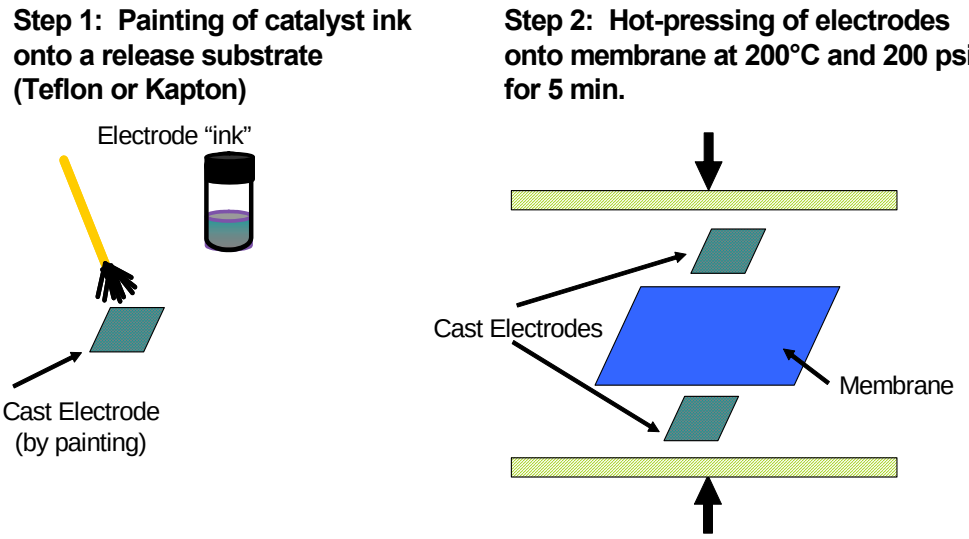

Figure 10-2 MEA fabrication technique

The main objective in this MEA fabrication technique is to achieve a good bond between the electrodes and the membrane. Good flow properties of a polymer ensure good bonding and adhesion with the electrodes. Therefore, a thorough understanding of the parameters affecting the flow properties of a polymer can serve to optimize processing conditions for MEA fabrication. These parameters include the processing temperature or the MEA bonding temperature, the polymer's molecular weight, and the water content in the polymer during fabrication. The MEA bonding temperature is normally close to the glass transition temperature of the polymer, as illustrated by the modulus vs. temperature graph depicted in Figure (10-3). In addition to glass transition temperature, controlling molecular weight and the water content in the copolymers can help optimize the processing temperature. The critical impact of the molecular weight and water content of a copolymer on processing temperature is discussed below.

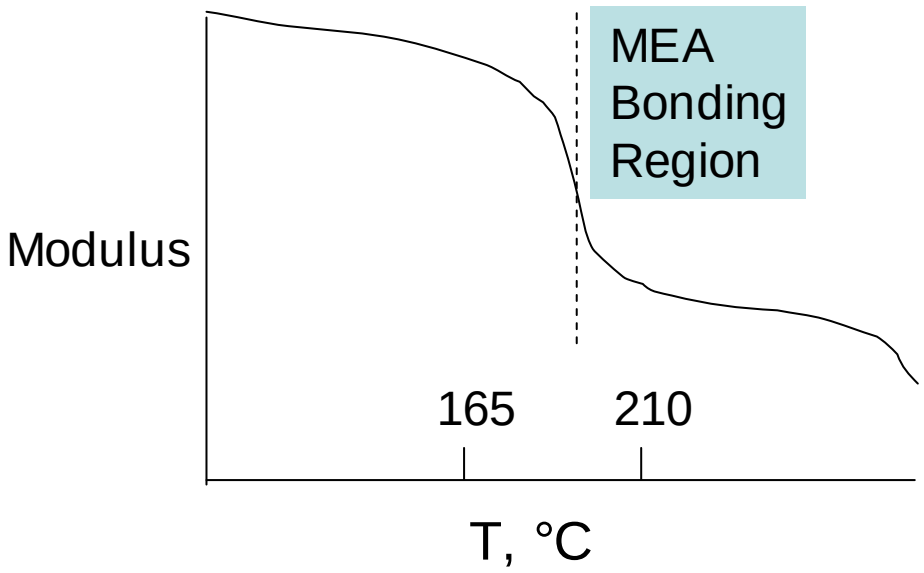

Figure 10-3 Modulus vs. temperature

10.1.1 Importance of molecular weight of the copolymer on processing temperature

For most copolymers, melt viscosity has a linear relationship with molecular weight up to a particular point, which is known as the entanglement molecular weight. Below the entanglement molecular weight, the flow properties of a copolymer are independent of the molecular weight. Above the entanglement molecular weight, however, the viscosity of a copolymer is proportional to the power of 3.4 of molecular weight. As a result, the processing temperature needs to be shifted to a higher temperature to compensate for the effect of the copolymer's increased viscosity.

10.1.2 The impact of water content in a copolymer on the processing temperature during MEA fabrication

Water is known to reside in hydrophilic copolymers in at least three different states, which can be categorized according to thermal properties.[4] *Non-freezing bound*

water is strongly associated with a copolymer, shows no thermal transition by differential scanning calorimetry, but depresses the T_g of the copolymer. *Freezable bound water* is weakly bound to the copolymer (or weakly bound to the non-freezing water), and displays a broad melting behavior around 0 °C. *Free water* shows a sharp melting point at 0°C. The tightly bound water acts as a plasticizer and, hence, can influence the flow temperature of a copolymer. Table (10-1) shows the depression of the glass transition temperature of BPSH and Nafion copolymers under fully hydrated conditions. The water content in the membrane when it undergoes MEA fabrication will influence the glass transition temperature and, hence, the processing temperature.

Table 10-1 Depression of glass transition temperature under hydrated conditions[4]

Copolymer	Water uptake (%)	T_g of dried sample (^oC)	T_g of fully hydrated sample (^oC)
BPSH-30	26.7	257	136
BPSH-40	49.5	267	126
BPSH-50	108.7	272	98
Nafion-1135	33.0	160	99

The main objective of this paper was to investigate the influence of water content and temperature on hot pressing conditions, as well as to determine how these variables influences fundamental transport properties such as proton conductivity. This paper will also describe the optimal processing conditions for fabricating membrane electrode assemblies. For this experimental study, disulfonated poly(arylene ether sulfone) random copolymers were chosen.[5] However, the fundamental findings obtained in this research can be applied to Nafion® as well.

10.2 Experimental

10.2.1 Copolymers studied

The synthesis of biphenol-based disulfonated poly (arylene ether sulfone) copolymers (BPSH-35; 35 mole percent disulfonated monomers) was successfully carried out via nucleophilic aromatic substitution.[5, 6] The molecular weight of the copolymer was 80,000 g/mole. The structure is given below [(1-x)=35%]

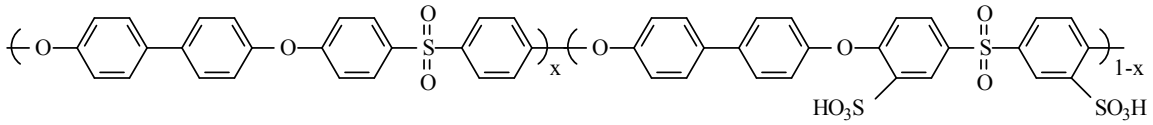

Figure 10-4 Chemical structure of BPSH-xx random copolymer

10.2.2 Differential scanning calorimetry (DSC) and thermogravimetric analysis (TGA)

Our DSC studies were performed in a TA DSC instrument using liquid nitrogen as a cooling medium for the sub-ambient experiments. Samples were equilibrated in a relative humidity oven (ESPEC SH 240) to achieve the desired hydration levels, then placed in thermally sealed pans capable of withstanding pressures up to 100 atm. Samples were cooled to -70 °C and then heated at a rate of 5 °C per min under a N_2 atmosphere.

The TGA studies were conducted using fully hydrated samples. Just before the experiment, the samples were removed from the water, blotted to remove any surface water, and placed in a TGA sample pan. The samples were heated at 10 ^{o}C/min under an air atmosphere.

10.2.3 Proton conductivity

Proton conductivity at 30 °C at full hydration (in liquid water) was determined in a window cell geometry[7] using a Solartron 1252+1287 Impedance/Gain-Phase Analyzer over the frequency range of 10 Hz -1 MHz following the procedure reported in the literature.[8]

10.2.4 MEA preparation and fuel cell characterization

Electrodes were fabricated by preparing an ink from glycerol, a Nafion dispersion, and a platinum/carbon-black mixture (20 wt% Pt). The ink was painted onto a Teflon substrate to produce a decal with a platinum loading of 0.4 mg. MEAs were prepared by hot pressing two of the electrode decals onto the BPSH-35 membrane as per the experimental design. A fuel cell test stand was used to measure high frequency resistance. The MEA was loaded into the single stack fuel cell. The fuel cell was operated with H_2/Air at 90 ^oC and 100% relative humidity. The hydrogen was fed into the anode at 200 sccm with a humidified temperature of 105 ^oC and the air flow into the cathode was 500 sccm at 90 ^oC.

10.2.5 Experimental design

The membrane was hot pressed both with (MEA) and without (blank) electrodes over a matrix of experimental conditions varying in water content and temperatures. The experimental matrix is given in Table (10-2), which shows, for example, that Sample 1 was equilibrated at 40% RH to achieve a particular water uptake and subsequently hot pressed at a temperature of 165 °C. The pressure was maintained at 2500 psi. For the MEAs, a similar set of experiments was performed, wherein the Pt loading was maintained at 0.2mg/cm.

Table 10-2 Experimental design

Sample BPSH-35	Temperature (°C)	RH (%)	MW (1000g/mole)
1	165	40	80
2	210	40	80
3	165	20	80
4	210	20	80
5	165	0	80

10.3 Results and discussion

10.3.1 Water uptake

Figure (10-5) depicts the retention of water in the presence of water vapor for samples equilibrated at 40 and 20 percent relative humidity. Samples equilibrated at 40% RH showed higher water uptake than the 20% RH samples over a range of temperatures. Correspondingly, a depression in the glass transition temperature (Table 10-3) was observed with increasing water uptake, as seen from DSC experiments.

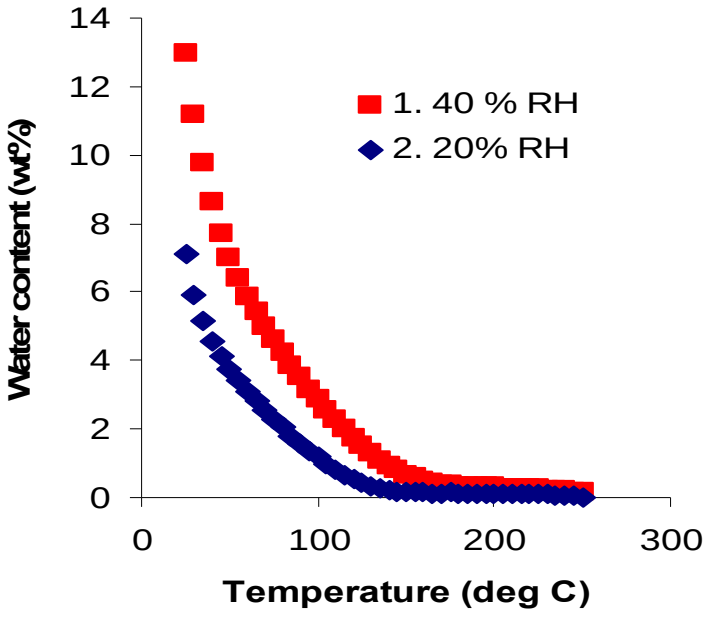

Figure 10-5 Retention of water as a function of temperature of the BPSH-35 random copolymer equilibrated at different relative humidities

Table 10-3 Depression of glass transition temperature of BPSH-35 with water uptake

Relative humidity (%)	Water content (%)	T_g (^oC)
0	0	260
20	7	188
40	13	165

10.3.2 Effect of hot pressing conditions on proton conductivity of the blanks and MEAs

The membranes were equilibrated at different water contents and hot pressed at different temperatures with (MEA) and without electrodes (blanks). After the hot pressing the blanks were equilibrated in liquid water, after which protonic conductivity was determined using a Solartron impedance analyzer at 30 °C. Table (10-4) represents the conductivity results run on the blank membranes. The MEA conductivity results were obtained from high frequency resistance values (HFR) measured at 80 °C. Conductivity decreased with the amount of water present in the membranes during hot pressing, as well as in response to the hot pressing temperature. Although the conductivity of Sample 5 did not appreciably decrease, the processing temperature was not sufficient to ensure good flow, as the Tg for the fully dried sample was around 260 °C. When membranes were equilibrated at 40% RH, conductivity dropped to 26 mS/cm when the hot pressing temperature was increased from 165 ^oC to 210 ^oC. The conductivity value for the unprocessed sample is a control and represents the value before hot pressing.

Table 10-4 Protonic conductivity of the hot pressed samples in liquid water

Sample BPSH35	T_g (°C)	RH (%)	MW 1000 g/mole	Proton conductivity* (mS/cm)
1	165	40	80	50
2	210	40	80	26
3	165	20	80	80
4	210	20	80	35
5	165	0	80	65
6	210	0	80	70
Control	–	–	80	85

*Liquid water, 30 °C, ± 5 %.

Similar observations were noted for the MEAs as well. Figure (10-6) represents the plot of MEA conductivity obtained from HFR measurements as a function of current density. Here also, MEA that were fabricated at 165 °C with a water content corresponding to 20% RH showed the highest conductivity.

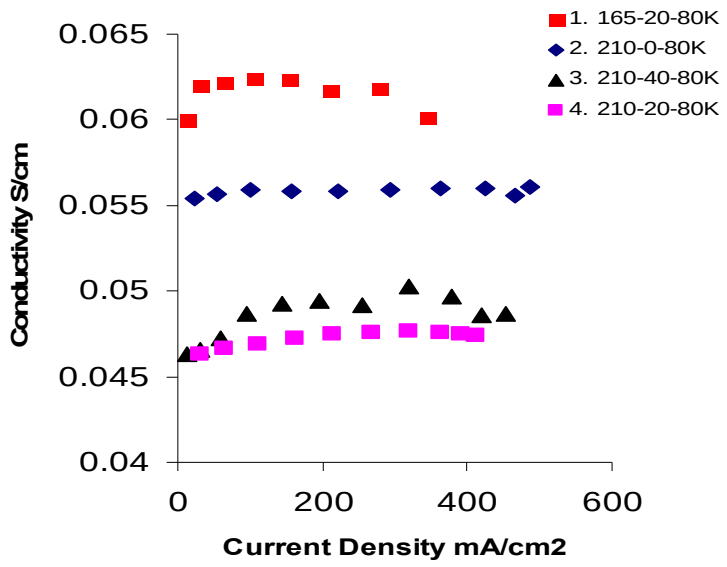

Figure 10-6 Conductivity vs. current density for the MEAs

Water uptake and DSC results indicated a depression in glass transition temperature with increasing water uptake. This trend shifted the flow temperature or the MEA bonding temperature for the copolymer to a lower value. The shift was more pronounced at higher water uptake levels. Processing the membranes at a temperature higher than the flow temperature may result in morphological changes or a relaxation within the copolymer. For example, in case of Nafion and other PEMs, conductivity initially increases with an increase in temperature, but then decreases once a particular temperature has been reached. This specific temperature has been found to be close to the hydrated α relaxation temperature.[2,5] Above the α relaxation temperature, the polymer undergoes relaxation, thereby disturbing the favored morphology needed for proton transport. Hence, conductivity decreases. Similar morphological changes are also observed for BPSH 35 copolymer at higher temperatures. Figure (10-7) represents the AFM images of BPSH 35 after exposure to different temperatures.[9]

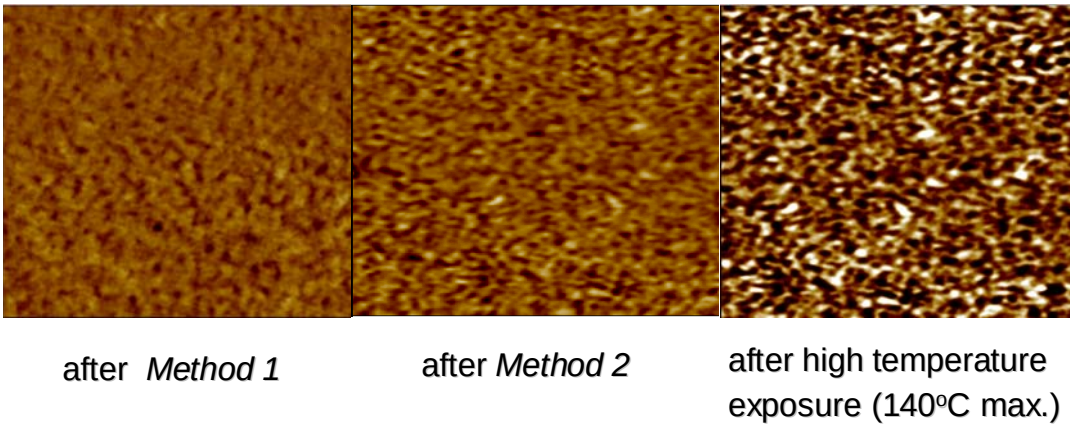

Figure 10-7 AFM images of the exposed BPSH 35 at different conditions. Reprinted from [9] with permission from Elsevier

Method 1 and Method 2 represent two different types of acidification treatments. In Method 1 the sample was exposed to 30 °C in water, and in Method 2 the sample was exposed to 100 °C, also in water. It is evident from the images that at 140 °C the sample experienced some morphological changes as the hydrated T_g for BPSH 35 copolymer under fully hydrated conditions was found occur at approximately that temperature. Hence, hot pressing the membranes at higher water contents and at higher temperatures

may have caused some morphological changes that resulted in a drop in conductivity values. To further investigate the effect of morphology on conductivity, the hot pressed samples (blanks) 2 and 4 were treated with boiling DI water for 2 h, which is known as a hydrothermal treatment.[5] Table (10-5) represents the conductivity values of the hot pressed samples after hydrothermal treatment.

Table 10-5 Proton conductivity values after hydrothermal treatment for the hot pressed samples

Sample	Temperature (^{o}C)	RH (%)	MW (1000 g/mole)	Initial* proton conductivity (mS/cm)	Final* Proton conductivity (mS/cm)
2	210	20	80	35	80
4	210	40	80	25	65

* liquid water, 30 ^{o}C.

For both Samples 2 and 4, conductivity values increased after hydrothermal treatment. In other words, the hydrothermal treatment produced a different morphology that facilitated the transport process as compared the samples' pre-treatment morphology. Although it is difficult to conclusively comment on the reestablishment of the morphology, it is evident that the decrease in conductivity was due to a morphology effect rather than a degradation effect.

The guidelines for fabricating MEAs can be summarized as follows:

- The MEA should be fabricated at a temperature close to the hydrated glass transition temperature of the copolymer, which is a function of both water content and molecular weight.
- If the processing temperature is too far below the hydrated Tg, the electrodes will not bind properly to the membrane and conductivity will be lowered.
- If the processing temperature is well above the hydrated Tg, the copolymer could undergo a morphological change that may lower its proton conductivity.

10.4 Conclusions

BPSH-35 random copolymers with a molecular weight of 80,000 g/mole were synthesized. The membranes were hot pressed both with (MEA) and without (blanks) electrodes over a matrix of experimental conditions varying in water content and temperature. The glass transition temperature or the flow temperature of the copolymer decreased with increasing water uptake, which impacted the bonding temperature of the MEA. Proton conductivity values determined both for the blanks and the MEAs decreased with both increasing water content and the temperature of the fabrication process. Processing the membranes at a temperature much higher than the flow temperature, may result in morphological changes and/or relaxation within the copolymer. Thus, MEAs should be fabricated at a temperature close to the hydrated glass transition temperature of the copolymer, which is a function of both water content and molecular weight.

The authors would like to thank UTC Fuel Cells (#PO3561) for their support.

10.5 References

1. Hickner, M. A.; Ghassemi, H.; Kim, Y. S.; Einsla, B. R.; McGrath, J. E., Alternative polymer systems for proton exchange membranes (PEMs). *Chemical Reviews* **2004,** 104, (10), 4587-4611.

2. Winter, M.; Brodd, R. J., What are batteries, fuel cells, and supercapacitors? (vol 104, pg 4245, 2003). *Chemical Reviews* **2005,** 105, (3), 1021-1021.

3. Carrette, L.; Friedrich, K. A.; Stimming, U., Fuel cells: Principles, types, fuels, and applications. *Chemphyschem* **2000,** 1, (4), 162-193.

4. Kim, Y. S.; Dong, L. M.; Hickner, M. A.; Glass, T. E.; Webb, V.; McGrath, J. E., State of water in disulfonated poly(arylene ether sulfone) copolymers and a perfluorosulfonic acid copolymer (nafion) and its effect on physical and electrochemical properties. *Macromolecules* **2003,** 36, (17), 6281-6285.

5. Wang, F.; Hickner, M.; Kim, Y. S.; Zawodzinski, T. A.; McGrath, J. E., Direct polymerization of sulfonated poly(arylene ether sulfone) random (statistical) copolymers: candidates for new proton exchange membranes. *Journal of Membrane Science* **2002,** 197, (1-2), 231-242.

6. Kim, Y. S.; Wang, F.; Hickner, M.; McCartney, S.; Hong, Y. T.; Harrison, W.; Zawodzinski, T. A.; McGrath, J. E., Effect of acidification treatment and morphological stability of sulfonated poly(arylene ether sulfone) copolymer proton-exchange membranes for fuel-cell use above 100 degrees C. *Journal of Polymer Science Part B-Polymer Physics* **2003,** 41, (22), 2816-2828.

7. Zawodzinski, T. A.; Neeman, M.; Sillerud, L. O.; Gottesfeld, S., Determination of Water Diffusion-Coefficients in Perfluorosulfonate Ionomeric Membranes. *Journal of Physical Chemistry* **1991,** 95, (15), 6040-6044.

8. Springer, T. E.; Zawodzinski, T. A.; Wilson, M. S.; Gottesfeld, S., Characterization of polymer electrolyte fuel cells using AC impedance spectroscopy. *Journal of the Electrochemical Society* **1996,** 143, (2), 587-599.

9. Kim, Y. S.; Dong, L. M.; Hickner, M. A.; Pivovar, B. S.; McGrath, J. E., Processing induced morphological development in hydrated sulfonated poly(arylene ether sulfone) copolymer membranes. *Polymer* **2003,** 44, (19), 5729-5736.

11.0 Structure Property Relationships of Proton Exchange Membranes

Abhishek Roy,[1] Michael A. Hickner,[2]

and

James E. McGrath [1]

[1] Macromolecules and Interfaces Institute

Virginia Polytechnic Institute and State University

Blacksburg, VA 24061

[2] Present Address: Department of Materials Science and Engineering

The Pennsylvania State University, University Park, PA 16802

Abstract

Over the last few years, our group has been synthesizing thermally and oxidatively stable sulfonic acid group containing poly(arylene ether sulfone) copolymers. The chemical structures and sequence distributions were varied to synthesize random, crosslinked and more recently the multiblock copolymers. The proton exchange membrane properties for the copolymers were characterized to develop concepts for establishing structure/property relationships between the functionality of the polymer backbone, the states of water, and the membrane transport. Experimentally determined water and proton transport data were successfully modeled to existing mathematical equations, regardless of the chemical nature of the copolymers. A relationship between transport properties and the volume fraction of the hydrophilic phase was established. This study led to the synthesis of copolymers with improved performance, particularly under partially hydrated conditions. Multiblock copolymers with phase separated morphology showed the best promise as next generation PEMs.

11.1 Introduction

Over the last two decades, proton exchange membrane based fuel cells (PEMFCs) have shown great promise in automotive applications as environmentally friendly alternatives to the internal combustion engine. [1-4] Significant research on PEMFCs were conducted by national and industrial research laboratories, by universities, as well as by automotive companies.[5,6] The major challenges associated with commercializing fuel cells are cost, the durability of the Pt electrodes, hydrogen storage and the need for improved performance from the polymeric membranes.[7] The McGrath research group has been principally involved with developing polymeric membranes with improved performance capabilities.[1] There are three major criteria for achieving improved PEM performance: (1) high proton conductivity under partially hydrated conditions and both sub-ambient and high temperatures; (2) reduced swelling-deswelling characteristics, and (3) low fuel or gas crossover. For the last five to six years, our group has been synthesizing wholly aromatic hydrocarbon based disulfonated poly(arylene ether sulfone)s as candidates for proton exchange membranes.[8-13] The rigid aromatic chemical backbone reduced fuel permeability significantly when compared to the commercially available membrane, Nafion®.[14] An earlier aspect of our research targeted the synthesis of random copolymers, where the sulfonic groups were distributed statistically throughout the copolymer backbone. The properties of the random copolymers were optimized by varying the chemical composition or the ion exchange capacity (IEC), as well as the chemical structure of the backbone.[12] Improved fuel cell performance under fully hydrated conditions, both for H_2 /Air and direct methanol fuel cells (DMFC) was achieved.[15] However, the isolated random hydrophilic domain morphology resulted in a drop in performance under partially hydrated conditions. However, by tailoring the morphology from a random architecture to a chemically phase separated multiblock copolymer, improved the performance significantly under partially hydrated conditions.[16-18] Unlike random copolymers, where phase separation between hydrophobic and hydrophilic domains occurs principally at higher ionic content and is water assisted, phase separation in multiblock copolymers occurs chemically. The multiblock copolymers consisted of both hydrophobic and hydrophilic blocks. The phase

separation between the blocks is a function of the molecular weight of the individual blocks and the difference between the hydrophobicity and hydrophilicity of the individual blocks. AFM and TEM studies revealed the formation of chemically phase separated, co-continuous, ordered hydrophobic and hydrophilic domains in the multiblocks.[19] Significant research has more recently been directed at designing ion containing multiblock copolymers with improved PEM performance characterstics.[16, 20-23] Our group has been involved in synthesizing thermally stable multiblock copolymers with varying chemical structures and compositions, ranging from highly fluorinated, to partially fluorinated, to hydrocarbon-based block copolymers.[19, 24-28] The hydrophilic segments in all these cases were kept same.

Regardless of the nature of the backbone, transport properties scaled with the block lengths of the copolymers. An increase in block length for a given series of block copolymers with the same ionic concentration was associated with increase in the self-diffusion coefficients of water and improved proton conduction under partially hydrated conditions. The continuous hydrophilic domains reduced the morphological barrier for transport even at low water content. Under fully hydrated conditions, proton conductivity and water uptake were found to be a function of the volume fraction of the hydrophilic phase.[29] However, also it was demonstrated that by synthesizing unequal block length materials, water uptake could be reduced without sacrificing proton conductivity.[16] For DMFC applications, the block copolymers showed very low methanol permeability and very high selectivity.[30] Hence, these materials are highly selective for both H_2/Air and DMFC systems. The states of water for multiblock copolymers were also investigated. Under similar ionic content, free water content increased with increasing block length.[29] Tightly bound water content was found to be higher compared to that of the random copolymers, which is critical in addressing both low and high temperature proton transport.

The main objective of this paper was to develop novel structure–property relationships applicable to all the random and multiblock copolymers studied in our group to date. By relating important transport properties with a copolymer's structural/physical properties, one can understand key parameters that control overall performance. The

major structural variables studied in these multiblock copolymers were block length, ion exchange capacity, and the chemical composition or the structure of the hydrophobic unit.

Three different series of both multiblock and random copolymers were chosen for this study. For the multiblocks, the ratio of individual block lengths was varied to afford both equal and unequal block length materials. The IEC was varied over a wide range by fluctuating the molar fraction of the hydrophilic block with respect to the hydrophobic block. The chemical structure of the hydrophobic blocks varied from fully hydrocarbon (BPSH-BPS, BPSH-PI) to partially fluorinated (BPSH-BisSF). For the random copolymers, the major structural variables were IEC and the chemical composition of the backbone. The IEC was varied by altering the molar fraction of the sulfonic acid units in the copolymers. The chemical structure was varied by changing the nature of the biphenol unit (BPSH-xx), the hydroquinone (HQSH-xx), and the 6F bisphenol (6FSH-xx). The structures of all the multiblock and random copolymers investigated in this study are given in Figure (11-1).

All these structural variables influence strongly phase separation characteristics of the hydrophobic and hydrophilic domains in these ion containing copolymers. The extent of phase separation correlates with the volume fraction of water or more precisely the volume fraction of the associated hydrophilic phase. This knowledge, coupled with various transport property measurements and states of water experimental results, will elucidate the novel structure property relationships for proton exchange membranes, leading to the synthesis of materials with improved properties.

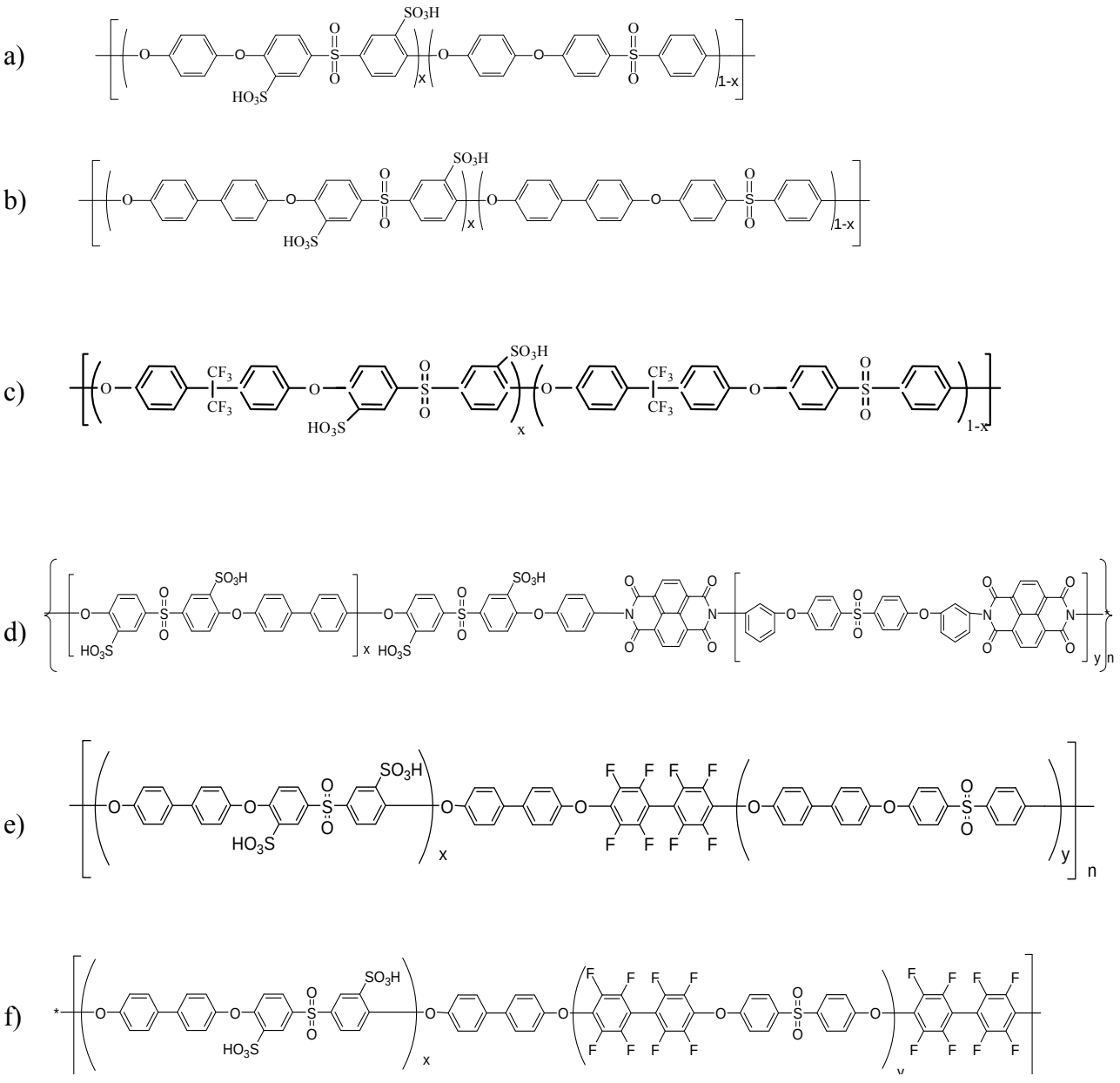

Figure 11-1 Chemical structures of a) HQSH-xx, b) BPSH-xx, c) 6FSH-xx, d) BPSH-PI(x:y), e) BPSH-BPS(x:y), f) BPSH-BisSF(x:y)

11.2 Experimental

11.2.1 Copolymers studied

The random copolymers evaluated for this study include BPSH-xx[9], HQSH-xx[16] and 6FSH-xx[12]. For the BPSH-xx, BP refers to the biphenol, S corresponds to the sulfone, H for the acid form, and xx indicates the degree of disulfonation. For the HQSH-xx and 6FSH-xx materials, HQ and 6F represent the hydroquinone and 6F bisphenol, respectively. The degree of disulfonation was varied over a wide range to vary the IEC. The multiblock copolymers considered were BPSH-BPS(x:y)[31], BPSH-PI(x:y)[19] and BPSH-BisSF(x:y)[27]. The BPSH with 100% degree of disulfonation represents the hydrophilic block with a molecular weight of x kg/mole. The BPS, PI, and the BisSF correspond to the hydrophobic blocks of the three multiblock copolymers with molecular weights of y kg/mole. Individual block lengths and IEC were varied. The chemical structures and physical properties are provided in Figure (11-1) and Table (11-1 and 11-2), respectively. The synthesis of all the copolymers was previously reported, and Nafion® 112 was purchased from Electrochem Inc. and used as received.

11.2.2 Characterization properties

The measurement techniques and all the data in this paper have been reported elsewhere, as listed for the following materials: HQSH-xx,[16] BPSH-xx,[9, 32] 6FSH-xx,[12] BPSH-BPS (x:y),[31, 32] BPSH-PI(x:y)[18, 19] and BPSH-BisSF(x:y).[17, 27]

Table 11-1 Summary of the physical properties of random copolymers

Sample	IEC (meq/g)	Density g/cc	IEC (meq/cc)	Water uptake (mass %)	Water volume fraction
Nafion 112	0.9	2.1	1.9	19	0.33
HQSH-35	1.8	1.4	2.4	160	0.78
HQSH-30	1.6	1.3	2.1	83	0.52
HQSH-25	1.4	1.3	1.8	60	0.42
HQSH-20	1.2	1.3	1.5	29	0.27
BPSH-50	2.1	1.4	3.0	232	0.77
BPSH-40	1.7	1.4	2.4	60	0.45
BPSH-35	1.5	1.3	2.1	37	0.33
BPSH-30	1.3	1.3	1.7	22	0.22
BPSH-20	1.1	1.3	2.7	16	0.15
6FSH-50	1.6	1.6	2.5	100	0.62
6FSH-40	1.3	1.5	2.0	34	0.34
6FSH-35	1.1	1.5	1.7	20	0.23
6FSH-30	1.0	1.5	1.4	16	0.19
6FSH-20	0.9	1.4	1.3	10	0.12

Table 11-2 Physical properties of multiblock copolymers

Sample	IEC (meq/g)	Density g/cc	IEC (meq/cc)	Water uptake (mass %)	Water volume fraction
BPSH-BPS(3:3)	1.3	1.3	1.7	30	0.28
BPSH-BPS(5:5)	1.4	1.5	2.0	33	0.32
BPSH-BPS(10:10)	1.3	1.4	1.8	60	0.45
BPSH-BPS(15:15)	1.4	1.2	1.6	83	0.50
BPSH-BPS(10:5)	1.8	1.6	2.8	100	0.61
BPSH-BPS(15:10)	1.7	1.5	2.6	90	0.58
BPSH-BPS(20:15)	1.7	1.4	2.4	70	0.49
BPSH-PI(5:5)	1.6	1.6	2.6	55	0.47
BPSH-PI(5:10)	1.1	1.6	1.7	23	0.26
BPSH-PI(5:20)	0.8	1.6	1.2	15	0.19
BPSH-PI(10:10)	0.5	1.5	0.8	12	0.15
BPSH-PI(10:15)	1.6	1.6	2.6	70	0.53
BPSH-PI(10:20)	1.2	1.6	1.9	40	0.39
BPSH-PI(15:10)	0.9	1.5	1.3	25	0.27
BPSH-PI(15:15)	1.8	1.5	2.7	156	0.70
BPSH-PI(15:20)	1.6	1.5	2.3	85	0.56
BPSH-PI(20:15)	1.1	1.5	1.7	38	0.37
BPSH-PI(20:20)	1.7	1.4	2.5	97	0.58
BPSH-BisSF(12:17)	1.5	1.6	2.3	40	0.38
BPSH-BisSF(12:17)	1.3	1.7	2.1	40	0.40
BPSH-BisSF(12:17)	1.1	1.7	1.9	25	0.30
BPSH-BisSF(16:25)	1.5	1.6	2.3	48	0.43
BPSH-BisSF(16:25)	1.3	1.6	2.1	40	0.39
BPSH-BisSF(16:25)	1.1	1.6	1.8	24	0.28
BPSH-BisSF(15:20)	1.3	1.7	2.2	26	0.31
BPSH-BisSF(10:15)	1.3	1.6	2.1	47	0.43
BPSH-BisSF(15:15)	1.3	1.5	2.0	78	0.54
BPSH-BisSF(8:10)	1.3	1.6	2.1	52	0.45
BPSH-BisSF(5:5)	1.3	1.6	2.1	31	0.33

11.3 Results and Discussion

11.3.1 Water absorption

The characteristic of note for hydrophilic copolymers is water absorption. Water residing within the hydrophilic domains increases phase separation and plays critical role in proton conduction. Water uptake on a mass basis was determined for all the multiblock and random copolymers. The water volume fraction of these copolymers was obtained from the density of the copolymers, as shown in Equation (11-1).[33]

$$\phi = \left(\frac{M_{H_2O} / \rho_{H_2O}}{\left[M_{H_2O} / \rho_{H_2O} + EW / \lambda \rho_{ionomer} \right]} \right) \qquad \textbf{Equation 11-1}$$

A water volume fraction can be approximated to the associated hydrophilic volume fraction as reported earlier.[34] IEC and block lengths are the two major variables influencing water uptake. Figure (11-2) plots water volume fraction as a function of IEC for all the random and multiblock copolymers noted in the experimental section. Throughout this paper, multiblock data are represented by filled points and random copolymer data by unfilled points. The multiblock copolymers were sub-categorized according to either block length or the individual molecular weight of the blocks. The individual blocks with a molecular weight of less than 5000g/mole are labeled as shorter blocks; whereas blocks with molecular weights higher than 5000g/ mole are labeled as longer blocks.

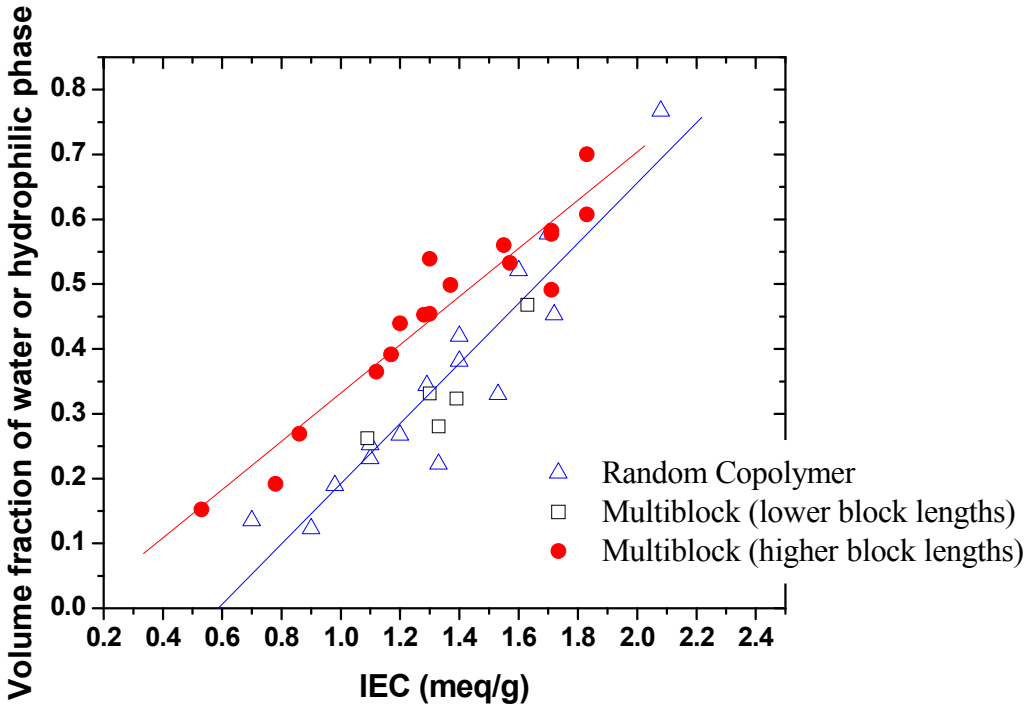

Figure 11-2 Influence of PEM microstructure on water absorption behavior

For both the multiblock and random copolymers, water absorption—or more precisely the volume fraction of the hydrophilic phase—increased with increasing IEC. At a given IEC, the higher block length multiblocks possessed higher volume fraction of water or hydrophilic phases. This was particularly evident for the lower IEC materials. Hence, at a given ionic content and irrespective of chemical structure, the multiblocks phase separated to a greater extent than the random copolymers. Interestingly, the two fitted lines tended to converge at higher ionic concentrations. The presence of a higher concentration of ionic groups influenced the sequence distribution in the random copolymers towards a microstructure similar to the multiblock copolymers.

The multiblock copolymers, featuring shorter block length hydrophobic and hydrophilic units, displayed water sorption characteristic similar to the random copolymers, which indicated a similar morphological structure. In such cases, the molecular weights of the individual blocks were not long enough to induce higher phase separation.

11.3.2 Water transport

Morphological studies using AFM and TEM techniques are widely used to study the morphology of PEMs. However, even though these techniques provide a useful overview of morphology, they fail to quantify or characterize the extent of connectivity between the hydrophilic domains. Understanding the influence of chemical composition, structure and sequence distribution on the extent of connectivity between the hydrophilic domains can provide a better picture of how the chemical nature of a phase separated copolymer influences its transport properties. Measuring water transport within the hydrophilic domains is definitely one of the more useful approaches.

The self-diffusion coefficient of water is an intrinsic water transport property which is related exponentially to the available free volume in the copolymer (V_t), as shown in Equation (11-2) below.[35]

$$D \propto \exp -\left(\frac{V^*}{V_t}\right) \qquad \textbf{Equation 11-2}$$
$$V_t \propto \phi$$

The free volume (V_t) was approximated to the volume fraction of the solvent, or in this case, the water (ϕ). The self-diffusion coefficient of water for each copolymer was determined using PGSE NMR techniques at 25 ^{o}C under fully hydrated conditions. Figure (11-3) represents the semi log plot of the self-diffusion coefficients of water vs. the reciprocal of the volume fraction of water. Over 50 different samples varying in chemical composition, structure, functionality of the backbone, and microstructure were considered. The experimental data was modeled to Equation (11-2) and a linear fit was obtained. At a given water volume fraction (i.e., by normalizing the water content effect), a higher self-diffusion coefficient value signifies greater phase separation or a better connectivity between the hydrophilic domains. The multiblock copolymers showed much higher diffusion coefficient values than the random copolymers and it is true over a wide range of water volume fractions. The region above the fitted line can be

assigned to the materials with a facilitated morphology, while the region below corresponds to materials with a restricted morphology.

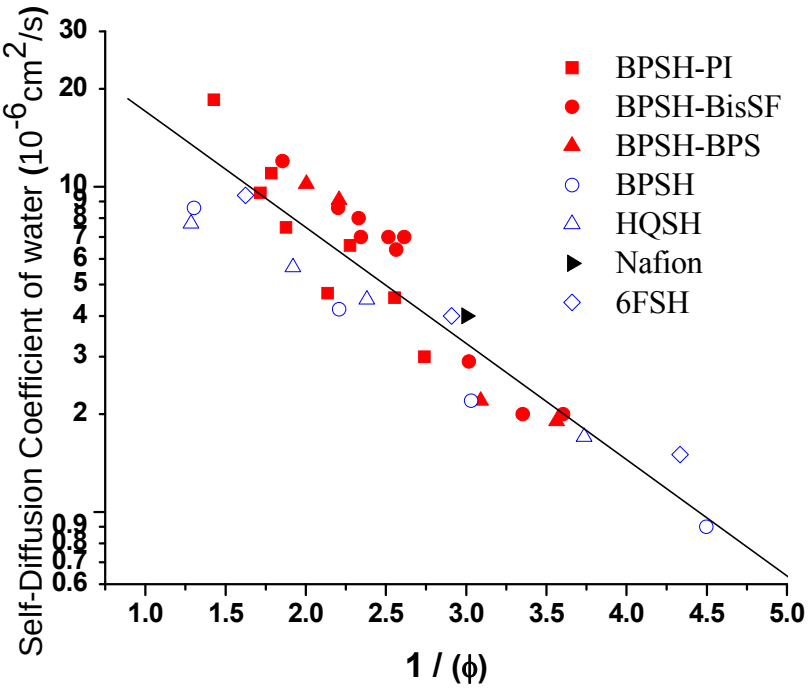

Figure 11-3 Self-diffusion coefficients of water scale with the volume fraction of water

The influence of the chemical structure on transport was also investigated. The BPSH-BisSF multiblocks (filled circles) consist of partially fluorinated hydrophobic blocks, in contrast to the fully hydrocarbon BPSH-BPS (filled triangles) and the BPSH-PI (filled squares) multiblocks. The presence of fluorine in the structure was expected to increase the hydrophobicity, and thus the extent of phase separation. This is reflected in the high diffusion coefficient values for the BPSH-BisSF system when compared to the other multiblocks at a given water content. Similarly, among the random copolymers, the 6FSH-xx copolymers showed improved transport properties in comparison to the hydrocarbon systems.

11.3.3 Proton transport

Proton flux for ion containing polymers can be described by the Nernst Plank equation,[34]

$$-j_p = D_p C_p \left(\frac{\nabla C_p}{C_p} + z_p \frac{F \nabla \psi}{RT} \right) \qquad \textbf{Equation 11-3}$$

where j_p is the proton flux, C_p is the concentration of the protons, D_p is the diffusion coefficient of the protons, z_p the proton charge, Ψ the electrostatic potential, R the gas constant, and F the Faraday constant. For a membrane with a constant thickness and a proton charge of +1, proton flux can be related to proton conductivity (σ).

$$\sigma \propto j_p \propto D_p C_p \qquad \textbf{Equation 11-4}$$

Thus, proton conductivity is a function of both the concentration and diffusion coefficient of the protons. While the concentration value is governed by the ionic composition of the copolymer, the diffusion value is dependent on structure or morphology.

$$\sigma = f(C, D) \qquad \textbf{Equation 11-5}$$

In case of random copolymers, proton conductivity—particularly under fully hydrated conditions—corresponded to the ion exchange capacity or the concentration of the ionic groups.[16] For the multiblocks, however, proton conductivity corresponded to both block length and IEC. Under similar IEC values, proton conductivity has been found to increase with increasing block length. The following percolation model was used to model our experimental data (measured at 30 ^{o}C in liquid water). The percolation model relates the transport of a species within a porous network to the volume available for transport. Mathematically, the percolation model is given by the following equation.[34]

$$\frac{\sigma}{\sigma_0} \alpha \left(\phi_1 - \phi_c\right)^{\gamma_D} \qquad \textbf{Equation 11-6}$$

where, σ is the proton conductivity, σ_0 is the intrinsic proton conductivity, Φ is the total free volume of the system which can be related to the water volume fraction, Φ_c is the critical volume fraction, and γ is the ideality factor. The critical volume fraction is related to the minimum volume fraction needed for transport to take place. Using this relationship, the experimental proton conductivity data for both the random and multiblock copolymers were modeled in a power law relationship with the volume fraction of water (Fig. 11-4).

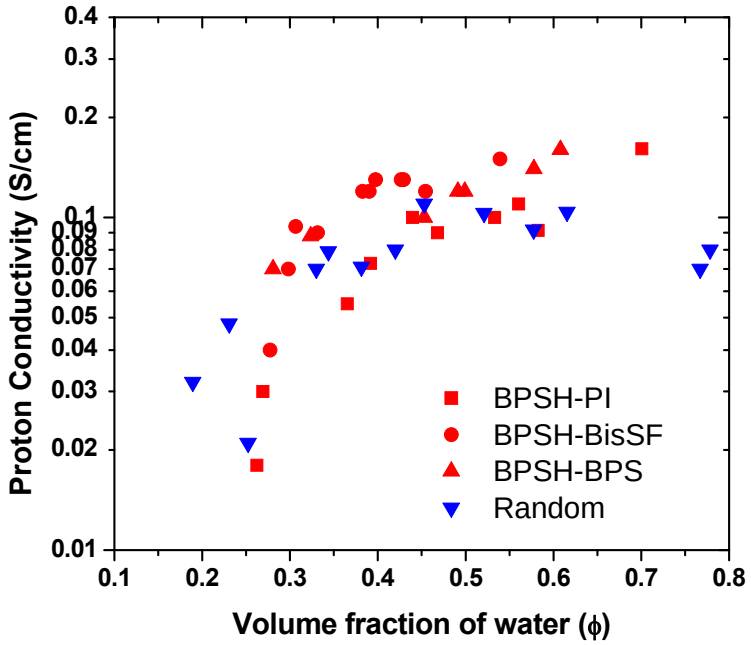

Figure 11-4 Proton conductivity measured in liquid water at 30 °C as a function of the volume fraction of water

This relationship allows one to compare the proton transport of different PEMs based on a single normalized physical property. For example, multiblocks with a better phase separated morphology showed higher proton conductivity than random copolymers over a wide range of water volume fraction. Similar to the water transport, presence of fluorine in the chemical backbone influences the proton transport also. BPSH-BisSF

having partial fluorination displayed highest proton conductivity among the multiblocks. One should also note that there was a subtle difference in the dependence of proton conduction on the volume fraction of water for the multiblock vs. the random copolymers. Particularly at higher water volume fraction levels, proton conduction decreases for the random copolymers, whereas a modest increase was observed in the case of the multiblocks. As discussed earlier, proton conductivity is a function of both effective charge concentration and proton diffusivity. Our investigation of these variables as a function of the volume fraction of water was useful in explaining this relationship. Figure (11-5) represents the plot of effective proton concentration vs. volume fraction of water. The proton concentration was varied by studying copolymers with varying IECs. The data is a representation of more than 50 different samples. Although the data is scattered, one can note that the effective proton concentration goes through a maxima for both the multiblock and random copolymers. At higher water volume fractions, the effective proton concentration decreases as the copolymer absorbs increasing amounts of water. A decrease in proton concentration is expected to decrease proton conductivity, especially when the concentration value is the dominant variable.

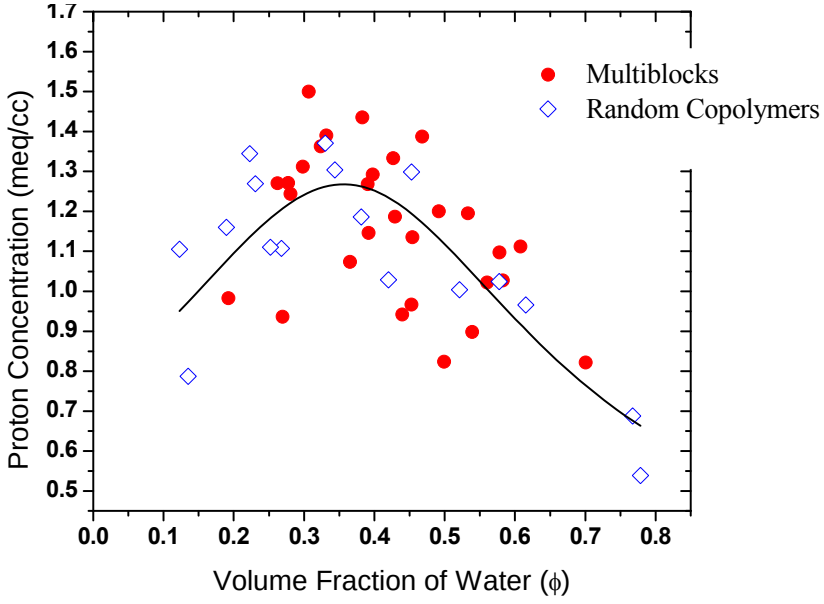

Figure 11-5 The effective proton concentration in PEMs decreases at higher water content

The proton diffusivity was calculated using the Nernst equation,[33] and ploted as a function of the reciprocal of the volume fraction of water (Fig. 11-6). At a higher volume fraction of water (lower 1/Φ), the diffusivity of the random copolymers was significantly lower than that of the multiblock copolymers. Hence, at high water volume fraction, the proton concentration term was identified as the dominant variable for the random copolymers, resulting in a decrease in proton conductivity. In contrast, in multiblocks, a comparably higher proton diffusivity offsets the decreasing protonic concentration trend and maintains the overall proton conductivity. Hence, the multiblock copolymer morphology allows one to maintain high proton conductivity even at high water content.

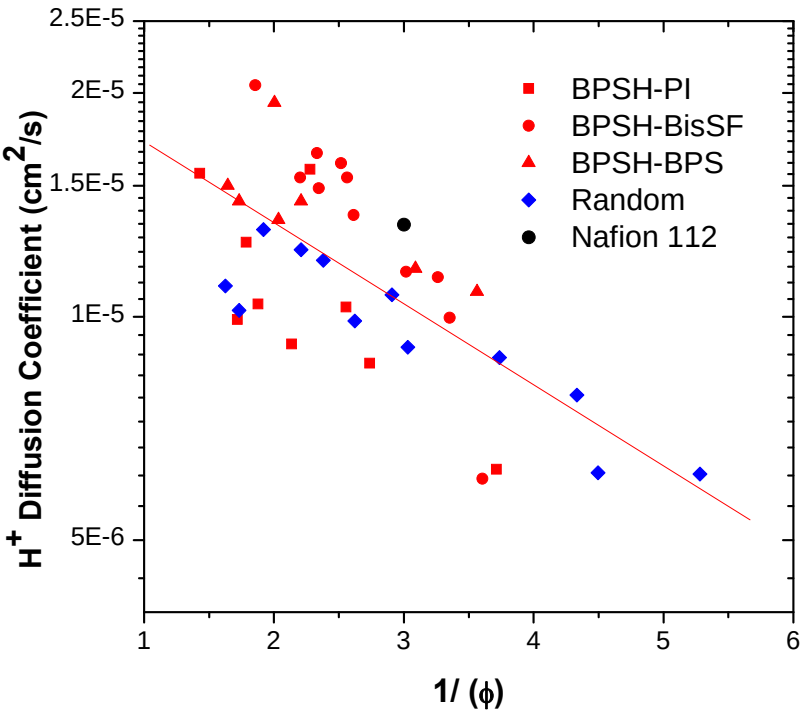

Figure 11-6 Multiblocks display higher proton diffusivity than the random copolymers at a given volume fraction of water

Proton conduction under partially hydrated conditions had been extensively studied for the multiblock copolymers. In general, performance under partially hydrated conditions scaled with increasing block length, with significant improvements achieved

compared to the random copolymers. Nanophase separation, e.g., the extent of connectivity between hydrophilic domains, is a function of block length, which lowers the morphological barrier for transport. As a component of this study, we investigated the extent to which nanophase separation correlated with improved performance. The extent of phase separation in non ionic block copolymers is identified by the product of two terms—the molecular weight of the individual blocks (N) and the Flory Huggins interaction parameter (χ).[36] Significant phase separation in the strong segregation limit is predicted when the product is > 10.5.

$$\chi N > 10.5 \qquad \textbf{Equation 11-7}\ ^{36}$$

On one hand, phase separation depends strongly on the molecular weights of the individual blocks. As discussed ealier, when block lengths was increased to 10,000-15,000 g/mole, a significant improvement in the properties of the copolymers were observed. Further increases in block length, however, increased water swelling and reduced performance due to swelling-deswelling issues.

On the other hand, the enthalpy term (χ parameter) which is a measure of the chemical dissimilarity between two blocks, controls the sharpness of phase separation also. For ion containing multiblock copolymers, it is difficult to estimate this parameter quantitatively. However, qualitatively it can be related to the difference between the hydrophobicity and hydrophilicity of the individual blocks. Hydrophilic blocks being kept same for all the multiblocks, the chemical structure of the hydrophobic unit only influenced the χ parameter. The influence of the hydrophobicity (i.e., the chemical structure of the hydrophobic blocks) on proton conductivity under partially hydrated conditions at 80 ^{o}C was studied, as shown in Figure (11-7).

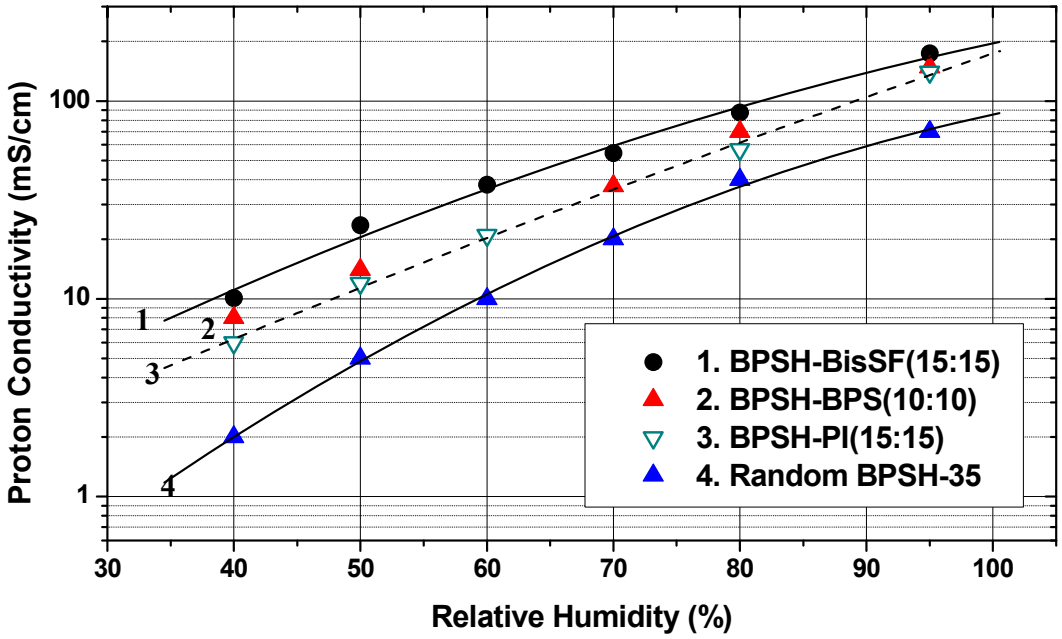

Figure 11-7 Influence of multiblock chemical structure on proton conduction under partially hydrated conditions at 80 °C

The multiblock copolymers chosen for this study were of high block lengths and similar IECs (1.4-1.5 meq/g). The fully hydrocarbon based BPSH-BPS(10:10) and BPSH-PI(15:15) copolymers showed similar behaviors under partially hydrated conditions. Significant improvements in performance were observed for the BPSH-BisSF(15:15) multiblocks. The partially fluorinated hydrophobic unit demonstrated increased hydrophobic characteristics compared to the hydrocarbon systems. This influenced the χ parameter, resulting in a possible increase in the sharpness of phase separation. This is consistent with the observed improvement in the water and proton transport properties of this particular multiblock under fully hydrated conditions. Hence, apart from tailoring the block lengths, altering the χ parameter or the chemical structure of the blocks, influences the sharpness of phase separation. This knowledge will contribute significantly in synthesizing new materials with improved performance characteristics.

11.3.4 States of water

As reported, there are at least three states of water that have been associated with water residing within the hydrophilic phases of a polymer.[11] The presence of these three states can be defined by their thermal properties. *Non-freezing bound water* is strongly associated with the polymer and depresses its T_g, but the water shows no melting endotherm as seen by differential scanning calorimetry (DSC). *Freezable bound water* is weakly bound to the polymer (or weakly bound to the non-freezing water), and displays broad melting behavior around 0 °C. *Free water* exhibits a sharp melting point at 0 °C. The states of water for the multiblocks and the random copolymers were characterized and quantified using DSC, NMR relaxation and TGA methods as reported earlier.[37] A strong relationship between the states of water and transport properties was revealed. In this paper, the nature of the distribution of the three types of water was investigated as a function of chemical composition and the microstructure of the copolymers and is related to their performance. Figure (11-8) represents the distribution of the three type of water on a percentage basis within the BPSH–xx [11] random copolymers, the BPSH-PI and BPSH-BPS multiblock copolymers, and Nafion® 112. The ion exchange capacity of the random copolymers was varied whereas it was kept similar for the multiblocks. Thus, block length was the only variable in the multiblock system. The tightly bound water for the random copolymers was independent of any observed changes in IEC, and similar to the multiblock copolymers, independent of block length.

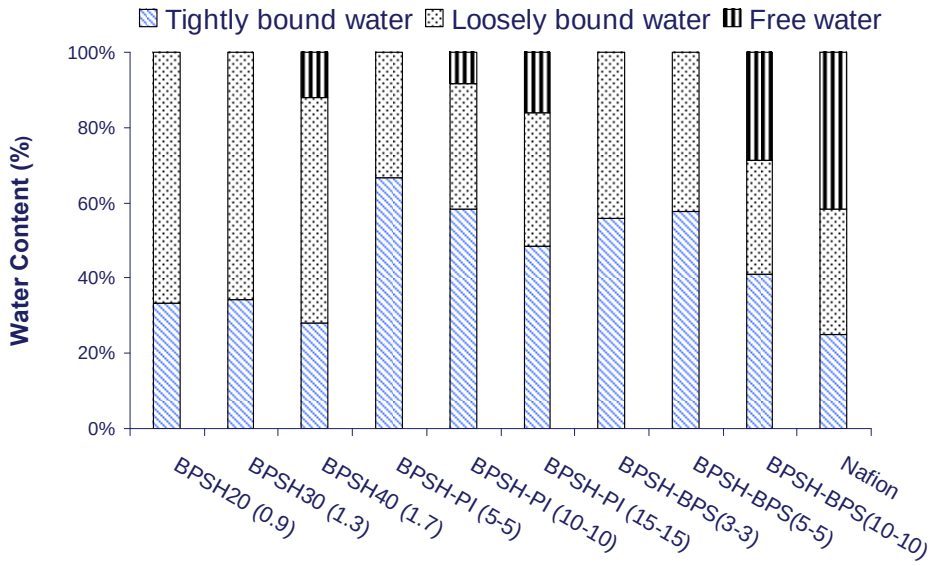

Figure 11-8 Distribution of different states of water in the PEMs as a function of the copolymer morphology and chemical compositions

For the random copolymers, free water was shown to develop after a particular ionic concentration. In spite of the constant IEC in the multiblock systems, free water developed as a function of increasing block length or morphology. The sharpness of the phase separation influenced free water content. The BPSH 40 random copolymer and the BPSH-BPS (10:10) multiblock copolymer displayed similar total water contents of 60%. However, the difference in chemical microstructure or morphology changed the distribution of the three types of water in the copolymers. Interestingly, Nafion®112 and the BPSH-BPS (10:10) displayed similar distributions of the three types of water, which indicated their similar morphological structure. This finding is reflected in the fact that it was possible to achieve very similar proton transport performance between the two over a wide range of hydration levels.

11.4 Conclusions

Novel structure-property relationships of transport properties with polymer physical properties were achieved for all the random and block copolymers. At a given ionic content, the extent or sharpness of phase separation controlled water absorption behavior. The self-diffusion coefficients of water were modeled to an exponential relationship with the inverse of the volume fraction of water. Proton conductivity followed a power law dependence on the volume fraction of water or the hydrophilic phase. At a given volume fraction, the block copolymers displayed both higher self-diffusion coefficients of water and improved proton conductivity as compared to the random copolymers. This improvement in transport properties indicates the presence of a desirable morphological structure for the block copolymers.

In proton exchange membranes, a tradeoff between the effective proton concentration and the volume fraction of water was observed. For both the random and multiblock copolymers, the effective proton concentration decreased at higher volume fractions of water. Because proton conductivity is both a function of proton concentration and diffusivity, it was shown to decrease for the random copolymers at higher water content. In contrast, the high proton diffusivity values for the multiblocks compared to the random copolymers resulted in increased proton conductivity even at high water content.

The extent of phase separation in multiblock copolymers is known to be a function of both the molecular weight of the individual blocks, as well as the hydrophobicity-hydrophilicity differences between the two blocks. Increasing either the block length or the hydrophobicity of the hydrophobic block resulted in significant improvements in proton transport under partially hydrated conditions. Nanophase separation (i.e., the extent of connectivity between hydrophilic domains) lowers the morphological barrier for transport. This highlights the importance of morphology on transport.

The states of water analyses showed a strong dependence of the distribution of the three types of water on the ion content and morphology of the copolymers. For the random copolymers, the formation of free water in the system occurred after reaching a certain ionic content. While for the block copolymers, in spite of having similar IECs, free water developed with increasing block length. The distribution of the states of water was found to be a function of the microstructure or the sequence distribution of the hydrophobic and hydrophilic segments. The multiblock copolymers consist of sulfonic acid groups attached to an aromatic hydrocarbon backbone. In contrast, Nafion® contains perflurosulfonic acid groups in a side chain. In spite of these chemical dissimilarities, the co-continuous morphology for the multiblocks allowed a similar distribution in the states of water as seen for Nafion®. Interestingly, the performance of the block copolymers (having higher free water content) under partially hydrated conditions equals to that of Nafion®, which is significantly better than the performance of random copolymers. It can be concluded that tailoring the microstructure of an aromatic hydrocarbon copolymer enables a favorable distribution of the three types of water, which improves proton conduction under partially hydrated conditions.

The authors wish to acknowledge the support of the National Science Foundation "Partnership for Innovation" Program (HER-0090556), Department of Energy (DE-FC36-01G01086, DE-FG36-06G016038), Nissan Motor Company, UTC Fuel Cell (#PO3561) and Sandia National Laboratories.

11.5 References

1. Hickner, M. A.; Ghassemi, H.; Kim, Y. S.; Einsla, B. R.; McGrath, J. E., Alternative polymer systems for proton exchange membranes (PEMs). *Chemical Reviews* **2004,** 104, (10), 4587-4611.

2. Mathias, M.; Gasteiger, H.; Makharia, R.; Kocha, S.; Fuller, T.; Xie, T.; Pisco, J., Can available membranes and catalysts meet automotive polymer electrolyte fuel cell

requirements? *Preprints of Symposia - American Chemical Society, Division of Fuel Chemistry* **2004,** 49, (2), 471-474.

3. Mauritz, K. A.; Moore, R. B., State of understanding of Nafion. *Chemical Reviews* **2004,** 104, (10), 4535-4585.

4. Winter, M.; Brodd, R. J., What are batteries, fuel cells, and supercapacitors? (vol 104, pg 4245, 2003). *Chemical Reviews* **2005,** 105, (3), 1021-1021.

5. Carrette, L.; Friedrich, K. A.; Stimming, U., Fuel cells: Principles, types, fuels, and applications. *Chemphyschem* **2000,** 1, (4), 162-193.

6. Brandon, N. P.; Skinner, S.; Steele, B. C. H., Recent advances in materials for fuel cells. *Annual Review of Materials Research* **2003,** 33, 183-213.

7. Zalbowitz, M.; S, T., Green Power. *Fuel Cells* **1999**.

8. Kim, Y. S.; Wang, F.; Hickner, M.; Zawodzinski, T. A.; McGrath, J. E., Fabrication and characterization of heteropolyacid (H3PW12O40)/directly polymerized sulfonated poly(arylene ether sulfone) copolymer composite membranes for higher temperature fuel cell applications. *Journal of Membrane Science* **2003,** 212, (1-2), 263-282.

9. Kim, Y. S.; Wang, F.; Hickner, M.; McCartney, S.; Hong, Y. T.; Harrison, W.; Zawodzinski, T. A.; McGrath, J. E., Effect of acidification treatment and morphological stability of sulfonated poly(arylene ether sulfone) copolymer proton-exchange membranes for fuel-cell use above 100 degrees C. *Journal of Polymer Science Part B-Polymer Physics* **2003,** 41, (22), 2816-2828.

10. Kim, Y. S.; Dong, L. M.; Hickner, M. A.; Pivovar, B. S.; McGrath, J. E., Processing induced morphological development in hydrated sulfonated poly(arylene ether sulfone) copolymer membranes. *Polymer* **2003,** 44, (19), 5729-5736.

11. Kim, Y. S.; Dong, L. M.; Hickner, M. A.; Glass, T. E.; Webb, V.; McGrath, J. E., State of water in disulfonated poly(arylene ether sulfone) copolymers and a perfluorosulfonic acid copolymer (nafion) and its effect on physical and electrochemical properties. *Macromolecules* **2003,** 36, (17), 6281-6285.

12. Harrison, W. L.; Wang, F.; Mecham, J. B.; Bhanu, V. A.; Hill, M.; Kim, Y. S.; McGrath, J. E., Influence of the bisphenol structure on the direct synthesis of sulfonated

poly(arylene ether) copolymers. I. *Journal of Polymer Science Part a-Polymer Chemistry* **2003,** 41, (14), 2264-2276.

13. Wang, F.; Hickner, M.; Kim, Y. S.; Zawodzinski, T. A.; McGrath, J. E., Direct polymerization of sulfonated poly(arylene ether sulfone) random (statistical) copolymers: candidates for new proton exchange membranes. *Journal of Membrane Science* **2002,** 197, (1-2), 231-242.

14. *DOE Program Review* **2005,** May 23-26, (Arlington,VA).

15. Kim, Y. S.; Sumner, M. J.; Harrison, W. L.; Riffle, J. S.; McGrath, J. E.; Pivovar, B. S., Direct methanol fuel cell performance of disulfonated poly-arylene ether benzonitrile) copolymers. *Journal of the Electrochemical Society* **2004,** 151, (12), A2150-a2156.

16. Roy, A.; Hickner, M. A.; Yu, X.; Li, Y.; Glass, T. E.; McGrath, J. E., Influence of chemical composition and sequence length on the transport properties of proton exchange membranes. *Journal of Polymer Science, Part B: Polymer Physics* **2006,** 44, (16), 2226-2239.

17. Roy, A.; Yu, X.; Dunn, S.; McGrath, J. E., Influence of Microstructure and Chemical Composition on Proton Exchange Membrane Properties for Disulfonated BisSF-BPSH Multiblock Copolymers. *To be Submitted* **2008**.

18. Roy, A.; Lee, H.-S.; McGrath, J. E., Structure-Property Relationships of BPSH-PI Multiblock Copolymers for Application in Proton Exchange Membrane Fuel Cells. *To be Submitted* **2008**.

19. Lee, H.-S.; Badami, A. S.; Roy, A.; McGrath, J. E., Segmented sulfonated poly(arylene ether sulfone)-b-polyimide copolymers for proton exchange membrane fuel cells. I. Copolymer synthesis and fundamental properties. *Journal of Polymer Science, Part A: Polymer Chemistry* **2007,** 45, (21), 4879-4890.

20. Roy, A.; Hickner, M. A.; Lee, H.-S.; Badami, A.; Yu, X.; Li, Y.; Glass, T.; McGrath, J. E., Transport properties of proton exchange membranes. *ECS Transactions* **2007,** 2, (24, Direct Methanol Fuel Cells), 45-54.

21. Kim, Y. S.; Einsla, M.; Hawley, M.; Pivovar, B. S.; Lee, H.-S.; Roy, A.; McGrath, J. E., Multiblock copolymers for low relative humidity fuel cell operation. *ECS*

Transactions **2007,** 11, (1, Part 1, Proton Exchange Membrane Fuel Cells 7, Part 1), 49-54.

22. Roy, A.; Lee, H.-S.; Badami, A. S.; Yu, X.; Li, Y.; Glass, T. E.; McGrath, J. E., Transport properties of multiblock hydrophilic-hydrophobic proton exchange membranes for fuel cells. *Preprints of Symposia - American Chemical Society, Division of Fuel Chemistry* **2006,** 51, (2), 660-661.

23. Roy, A.; Hickner, M.; Glass, T.; Li, Y.; Einsla, B.; Wiles, K. B.; Yu, X.; McGrath, J. E., States of water- investigating the water-polymer interactions and transport phenomenon in proton exchange membranes. *Preprints of Symposia - American Chemical Society, Division of Fuel Chemistry* **2005,** 50, (2), 699-700.

24. Ghassemi, H.; Ndip, G.; McGrath, J. E., New multiblock copolymers of sulfonated poly(4 '-phenyl-2,5-benzophenone) and poly(arylene ether sulfone) for proton exchange membranes. II. *Polymer* **2004,** 45, (17), 5855-5862.

25. Ghassemi, H.; McGrath, J. E., Synthesis and properties of new sulfonated poly(p-phenylene) derivatives for proton exchange membranes. I. *Polymer* **2004,** 45, (17), 5847-5854.

26. Li, Y.; Roy, A.; Badami, A. S.; Hill, M.; Yang, J.; Dunn, S.; McGrath, J. E., Synthesis and characterization of partially fluorinated hydrophobic-hydrophilic multiblock copolymers containing sulfonate groups for proton exchange membrane. *Journal of Power Sources* **2007,** 172, (1), 30-38.

27. Yu, X.; Roy, A.; Dunn, S.; Yang, J.; McGrath, J. E., Synthesis and characterization of sulfonated-fluorinated, hydrophilic-hydrophobic multiblock copolymers for proton exchange membranes. *Macromolecular Symposia* **2006,** 245/246, (World Polymer Congress--MACRO 2006), 439-449.

28. Wang, H.; Badami, A. S.; Roy, A.; McGrath, J. E., Multiblock copolymers of poly(2,5-benzophenone) and disulfonated poly(arylene ether sulfone) for proton-exchange membranes. I. Synthesis and characterization. *Journal of Polymer Science, Part A: Polymer Chemistry* **2006,** 45, (2), 284-294.

29. Roy, A.; Yu, X.; Lee, H.-S.; Badami, A. S.; Dunn, S.; McGrath, J. E., Proton exchange membranes for fuel cell applications. *Polymer Preprints (American Chemical Society, Division of Polymer Chemistry)* **2007,** 48, (1), 246-247.

30. Roy, A.; Hickner, M. A.; Xiang, Y.; Lee, H.-S.; McGrath, J. E., *ECS Transactions* **2007,** 2, (24).

31. Lee, H.-S.; Roy, A.; Lane, O.; Dunn, S.; McGrath, J. E., Hydrophilic-hydrophobic multiblock copolymers based on poly(arylene ether sulfone) via low-temperature coupling reactions for proton exchange membrane fuel cells. *Polymer* **2008,** 49, (3), 715-723.

32. Roy, A.; Lee, H.-S.; McGrath, J. E., Hydrocarbon based BPSH-BPS Multiblock Copolymers as Novel Proton Exchange Membranes Part-B. *To be Submitted* **2008**.

33. Schuster, M.; Kreuer, K.-D.; Andersen, H. T.; Maier, J., Sulfonated poly(phenylene sulfone) polymers as hydrolytically and thermooxidatively stable proton conducting ionomers. *Macromolecules* **2007,** 40, (3), 598-607.

34. Elabd, Y. A.; Napadensky, E.; Sloan, J. M.; Crawford, D. M.; Walker, C. W., Triblock copolymer ionomer membranes Part I. Methanol and proton transport. *Journal of Membrane Science* **2003,** 217, (1-2), 227-242.

35. Yasuda, H.; Lamaze, C. E.; Ikenberry, L. D., Permeability of Solutes Through Hydrated Polymer Membranes. *Die Makromoleculare Chemie* **1968,** 118, (NR-2858), 19-35.

36. Leibler, L., Theory of Microphase Separation in Block Copolymers. *Macromolecules* **1980,** 13, (6), 1602-1617.

37. Roy, A.; Hickner, M. A.; Lee, H.-S.; Glass, T. E.; McGrath, J. E., States of Water of Proton Exchange Membranes Part-A- Influence of Chemical Structure and Compositions. *To be Submitted* **2008**.

12.0 Suggested Future Research

12.1 Scope

The novel structure property relationships investigated during the course of this research highlight the importance of a phase separated morphology in achieving improved PEM performance. Initially, the acidity of a proton exchange membrane was considered to be the most important criterion for achieving high proton conductivity. However, the current research underscores the importance of the extent of connectivity between the hydrophilic domains as the major factor in controlling proton transport, particularly under partially hydrated conditions. The research also identified important PEM properties that need to be addressed in synthesizing new materials. For example, the copolymer should have a facilitated morphological structure that promotes both water and proton transport. Quantitatively, the self-diffusion coefficient of water should be in the favorable morphological region as mentioned Figure (11-3). The relationships between the self-diffusion coefficients of water and the volume fraction of water can be used as a modeling tool in predicting the extent of connectivity within hydrophilic domains.

This study also pointed out the importance of low water uptake—or more precisely, the significance of low water swelling. The proton concentration in the PEM is a strong function of the water swelling. A reduced water uptake increases the effective proton concentration. In addition to enhancing performance, water swelling also influences the overall durability of a PEM. Constraining the hydrophilic unit by physical or chemical crosslinking can reduce swelling and improve the durability of a PEM.

In view of the fact that durability and fuel efficiency are essential in designing a proton exchange membrane, low gas or fuel crossover are required. The copolymer structure strongly influences fuel permeability as reported for both H_2/Air and DMFC systems. In addition to the rigid polymeric backbone, the nature of the sequence

distribution of the hydrophobic unit controls the permeability of gases and methanol within the polymer matrix.

The distribution of different types of water within the copolymer also influences PEM properties. Each type of water (i.e., strongly bound, loosely bound, and free) has its own unique impact on the properties of a PEM. Thus, the proper balance of these three types of water in a PEM is a function of the chemical composition and morphology of the copolymer. By tailoring structural variables, the relative amount of the each type of water can be varied, which in turn impacts properties.

The above-mentioned criteria can be achieved by synergistic research exploring the synthesis and characterization of proton exchange membranes. Some possible approaches are discussed below.

12.2 Synthetic strategies

The primary objective of the proposed synthesis is to achieve both improved phase separation and reduced water uptake for the copolymers in comparison to the state-of-the-art material, Nafion®. The research is based on the foundation developed for multiblock copolymer chemistry. For ionic multiblock copolymers, phase separation was found to be a function of both block length and the hydrophobicity-hydrophilicity differences between the individual blocks. Increasing the hydrophobicity of the hydrophobic block through partial fluorination (BPSH-BisSF) resulted in significantly improvement performance. Specifically, increased hydrophobicity was expected to increase the extent of phase separation. However, for all the multiblocks synthesized, the hydrophilic block was kept the same. A change in the hydrophilicity of the hydrophilic block is also expected to influence phase separation. Hydrophilicity can be controlled by manipulating the ionic concentration in the hydrophilic block.

In our earlier study of the hydroquinone-based HQSH-xx random copolymers, a higher ion exchange capacity was achieved with a same degree of disulfonation used for our biphenol systems (BPSH). This is related to the difference in the individual molar

mass of the two bisphenol units. Hence, a HQSH-100 hydrophilic block will have a higher IEC compared to a BPSH-100 hydrophilic block. This variable is expected to alter the hydrophobicity-hydrophilicity differences in the block copolymers and significantly improve phase separation. In addition, changing the hydrophobic unit from a hydrocarbon to a partially fluorinated unit can be another important modification. These two structural alterations are expected to greatly enhance phase separation and, therefore, the desired properties for multiblock systems over existing systems. Besides changing the bisphenol units in the polymeric backbone, the functional groups can also be altered to add other structural variables. The ketone and sulfone are the variables as functional groups.

The possible chemical structures of this proposed array of multiblock copolymers are summarized in Figure (12-1), where X, Y and Z are the variables.

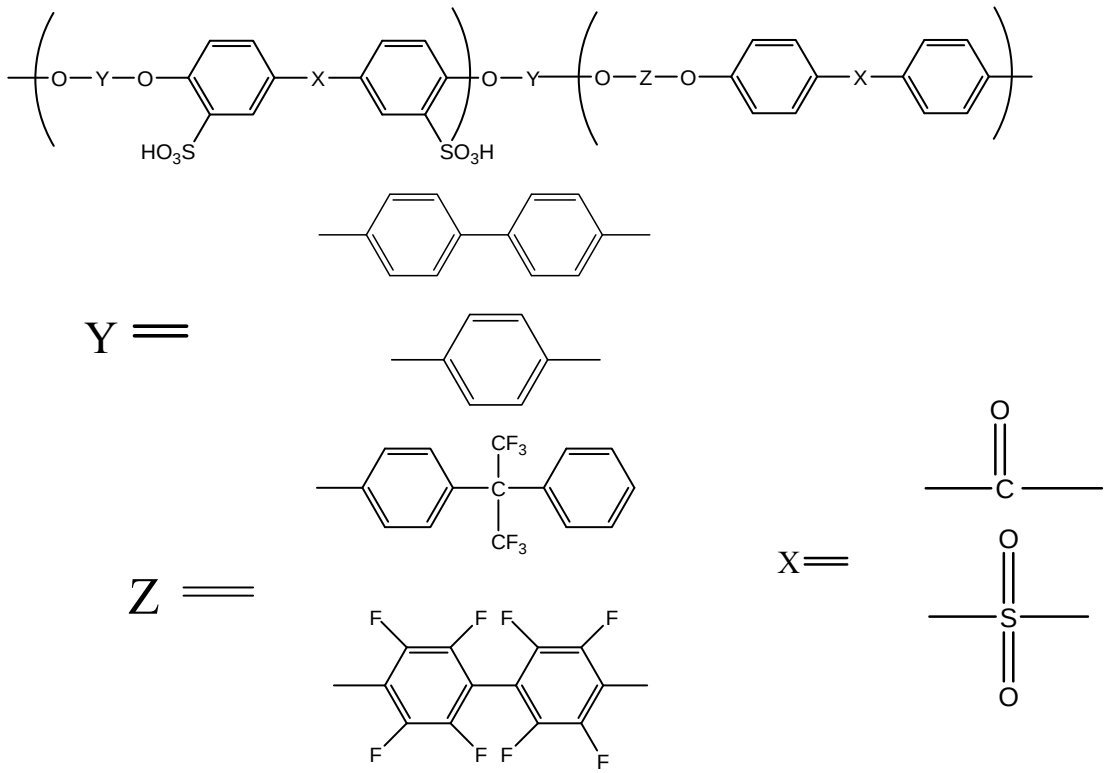

Figure 12-1 Variation in chemical structures for the proposed multiblock copolymers

The sharpness of phase separation in the multiblock copolymers was associated with increasing water uptake. As we documented, higher water uptake reduces proton concentration and, hence, overall proton conductivity. Because transport is controlled by the extent of phase separation, and proton concentration is controlled by water uptake, maximizing both these factors will maximize overall proton conductivity. Water uptake can be controlled to a certain extent by increasing the hydrophobic block length over the hydrophilic block length. This is analogous to physical crosslinking, whereby the hydrophobic units constrain the hydrophilic blocks. However, there is a certain limit to which the hydrophobic–hydrophilic block length ratio can be altered. A higher ratio changes the morphological structure from a continuous to a discontinuous hydrophilic domain morphology, thereby reducing performance. Chemical crosslinking is an alternative approach. By crosslinking the equal block length multiblock copolymers, one may retain the ideal morphological structures, while at the same time reducing water uptake. Recently, Riffle et al.[1] have reported the synthesis of thermally stable epoxy–crossslinked disulfonated poly(arylene ether sulfone) copolymers, which have shown promise. For the random copolymers, the chemistry was established and significant improvements in PEM selectivity were achieved. Extending the chemistry for the multiblocks is an approach for chemical crosslinking the ionic multiblocks. Both improved performance under partially hydrated conditions and reduced water swelling can be achieved from the proposed crosslinked mutliblock copolymers.

We also proposed that introducing thermally stable crosslinking groups to the polymer matrix would reduce the fuel permeability of the system. A significant reduction in salt permeability was observed with increasing crosslinking density for the epoxy crosslinked random copolymer systems.[1] A similar influence of crosslinking on gas and methanol permeability is also expected. In addition to rigid aromatic backbones, the multiblock morphology and crosslinking are proposed to improve the durability of the membrane by reducing both gas and methanol crossover.

We also confirmed that the states of water are a strong function of the ionic content and morphology of the system. Specifically, free water content increased with an

increasing extent of phase separation. Moreover, increased free water content increased swelling and may reduce selectivity. By crosslinking, however, it was possible to reduce the amount of free water in the system. By effectively controlling the multiblock morphology and crosslinking density, optimize distribution of the three types of water in the copolymer can be achieved.

In summary, the synthetic principles we established show great promise for the next generation of proton exchange membranes—especially since structural variables can be synthetically tailored to achieve the desired properties.

12.3 Characterization

The synthesis of these materials will broaden the spectrum for further structure-property relationship studies. Apart from the measurement techniques we discussed herein, several new experimental designs can be proposed. New characterization techniques will be essential for further understanding the influence of chemical structures on PEM properties. Over the several years, our group has been involved in microscopic studies on the morphology of multiblock systems using AFM and TEM techniques. Both of these microscopic techniques were successful in revealing the co-continuous morphological structure of the hydrophilic-hydrophobic domains. However, on a quantitative scale, it was difficult to estimate the size of these domains. Small angle X-ray diffraction studies will be valuable in assessing the size of these domains as a function of the multiblock copolymer morphology. Water dynamic studies and the states of water were examined using NMR relaxation techniques. It is expected, however, that neutron scattering techniques will be useful in revealing further information about water–polymer interactions.

In addition to this fundamental investigation, a number of important fuel cell and electrochemical experiments are ongoing, including MEA fabrication and the evaluation of fuel cell performance under low relative humidity and high temperature. Several of these tests, in fact, have disclosed encouraging preliminary results.[2] In conjunction with

these fuel cell experiments, freeze-thaw cycling and low RH cycling experiments are suggested to predict the lifetime and real-time performance of these membranes.

12.4 References

1. Paul, M.; Park, H. B.; Freeman, B. D.; Roy, A.; McGrath, J. E.; Riffle, J. S., Synthesis and crosslinking of partially disulfonated poly(arylene ether sulfone) random copolymers as candidates for chlorine resistant reverse osmosis membranes. Polymer, available online, doi:10.1016/j.polymer.2008.02.039, **2008**.

2. Kim, Y. S.; Einsla, M.; Hawley, M.; Pivovar, B. S.; Lee, H.-S.; Roy, A.; McGrath, J. E., Multiblock copolymers for low relative humidity fuel cell operation. *ECS Transactions* **2007,** 11, (1, Part 1, Proton Exchange Membrane Fuel Cells 7, Part 1), 49-54.

List of Symbols

j_p	Proton flux
C_p	Concentration of protons
D_p	Diffusion coefficient of protons
Z_p	Protonic charge
Ψ	Electrostatic potential
R	Gas constant
F	Faraday
σ	Proton conductivity
A	Cross sectional area
Z’	Real impedance response
λ	Hydration number
A	NMR signal intensity
γ	Gyromagnetic ratio
δ	Length of gradient pulse
Δ	Time between gradient pulse
Δr	Mean square displacement
D_{eff}	Effective self-diffusion coefficient of water.
H	Partition coefficient
Φ	Volume fraction of water

Vita

Abhishek Roy, son of Mr. Arunabha Roy and Mrs. Manju Roy was born in Calcutta, India. After completion of schooling from Nava Nalanda High School, he earned his B.S. in Chemistry from University of Calcutta in 1999. He moved on to earn a post graduate engineering degree in Polymer Science and Technology from University of Calcutta in 2002. He continued his graduate education at Virginia Polytechnic Institute and State University in pursuing Ph.D. degree in Macromolecular Science and Engineering program. Upon completion, he plans to join Dow Chemical Company in Midland, MI.